Author:
Luvira, Viravarn

Title:
High-throughput proteomic analysis of the dengue virus secretome and the identification of plasma biomarkers of disease severity

High-throughput proteomic analysis of the dengue virus secretome and the identification of plasma biomarkers of disease severity

Viravarn Luvira

A dissertation submitted to the University of Bristol in accordance with the requirements for award of the degree of Doctor of Philosophy in the School of Cellular and Molecular Medicine.

Oct 2019

Word count (excluding preliminary pages, references and appendices): 76,302

Abstract

Dengue virus (DENV) causes the most important arthropod-borne viral disease of humans. Dengue (DEN) pathogenesis is not well understood and there are neither fully protective vaccines nor antiviral drugs to prevent DEN. A diagnostic test to predict disease severity is also lacking. A greater understanding of the cellular changes that occur in response to DENV infection will increase our understanding of pathogenesis and potentially lead to the development of new treatment options. In this study, quantitative mass spectrometry (MS) was therefore used to systematically analyse the host response to DENV infection both *in vitro* and *in vivo*.

Initially, the proteome and secretome of DENV infected HEK293T cells and HEK293T cells expressing a DENV replicon were compared. Bioinformatic analysis of the results showed that the replicon system was good surrogate for viral replication studies.

The combined proteomic/secretomic analysis was then extended to DENV infected Huh-7 liver cells. Bioinformatic analysis of the results showed that the predominant effect of infection was a significant decrease in the levels of proteins, both in the proteome and secretome, that were involved in “complement and coagulation cascades” and “lipid metabolic” processes.

Proteomic analysis of serum from patients with different grades of DEN identified proteins that were significantly altered in response to DENV infection and two proteins, C-reactive protein and apolipoprotein CII, that could be used to discriminate disease states.

The results of the proteomic analyses using cell-based models and patient serum were then compared, which revealed that Huh-7 cells provide a good model for studying the role of complement, coagulation and acute phase proteins (APPs) in DEN.

The results of the proteomic analyses were validated for selected APPs. The levels of APPs in DENV infected Huh-7 cells could be rescued by treatment with MG132, suggesting liver APPs are degraded by the proteasome in DENV infection.

Dedication and Acknowledgements

A PhD is just a degree but I have leant much about life and science during these four years. This learning would not have been possible without the support of a number of people. I therefore would like to express my gratitude to them.

First of all, I would like to thank my beloved supervisor, Dr. Andrew Davidson. This work would be impossible without his continuous support, recommendation, guidance and his infinite patience. I know it was a big challenge (the optimistic word for problem) to train a medic without lab skills and basic science knowledge from the very first step through to the culmination which is this work achievement; I know I am really lucky to have him as my supervisor.

I would like to acknowledge the Faculty of Tropical Medicine, Mahidol University and the Mahidol University's Academic Development Scholarship for granting my PhD study. I would like to express my gratitude to my head of department and Dean, Prof. Punnee Pitisuttithum, Assist Prof. Weerapong Phumratanaprapin and Prof. Yaowalark Sukthana for their understanding and continuous support.

I would like to thank my co-advisor, Dr. David Morgan, for his support and inspiring talks over coffee. I also would like to thank Dr. David Matthew for his great and impressive comments to my annual progress reports. I would like to thank Dr. Kate Heesom and the staff in proteomic facility for their technical assistance throughout the study. Furthermore, I would like to thanks my examiners, Prof. Julian Hiscox and Dr. Laura Rivino, for the great comments to improve this wotk.

For me, the E-50 virology lab is a wonderful place full of wonderful and unique people. I love all the lab members and would like to thank them for sharing laughter and tears throughout successful and failed experiments. I would like to thank my proteomic Jedi, Dr. Phillip Lewis, and my real life heroines, Dr. Maia Kavanagh Williamson and Dr. Holly Baum, for their invaluable training, advice and help. I also would like to thanks Dr. Amjad Yousuf and Dr. Abulrhman Al Zilay for their technical advice as well as Alistair Antonopoulos, Joshua Lee, I'ah Donovan-Banfield and Alina Rozanova for their technical assistance. Furthermore, I would like to thank all support for the E-floor technician team especially Dr. Natalie Griffiths-Stubbs. In Addition, I thanks all my friends in Bristol and Thailand, especially my sis, Dr. Punyawee Dulyayangkul.

I would like to express my love and deepest gratitude to Dr. Danabhand Phiboonbanakit, Dr. Kitti Trakulhun, Prof. Punnee Pitisuttithum, Dr. Sopon Iamsirithaworn, Wassana Piwsa-Ard, Assist. Prof. Prakaykaew Charunwatthana, Dr. Naiyarat Prasongsook, Dr. Navapan Issariyakulkarn, Dr. Virisorn Wongsrichanalai, Dr. Khemthong Tonsakulrungruang and Kollawat Somsri for their friendship and continuous support throughout the study period and my difficult time. Their love is always beside me wherever I am and whenever I need it.

Finally, I would like to thank my parents and my family for invaluable and infinite love. I have no word to express how much I appreciated their love and support. I believe that my father who was my inspiration for PhD studies would be proud of me, if he could see my achievement.

I declare that the work in this dissertation was carried out in accordance with the requirements of the University's Regulations and Code of Practice for Research Degree Programmes and that it has not been submitted for any other academic award. Except where indicated by specific reference in the text, the work is the candidate's own work. Work done in collaboration with, or with the assistance of, others, is indicated as such. Any views expressed in the dissertation are those of the author.

SIGNED: DATE: 22 December 2019

Table of Contents

Table of Figures

Table of Tables

Abbreviations

aa	amino acid(s)
ADE	antibody-dependent enhancement
AGC	automatic gain control
AGT	angiotensinogen
ALB	albumin
AMBP	protein AMBP
APO	apolipoprotein A1
APOA1	apolipoprotein
APOB	apolipoprotein B
APOC2	apolipoprotein C2
APPs	acute phase proteins
APS	ammonium persulphate
ATF6	activating transcription factor-6
AUFI	acute undifferentiated febrile illness
BCA	bicinchoninic acid
CALR	calreticulin
cDNA	complementary DNA
CFI	coagulation factor I
CFH	coagulation factor H
CIC	circulated immune complexs
CM	complete media
CNX	caknexin
CPE	cytopathic effect
Co-IP	co-immunoprecipitation
COX	cytochrome c oxidase
COX6C	Cytochrome c oxidase subunit VIc
CRP	C-reactive proteins
DAPI	4',6-diamidino-2-phenylindole
DAVID	Database for Annotation, Visualization and Integrated Discovery
DC-SIGN	dendritic cell-specific intercellular adhesion molecule-3-grabbing non-integrin
DDX	DEAD-Box Helicase
DEN	dengue
DENV	dengue virus
DF	dengue fever
DHF	dengue haemorrhagic fever
DIC	disseminated intravascular coagulation
DMEM	Dulbecco’s modified Eagles medium
DMSO	dimethyl sulfoxide
DNA	deoxyribonucleic acid

DSS	dengue shock syndrome
DTT	dithiothreitol
EDTA	ethylenediaminetetraacetic acid
eIF2A	alpha subunit of eukaryotic initiation factor 2
ENO1	alpha enolase
ER	endoplasmic reticulum
FASN	fatty acid synthase
FBLN1	fibulin-1
FBG	fibrinogen
FBS	foetal bovine serum
FDR	false discovery rate
FFU	focus forming units
FGA	fibrinoge alpha
FGB	fibrinogen beta
FGG	fibrinogen gamma
FGL1	fibrinogen-like protein 1
FUCA2	plasma alpha-L-fucosidase
F2	prothrombin
F13B	coagulation factor XIII B chain
g	gram
g	gravity
GES	group enrhichment score
GFP	green fluorescent protein
GO	Gene ontology
GOBP	Gene ontology biological process
GOCC	Gene ontology cellular component
GOMF	Gene ontology molecular function
GRP78	glucose-regulated protein 78
GWAS	genome-wide study
h	hour(s)
hpi	hour poost-infection
Hct	hematocrit
HDL	high-density lipoproteins
HEPES	4-(2-hydroxyethyl)-1-piperazineethanesulfonic acid
HIST1H4L	histone H4
HIV-1	human immunodeficiency virus type 1
HLA	human leukocyte antigen
HNF4A	hepatocyste nuclear factor 4 alpha
HNRNPH1	heterogeneous nuclear ribonucleoprotein H1
HP	haptoglobin
HRP	horseradish peroxidase
HSP	heat shock protein
HSPA5	endoplasmic reticulum chaperone BiP

ICAT	isotope-coded affinity tags method
IF	imunofocus
IFA	immunofluorescence assay
IFITM3	Interferon-induced transmembrane protein 3
IFN	interferon
Ig	immunoglobulin
IL-6	interleukin-6
IL-8	interleukin-8
IPA	ingenuity pathway analysis
IRE1	inositol-requiring protein-1
iTRAQ	isotope tags for relative and absolute quantitation
JEV	Japanese encephalitis virus
k	kilo
kDa	kilo-Dalton
l	liter
LAMP1	lysosome-associated membrane proteins 1
LC	liquid chromatography
LD	lipid droplet
LDL	low densitry lipoproteins
m	milli
M	Molar
MALDI-TOF	matrix-assisted laser desorption/ionization time-of-flight
MAN1A1	mannosyl-oligosaccharide 1,2-alpha-mannosidase IA
MEM	minimal essential medium
MHC	major histocompatibility complex
MIF	macrophage migration inhibitory factor
min	minute(s)
miRNA	microRNAs
MOI	multiplicity of infection
MS	mass spectrometry
MS/MS	tandam mass spectrometry
n	nano
NCR	noncoding regions
NEAA	non-essential amino acids
NF-κB	nuclear factor-κB
NH4Cl	ammonium chloride
NID1	nidogen-1
NLS	nuclear localisation signal
NPC	nuclear pore complex
NS	non-structural
NTPase	nucleotide triphosphatase
NUPs	Nucleoporins
NUP37	nucleoporins 37

OFI	other febrile illness
ORF	open reading frame
ORM1	alpha-1-acid glycoprotein 1
ORM2	alpha-1-acid glycoprotein 2
p	pico
PBS	phosphate buffered saline
PCR	polymerase Chain Reaction
PDL	poly-D-lysine
PEP	posterior error probability
PERK	PKR-like endoplasmic reticulum kinase
pi	post-infection
Plt	platelet
PLTP	phospholipid transfer protein
PPH	primary human hepatocytes
PROC	protein C
PROS1	protein S
PSMs	peptide-to-spectrum matches
PTM	post translational modification
PVDF	polyvinylidene difluoride
qRT-PCR	real-time reverse-transcription PCR
RBP4	retinol binding protein 4
RC	replication complex
REP	HEK293T-DV-Rep
RNA	ribonucleic acid
RP	reversed-phase
rpm	revolutions per minute
RT	reverse transcription
RTemp	room temperature
RT-PCR	reverse transcription PCR
sec	second(s)
SEC61	protein transport protein Sec61
SERPINA1	alpha-1-antitrypsin
SERPINA5	protein C inhibitor
SERPINC1	antithrombin III
SERPIND1	heparin cofactor II
SERPING1	C1 inhibitor
SFM	serum free media
SILAC	Stable Isotope Labelling by Amino acids in Cell culture
shRNA	short hairpin RNA
siRNA	small interfering RNA
sNS1	secreted nonstructural protein 1
SPPL3	Signal Peptide Peptidase-Like 3
STAT1	signal transducer and activator of transcription 1

STAT3	signal transducer and activator of transcription 3
STRING	Search Tool for the Retrieval of Interacting Genes/Proteins
TCA	trichloroacetic acid
TCEP	Tris (2-Carboxyethyl) phosphine Hydrochloride
TCID50	50% tissue culture infective dose
TEAB	triethyl ammonium bicarbonate
TEMED	tetramethylethylenediamine
TG	triglycerides
TGN	trans-Golgi network
TMT	Tandam Mass Tag
TRX	thioredoxin
U	unit(s)
UBE1	ubiquitin-activating enzyme E1
UP	Uniport
UPR	unfolded protein response
UPS	ubiquitin proteasome system
UTR	untranslated region
V	volts
VDAC1	voltage-dependent anion channel 1
v/v	volume/volume
VLDL	very low density lipoproteins
WHO	World Health Organization
WNV	west Nile virus
WS	warning signs
XRCC5	X-ray repair cross-complementing protein 5
w/v	weught/volume
YFV	yellow fever virus
ZIKV	Zika virus
2D-DIGE	two-dimensional Differential in-Gel Electrophoresis
2D-PAGE	two-dimensional polyacrylamide gel electrophoresis
°C	degrees Celsius
α	alpha
β	beta
γ	gamma
δ	delta
ε	epsilon
μ	micro

CHAPTER 1. GENERAL INTRODUCTION

1.1 Dengue: Global impact and challenges

1.1.1 Global burden

Dengue (DEN), a mosquito-borne disease caused by infection with dengue virus (DENV) serotypes 1-4, has been a major global public health problem for decades. Despite much effort to prevent infection and improve treatment, morbidity and mortality due to DEN is high and constantly increasing. The true burden of DEN is unknown. The most cited report estimates an incidence of 390 million DENV infected cases with 96 million symptomatic cases annually, worldwide (WHO, 2019; Bhatt *et al.*, 2013). Among the symptomatic cases, ~22,000 deaths are reported annually, a mortality rate of ~2.5% (WHO, 2019; Lam, 2013). However, this number was estimated in 2013 based on the official report cases which was believed to be only 8% of symptomatic cases (Stanaway *et al*., 2016).

1.1.2 Clinical spectrum of DEN disease

DEN has a wide range of clinical presentations and complications as well as an unpredictable clinical course. The classic clinical course starts with high grade fever and non-specific symptoms lasting for 2-7 days during the "febrile phase", followed by a "defervescence" or "critical phase" which usually lasts 24-48 h and a "recovery phase" (WHO, 2012) (Figure 1.1). In the febrile phase, patients have fever with two or more of the following symptoms and signs: headache, retroorbital pain, myalgia, arthralgia, rash, haemorhagic manifestations and/or leucopenia (WHO, 1997). However, some patients can present with fever with non-specific symptoms and signs. Dehydration (from fever and vomiting) and spontaneous bleeding can be found as complications in this phase. Following the febrile phase, fever abruptly subsides and most individuals recover, however some individuals enter a critical phase when plasma leakage and more severe complications may occur. In mild cases, fever disappears spontaneously without signs of plasma leakage and patients recover from illness with improvement of laboratory parameters. For other individuals, leakage of the intravascular volume to interstitial spaces results in a decreased blood volume, increased concentration of red cells (increased haematocrit; (Hct)), ascites

and pleural effusion. Together with leakage, platelets and white blood cell count markedly decrease in this period. The severity of disease and the nature of complications during this phase varies. In the most severe case, patients suffer from shock, severe bleeding and multiple organ failures. The organ failures in this phase occur from both the direct pathology of DENV infection (Povoa *et al.*, 2014) and as a result of shock and disseminated intravascular coagulopathy (DIC). In severe cases, the multi-organ failures which are a consequence of prolonged shock in the critical phase continues and congestive heart failure from fluid overload occurs. The vicious cycle of uncontrolled shock, multi-organ failure, DIC and bleeding finally leads to death. However, most individuals enter a recovery or convalescent phase, during which fluid reabsorbs back to the circulation and the laboratory parameters gradually improve. Patients return to a normal appetite and might develop a convalescent rash, which is a hallmark sign of this phase.

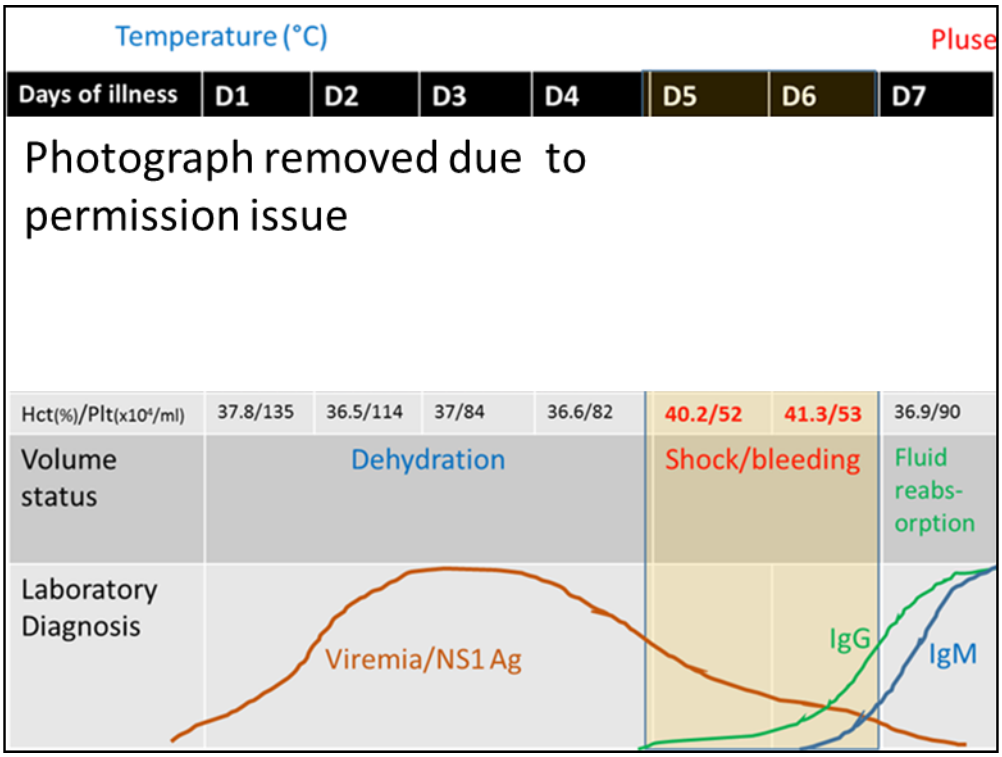

Figure 1.1 The course of DEN illness.

The classic clinical parameters and laboratory results of DEN disease progression can be divided in to three phases (febrile, critical and recovery phases). The body temperature (°C) and pulse rate (/min) are plotted in blue and red, respectively. In the febrile phase, the patient suffers from dehydration. The haematocrit (Hct) gradually increases and reaches a peak in the day that fever subsides when plasma leakage may occur. In contrast, platelets (Plt) decrease to the lowest level in the critical phase. Spontaneous bleeding may occur in the critical phase. After the critical phase which lasts 24-48 h, fluid reabsorbs into the circulation, the Hct decreases, Plt increases and the patient recovers. For diagnosis, DENV viremia and antigenemia can be detected in the febrile phase whilst the antibody response (IgG and IgM) gradually increases during the recovery phase.

Moreover, the spectrum of disease ranges from asymptomatic infection, undifferentiated febrile illness, dengue fever (DF), dengue haemorrhagic fever (DHF) and dengue shock syndrome (DSS) as classified by the World Health Organisation (WHO) in 1975 and 1997 (WHO, 1997) (Figure 1.2A). In 2009, the WHO announced a new classification scheme for DEN infection which divided clinical symptoms into DEN without warning signs (DEN w/o WS), DEN with warning signs (DEN w WS) and severe DEN (SD) (WHO, 2009) (Figure 1.2B). This classification scheme is very useful for patient triage in the resource limited countries. However, it might not reflect the true severity of leakage, which is the hallmark of pathogenesis and therefore may not be the best classification system for studies on the pathogenesis of disease. Furthermore, there have been increasing reports of unusual manifestations of DEN which were not previously included in the classification schemes. Thus, the WHO (regional office of South-East Asia) launched a new classification scheme in 2011 (WHO 2011) (Figure 1.2C). In brief, this definition used DF and DHF as in the 1997 scheme, but added a broader range of clinical signs including undifferentiated fever and expanded DEN, syndrome/isolated organopathy.

Therefore, the major challenges of managing DEN clinically, are how to distinguish DEN from other febrile diseases which have the specific treatments and how to diagnose and manage SD cases.

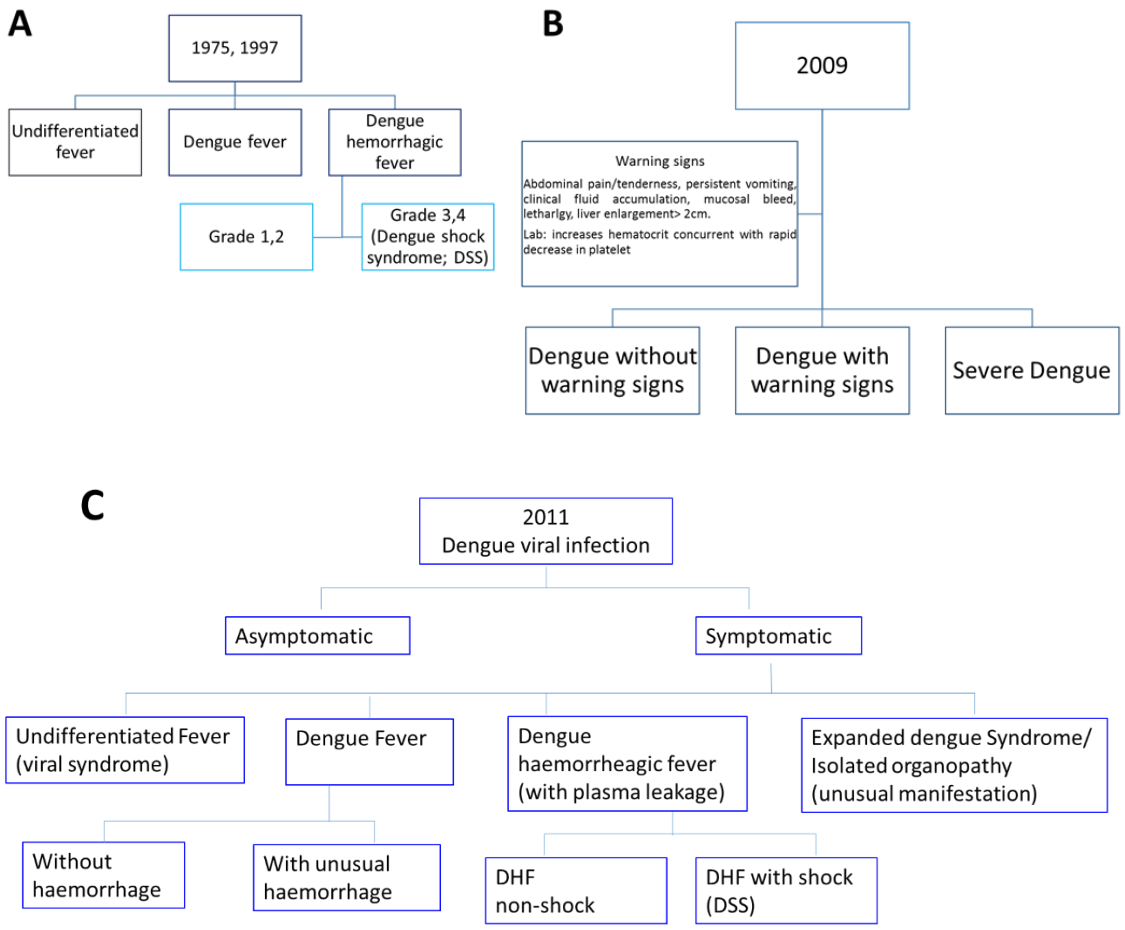

Figure 1.2 DEN case classifications.

WHO DEN case classifications are summarised. **(A)** WHO 1975 and 1997 **(B)** WHO 2009 and **(C)** WHO 2011.

1.1.3 Gaps in clinical practice

Due to the wide spectrum and complications of DEN, as well as limited therapeutic and preventative methods, there are many gaps in clinical practice that urgently require scientific investigation. According to a study modelling the natural history of DEN, only 5% of those exposed to DEN has infection and one-fourth of them have symptoms (Shepard *et al*., 2004). An increased understanding of disease pathogenesis, especially in regards to the host factors contributing to disease, has the potential to improve methods to predict symptomatic cases and effectively prevent disease.

For patients with febrile illnesses, distinguishing patients with viral syndrome (acute undifferentiated febrile illness; AUFI) and DF is difficult but necessary. In tropical areas, a number of other common febrile illnesses mimic DEN symptoms, including bacterial infections such as salmonellosis, leptospirosis, and rickettsiosis, which require specific antibiotic treatments (Luvira *et al*., 2019). Currently available diagnostic tests for DEN such as antigen and viral detection are only of use in the early phase of fever (before five days after onset) while there is no effective diagnostic test for patients who present in the critical phase of disease. Serology tests can be detected during/after the critical period but have a low sensitivity and need follow up convalescent specimens for confirmation. For patients with severe DEN that present clinically with shock and bleeding, it is difficult to distinguish DEN from severe forms of specific bacterial infections by clinical parameters, although the treatment of the two conditions are totally different. Thus, biomarkers for the diagnosis of DEN, especially in late phase of disease are still required.

The most important problem in the management of DEN is that there are no tools available that physicians can use to predict those patients at risk of progressing to severe disease. The 2009 WHO classification of DEN w WS (Figure 1.2B), primarily aimed to identify potentially severe cases for management. However, the definition and criteria are not well defined and mostly subjective (Srikiatkhachorn *et al*, 2011). Moreover, Kalayanarooj (Kalayanarooj, 2011) reported that the application of guidelines of "warning signs" in children led to a two-fold increase in healthcare provider demand. In order to identify patients that may progress to severe disease early and to ensure close observation

and care of patients whilst not overburdening the healthcare system, the identification of reliable biomarkers for predicting the severity of disease are urgently needed.

Finally, there is no available specific treatment for DEN. Aside from developing antivirals, understanding the host response/s to DENV infection has the potential to improve therapeutic invention measures, as the major pathology of severe DEN results from an overexuberant host immune response.

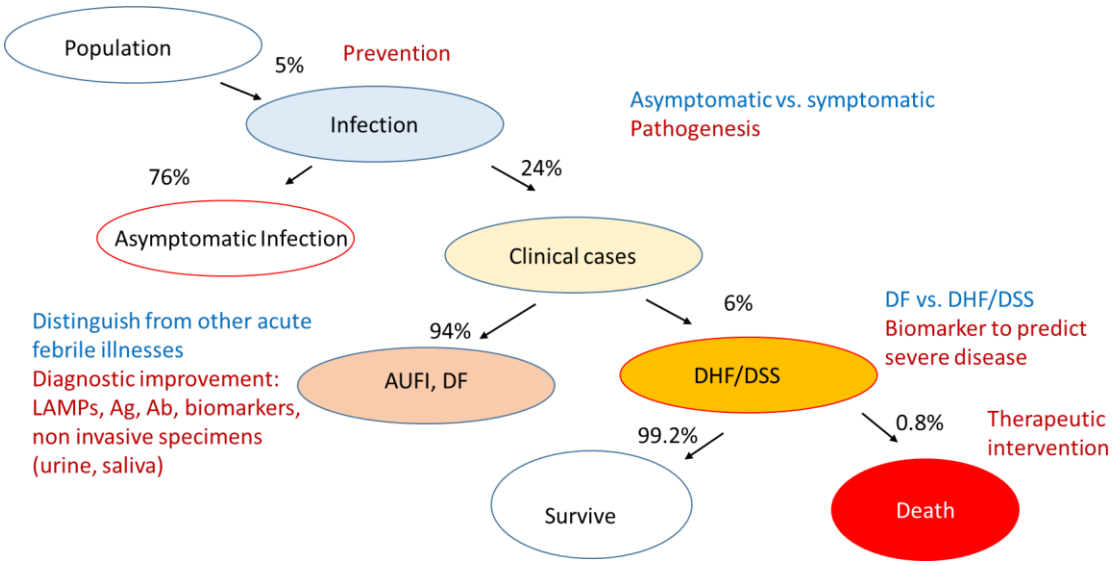

Figure 1.3 Spectrum of disease and gaps in clinical practice.

The estimation of disease progression without vaccination (Modified from Shepard *et al.*, 2004) based on a modelling study using data from South-East Asia. The clinical challenges and proposed study solutions are described.

1.2 Dengue virus (DENV)

DENV is an enveloped virus belonging to the *Flaviviridae* family, genus *Flavivirus*. Using serological methods, DENV has been antigenically classified into four serotypes: serotypes 1-4. The *Flaviviridae* family can be classified into clusters based on vector: non-vector (eg. hepatitis C virus; HCV), mosquito-borne, tick borne (eg. tick-borne encephalitis virus; TBEV) and viruses with no known vectors (Kuno *et al*, 1998; Daep *et al.*, 2014). Flaviviruses of importance to human health in the mosquito-borne cluster include; yellow fever virus (YFV), Japanese encephalitis virus (JEV), West Nile virus (WNV), Zika virus (ZIKV) and DENV. Antigenic relatedness amongst flaviviruses results in serological cross-reactivity when testing for viral infections which circulate in the same geographic areas especially for DENV, ZIKV and JEV (Muller *et al*., 2017; Ngono and Shresta, 2018). Humans are generally a dead-end host for most flaviviruses, which circulate between arthropod vectors and mammalian or avian hosts. Sylvatic forms of DENV exist and are maintained in transmission cycles between non-human primate hosts and forest mosquitoes. However DEN outbreaks in humans arise from DENV strains maintained in human to mosquito transmission cycles which involve no intermediate hosts (Daep *et al.*, 2014). *Aedes* mosquitoes, including *A. aegypti* and *A. albopictus* are the major DENV vectors.

1.2.1 DENV particle and genome organisation

The DENV particle (~ 50 nm in diameter) consists of an envelope and nucleocapsid which contains the RNA genome surrounded by the capsid (C) protein (Bartenschlager and Miller, 2008). The envelope consists of a host derived bilayer lipid membrane and an outer glycoprotein shell which is formed by 180 copies of the envelope (E) protein and precursor of membrane/membrane (prM/M) protein (Perera and Kuhn, 2009).

Similarly to other flaviviruses, DENV has a single–stranded positive sense RNA genome ~11 kilobases in size, which contains a single long open reading frame (ORF) flanked by 5′ and 3′ untranslated regions (UTR) (Figure 1.3). The ORF encodes a large polyprotein (~3400 amino acids) that is proteolytically processed into ten proteins and two peptides (ER and 2K) (Meng *et al*., 2015). There are three structural proteins including C,

prM and E and seven non-structural proteins (NS) including NS1, NS2A, NS2B, NS3, NS4A, NS4B and NS5. These proteins are multifunctional and play important roles in viral replication and the modulation of host cell processes. The known character and functions of each protein are listed in Table 1.1.

1.2.2 DENV structural proteins

Capsid protein

The DENV C protein is a 12 kDa homodimer which interacts with the RNA genome to form the nucleocapsid. It plays a role in DENV assembly and releases the genome after cell entry. It localizes in both nucleus and cytoplasm of DENV infected cells. In the nucleus, the C protein accumulates in nucleoli, whilst it is distributed between endoplasmic reticulum (ER) membranes and lipid droplets in the cytoplasm (Byk and Gamarnik *et al*, 2016). The C protein has been found to interact with lipid droplets in both mosquito and human cell models as well as with very low density lipoproteins (VLDL) isolated from human blood (Faustino *et al.*, 2014).

prM/M protein

The prM/M protein stabilizes the E protein structure and prevents the E protein from prematurely fusing with host cell membranes. The prM protein is initially localised to the ER and interacts with the E protein to form a heterodimer in the immature virion. During release of the immature virus particle, prM is cleaved to pr and M by a cellular furin-like protease. The M protein is found on the mature virion (Cruz-Oliveira *et al*, 2014). The M protein has also been localised to the cell surface and can be found secreted as dimer and tetramer (Wong *et al*., 2012). Antibodies to prM (anti-PrM) have been proposed to precipitate antibody dependent enhancement (ADE) and therefore play a role in pathogenesis.

E protein

The E protein, a 53 kDa protein, consists of three domains (Cruz-Oliveira *et al*., 2014). In the immature virion, the E protein is found as a prM-E heterodimer on the surface. After cleavage of the prM protein, the E protein rearranges to form a dimer in the mature virus particle. The first domain, DI is a central structural domain. The second domain, DII

is the dimerization domain, and plays a role in the fusion of the viral particle with cellular membranes during the viral entry process. The third domain, DIII has an immunoglobulin-like structure and is more exposed on the surface of virus.

The E protein is important in viral attachment and membrane fusion during viral entry. DIII is the attachment site or receptor binding site, while DII mediates rearrangement of E into a trimer which forms a fusion pore between virus and host cell membranes (Modis *et al.,* 2004). Moreover, glycosylation of the E protein on Asn-67 or -153 plays a role in viral –host cell attachment. As the E protein mediates attachment of the virus particle to the host cell, it is a major target for drug development and neutralizing antibody studies (Heinz and Stiasny, 2012).

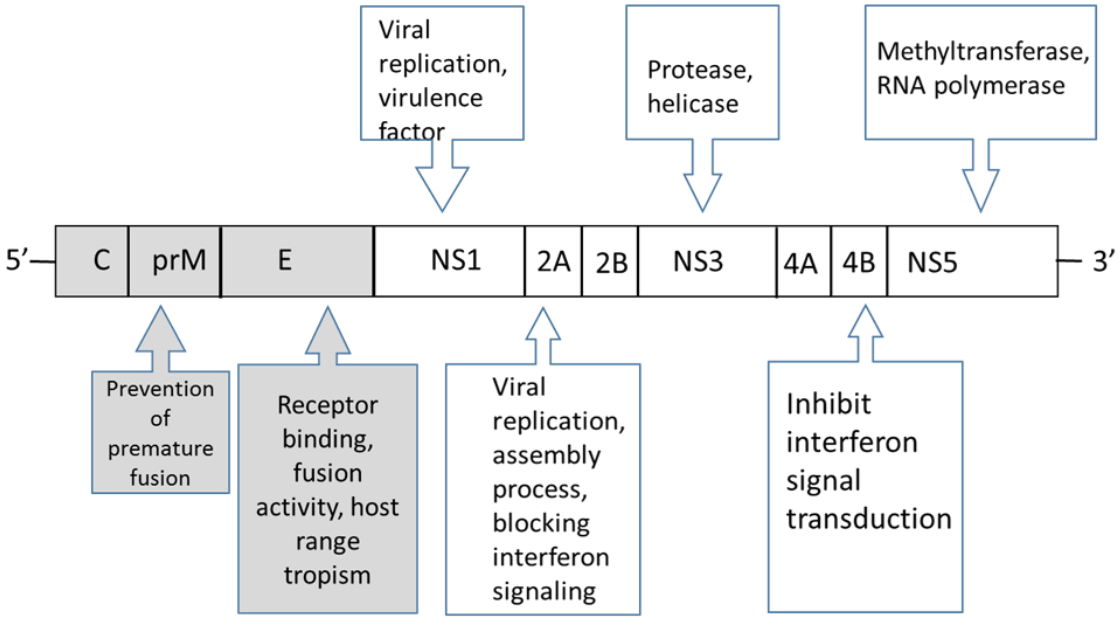

Figure 1.4 Structure of the flavivirus genome and brief functions of the structural and non-structural proteins.

Figure modified from Rodenhuis-Zybert *et al*. 2010

Table 1.1 Summary of DENV proteins

Structure	Localization	Functions
C protein	Nucleoli and cytoplasm, virus particle	Packaging and protection of the viral genome
E protein	Lumen of ER, virus particle	Viral attachment and membrane fusion in viral entry, major antigen
PrM/M protein	Pr- lumen of ER M-transmembrane protein, virus particle	Prevention of premature fusion
NS1	Intracellular NS1- lumen of ER, cell surface, secreted NS1- sera	Intracellular NS1: co-factor for viral replication Secreted NS1: virulence factor
NS2A	Transmembrane protein	Part of the replication complex , assembly process, an antagonist of type I interferon (IFN) signalling
NS2B	Transmembrane protein	Cofactor for the protease domain of NS3
NS3	Cytoplasm	Enzyme for viral replication: protease, helicase and NTPase
NS4A	Transmembrane protein	Part of the replication complex, modulates intracellular membranes
NS4B	Transmembrane protein	Part of replication complex, an antagonist of host IFN signalling
NS5	Cytoplasm	Enzyme for viral replication: methyltransferase and RNA polymerase, an antagonist of host IFN signalling

1.2.3 DENV non-structural proteins

NS1 protein

The NS1 protein plays important roles in viral replication and as a virulence factor. It is a 45 kDa glycoprotein, found in multiple oligomeric forms and can be detected in multiple locations in the infected cell (Muller and Yong, 2013). The NS1 protein is divided into three domains: a "β roll" domain, a "wing" domain and a "β-ladder domain". Intracellular NS1 forms a dimer which is found in the ER lumen and on the cell surface (Akey *et al*., 2015). Whilst, secreted NS1 (sNS1) is a lipid associated hexamer.

Intracellular NS1 is co-factor for viral replication while sNS1 plays a major role in immune associated pathogenesis. There are two glycosylation sites in NS1, at Asn-130 and Asn-207 and twelve conserved cysteine (Cys) residues. Interestingly, sNS1 circulates in the sera of acute DENV infected patients. Circulating sNS1 and antibodies recognising it are used in diagnostic tests. Moreover, sNS1 is a target for antiviral and vaccine development (Muller and Yong, 2013).

NS2A protein

The NS2A protein is a small hydrophobic protein (~22 kDa in size) which has multiple functions. It facilitates the viral replication and assembly processes and is involved in virus-induced membrane formation (Idrees and Ashfaq, 2012). Moreover, NS2A can inhibit interferon-β. NS2A can be found in cytoplasm of DENV infected cells.

NS2B protein

NS2B, a 14 kDa hydrophobic protein, is required as a cofactor for the protease function of the NS3 protein (described in more detail below) (Idrees and Ashfaq, 2012).

NS3 protein

The NS3 protein a ~70 kDa protein, contains two domains which have protease and helicase activity. These two viral enzyme activities are essential in many viral processes involved in viral replication and virus infectivity. NS3 is a conserved viral protein which has 77% similarity amongst the four serotypes. Thus, NS3 has been a target for antiviral development.

The serine protease domain, encompassing the N-terminal 180 amino acid residues, forms a complex with NS2B. The main function of the NS2B-NS3 serine proteinase is to cleave the viral polyproteins at multiple sites internal sites including; C-Canchor NS2A-NS2B, NS2B-NS3, NS3-NS4A, NS4A-2K, NS4B-NS5 and within NS3 itself (Luo *et al*., 2008). Whilst host furin and signalase proteases cleave the remainder of the viral polyprotein at the Canchor-prM, pr-M, prM-E, E-NS1, NS1-NS2A and 2K-NS4B junctions. Moreover, the NS2B-NS3 proteinase influences the enzymatic activity of the helicase domain (Perera and Kuhn, 2008).

The C-terminal domain (residues 181-618) of NS3, contains 3 subdomains and possesses RNA helicase/NTPase/RTPase activities. The NS3 helicase is essential for RNA binding. Moreover, the helicase domain was found to be involved in DENV viral assembly.

NS4A protein

The NS4A protein is a 16 kDa transmembrane protein that forms part of the replication complex. NS4A can induce ER hypertrophy and the unfolded protein response (UPR) (Guzman and Harris, 2014). NS4A is found in the cytoplasm of infected cells and colocalizes with double-stranded RNA.

NS4B protein

NS4B, is a 27 kDa integral hydrophobic membrane protein, which has been found to interact with many viral proteins including; NS1, NS2B, NS3 and NS4A in order to regulate viral RNA replication (Xie *et al,* 2015). In addition, NS4B is involved in antagonising the IFN response by acting to inhibit phosphorylation of signal transducer and activator of transcription 1 (STAT1), preventing downstream signalling and has also been shown to potently suppresses RNA interference (RNAi) (Xie *et al*, 2015). As such, NS4B is a major target for anti-DENV drug discovery.

NS5 protein

The NS5 protein is the largest and most highly conserved DENV protein, it is ~ 104kDa in size and contains 900 amino acid residues. It has two domains. The N-terminal domain contains N7 and 2′-*O*- methyltransferase (MTase) activities whilst the C-terminal

domain contains RNA polymerase activity (Perera and Kuhn, 2009). The MTase activities are required for capping of the viral genome whilst the RNA dependent RNA polymerase activity of NS5 plays a key role in RNA replication. The NS5 protein has been shown to localise to the nucleus in a serotype specific fashion (Hannemann *et al*., 2013). NS5 also plays an important role in inhibiting the IFN response as it binds to STAT2 and targets it for proteasomal degradation (Ashour *et al*., 2008; Mazzon *et al.*, 2009).

1.2.4 DENV life cycle

After infection, DENV enters the host cell and uses the host machinery to produce new virus particles. The processes are virus attachment and entry, viral replication, and viral maturation and release (Figure 1.5).

A number of cell surface receptors have been identified to bind the DENV particle including; heparan sulfate, mannose receptor, dendritic cell-specific intercellular adhesion molecule-3-grabbing non-integrin (DC-SIGN), heat shock protein (HSP) 90/HSP70, macrophage Fc receptor, endoplasmic reticulum chaperone BiP (HSPA5) and CD14 (Cruz-Oliveira *et al.*, 2015). After viral attachment, the virus is taken into the cell by receptor-mediated endocytosis followed by fusion of the viral membrane with that of the endosome to mediate virus release. These processes are mainly mediated by the E protein and triggered by acid pH as the endosome becomes acidified (Rodenhuis-Zybert *et al.*, 2010). After that, the DENV genome is uncoated and translated in association with perinuclear ER membranes. The viral non-structural proteins induce changes to the host ER morphology to form a virus induced membrane enclosing the viral RNA and viral proteins, termed a "replication complex" (Welsch *et al*., 2009). Viral genome replication occurs in the replication complex *via* the formation of a negative strand RNA that is complementary to the viral genome. The negative sense RNA is used in turn, as a template for the production of new positive strand genomes that are either used for further rounds of translation and replication or are extruded from the replication complex to associate with the C protein to form a nucleocapsid. The nucleocapsid buds into the ER lumen, acquiring a lipid envelope containing the prM and E proteins. At the end of this process the immature virion is released from ER. The immature virion consists of a nucleocapsid covered with prM/E heterodimers outside of the envelope (Perera and Kuhn, 2008). The immature virion

then transits through the trans-Golgi network (TGN) where glycoprotein processing occurs. The slight acidity of the TGN triggers prM cleavage by a cellular furin-like protease to generate the mature particle (Rodenhuis-Zybert *et al*., 2010). When the mature virus particles are secreted, the pr peptide is released from the virions. However, for some virus particles processing is incomplete, resulting in a mixture of immature and the partially immature virions secreted from infected cells (Guzman *et al.*, 2015) (Figure 1.5). The viral NS1 protein is initially translocated into the ER lumen where it is glycosylated and plays a crucial role in genome replication. However, it is also secreted from cells in a hexameric form.

DENV modulates multiple host proteins and processes throughout its life cycle. The main cellular processes modified by DENV infection/replication are the unfolded protein response (UPR), ubiquitin proteasome system (UPS), lipid metabolism/autophagy and the IFN response (Fischl and Bartenschlager, 2011).

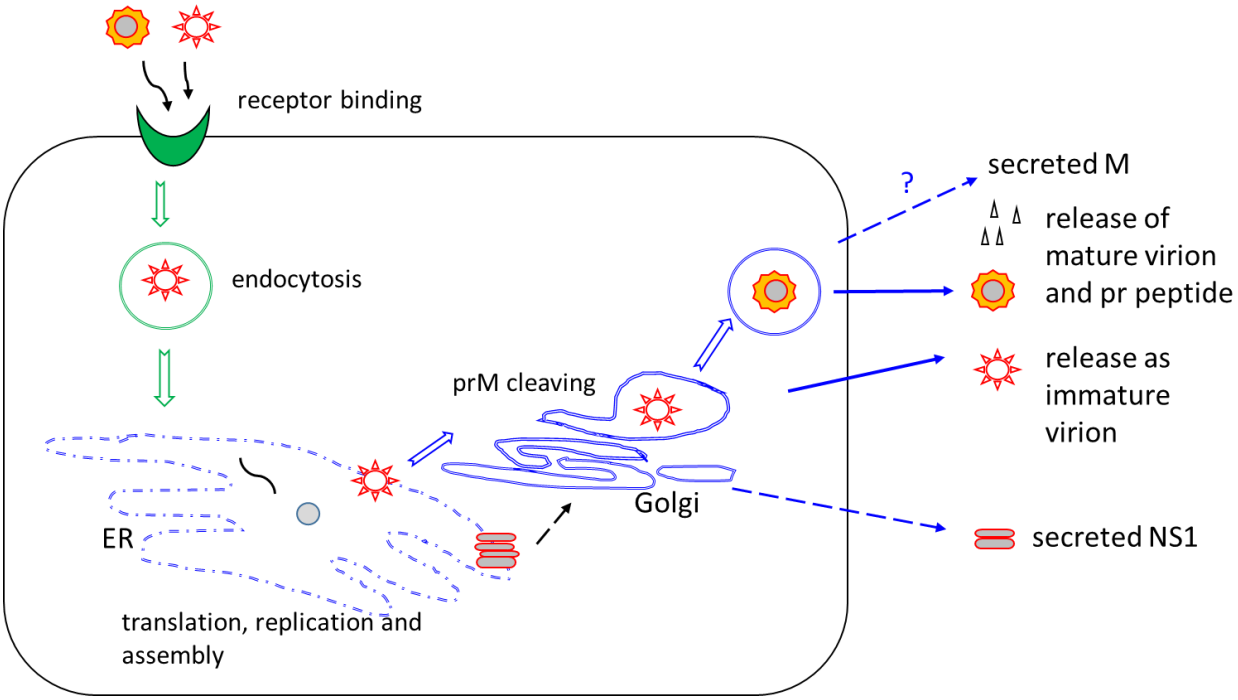

Figure 1.5 DENV life cycle.

Adapted from Rodenhuis-Zybert *et al.*, 2010 and Guzman and Harris E, 2015.

Modulation and remodeling of ER structures during DENV replication and virion secretion results in ER stress (Blazquez *et al.*, 2014). Activation of the UPR as a response to ER stress has been documented for many flaviviruses including DENV (Blazquez *et al.*, 2014). The interaction between misfolded proteins and HSPA5, stimulates the UPR response *via* three main ways: phosphorylation of protein kinase RNA-like endoplasmic reticulum kinase (PERK), cleavage of activating transcription factor 6 (ATF6) and phosphorylation of inositol-requiring enzyme 1 (IRE1). Moreover, there is crosstalk between the UPR and autophagy by PERK and IRE1 signaling pathways. Lee and co-workers demonstrated an activation in PERK and IRE1 signaling pathways during early DENV infection whilst the ATF6 pathway was not found to be activated by DENV infection (Lee *et al.,* 2018). In addition to reducing cellular stress in the infected host cells, the UPR is also required for DENV replication. Inhibition of PERK and IRE1 signaling pathways by shRNA transfection resulted in a decrease in the level of NS1 and autophagy markers as well as a reduction in viral titre (Lee *et al.,* 2018).

DENV replication involves lipid metabolism in many ways: host lipid droplets (LD) are used as an energy supply, the virus attaches and enters *via* lipid rafts and LDL receptors and hijacks the ER, the organelle used for cholesterol and fatty acid synthesis, to form the RC. In addition, the sNS1 hexamer has lipoprotein content (Fischl and Bartenschlager, 2011; Osuna-Ramos *et al*., 2018). Autophagosome formation was proposed to enhance DENV replication and prevent apoptosis of host cells (Orozco-García and Gallego-Gómez, 2016). Moreover, autophagic processes produce energy for viral replication by autophagy-dependent processing of LD, free fatty acids and triglycerides (Heaton and Randall, 2010).

The UPS which involves regulated protein degradation is also stimulated during DENV replication. The UPS is required for the uncoating of a number of RNA viruses, including DENV, so it is a vital host process for viral replication (Byk *et al.*, 2016). Blocking ubiquitin-activating enzyme E1 (UBE1) by a specific inhibitor was shown to block the step of viral uncoating (Byk *et al*., 2016) and caused a decrease in DENV protein synthesis and infectivity (Kanlaya *et al.*, 2010). DENV infection also results in the degradation of STAT-2 by the UPS which antagonises the IFN response, therefore the UPS

is required for viral escape from the host innate antiviral response (Fischl and Bartenschlager, 2011).

1.2.5 Replicon

Replicons are subgenomic viral RNAs that lack the genes encoding one or more of the viral structural proteins, whilst retaining key nonstructural genes required for RNA replication. Replicons are therefore capable of replication in permissive cells without the production of infectious virus particles. The introduction of genes into flavivirus replicons, encoding selectable markers in place of the structural genes, typically C-prM-E or prM-E, allows cells containing replicons (once introduced by transfection) to be selected and grown continually in the presence of the selection agent (Figure 1. 6). A number of studies have reported the production of DENV replicons and cell lines stably containing the replicons. Such cell lines have been demonstrated to be useful models for investigating viral replication and its effect on the host cell as well as for screening antiviral agents (Ward and Davidson, 2008). To date, proteomic studies have not been done using DENV replicon containing cells.

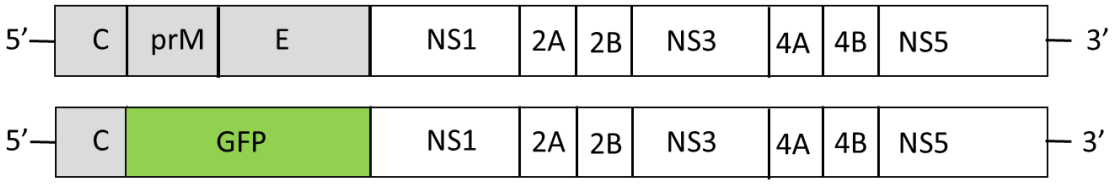

Figure 1.6 Structure of DENV replicon genome.

1.3 Dengue pathogenesis

The pathogenesis of DEN is not completely understood and it is believed to be multifactorial (Martina *et al*., 2009). The hallmarks of severe DEN disease are an increase in vascular permeability, thrombocytopenia and coagulopathy which are believed to be immune mediated. Many factors are believed to play a role in pathogenesis including; host factors (genetics, age, underlying diseases and nutritional status), viral virulence factors (strains) and immune status (primary or secondary infection).

1.3.1 The virus - host interaction

Initial infection to systemic infection

After the bite of a DENV infected mosquito, the first infected cells are skin dendritic cells, macrophages and mast cells. After that, a local inflammatory process, *via* natural killer cells (NK cells) and T-cells, clears the infection from the skin. A systemic infection starts after infected DENV cells are drained to the lymphatic system. A viremic stage occurs 24-48 h before the onset of symptoms (St John *et al*., 2013) and lasts for 4-5 days after onset (range 2-12 days) (Gubler *et al.*, 1981).

Target cells

The major target cells of DENV are monocytes, endothelial cells, liver cells, splenic macrophages, tissue macrophages and stromal cells of the bone marrow (Martina *et al*., 2009). Moreover, DENV has been isolated from other organs such as the skin, lymph nodes, lungs, kidneys, thymus and brain (Martina *et al.*, 2009).

1.3.2 Mechanisms of pathogenesis

1.3.2.1 1.3.2.1 Antibody-Dependent Enhancement of Dengue (ADE)

In a secondary DENV infection, a non-neutralising cross-reactive antibody response from a previous infection has been proposed to enhance infection. After primary DENV infection, patients are believed to have long term protection to that serotype due to the production of serotype-specific neutralising antibodies. However, the cross reactive antibodies are believed to be a key factor in the development of severe disease during a subsequent infection with a different serotype, this phenomenon was first described by

Halstead *et al*. as antibody-dependent enhancement of DEN or ADE (Halstead, 1979; Halstead *et al.*,1980; Alan L Rothman, 2011). ADE occurs when a cross reactive antibody-virus complex binds to a Fc receptor on a suitable target cell (monocytes, macrophages and others) leading to enhanced uptake of the virus and infection. This in turn leads to an increase in the secretion of vasoactive cytokines and vascular mediators from these cells or cells that recognise them (T-cells) during infection.

The antibodies which play major roles in ADE are anti-E and anti-prM antibodies. Although antibodies to highly conserved regions of the E protein have high serotype specificity and neutralising ability, antibodies to other parts of the E protein are cross reactive and induce ADE (Guzman and Harris, 2015; Rothman, 2011). During the process of viral assembly, some immature virions are released from cells. Antibodies to the prM protein can enhance the entry of immature virions in secondary DENV infection (Rothman, 2011).

1.3.2.2 1.3.2.2 Cell mediated immunity

B cells clearly play a major role in DEN pathogenesis *via* antibody production; however, the role of T cells in preventing and contributing to disease is still unclear (Malavige and Ogg, 2013). $CD8^+$ T cells are believed to play a more important role in DENV protection than $CD4^+$ T cells (Ngono and Shresta, 2018). $CD8^+$ T cell responses are directed against epitopes in the NS3, NS4B, and NS5 proteins while $CD4^+$ T cells target epitopes in the C and E proteins as well as sNS1 protein (Rivino, 2018). It has been proposed that cross reactive memory T cells from a prior DENV infection have an effect on the severity of DENV infection via the secretion of pro-inflammatory and immunosuppressive cytokines including IFN-ɤ, TNF-α and IL-13 (Malavige and Ogg, 2013; Martina *et al.,* 2009). The ineffective T cell response during a secondary infection due to stimulation of a response to prior DEN infection has been described as “original antigenic sin” (Mongolsapaya *et al*., 2003). However, there is evidence that activated DENV-specific $CD8^+$ T cells can produce antiviral effectors in acute DEN (Rivino *et al.*, 2015). Thus, to date, the consequence of “original antigenic sin” is unclear whether it is enhanced protective immunity or immunopathology for secondary DENV infection

(Rivino, 2016). Furthermore, HLA alleles were reported to have effect on the extent of both the $CD4^+$ and $CD8^+$ T cell responses (Weiskopf and Sette, 2014).

1.3.2.3 1.3.2.3 Autoimmune response

Thrombocytopenia caused by cross reactivity of antibodies to the NS1 protein with human platelets and plasma leakage caused by cross reactivity of those autoantibodies with endothelial cells (Lin *et al.,* 2016) has been reported and may also play a role in pathogenesis. Supporting evidence is the similarity of the protein structure of the DENV E and NS1 proteins and human coagulatory molecules (Lin *et al,* 2011). Furthermore, Lin *et al.* showed that the levels of antibodies to NS1 in DHF/DSS cases were significantly higher than those in DF cases and could induce endothelial apoptosis (Lin *et al.*, 2004).

1.3.2.4 1.3.2.4 NS1

The NS1 protein has been proposed as a key virulence factor in DEN pathogenesis. There is a high level of secreted NS1 in early DENV infection which has been correlated with disease severity (Libraty *et al*., 2002; Aviruntnan *et al.,* 2006). Furthermore, a higher titre of anti-NS1 antibody was found in severe acute secondary DEN infection compared with non-severe cases (Jayathilaka *et al.,* 2018). In addition to its role in viral replication, NS1 has been well characterised to activate the complement cascade followed by the induction of proinflammatory cytokines. Furthermore, Aviruntnan *et al.* (Aviruntnan *et al.,* 2006) demonstrated NS1 purified from the supernatants of DENV infected cells could also activate complement. Furthermore, binding of NS1 with prothrombin resulted in the inhibition of prothrombin activation and a prolonged activated partial thromboplastin time (APTT) (Lin *et al.,* 2012). More recently, NS1 from all DENV serotypes has been shown to directly increase human pulmonary microvascular endothelial cell permeability *in vitro* (Beatty *et al.,* 2015; Modhiran *et al.,* 2015).

One theory alone cannot explain all aspects of DEN pathogenesis and most studies have been based on *in vitro* studies or the use of mouse models which do not fully recapitulate human disease. More research is required to understand DEN pathogenesis.

1.4 Treatment and Prevention of DEN

1.4.1 Treatment

Treatment of DEN basically relies only on good supportive care; close monitoring and fluid resuscitation as well as treatment of complications such as bleeding and shock. Proper volume evaluation and resuscitation is the key treatment for case of shock; inadequate volume replacement in the leakage stage results in prolonged shock and leads to organs damage while over-replacement of fluid can lead to fluid overload in the recovery phase. Many compounds have been shown to have promising antiviral properties *in vitro* but were not effective at suppressing DENV replication in clinical trials (Low *et al*, 2017). To suppress the immune response associated with DEN, many anti-inflammatory drugs such as corticosteroid and statins (3-hydroxy-3-methyl-glutaryl coenzyme A (HMG-CoA) reductase inhibitors) have been tested in clinical trials, but all failed to improve the outcome of disease (reviewed in Chan and Ooi, 2015)

There are many ongoing *in vitro* studies aiming to identify drugs that target DENV entry/fusion and/or the E glycoprotein, which play a key role in viral attachment (Guardia and Lleonart, 2014). Examples of these agents include DN59 (a fusion inhibitor, E protein stem and E trimer binder) and tetracycline derivatives such as doxycycline and rolitetracycline (fusion inhibitors and E protein hydrophobic pocket binder). Celgosivir, an alkaloid castanospermine, inhibits ER-associated α glucosidase causing E, prM and NS1 protein misfolding during maturation and glycosylation of these proteins. Despite a successful inhibitory profile *in vivo* using a mouse model, a Phase Ib clinical trial of celgosivir in DEN patients showed no difference in virological reduction and clinical parameters between treatment and placebo groups (Low *et al.,* 2014)

Other direct-acting antiviral agents have been developed that target NS3 (both helicase and protease inhibitors), NS4B and NS5. Among these, only Balapiravir which is an NS5 polymerase inhibitor was trialled clinically. Although Balapiravir was able to inhibit replication of all serotypes of DENV *in vitro*, it failed to decrease viremia and NS1 Ag in a randomized control trial of DEN infected patients (Nguyen *et al.,* 2013).

1.4.2 Prevention

DEN surveillance and vector control have been applied as a public policy in all endemic areas; however, the increase in prevalence of DEN reflects the failure to control the spread of DENV and requires urgent development of other preventive methods. DEN vaccines have been in development for decades and the first licenced DEN vaccine was launched in 2015.

CYD-TDV (Dengvaxia®) is a recombinant live-attenuated vaccine containing the yellow fever 17D vaccine virus backbone chimerized with the prM and E proteins from DENV 1-4. Three doses of a live attenuated tetravalent vaccine at 0, 6 and 12 months showed an efficacy of 56.5% and 60.8% in phase III trials in Asian and Latin American children, respectively (Capeding e*t al.*,2014; Villar *et al.*, 2015). However, the efficacy is serotype-specific; 50.3% for serotype 1, 42.3% for serotype 2, 74.0% for serotype 3, and 77.7% for serotype 4 (Villar *et al.*, 2015). Unfortunately, post-marketing reanalysis of data associated with the trials revealed a higher risk of more severe DEN and hospitalizations among the subgroup of vaccinated children with no prior DEN infection (Sridhar *et al,* 2018). It has been hypothesised that CYD-TDV acts similarly to a primary infection for DEN naïve children, so they become prone to the development of more severe disease in natural infection from ADE.

A number of other vaccine candidates are in phase III clinical trials including; TV003/TV005 and DENVax. The TV003/TV005 vaccine candidate is a live attenuated tetravalent vaccine developed by deletion of 30 nucleotides from 3´ UTR of DENV-1, DENV-3 DENV-4, and a chimeric DENV-2/DENV-4 (rDEN1Δ30, rDEN3Δ30/31, rDEN4Δ30 and rDEN2/4Δ30) (Whitehead, 2016). In DENVax, the prM and E genes of an attenuated DENV-2 strain PDK-53, has been replaced with the prM and E genes of other serotypes (DENV-2/-1, -2/-3, and -2/-4 chimeras). Other vaccine approaches in early clinical phase development include an inactivated vaccine (purified formalin-inactivated virus; PIV), DNA vaccines (monovalent DENV-1 and tetravalent prM/E), a subunit vaccine (V180) and prime/boost strategies (Prompetchara *et al.*, 2019).

1.5 High throughput proteomic techniques to identify changes in host protein amounts

1.5.1 Discovery proteomics

Mass spectrometry (MS) based proteomics can be classified into "Discovery" or "Shot gun" based strategies and "Targeted" strategies. The goal of discovery-based proteomics is the identification and possible quantitation of as many proteins as possible whilst targeted proteomics aims to identify and monitor a selected number of target proteins (Doerr, 2013). Thus, discovery proteomics is a popular method for identifying candidate biomarkers before developing targeted proteomic methods for clinical diagnosis. A challenge of discovery proteomics is the validation of candidate biomarkers and to translate the results so they can be used clinically (Harlan and Zhang, 2014).

Discovery proteomics can be divided into "bottom-up" and "top-down" approaches. In bottom-up proteomics, proteins are digested into peptides using specific proteases before identification and quantitation by MS, simplifying analysis. On the other hand, top-down proteomics involves direct analysis of intact proteins, which provides more data on protein isoforms and post-translational modifications (PTM) (Hung and Tholey, 2012)

1.5.2 Quantitative proteomics

Many proteomic techniques can be used to quantify proteins by MS. The traditional approach has been to use 2D SDS-PAGE to identify differentially expressed proteins, before excision of protein spots of interest, followed by protein identification by MS. Although this method can provide information on PTMs, it is limited in its reproducibility and the low dynamic range of detection (Rhea *et al.*, 2010).

For high-throughput analysis, peptides/proteins can be relatively quantified by stable isotope labelling. There are many stable isotope labelling techniques with different advantages and limitations. The Stable Isotope Labelling by Amino acids in Cell culture (SILAC) is the method of choice for *in vivo* labelling of cells in continuous cell culture; however, SILAC cannot be used to analyse clinical specimens such as sera and body fluids. Other stable isotope labelling methods including Isotope-Coded Affinity Tags (ICAT) and

Isotope Tags for Relative and Absolute Quantitation (iTRAQ) are commonly used *in vitro*. The use of ICAT can reduce the complexity of the sample and variation, but there is a selective detection of proteins containing high cysteine amounts and there are limitations on the detection of acidic proteins. The use of iTRAQ has the advantages that four - eight specimens are analysed in the same run and internal controls can be included, but the need for enzymatic digestion and fractionation before MS analysis makes the sample preparation more complex (Rhea *et al*., 2010).

The advance stable isotope labelling, tandem mass tags (TMT) was first invented by Thompson and team (Thompson *et al*., 2003). The use of isobaric tags means that identical TMT labelled peptides from different samples have an equal mass and coelute better in chromatography fractionation steps compared to previous techniques which use heavy/light isotope labelling. TMT labelling also results in the detection of peptides with a high sensitivity and reproducibility compared to other stable isotope labelling techniques. TMT can be used for both *in vitro* analysis and to analyse clinical specimens. Moreover, up to 11 samples can be analysed in one run and internal standards included to normalise between runs.

1.6 Role of the "Proteome" and "Secretome" in biomarker identification

1.6.1 Proteomic analysis of DENV infected cells

A number of studies have reported the proteomic analysis of DENV infected cells in order to identify host cell proteins that are modulated in response to infection. Such studies have the potential to increase our understanding of pathogenesis and also to identify biomarkers and targets against which therapeutic agents can be developed. Previous proteomic studies have been performed using various cell lines and different proteomic techniques and are summarised in Table 1.2.

Many interesting host proteins and important biological processes were identified to be dysregulated during DENV infection by pathway analysis; however, much still needs to be done to identify key proteins involved in DEN pathogenesis and to identify biomarkers to predict disease severity. In particular more studies are required to correlate

the results obtained from the proteomic analysis of *in vitro* and *in vivo* samples, in order to understand the relevance of cell based models to DENV infection *in vivo*.

Table 1.2 Summary of cellular proteome studies.

	Cell line	Condition and % infection	Proteomic technique	Total number of differentially expressed proteins identified	No. and important** differential expression proteins (DENV/mock)		Validation	Functional classification/ IPA
					Increased	Decreased		
Pattanakitsakul *et al*., 2007	HepG2, liver	DENV-2 MOI=1 24 hpi 80.06%	2D-PAGE followed by QTOF-MS	17	10: EF-tu, DEAD box protein p72, PRP4*, elongin C*, annexin5, V-type proton ATPase subunit H	7: vinculin	2D WB: EF-Tu, vinculin	**Upregulated** -transcription and translation processes
Kanlaya *et al.*, 2009	EA.hy926, endothelial	DENV-2 MOI=10 24 hpi 93.59%	2D-PAGE followed by MS and/or MS/MS	15	9: hnRNP K, hnRNPH1 and hnRNP C1/C2, proteasome β subunit, β actin	5:EF-2	2D WB: EF-2, hnRNP K Functional assay: alteration in actin cytoskeleton assemmbly	mRNA stability/processing, transcription/translation regulation, molecular chaperone, oxidative stress response/ regulation, cytoskeletal assembly, protein degradation, cellular metabolism
Kanlaya *et al.*, 2010	HUVECs, endothelial	DENV-2 MOI=10 24 hpi 70%	2D-PAGE followed by MS and/or MS/MS	38	16: UBE1, MxA, annexin A5, proteasome 26S ATPase subunit2, GSS	22: EF-2, hnRNP H, valosin-containing protein, annexin A2, EF1α, TrxR1, Prx1, proteasome β3 subunit	WB: annexin A2, UBE1, hnRNP H, EF-2 IFA: MxA Functional assay: UBEI-41	mRNA stability/processing, oxidative stress response, protein degradation, nuclear structure, cytoskeleton assembly, protein translation, cell cycle regulation, calcium-dependent membrane binding, cell differentiation, signaling,

								cellular metabolism, antiviral response
Pattanakitsakul *et al*., 2010	EA.hy926, endothelial Subcellular fractionation	DENV-2 MOI=10 24 hpi 92.31%	2D-PAGE followed by MS and MS/MS	35	21: Alix, transferrin, valosin-containing protein	13: HSP70, HSP90	WB: Alix Functional assay: Alix involved in DENV replication (late endosome stage)	**Upregulated** - endocytosis system Downregulated- molecular chaperone
Mishra *et al.*, 2012	THP1 (monocyte)	DENV-2 MOI=1 72 hpi NA	2D-PAGE followed by MALDI-TOF	-	hnRNP-H and PDIA3	-	WB: hnRNP-H, PDIA3 Functional assay: hnRNP-H and PDIA3 assist DENV replication	-
Pando-Robles *et al.*, 2014	Huh-7, liver	DENV-2 MOI=1 24 hpi 13.96%	Label-free LC-MS/MS	155	64: PYCR1, HSPA5, EIF2α, eIF4A1, EF1A1	91: hnRNPH1, AnnexinA4, HSPB1, HSP90, HSP9, HSPE1, V-type proton ATPase subunit H	NA	**Downregulated** - glycolytic pathway, citrate, and pyruvate metabolism
Chiu *et al*., 2014	A549, lung	DENV-2 MOI=5 28 hpi	Nuclear and cytoplasm fractionation before SILAC LC MS/MS	400 (≥1.5 fold)	Both nuclear and cytoplasm 3: signal recognition particle receptor subunit a,	Both nuclear and cytoplasm 19: CDK1, CDK2, CDK4, CCNB1, AURKA, AURKB	WB: CTSL1, ERC1, KPNA2, MFN1, PRAF2, UBE2S, HYOU1 IFA: PRAF2, ERC1	**Upregulated** -Nuclear: signal recognition particle/Heat shock/protein export -Cytoplasm: type I interferon-mediated signaling pathway/ER membrane **Downregulated**

					HSPA5, HYOU1			-Nuclear: cell cycle -Cytoplasm: positive regulation of cell cytokinesis, ER membrane
Martínez-Betancur *et al.*, 2016	U937, monocyte	2 strains: of DENV-2 48 hpi (infection rate-NA)	2D-PAGE followed by MALDI-TOF	DENV-2 /NG : 9	4: α-enolase, tubulin β, HSP90AA1, pyruvate kinase M2	5: hnRNPH1, α-enolase, HSP70 protein 9, fatty acid-binding protein, protein disulfide isomerase	NA	NA
				DENV-2 /16681 : 6	4: pyruvate kinase M2, pyruvate kinase, transaldolase, Phospholipase Cα	2: annexin IV, phosphotyrosine phosphatase		
Miao *et al.*, 2019	K562, lymphblast	DENV-2 MOI=10 48 hpi	Dimethyl labelling LC-MS/MS	321 regulated proteins	201: HDAC1, EIF3E, GRB2, BID, SAP18, PREB, SETD2, HMGN2, EIF3E, EIF3J, EIF4A2, EIF5, EIF4EBP2 and TSFM	120: EEF1B2, EEF2K	WB: HDAC1, EIF3E, GRB2, BID, SAP18	Transcription regulation, RNA splicing and processing, immune system, cellular response to stimulus, and macromolecule biosynthesis.

				160 regulated phospho-proteins	103: ZRANB2, MYBB1A	85:HMGA1, PA2G4		

* detected in only DENV infected cells

**Proteins that were focused and /or discussed in the studies

IPA=Ingenuity pathway analysis, EF =elongation factor, PRP4=Pre-mRNA processing factor 4 homologue, Alix= apoptosis-linked gene-2-interacting protein X, UBE1= ubiquitinactivating enzyme E1, MxA= interferon induced Mx protein, GSS=glutathione, TrxR1= synthetase thioredoxin reductase 1, Prx1=peroxiredoxin 1, PYCR1= pyrroline-5-carboxylate reductase 1, mitochondrial, GRP78= glucose-regulated protein 78, EIF= eukaryotic initiation factor, hnRNPH1= heterogeneous nuclear ribonucleoprotein, HSP= heat shock protein, PDIA3= Protein Disulfide Isomerase A3, HSPA5= Endoplasmic reticulum chaperone BiP, HYOU1= hypoxia up-regulated protein 1, CDK=cyclin dependent kinases, CCNB1=cyclin B1, AURK= aurora kinases, PA2G4= proliferation-associated protein 2G4, ZRANB2=zinc finger Ran-binding domain-containing protein 2, HMGA1= mobility group AT hook1, PREB =prolactin regulatory element binding protein, HDAC1= histone deacetylase 1, GRB2= growth factor receptor-bound protein 2, BID= BH3 Interacting Domain Death Agonist, SAP18= Sin3A Associated Protein 18, SETD2= SET domain containing 2, HMGN2=high mobility group nucleosomal binding domain 2

1.6.2 Secretome analysis of DENV infected cells

In terms of cell models of infection, the secretome consists of both pathogen and host cellular proteins secreted in response to infection and may include; virulence factors encoded by the pathogen, intracellular processes (pathogens' and cellular enzymes), proteins involved in cell-cell signal transduction (cytokines and chemokines), as well as host immune components (antibodies) (Ranganathan and Garg, 2009; Cao *et al*., 2011). The use of high-throughput proteomics to investigate the cellular secretome in response to virus infection potentially provides knowledge that can be used to gain a deeper understanding of pathogenesis and hopefully leads to the identification of proteins that can be used clinical as biomarkers or can be targeted to develop new treatments/vaccines (Ranganathan and Garg, 2009).

There have been only two studies investigating the changes in the cellular secretome in response to DENV infection. A study by Higa and colleagues (Higa *et al.*, 2008) used 1D SDS-PAGE and liquid chromatography (LC) coupled with tandem MS (MS/MS) to characterise the secretome of DENV-2 infected human HepG2 liver cells. The proteins that were identified and analysed focused in this study were α-enolase (ENO1), superoxide dismutase (SOD), peptidyl-prolyl isomerases A and B (cyclophilins A and B), tissue inhibitor of metalloproteinases 1 and 2 (TIMP-1 and 2) and macrophage migration inhibitory factor (MIF) (Higa *et al.*, 2008). A second study was also done on DENV-2 infected HepG2 cells using two different proteomic approaches: tryptic digestion of proteins followed by bottom up MS analysis and top down MS analysis of whole intact proteins strategies (Caruso *et al.,* 2017). The dual analysis identified 175 proteins; 57, 59 and 59 proteins were detected only in mock infected cells, DENV-2 infected cells and both cell types, respectively. The study focussed on proteins identified to play a role in proteolytic processes and identified inter-alpha-trypsin inhibitor (heavy chain H2) and ADAM10 only in the secretome of mock infected cells whereas tissue factor pathway inhibitor (TFPI), neurotrypsin and trypsin were only identified in the secretome of DENV-2 infected cells.

Thus, more studies examining the secretome of DENV infected cells are needed in order to better understand the host response to viral infection and determine if DENV infection dysregulates cellular secretion.

1.7 Biomarkers: a new hope from translation medicine

Currently, there is no reliable biomarker available to predict whether DEN patients in the early phase of disease will progress to severe disease. Furthermore, reliable tests to diagnose patients with DEN after the viremic phase need to be improved. Biomarkers proposed for purely diagnostic use and to predict disease severity can be divided into a number of categories; viral markers, immune activation markers, coagulation and endothelial activation markers, other soluble factors, biochemical markers and host genetic markers (Srikiatkhachorn and Green, 2010; Yacoub *et al* 2014; John *et al*., 2015).

Biomarkers currently used in clinical practice for distinguishing DEN from other febrile illness (AUFI) include; NS1 a surrogate of viremia and clinical laboratory markers such as liver function tests, the percentage of atypical lymphocytes and platelet count (Luvira *et al*., 2019). Low white blood cell count, low levels of C-reactive proteins (CRP) and procalcitonin were also proposed as a biomarkers to diagnose viral infection, mainly DEN, from other bacterial infections in tropical areas (Wangrangsimakul *et al*., 2018).

Biomarkers proposed for predicting disease severity in the early febrile phase include; viral markers (NS1) and IFNα (Srikiatkhachorn and Green, 2010). High levels of NS1 and anti-NS1 antibody as well as high viral loads have been proposed as markers of disease severity (Jayathilaka *et al*., 2018, Vaughn *et al*., 2000). However, decreased levels of NS1 reported in secondary DENV infection (de la Cruz-Hernandez *et al.*, 2013) might limit its usage as a biomarker. Moreover, a higher level of viremia in DF compared with DHF has been reported (de la Cruz-Hernandez *et al*., 2013). Elevated levels of CRP have also been proposed as marker of DSS in the early febrile phase (Chen *et al*., 2015). Biomarkers proposed in late febrile phase include i) cytokines such as IL-10, CXCL3, complements C3a and C5a, ii) soluble receptors including TNF-α receptor, IL-2 receptor, vascular endothelial growth factor (VEGF) and soluble $CD4^+$/$CD8^+$ T-cells iii) endothelial activation markers including von Willebrand factor (vWF), ADAMTS-13,

thrombomodulin, IL-8, intercellular adhesion molecule (ICAM)-I and vascular cell adhesion molecule (VCAM)-I as well as vascular endothelial growth factor (VEGF) (Srikiatkhachorn and Green, 2010; Yacoub *et al* 2014). The levels of specific serum lipoproteins have also been proposed as useful predictors of DEN severity but racial and age differences need to be taken into account (Lima *et a*l., 2019).

However, at the present time there are no universal biomarkers to predict DEN disease severity and there are conflicting results amongst the studies that have been undertaken. Many factors need to be taken into account in studies aiming to identify biomarkers and translate them clinically; for example, variation between serotypes, host factors (race, age and sex) and immune response (Yacoub *et al.*, 2014) as well as the specimen type (serum or plasma) and methods of testing (Srikiatkhachorn and Green, 2010). Furthermore, the timing of specimen collection is an important factor that affects the results; thus, biomarkers should be examined by the time of defervescence, instead of at the onset of fever (Srikiatkhachorn and Green, 2010). Ideally, sequential sample collections are needed for a better understanding of predictive biomarkers (Srikiatkhachorn and Green, 2010). Hopefully, the study of host proteins that are modulated in response to DENV infection, both *in vitro* and *in vivo*, will facilitate biomarker discovery.

1.8 Proteomic analysis of serum/plasma from DEN patients.

A number of researchers have used LC-MS/MS based approaches to identify potential biomarkers of SD. However, the studies used different methodologies leading to different results. Fragnoud and colleagues (Fragnoud *et al*., 2012) used Isotope Coded Protein Labeling (ICPL) coupled with MS/MS to analyse pooled sera from patients with SD and DF as well as healthy people, analysing five samples in each group. There were seven proteins identified that significantly increased or decreased in amount (>1.6 fold) in the sera from patients with SD compared to DF: (peroxyredoxin-2, vitamin D Binding-Protein (VitDBP), afamin, fibronectin, leucine-rich alpha-2 glycoprotein 1 (LRG1), galectin 3 Binding-Protein, CRP and ferritin light-chain). The amounts of three proteins (VitDBP, LRG1, and ferritin light-chain) were validated by Western blotting and suggested to have potential as biomarkers (Fragnoud *et al*., 2012). However, using pooled sera and

excessive depletion of serum proteins might have been a limitation of the study. Another approach used discovery proteomics together with a nonparametric modeling pipeline (Brasier *et al*., 2012). Matrix Assisted Laser Desorption/Ionization/ Time of Flight MS (MALDI TOF/TOF) was used to analyse proteins from 42 DF and 13 DHF cases. The data obtained was then combined with clinical data relating to the samples, leading to the analysis of two cytokines and 42 proteins by multivariate adaptive regression splines (MARS) to assess their potential as biomarkers. The most accurate model that correlated with 100% of DHF cases, was based on IL-10, C4A, fibrinogen, tropomyosin, immunoglobulin G and three isoforms of albumin (Brasier *et al*., 2012). This complicated model still requires verification in a large sample size. Kumar and colleague's (Kumar *et al*., 2012) sequentially examined patient sera sampled during the course of disease using Quadrupole Time-of-Flight (Q-TOF) LC-MS. Samples from 44 DF and 18 DHF cases, collected at three time points during infection for each patient (early febrile, defervescence and convalescent phase) were examined. Multiple statistical methods were then used to classify a subset of markers for DHF prediction. The elevated acute phase proteins which were observed from this study were CRP, serum amyloid A2, haptoglobin, alpha-2 macroglobulin and ferritin (Kumar *et al.,* 2012). The use of pooled sera might be a limitation of this study.

1.9 Aims of the project

The **OVERALL AIM** of this project is to use high-throughput proteomics to analyse the cellular proteome and secretome of DENV infected cells and patient sera to conduct combined proteomic/secretome analysis and sera proteomic analysis in response to DENV infection.

Specific Aims

1) To analyse the proteome and secretome of DENV infected human HEK293 and Huh-7 liver cells using high-throughput proteomics to identify proteins modulated in response to infection.

2) To analyse the proteome and secretome of human HEK293 cells containing a DENV replicon to determine if there are changes in the cellular secretome.

3) To analyse the results of a high-throughput analysis of clinical samples from DENV infected individuals to determine if changes in the abundance of specific proteins correlate with disease diagnosis and severity prediction.

4) To determine whether DENV replication in cultured cells results in changes in the levels of secreted proteins that are also modulated in clinical samples from DENV infected individuals and to investigate the mechanisms involved.

CHAPTER 2. METHOD AND MATERIALS

2.1 Cells and cell culture

2.1.1 Cells and cell culture

Human hepatocellular carcinoma (Huh-7), human embryonic kidney (HEK293T) and HEK293T cells containing the DENV replicon DV-Rep-GP2A (HEK293T-DV-Rep-GP2A (REP)) cells (Masse *et al*. 2010), were cultured in Dulbecco's modified Eagle's medium (DMEM) (Lonza, Basel, Switzerland) supplemented with 10% heat-inactivated foetal bovine serum (FBS) (Gibco^{TM}, Thermo Fisher Scientific, MA, USA), 100 µg/ml streptomycin and 100 U/ml penicillin (Gibco^{TM}, Thermo Fisher Scientific), 0.1 mM non-essential amino acids (NEAA) (Gibco^{TM}, Thermo Fisher Scientific) and 2 mM L-glutamine (Gibco^{TM}, Thermo Fisher Scientific). REP cells were maintained under 3.5 µg/ml puromycin (Sigma-Aldrich, Gillingham, UK) selection. All cells were maintained in a humidified incubator at 37 °C and 5% CO_2. For serum free experiments, cells were grown in Pro293a-CDM serum free media (SFM) (Lonza) supplemented with streptomycin, penicillin, NEAA and 2 mM L-glutamine as described above. Vero cells, kidney epithelial cells isolated from an African green monkey, were cultured in Eagle's medium M199 (Gibco^{TM}, Thermo Fisher Scientific) with 5% FBS at 37 °C in a humidified incubator with 5% CO2. The C6/36 mosquito cell line isolated from *Aedes albopictus* (Igarashi *et al*., 1978) was maintained in Leibowitz's L-15 medium (Lonza) supplemented with 10% FBS, 8% (v/v) tryptose phosphate broth (Gibco^{TM}, Thermo Fisher Scientific), 0.1 mM NEAA and 2 mM L-glutamine. Cells were maintained in a humidified incubator at 28 °C with atmospheric CO_2.

To passage cells, the growth medium was removed before washing cells once with warm Dulbecco's phosphate buffered saline (PBS) (Lonza). An appropriate volume of 0.05% trypsin/EDTA (Gibco^{TM}, Thermo Fisher Scientific) was added to cover the cell monolayer. The cells were incubated at 37 °C until they detached. The appropriate media was added and the cells collected by centrifugation at 150 g for 8 min before resuspension of the cell pellet in the appropriate media. Finally, the desired proportion of cells was added to a new flask containing new media.

To seed cells for secretomes experiment, poly-D-lysine (PDL) (Sigma-Aldrich) diluted in PBS at the concentration of 0.1 mg/ml was coated to flask for 5 min before three times washing with PBS.

As required for cell seeding, the cell number was counted using a haemocytometer. In order to assess the number of viable cells, 0.4 % (w/v) trypan blue (Sigma-Aldrich) was added in a 1:1 ratio.

In some of the experiments performed, the following agents were added to media either before or after infection, as indicated.

- Recombinant human IL-6 (R&D systems, Minneapolis, USA), prepared by dilution in 0.1% bovine serum albumin (BSA) (Sigma-Aldrich)

-MG132 (Alfa Aesar™, Thermo Fisher Scientific), prepared by dilution in DMSO (Sigma-Aldrich).

2.1.2 Cell viability assay

Cell viability was determined using a Vybrant MTT assay (Invitrogen™, Thermo Fisher Scientific). Cells were seeded in PDL coated 96 well plates at a density of 30,000 cells each/well and cultivated in DMEM with 10% FBS for 24 h. The supernatant was removed, the cells were washed three to five times with warm PBS, and then cultured in either Pro293a-CDM with 10% FBS or Pro293a-CDM SFM for either 30 h (Huh-7) or 48 h (HEK293T). The media was then removed and replaced with 100 µl of either Pro293a-CDM containing 10 % FBS or Pro293a-CDM SFM alone followed by the addition of 10 µl of 12 mM MTT stock solution (Appendix A). The plate was incubated for 4 h before 100 µl of SDS-HCl solution was added (Appendix A) and mixed well by pipetting. The plate was incubated for a further 4-6 h and mixed again by pipetting. The absorbance was then measured at 570 nm on a plate reader (SpectraMax 190 microplate reader, Molecular Devices, Silicon Valley, California, USA). The percentage of cell viability was calculated using the formula:

$$\text{cell viability (\%)} = \frac{\text{(absorbance value of sample – absorbance value of blank)}}{\text{(absorbance value of control – absorbance value of blank)}} \times 100$$

2.1.3 Cell culture supernatant preparation for secretome analysis

Cells (~ 2.6E+06/ T25 flask) were then seeded into the PDL coated flasks and cultivated in the appropriate media (containing FBS) for 24 h until they were 60-80% confluent. The supernatant was then removed, and the cells were gently washed five times with warm PBS to remove all traces of serum. An appropriate volume of SFM was added to each flask. The supernatant was collected and centrifuged at 2000 g for 10 min to remove any cells. The supernatants were then concentrated ~ 40 fold using a 3 kDa cut-off Amicon® Ultra-4 Centrifugal Filter Unit (Merck-Millipore, Hertfordshire, UK) by centrifugation at 4,000 g for 45-50 min at 4 °C. The concentrated samples were then stored at -80 °C before analysis by either LC-MS/MS or Western blotting. The confluency and condition/morphology of the cells, as well as the final culture supernatant volume after concentration were recorded.

2.2 Virus growth, infection and assay

2.2.1 Virus infection conditions

Huh-7 and HEK293T cells (including replicon containing) were grown either in T25 flasks or on coverslips in a 24 well plate until ~ 60-80% confluent. The media was removed and cells were washed with warm PBS, which was then removed and replaced with the virus inoculum diluted to the required multiplicity of infection (MOI) in MEM (minimal essential medium (MEM) containing Earles salts (Lonza) supplemented with 2% FBS, 0.1 mM NEAA and 2 mM L-glutamine). Heat inactivated virus was prepared by heating the same lot of virus at 55 °C for 1 h and then diluting to the same MOI. The flasks/coverslips were then incubated in a humidified incubator at 37 °C and 5% CO_2 and gently rocked every 15 minutes. After 90 min, the inoculum was removed and the cells were gently washed five times with warm PBS, then cultured in either MEM maintenance medium or SFM at 37 °C and 5% CO_2. The culture supernatants were harvested 30 h post infection (hpi) for Huh-7 cells and at 48 hpi for HEK293T cells. The supernatants were concentrated as described above. Cells were then washed twice with warm PBS. The cells were harvested using a cell scraper and stored at -80 °C. Cells grown on coverslips were analysed by an immunofluorescence assay as described below.

2.2.2 Virus stock production

DENV-2 strain New Guinea C (NGC) produced from the DENV-2 infectious clone pDVWS601 (Pryor *et al*., 2001; Gualano *et al*., 1998) was used in this study. C6/36 cells were cultured in a T225 flask until they reached 80-90% confluence. The media was removed and cells were washed with warm PBS. DENV-2 stocks were diluted in L-15 medium (L-15 medium supplemented with 2% FBS, 0.1 mM NEAA and 2 mM L-glutamine) and added to the mosquito cell monolayer. Flasks with the viral inoculum were incubated in a humidified incubator at 28 °C with atmospheric CO_2 for 90 min with gentle rocking every 20 min. Additional L-15 medium was then added to each flask and further incubated at 28 °C with atmospheric CO_2.

Culture supernatants containing virus were harvested when either the infected cells showed ~ 80% cytopathic effect (CPE) or 5-6 days after infection. The culture supernatants were clarified by centrifugation at 4000 g for 10 min followed by the addition of 1M HEPES pH 8.0 (Gibco^{TM}, Thermo Fisher Scientific) to a final concentration of 25 mM. Culture supernatants were aliquoted and stored at -80 °C.

2.2.3 Virus immunofocus assay

Vero cells were seeded in PDL-coated 24 well plates and grown until 90% confluent. Tenfold serial dilutions of virus stock or cell culture supernatant were prepared in MEM. The growth medium was removed and the cells washed twice with PBS before 200 µl of virus diluent was added. The plates were incubated in humidified incubator at 37 °C with 5% CO_2 for 90 min and rocked intermittently. The virus inoculum was then removed and the cells washed twice with warm PBS before a 1:1 mixture of Avicell (RC-581; FMC Biopolymer) and 2X MEM (Appendix A) was added into each well. The plates were then incubated at 37 °C for 3-4 days, after which time the overlay medium was removed. The cells were washed twice with warm PBS and then fixed with cold methanol for 5 min. Subsequently, blocking solution (2% (w/v) skim milk powder in PBS) was added to the cells and incubated for 30 mins at room temperature (RTemp). The blocking solution was removed and then the cells were incubated with an in-house anti-DENV E (4G2) antibody diluted in blocking solution for 1 h at RTemp. The antibody solution was then removed and the cells washed four times with PBS for 5 min. The cells were further incubated with

a horseradish peroxidase (HRP) conjugated secondary antibody in blocking solution by rocking for 1 h at RTemp, followed by four 5 min washes in PBS. Finally, 200 µl of TrueBlue™ Peroxidase substrate (SeraCare Life Sciences Inc., Massachusetts, USA) was added into each well and the plates were incubated at RTemp until well-defined plaques were visible. The plaques were counted in each well (when not too numerous to count) and the viral titre was calculated as focus forming units (FFU)/ml (taking into account all dilution factors). All experiments were done in duplicate and the average viral titre reported.

2.2.4 50% Tissue culture infectious dose ($TCID_{50}$) assay

Vero cells were seeded at a density of 1 x 10^4 cells/well into 96-well plates in 100 µl of Eagle's medium M199/well. Tenfold serial dilutions of virus were prepared in MEM. Each dilution (100 µl /well) was added to 12 wells of the plate. Plates were incubated at 37 °C with 5% CO_2 until CPE was observed. At this time, the number of wells positive and negative for CPE in a 96-well plate were recorded and used to calculate the $TCID_{50}$ titre following the method of Reed and Muench (Reed and Muench, 1938).

2.3 Protein detection

2.3.1 Protein sample preparation

Total cell lysates were prepared from adherent cells. The cell monolayer was washed twice with PBS. Following this, 2X sample buffer (~ 50 – 100 µl / 1 x 10^6 cells; Appendix A) was added to the cells, which were then detached using a cell scraper and transferred to a tube. This cell lysate was heated at 95 °C for 5 min and placed on ice before being passed through a 25-gauge needle. Lysates were either used immediately or stored at -80 °C until required for analysis.

For co-immunoprecipitation (co-IP), adherent cells were washed twice with PBS. Co-IP lysis buffer (Appendix A) (1 ml/ 8x 10^6 cells) was added to the cell monolayer on ice and incubated for 5 min before the cells were detached with a cell scraper and transferred to a tube. The lysate was incubated on ice for a further 30 min, before being passed through a 25-gauge needle, then centrifuged at 14,000 g for 10 min at 4 °C and

finally transferred to new tube. Lysates were either used immediately or stored at -80 °C until required for analysis.

Secretome lysates were prepared from cell cultured supernatants for proteomic analysis as described in Section 2.1.3. For Western blotting, the proteins in the culture supernatants were either concentrated by ultra-centrifugation or by trichloroacetic acid (TCA) (Sigma-Aldrich) precipitation. For TCA precipitation, the supernatants were centrifuged at 2,000 g for 10 min to remove cell debris and 100% (w/v) TCA added to the clarified supernatant to a final concentration of 20%. The solutions were mixed and incubated on ice for 1 h and then centrifuged at 17,000 g for 30 min at 4 °C. The resulting pellet was washed twice with 500 µl of ice-cold acetone, collecting the pellet by centrifugation at 10,000 g for 5 min at 4 °C each time. The pellet was air-dried and resuspended in 80 µl of 2X sample buffer before being heated to 95 °C for 5 min. The samples were either used immediately or stored at -80 °C until required for analysis.

2.3.2 Protein quantification (BCA Protein Assay)

The protein concentration of all lysates was determined using a Pierce™ BCA Protein Assay Kit (Thermo Fisher Scientific), as per the manufacturer's instructions. Briefly, BSA standards of known protein concentration and samples of unknown protein concentration were seeded in 96 well plates. A working reagent (Reagent A and Reagent B, 50:1) was made up and added to all wells. Plates were incubated at 37 °C for 30 min and absorbance at 562 nm of each well measured on a plate reader (SpectraMax 190 microplate reader, Molecular Devices). The protein concentration in each sample was calculated by comparison to the standard curve produced using the BSA standards and taking into account any dilution factor.

2.3.3 Sodium Dodecyl Sulphate-Polyacrylamide Gel Electrophoresis (SDS-PAGE)

Protein lysates were prepared by the addition of 4X Laemmli buffer (Bio-rad, California, USA) containing either 355 mM β-mercaptoethanol (BME) or 100 mM dithiothreitol (DTT) as reducing agents and heated to 95 °C for 5 min. Proteins were then separated by SDS-PAGE on 10% or 15% gels at 80-120 V in running buffer (Appendix A) using a Bio-Rad mini-PROTEAN® apparatus (Bio-Rad) and compatible power pack (Bio-

Rad Power AC300, Bio-Rad) following the method of Laemmli (Laemmli UK, 1970). Protein molecular masses were estimated by omparison with a PageRuler™ Prestained protein ladder (Thermo Fisher Scientific) run in an adjacent well.

2.3.4 Coomassie blue staining

Proteins in SDS-PAGE gels were detected by staining with a Coomassie Brilliant Blue R-250 staining solution for 1-2 h by rocking at RTemp (Appendix A). The gels were subsequently destained using destain solution for at least 4 h at RTemp (Appendix A).

2.3.5 SYPRO Ruby staining

Proteins in SDS-PAGE gels were detected by staining with a SYPRO® Ruby (Molecular Probes™, Invitrogen, Thermo Fisher Scientific) dye staining solution according to manufacturer's protocol. Briefly, gels were fixed in 100 ml of fix solution containing 50% methanol and 7% acetic acid for 30 min before overnight stained in 60 ml of SYPRO Ruby dye by rocking at RTemp under cover to exclude from light. The gels were then transferred to a new container and washed twice with 100 ml of wash solution (10% methanol, 7% acetic acid) 30 min each by rocking at RTemp. Finally, the gels were scanned by Typhoon™ Variable Mode Imager (Amersham Biosciences, GE Healthcare, Buckinghamshire, UK) using ImageQuant™ Image Analysis Software.

2.3.6 Western blotting

Sample preparation and SDS-PAGE were performed as described above except using a Precision Plus Protein™ Kaleidoscope™ standard (Bio-Rad) as a marker. After electrophoresis was complete, the separated proteins were transferred from SDS-PAGE gels to a polyvinylidene difluoride (PVDF) membrane (GE Healthcare) using a Trans-Blot Semi-Dry Transfer Cell (Bio-Rad). Following electrophoresis, gels were equilibrated in transfer buffer (Appendix A) at RTemp. PVDF membrane was activated by subsequent soaking in methanol, water and transfer buffer.

After the transfer was complete, the membrane was incubated in blocking solution (5% (w/v) skim milk powder in PBST (Appendix A) either for 1 h at RTemp or overnight at 4 °C. The membrane was then washed with PBST and incubated in a solution containing an appropriate primary antibody (Table 2.1) diluted in 5% (w/v) skim milk powder in PBST

for either 1 h at RTemp or overnight at 4 °C. The antibody containing solution was removed and the membrane was then washed four times with PBST for 5 min each time. The membrane was then incubated with the appropriate secondary antibody (Table 2.2) diluted in 5% (w/v) skim milk powder or 5% (w/v) BSA in PBST for 1 h at RTemp before four washes with PBST each for 5 min. The membrane was drained and incubated for 1 min in LumiGLO® Chemiluminescent Substrate (Kirkegaard & Perry Laboratories, Inc, Maryland, USA). The membrane was drained, placed in a plastic envelope and transferred into an X-ray cassette with a sheet of X-ray film (Amersham Hyperfilm^{TM} ECL, GE Healthcare Limited) exposed to the membrane. The film was developed using a Compact X4 Automatic X-ray Film Processor (Xograph Healthcare, Gloucestershire, UK).

Where necessary, membranes were stripped and reprobed with new antibody. To do so, used membranes were incubated in Abcam mild stripping buffer (Appendix A) for 5-10 min by rocking at RTemp followed by two times washes with PBS each for 10 min and two times washes with TBST each for 5 min. The membrane was then ready to block with blocking agent.

Table 2.1 Primary antibodies used for Western blot analysis.

Antibody	Target protein molecular weight (kDa)	Source	Working dilution	Catalogue number	Manufacturer
Anti-DENV NS1	40	Rabbit	1:500	GTX124280	GeneTex (California, USA)
Anti-DENV NS4B	27	Rabbit	1:1000	GTX103349	GeneTex
Anti-DENV NS5	105	Rabbit	1:500	----------	Dr A. Davidson
Anti-DENV E	60	Mouse	1:500	----------	Dr A. Davidson
Anti-DENV E	60	Rabbit	1:500	NBP2-52666	Novus Biological (Bio-Techne, Abingdon, UK)
Anti-DENV prM	60	Rabbit	1:1000	GTX128092	GeneTex
Anti-GAPDH	36	Rabbit	1:5000	GTX100118	GeneTex
Anti-APOH	38	Mouse	1:200	sc-515677	Santa Cruz Biotechnology (Texas, USA)
Anti-C4A	193	Mouse	1:200	sc-271181	Santa Cruz Biotechnology
Anti-HSPA5	72	Rabbit	1:1000	ab108613	Abcam (Cambridge, UK)
Anti-ERC1	128	Mouse	1:2000	ab50312	Abcam
Anti-CALR	48	Rabbit	1:1000	ab92516	Abcam
Anti-FGA	95	Rabbit	1:3000	ab92572	Abcam
Anti-FGB	56	Rabbit	0.4 µg/ml	NBP1-90956	Novus Biological
Anti-FGG	52	Rabbit	1:500	GTX108640	GeneTex

Anti-SERONINC1	55	Rabbit	1:500	ab126598	Abcam
Anti-SERPINA1	52	Mouse	1:1000	ab9400	Abcam
Anti-CLU	α-chain: 36-39 β-chain: 34-36	Mouse	1:200	sc-8354	Santa Cruz Biotechnology
Anti-VTN	54	Mouse	1:500	ab13413	Abcam
Anti-APOA1	31	Rabbit	1:1000	ab52945	Abcam
Anti-HNF4A	53	Rabbit	1:1000	ab92378	Abcam
Anti-HP	45	Rabbit	1:1000	ab131236	Abcam
Anti-APOC2	8, 12	Sheep	0.5 µg/mL	AF4497	R&D systems (Minneapolis, USA)
Anti-DICER1	219	Rabbit	1:2000	NBP1-06521	Novus Biological
Anti-HMGA2	12	Mouse	1:500	NBP2-43640	Novus Biological
Anti-STAT2	113	Mouse	1:1000	sc-514193	Santa Cruz Biotechnology

Table 2.2 Secondary antibodies used for Western blot analysis.

Antibody	Working dilution	Catalogue number	Manufacturer
Goat anti-mouse IgG, HRP conjugated	1:1000	12-349	Millipore-Merck (Burlington, USA)
Goat anti-rabbit IgG, HRP conjugated	1:5000	sc-2054	Santa Cruz Biotechnology
Goat anti-rabbit IgG, HRP conjugated	1:5000	ab216777	Abcam

2.3.7 Immunofluorescence assay (IFA)

Cells were grown on glass coverslips which were coated with PDL (0.1 mg/ml in PBS) when appropriate. For each experiment the culture media was removed, the coverslips were washed twice with warm PBS and fixed by the addition of ice-cold methanol for 5 min. The fixed cells were then allowed to air dry and either stored at -80 °C or used directly for IFA.

Coverslips were washed with PBS and incubated in blocking solution (10% (v/v) FBS in PBS) for 1 h at RTemp, before being incubated with the appropriate primary antibody (Table 2.3) diluted in blocking solution for 1 h at RTemp. The antibody containing solution was removed and the coverslips were washed four times with PBS for 5 min per wash and subsequently incubated with an appropriate secondary antibody (Table 2.4) diluted in blocking solution for 1 h at RTemp. The secondary antibody was removed and the coverslips were washed again four times with PBS for 5 min per wash. Finally, the coverslips were drained and mounted with VectaShield containing 4′,6-diamidino-2-phenylindole (DAPI) (Vector Laboratories, Burlingham, USA). The cells were analysed with either a widefield imaging system (Leica DM IRB inverted epifluorescence microscope, Leica Microsystems GmbH, Wetzlar, Germany) or using a confocal laser imaging system (Leica SP5-AOBS confocal laser scanning microscope, Leica Microsystems GmbH) in the Wolfson Bioimaging Facility (Faculty of Life Sciences, University of Bristol). The software Leica Application Suite X (LAS X) and ImageJ (version 1.8.0) were used to collect and analyse cell imaging data.

Table 2.3 Primary antibodies used for IFA.

Name	Target protein Mw (kDa)	Source	Working dilution	Catalogue number	Manufacturer
Anti-DENV E (4G2)	60	Mouse	1:400	In house	Dr A. Davidson
Anti-DENV E	60	Rabbit	1:500	NBP2-52666	Novus Biological
Anti-DENV NS1	46	Mouse	1:200	In house.	Dr A. Davidson
Anti-FGB	56	Mouse	1:50	sc-271035	Santa Cruz Biotechnology
Anti-FGG	52	Mouse	1:50	sc-133156	Santa Cruz Biotechnology

Table 2.4: Secondary antibodies used for IFA.

Name	Working dilution	Catalogue number	Manufacturer
Alexa Fluor® 568 Goat anti-rabbit IgG (H+L) antibody,	1:1000	A11036	Invitrogen™, Thermo Fisher Scientific
Alexa Fluor® 568 goat anti-mouse IgG (H+L) antibody	1:1000	A11004	Invitrogen™, Thermo Fisher Scientific
Alexa Fluor® 488 goat anti-mouse IgG (H+L) antibody,	1:1000	A11029	Invitrogen™, Thermo Fisher Scientific
Alexa Fluor® 488 goat anti-rabbit IgG (H+L) antibody	1:1000	A11008	Invitrogen™, Thermo Fisher Scientific

2.3.8 Co-immunoprecipitation (Co-IP) assay

One ml of unconcentrated cell culture supernatant or cell lysate (prepared as described in Section 2.3.1) was incubated with 10 µg of an appropriate antibody (Table 2.5) overnight at 4 ºC under gentle agitation. 40 µl of packed bead volume of Pierce™ Protein A or G Magnetic Beads (Thermo Fisher Scientific) were pre-equilibrated with washing buffer (Appendix A) as per the manufacturers' instructions. The magnetic beads were then added to the lysate/antibody mixture and incubated by rotation at RTemp. After 1 h, the beads were magnetically collected and washed twice with equilibration buffer, before a final wash with ultrapure water. Protein was eluted from the beads by adding 80 µl of 2X SDS-PAGE reducing sample buffer (Appendix A) to the tube and either heating at 95 ºC for 10 min (Protein G beads) or incubation at RTemp for 10 min with rotation (Protein A beads). The beads were captured magnetically and the supernatant was removed for further analysis.

Table 2.5: Antibodies used for Co-IP.

Name	Target protein Mw (kDa)	Source	Catalogue number	Manufacturer
Anti-APOH	38	Mouse	sc-515677	Santa Cruz Biotechnology
Anti-C4A	193	Mouse	sc-271181	Santa Cruz Biotechnology
Anti-FGG	52	Mouse	sc-133156	Santa Cruz Biotechnology
Normal mouse serum (used as control)	NA	Mouse	sc-45051	Santa Cruz Biotechnology

2.4 RNA quantification

2.4.1 Total RNA isolation from adherent cells

RNA was isolated using an SV Total RNA Isolation System (Promega, Madison, USA) according to the manufacturer's instruction. Briefly, 200 µl of RNA lysis buffer containing BME was added to a T25 flask, containing ~2.6 x 10^6 cells and the cells were removed by scraping. The microcentrifugation purification method was applied as described by the manufacturer. Finally, the purified RNA was eluted in a final volume of 100 µl with nuclease-free water and stored at -70 °C. The RNA concentration was measured using a Nanodrop™ spectrophotometer (Thermo Fisher Scientific).

2.4.2 Extraction of viral RNA from cell culture fluids

A QIAamp Viral RNA Mini Kit (Qiagen, Hilden, Germany) was used to extract DENV RNA from 140 µl of culture supernatant from infected cells according to the manufacturer's instructions. The mini spin procedure was applied. The purified RNA was finally eluted in 60 µl of AVE buffer (0.04% sodium azide in RNase-free water) and stored at -70 °C.

2.4.3 Two-step reverse-transcription PCR (RT-PCR)

Two-step RT-PCR was performed. RNA extracted from adherent cells and supernatants were used for cDNA synthesis in the first step followed by PCR in the second step.

2.4.3.1 2.4.3.1 Reverse transcription (RT) reaction

The cDNA was synthesized from equal amounts of RNA in each sample using the ImProm-II™ Reverse Transcription System (Promega). Firstly, 0.2 µg of random hexamers (Promega) was added to 0.5 µg RNA and the volume adjusted to 10 µl with nuclease-free water.

For RT of viral RNA, either 5 ng of an *in vitro* transcribed DENV-2 transcript or 2 µl of DENV RNA (from an eluate of 60 µl (as described above)) was used with 0.5µM of the DENV specific primer DV2-C69Br (10 pmol/ul) (sequence was listed in Table 2.6) in

a final volume of 10 µl. The *in vitro* transcribed RNA were produced by using a T7 RNA polymerase based RiboMAX^{TM} Large Scale RNA Production System (Promega). The reaction mixture consisted of 3-4 µg of linear DNA template, 7.5 mM of rNTPs (ATP, CTP, GTP, and UTP), T7 Transcription 1X Buffer, enzyme mix (T7) and nuclease-free water to a final volume of 50 µl. The reaction mixture was incubated at 37 °C for 4 h before adding 3-4 µl of RQ1 RNase-Free DNase (1 U/µg RNA; Promega) and further incubating at 37 °C for 1 h.

Subsequently, the tubes containing the RNA/primer mixtures were incubated at 70 °C for 5 min and then quickly chilled on ice. An RT reaction mix was then added to the denatured RNA/primer mix on ice. Each RT reaction mix contained 4 µl of ImProm-II™ 5X Reaction Buffer (Promega), 25 mM $MgCl_2$, 0.5 mM dNTPs, 1 µl of ImProm-IITM Reverse Transcriptase (Promega) and nuclease-free water to a final volume of 10 µl. Finally, the tubes were placed in a GS1 thermocycler machine (G-Storm, UK) with a heated lid set to 100 °C and incubated as follows: 25 °C for 5 min, 42 °C for 60 min and 70 °C for 15 min. The final cDNA product was either processed for further analysis or stored at -70 °C.

2.4.3.2 2.4.3.2 PCR amplification

For the PCR step, the cDNA template was diluted with nuclease free water to a final concentration of 5 ng/µl (based on the starting concentration of input RNA used for RT). A PCR master mix was added to 2 µl of cDNA template. Each PCR master mix contained 2.2 µl of a gene specific primer set (Qiagen) (Table 2.6), 2 µl of 10 X Maxima Hot Start Taq buffer, 2 µl of 0.5 mM dNTPs, 2 mM $MgCl_2$, 1U of Maxima Hot Start Taq DNA Polymerase (Thermo Fisher Scientific) and nuclease free water to a final volume of 18 µl. For quantification of DENV RNA, the gene specific primers were substituted with the DENV specific primers (listed in Table 2.7), 0.3 µM forward primer and 0.3 µM reverse primer. Finally, the reactions were placed in a PCR machine (with a heated lid set to 100 °C) and cycled as follows: 95 °C for 15 s followed by 42 °C for 60 s for 35-40 cycles. The PCR products were then analysed by agarose gel electrophoresis.

2.4.4 Primers optimization and efficiency

Optimisation of primer sets was performed using PCR (Section 2.3.4.2) on RT-PCR product samples and agarose gel electrophoresis (Section 2.4.6). Efficiency of the primers was then determined by quantitative real time RT-PCR (qRT-PCR) (section 2.4.5)

2.4.5 Quantitative real time RT-PCR (qRT-PCR)

The efficiency of the primers for qRT-PCR analysis was analysed as follows. Ten-fold serial dilutions of the cDNA templates (derived from cellular or viral RNA/*in vitro* RNA transcripts) were made in nuclease-free water to generate the standard curves for qRT-PCR. 1 µl of diluted cDNA template was then mixed with 11.5 µl of qPCR reaction mixture. The qPCR reaction mixture consisted of 6.25 µl of the 2X Maxima Hot Start Taq buffer (Thermo Fisher Scientific), 1.25 µl of the appropriate gene specific primer set (QIAGEN) (Table 2.7) and made to a final volume of 11.5 µl with sterile nuclease-free water. For quantification of DENV RNA, the forward and reverse primers (Table 2.7) were used at a concentration 0.3 µM. Subsequently, the qPCR reaction was performed using a Stratagene Mx3005P QPCR System (Agilent Technologies, California, USA). The program was set for initial activation at 95 °C for 10 min, followed by 40 cycles of denaturation (15 s at 95 °C) and annealing (60 s at 60 °C). Finally, C_T values were used for calculating the amount of mRNA. SoftMax Pro program was used to quantify C_T value and calculate the efficiency curves.

Once the specificity, sensitivity and efficiency of the primers was validated, qRT-PCR reactions were set up using 1 µl of cDNA template (≤500 ng) and 11.5 µl of qPCR reaction mixture using the cycling conditions described above. C_T values were used for quantitation of mRNA. The relative quantification was determined by the double-delta Ct (ΔΔCt) analysis. The value-of-interested gene was firstly normalized by those of a reference gene from the same sample; GAPDH was used as the reference gene. Then the ΔΔCt value was calculated for each gene in each cell type, as described in (Livak and Schmittgen, 2001), using Microsoft Excel. Gene expression values obtained from mock infected cells were used as control.

Gene specific primers using in this study were purchased from QIAGEN (Hilden, Germany) as summarised in table 2.6.

Table 2.6: Oligonucleotide primers used in this study

Gene	Source	Catalog number	Amplicon length (bp)
GAPDH	Qiagen	QT00079247	95
FGA	Qiagen	QT00046711	113
FGG	Qiagen	QT01000727	64
FGB	Qiagen	QT00031003)	105
HNF4A	Qiagen	QT00019411	90
SERPINA1	Qiagen	QT00077469	87
SERPINC1	Qiagen	QT00013013	145
HP	Qiagen	QT00071449	94
F2	Qiagen	QT00013314	103
CEBP	Qiagen	QT00203357	88
F13B	Qiagen	QT00056945	87
IL6	Qiagen	QT00083720	107

Table 2.7 DENV-specific primers used for qPCR and their sequences

Type	Primer	DENV-2 target	Primer sequence (5' → 3')
Forward	C14A	C gene	AATATGCTGAAACGCGAGAGAAACCGCG
Reverse	DV2-C69Br	C gene	CCCATCTCTTCAGTATCCCTGCTGTTGG
Reverse	DV-C69Br-AM	C gene	CCCATCTCITCAIIATCCCTGCTGTTGG

*I indicates Deoxyinosine substituted at position

2.4.6 Agarose gel electrophoresis

PCR products were mixed with 6X gel loading buffer (Appendix A) and separated on a 4 % (w/v) agarose gel by electrophoresis using 1X TBE running buffer (Appendix A) containing 0.5 µg/ml ethidium bromide. An O'RangeRuler 20 bp DNA Ladder (Thermo Fischer Scientific) was used as a marker. The PCR products were imaged using a BioDoc-IT™ System Ultraviolet transilluminator (UVP, CA, USA).

2.5 Clinical specimen selection

The clinical specimens assessed by proteomic analysis were obtained from patients and volunteers in the Philippines (kindly provided by Dr Raul Destura, National Institute of Health, University of the Philippines Manila (NIH UPM)).

The retrospective study used archived sera from the biobank housed at NIH UPM. Serum samples were collected upon admission hospitals from patients with febrile illness (Project number UPMREB 2016-110-01; Research Ethics Board, University of the Philippines Manila).

The DEN infection case was defined by clinical symptoms and positive laboratory confirmation (DENV specific RT-PCR and/or NS1 antigen testing and/or DENV IgM testing). Sera from healthy individuals were used as control groups. DEN-positive cases were then further classified based on clinical outcome by severity into 3 groups according to the WHO 2009 definition: DEN w/o WS, DEN w WS and SD (WHO 2009).

From the available samples, specimens were prioritised for analysis based on an early sampling time (day after fever onset) with a similar proportion of ages (where possible) and genders in all groups.

2.6 Preparation of samples for LC-MS/MS analysis

2.6.1 Preparation of cell lysates and cell culture supernatant specimens for MS analysis

Cells were washed twice with PBS, detached by cell scraper and collected by centrifugation. RIPA buffer containing protease inhibitors (Appendix A) was added and the resulting lysates were incubated on ice for 30 min and passed through 23-gauge blunt needles. Cell lysates were used for further BCA and LC-MS/MS analysis or kept at -80°C.

Before labelling by 10-plex tandem mass tagging (TMT) and proteomic analysis, the protein concentration in cell lysates and concentrated supernatants were determined by BCA assay as described previously. The sample volumes were then adjusted (with PBS) to reflect equal starting volumes and approximate cell numbers with no sample containing greater than 100 μg of protein. All experiments were repeated three times.

2.6.2 Preparation of clinical specimens for mass spectrometry analysis

Serum samples from patients with different grades of dengue disease severity were depleted of human serum albumin (ALB) and IgG using a ProteoPrep® Blue Albumin and IgG Depletion kit (Sigma-Aldrich) following the manufacturer's instructions. Briefly, 75 µl of each serum sample was applied to the equilibrated resin. The eluate was applied to the resin again before washing of the resin with equilibration buffer. The eluate and wash were combined to give a final volume of ~ 175 µl. The concentration of protein in each sample was determined using a BCA assay using a 1:25 dilution of each sample. A "mastermix" reference sample was produced by combining proportional amounts of each sample used in the analysis.

2.7 Quantitative mass spectrometry analysis

2.7.1 TMT labelling and high pH reversed-phase chromatography

The protein concentration for each sample prepared as described in 2.6.2 was determined via BCA assay. For samples which could not contain DENV; 100 µg of each sample was sent to the Proteomics Facility for TMT labelling using a TMT10plex Isobaric Label Reagent Set (Thermo Fisher Scientific) by Dr Kate Heesom and co-workers. If the samples potentially could have contained inactivated DENV then the first steps of the TMT labelling were done in the BL3 laboratory before sending to the Proteomics Facility as follows. 100 µg of sample was adjusted to a volume of 50 µl using nuclease free water and then adjusted to a final volume of 100 µl with 100 mM triethyl ammonium bicarbonate (TEAB). 5 µl of 200 mM Tris (2-Carboxyethyl) phosphine Hydrochloride (TCEP) was added and the samples incubated at 55 °C for 1 h. Then 5 µl of 375mM iodoacetamide (prepared immediately before use by dissolving 9 mg of iodoacetamide in 132 µl of 100 mM TEAB) was added to each sample, mixed and incubated for 30 min at RTemp, protected from light. Six volumes (~600 µl) of pre-chilled acetone was then added to each tube and proteins precipitated overnight at -20 °C. The precipitated proteins were then sent to the Proteomics Facility for further processing as follows. Briefly, the precipitated proteins were collected by centrifugation and then digested with trypsin (2.5 µg of trypsin per 100 µg protein) overnight at 37 °C and labelled with TMT 10Plex reagents according

to the manufacturer's instruction (Thermo Fisher Scientific). A different isobaric tag was applied to each sample. All 10 samples were then mixed together before fractionation and clean-up.

The pooled sample was evaporated to dryness, resuspended in 5% formic acid and desalted using a SepPak cartridge according to the manufacturer's protocol (Waters, Milford, Massachusetts, USA). Eluate from the SepPak cartridge was then evaporated to dryness and resuspended in buffer A (20 mM ammonium hydroxide, pH 10) then fractioned by high pH reversed-phase (RP) chromatography using an Ultimate 3000 liquid chromatography system (Thermo Scientific). The sample was loaded onto an XBridge BEH C18 Column (130Å, 3.5 µm, 2.1 mm x 150 mm, Waters) in buffer A and ran in gradient of buffer B (20 mM Ammonium Hydroxide in acetonitrile, pH 10) from 0-95% over 60 min. The resulting fractions were evaporated to dryness and resuspended in 1% formic acid prior to analysis by nano-LC MSMS using an Orbitrap Fusion Lumos mass spectrometer.

2.7.2 Nano-LC Mass Spectrometry

High pH RP fractions were further fractionated using an Ultimate 3000 nano-LC system in line with an Orbitrap Fusion Lumos mass spectrometer. Briefly, peptides in 1% formic acid were injected onto an Acclaim PepMap C18 nano-trap column (Thermo Scientific). After washing with 0.5% acetonitrile, 0.1% formic acid, peptides were resolved on a 250 mm × 75 µm Acclaim PepMap C18 RP analytical column (Thermo Scientific) over a 150 min organic gradient, using 7 gradient segments (1-6% solvent B over 1min., 6-15% B over 58min, 15-32%B over 58min, 32-40%B over 5min, 40-90%B over 1 min, held at 90%B for 6 min and then reduced to 1%B over 1 min) with a flow rate of 300 nl/min. Solvent A was 0.1% formic acid and Solvent B was aqueous 80% acetonitrile in 0.1% formic acid. Peptides were ionized by nano-electrospray ionization at 2.0 kV and temperature of 275°C.

All acquired spectra from the Orbitrap MS controlled by Xcalibur 4.1 software (Thermo Scientific) were operated in data-dependent acquisition mode using an Synchronous Precursor Selection (SPS)-MS3 workflow. FTMS1 spectra were collected at a resolution of 120,000 with an automatic gain control (AGC) target of 200,000 and a max

injection time of 50 ms. Precursors were filtered with an intensity threshold of 5,000 according to charge state (to include charge states 2-7) and with monoisotopic peak determination set to Peptide. Previously interrogated precursors were excluded using a dynamic window (60s +/-10ppm). The MS2 precursors were isolated with a quadrupole isolation window of 0.7 m/z. Then the ITMS2 spectra were collected with an AGC target of 10,000 max injection time of 70 ms and CID collision energy of 35%.

For FTMS3 analysis, the Orbitrap was operated at 50,000 resolution with an AGC target of 50,000 and a max injection time of 105 ms. Precursors were then fragmented by high energy collision dissociation (HCD) at a normalised collision energy of 60% to ensure maximal TMT reporter ion yield. SPS was enabled to include up to five MS2 fragment ions in the FTMS3 scan.

2.7.3 Data Analysis

The raw data files were processed and quantified using Proteome Discoverer™ software v2.1 (Thermo Scientific) and searched against the UniProt Human database (downloaded September 2018: 152927 entries) and the DENV-2 New Guinea C strain (GenBank accession number: AF038403) using the SEQUEST algorithm. Peptide precursor mass tolerance was set at 10 ppm, and MS/MS tolerance was set at 0.6 Da. Search criteria included oxidation of methionine (+15.9949) as a variable modification and carbamidomethylation of cysteine (+57.0214) and the addition of the TMT mass tag (+229.163) to peptide N-termini and lysine as fixed modifications. Searches were performed with full tryptic digestion and a maximum of 2 missed cleavages were allowed. The reverse database search option was enabled and all data was filtered to satisfy false discovery rate (FDR) of 5%. The main search was done by Dr Kate Heesom and the ThermoFischer .msf file and excel spreadsheet produced for further analysis. The above proteomics analysis, and as such the protocols listed in sections 2.7.2 and 2.7.3, are provided as a service from the faculty proteomics facility.

2.8 Quantification and bioinformatics analysis

The raw dataset was filtered to exclude proteins identified by less than 2 peptides. The data was then analysed further using the Perseus software application (Tyanova *et al*.,

2016). The ratios were log2 transformed and normalised by subtraction of the median ratio in each comparison from the other ratios. Proteins were used for statistical analysis where a valid value was present for at least 2 of 3 experiments. An unpaired two-sample student *t-test* with the permutation-based FDR 0.05 was performed. Proteins that increased or decreased in amount (≥ 1.3 fold and ≥ 1.5 fold) in the condition under investigation compared to the control condition were analysed using the Database for Annotation, Visualization and Integrated Discovery (DAVID) version 6.8 (Huang *et al.,* 2009) and the Search Tool for the Retrieval of Interacting Genes/Proteins (STRING) 9.1 database (Franceschini *et al.,* 2013) to identify groups of functional enriched proteins corresponding to specific gene ontology terms and identify protein networks and processes over-presented in DENV infected cells.

The STRING analysis produces an interaction network with each protein represented as a node (labelled with the gene symbol) and predicted functional links shown by up to eight coloured lines representing different types of evidence for the link. STRING uses the following evidence terms: "Neighborhood" = genes in immediate neighbourhood on the genome; "Gene Fusion"; "Occurrence" = two genes have a similar phylogenetic profile; "Coexpression" = two genes have been detected to have similar expression profiles; "Experiments" = protein-protein interaction detected by physical association or co-localisation; "Database"= do the two genes occur in annotated pathways in databases; "Textmining" = protein is mentioned with other proteins in publications.

The FunRich program version 3.1.3 (Pathan *et al,* 2015) was used to identify overlapping of data sets and produce Venn diagram.

Following the HUGO Gene Nomenclature Committee's general guidelines (Wain *et al,* 2002), the protein names and symbols in this thesis are the same as the gene symbol, but not italicised.

2.9 Statistical analysis

Statistical analysis of significance was calculated by using Student's t-test and statistical significance was defined as P-value < 0.05. Data were analysed by using Excel program and GraphPad Prism program.

CHAPTER 3. OPTIMISATION OF METHODS FOR LC-MS/MS ANALYSIS OF CULTURE SUPERNATANTS

3.1 Introduction

The study of cell secretomes by high through-put proteomics is still a growing and developing field. Compared to the proteomic analysis of cell lysates there are a number of challenges that must be overcome. Methods must be determined and optimised to remove abundant bovine serum proteins present in typical cell culture media and concentrate the proteins in cell culture supernatants for subsequent LC-MS/MS analysis. The latter is important due to the decrease in concentration of cellular proteins that occurs, when they are secreted into the culture supernatant, which is much larger in volume compared to the cell volume. Additionally, it is not trivial to normalise the amounts of proteins present in different samples using a loading control, which is typical when analysing the amounts of proteins in cell lysates by Western blotting.

Highly abundant proteins in FBS, such as BSA and IgG, need to be removed, as much as possible, from cell culture supernatant samples before LC-MS/MS analysis, as they may mask the detection of lower abundant secreted proteins (Stastna and Van Eyk, 2012). To achieve this, in many previous secretomes studies, cultured cells were initially grown in media containing serum, before removal of the media, washing several times with PBS or SFM and changing the media to SFM. However, the details of each method varied. For example, in studies analysing the secretome of DENV-2 infected HepG2 cells, the cells were initially grown and infected in complete media (CM). Further incubation in CM occurred until 32 hpi when the cells were extensively washed with PBS followed by further incubation of the cells in SFM for 16 h before harvest and analysis (Higa *et al*., 2008; Caruso *et al*., 2017). Whereas in a study analysing the secretome study of chikungunya virus infected WRL68 cells, the cells were grown in CM overnight, infected in SFM and then extensively washed with SFM and incubated with SFM for a further 24 hpi before harvesting and analysis (Thio *et al*., 2015). Starving cells of serum and extensive washing

may affect normal cell growth and function, thus the effects of each protocol for secretome preparation requires validation to ensure the optimal growth of cells (Stastna and Van Eyk, 2012). Although previous studies revealed no significant differences in the growth of cells in SFM compared with CM, as determined by cell lysis and viability assays, they used different cell lines and conditions to those planned in this study (Higa *et al*., 2008; Thio *et al*., 2015).

An alternative approach to the use of SFM is to grow cells in CM throughout but remove highly abundant serum proteins such as albumin and IgG, before proteomic analysis. However, the depletion methods risk losing proteins bound with albumin and IgG (Stastna and Van Eyk, 2012).

Typically, cell culture supernatants need to be concentrated before proteomic analysis. Three major techniques are used for this purpose; ultrafiltration, precipitation and/or dialysis. The most common approach is to concentrate supernatants (both for LC-MS/MS and Western blotting) using membrane ultrafiltration concentrators. Different studies have used membranes with different molecular weight cut-offs, depending on the proteins to be analysed. Whilst proteins > 10 kDa in size were studied by Higa and colleagues (Higa *et al*., 2008), Caruso and colleagues used two ultrafiltration steps to isolate proteins < 10 kDa but > 3 kDa in size, as the study focused on an examination of the products of protein proteolysis (Caruso *et al*., 2017).

Protein precipitation techniques using reagents such as TCA/acetone and ethanol/acetone have also been used to concentrate and prepare cell culture supernatants for MS analysis and Western blotting (Geddes *et al*., 2015). Dialysis methods in which the cell culture supernatant is first dialysed against water/buffer using a cut-off membrane before concentration of the supernatant by vacuum concentration or ultrafiltration have also been used prior to MS analysis (Cao J *et al*., 2011; Romanello M. *et al*, 2014). Although dialysis is simple, it is time consuming, taking up to 2 days. A study that compared different secretome preparation methods using the culture supernatant from a hepatocellular carcinoma cell line, revealed that ultrafiltration was most efficient in terms of protein concentration whilst precipitation resulted in the highest amount of protein

identifications and a greater detection of low molecular weight proteins by MS analysis (Cao J *et al*., 2011).

Thus, the work reported in this chapter was aimed at developing a protocol to optimise the conditions required to prepare culture supernatants derived from DENV infected cells for proteomic analysis, whilst ensuring normal cell growth.

Results

To comprehensively analyse the cellular proteomes and secretomes of DENV and mock infected cells, simultaneous proteomic analysis of both cell lysates and the corresponding cell culture supernatants was planned. The time of harvest post-infection was chosen according to the results of previous proteomic analyses of DENV infected cells, done in the laboratory; 30 and 48 hpi for Huh-7 and HEK293T cells, respectively (Yousuf, 2016; Chiu *et al*., 2014). At these times the virus was still in the exponential phase of replication but there was little cell death. However, before the combined proteomic/secretome analyses could be undertaken, a number of optimisation experiments were done to determine the optimal conditions for secretome analysis, which had not previously been undertaken in the laboratory.

3.2 Establishment of conditions for minimising serum proteins in the secretome

Based on previous secretome studies (reviewed in section 3.1), it was planned to grow the cells in CM, prior to DENV infection and then exchange the media with SFM, after DENV infection, to ensure that abundant proteins contained in the FBS added to CM did not interfere with the secretome analysis. Furthermore, the washing step and change from CM to SFM were done immediately after infection, to prevent any interruption in protein secretion that may occur early after infection.

Initially, conditions were optimised to ensure removal of exogenous bovine serum proteins from the secretome. Uninfected Huh-7 cells were seeded and grown in CM for 24 h, at which point they were ~ 60-80% confluent. The CM was then removed and the cells extensively washed with PBS five times before replacing the media with either fresh CM

or SFM. The cells were incubated for up to 48 h after changing the media, to simulate the conditions to be used for viral infection. Analysis of the culture supernatants by SDS-PAGE and Coomassie blue staining revealed a protein of ~ 69 kDa, which is the molecular mass of BSA, in the culture supernatants prepared with CM, but no comparable band in the culture supernatants prepared using SFM after initial growth in CM (Figure 3.1A).

To ensure cells were not lost during the extensive wash procedure, the flasks were pre-coated with PDL before the cells were seeded into the flasks. The effect of PDL coating was tested, to ensure proteins in CM did not bind to the PDL. PDL coated flasks (with no cells) were incubated with either CM or SFM alone for 24 h followed by a 48 h incubation with SFM (without a washing step). To ensure sensitive detection of any serum proteins, the culture supernatants were concentrated by ultrafiltration, using a membrane with a 3 kDa cut-off and examined by SDS-PAGE and Coomassie blue staining (Figure 3.1B). An ultrafiltration device with a 3 kDa cut-off was chosen to retain as many secreted proteins as possible in the concentrated culture supernatants. Coating flasks with PDL did not result in the detectable (by Coomassie blue staining) retention of any proteins from CM.

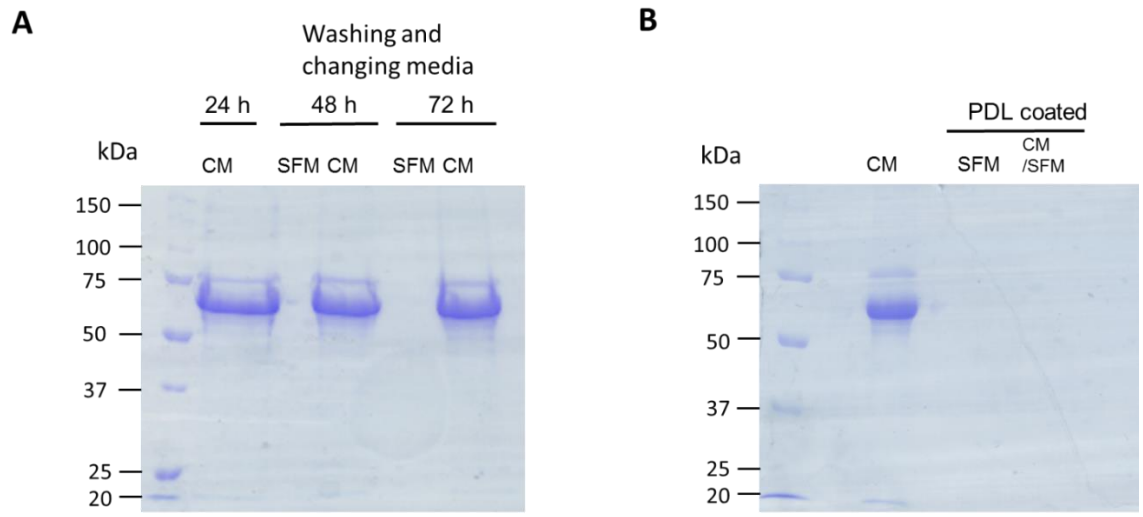

Figure 3.1 SDS-PAGE analysis of cell culture supernatants from cells grown in CM and SFM.

(A) Culture supernatants from Huh-7 cells grown in CM were harvested at 24, 48 and 72 h after seeding. Cells were seeded and grown in CM for 24 h before being washed with PBS and the media exchanged to SFM. The culture supernatant from cells further incubated in SFM were harvested at the same time point. Proteins in the cell culture supernatants (10 µl of each supernatant) were denatured in 2X sample buffer and analysed by 10% SDS-PAGE followed by Coomassie blue staining. **(B)** Flasks without cells were coated with PDL and then incubated with either SFM alone for 72 h, or complete media for 24 h followed by a 48 h incubation with SFM (COM/SFM). Equal volumes of media were then harvested and concentrated to the same volume (~ 40X) by ultrafiltration using a membrane with a 3 kDa cut-off (Amicon® Ultra 4 Centrifugal filter unit). Proteins in the concentrated media (10 µl of each supernatant) were denatured with 2X sample buffer and analysed by 10% SDS-PAGE and Coomassie blue staining. Concentrated CM (CM; not in contact with a PDL coated flask) was analysed in parallel as a control. The molecular masses (in kDa) of protein markers are shown on each figure.

The efficiency of the PBS wash step in the removal of serum proteins was examined in more detail. All cell lines planned to be used in this study (HEK293T, HEK293T-DV-Rep (REP) and Huh-7 cells) were seeded in PDL coated flasks and grown for 24 h in complete medium. The cells were then washed with PBS five times and SFM added to the flasks. Equal volumes of unconcentrated and ultrafiltration-concentrated cell culture supernatants were analysed by SDS-PAGE followed by Coomassie blue staining (Figure 3.2). Analysis of the unconcentrated cell culture supernatants showed that there were undetectable levels of protein after washing and growth in SFM. However, analysis of the concentrated cell culture supernatants revealed that despite the wash step there was still residual protein, of the size expected for BSA, in the media of some samples. By contrast, protein was not detected in the concentrated media that was obtained after incubation with PDL coated flasks in the previous experiment (Figure 3.1B), suggesting that the abundant protein observed may have been secreted from the cells.

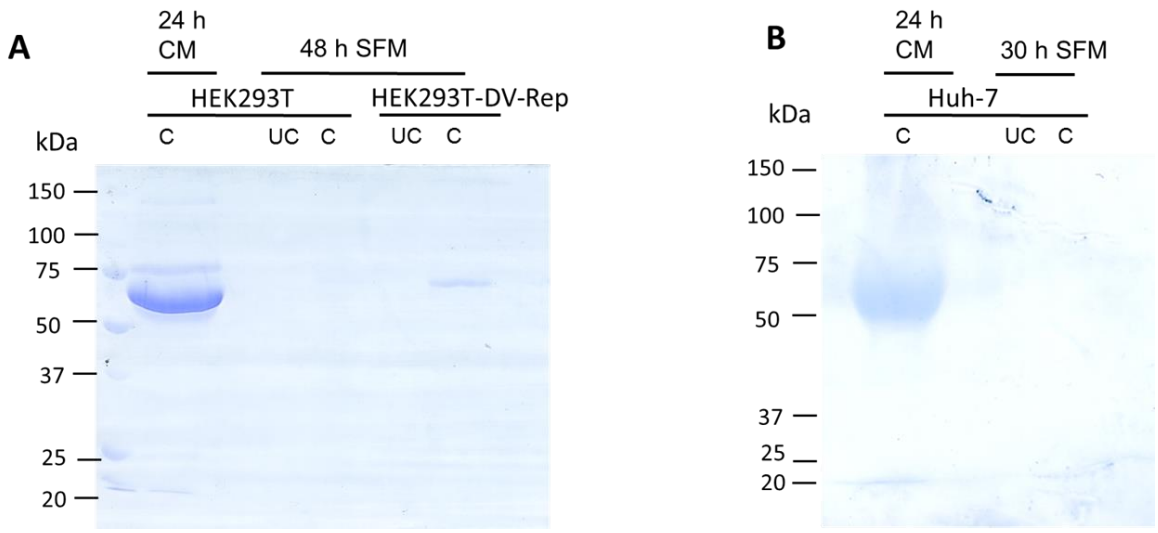

Figure 3.2 Analysis of concentrated cell culture supernatants from HEK293T, REP and Huh-7 cells grown in SFM.

HEK293T and REP **(A)** as well as Huh-7 **(B)** cells were grown in CM for 24 h until reaching 80% confluency before extensive washing with PBS. The cells were then grown in SFM for a further 48 h (HEK293T and HEK293T-DV-Rep) or 30 h (Huh-7). The cell culture supernatants, before media exchange (containing FBS; 24 h CM) and at harvest time (48 h or 30 h after media exchange) were collected and 4 ml of each supernatant concentrated to 90 µl. Twenty µl of the unconcentrated (UC) and concentrated (C) culture supernatants were analysed by 10% SDS-PAGE analysis and Coomassie blue staining. The molecular masses (in kDa) of protein markers are shown on each figure.

3.3 Effects of SFM on cell growth and virus infection

Growing cells in the absence of serum may affect cell growth and virus infection. The effects of serum starvation had not previously been tested using the cell lines and time points used in this study. Therefore, initially, Huh-7 and HEK293T cells were examined by microscopy after growth in CM for 24 h, washing with PBS and changing the media to SFM, for 30 and 48 h, respectively. The results revealed that the cells grown in SFM still had a normal healthy appearance and grew to confluency at a similar rate to cells grown in CM (data not shown). The viability of the HEK293T and Huh-7 cells after growth in CM or SFM (using the protocol described above) was then determined using a MTT assay (Figure 3.3). The results revealed that there was no significant change in the viability of HEK293T and Huh-7 cells grown in SFM compared with complete media with 78.7% (P-value = 0.20) and 77.8% (P-value = 0.33) viability for HEK293T and Huh-7 cells respectively.

To confirm that the growth of the cells in SFM did not affect DENV infection, HEK293T and Huh-7 cells were grown in CM, infected with DENV-2 at a MOI of 5, washed with PBS and then grown in SFM. At 30 and 48 hpi, for Huh-7 and HEK293T cells respectively, the cells were fixed and analysed by IFA using an anti-E antibody. The results showed that when the cells were grown in SFM conditions, the infection rate (determined by IFA) was still 90-95% of that using CM for both cell types (data not shown).

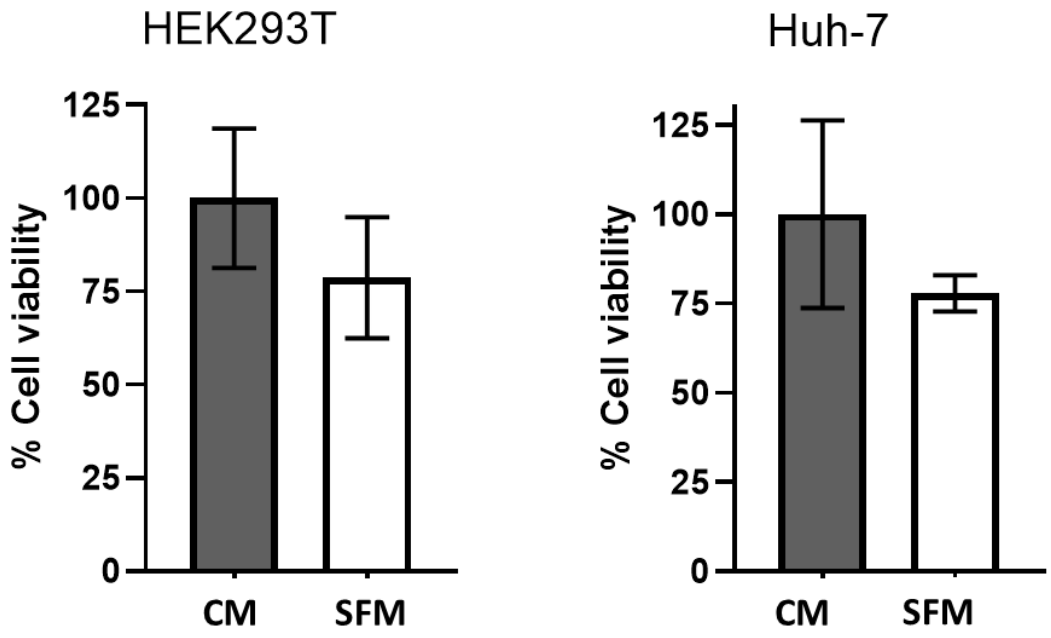

Figure 3.3 Cell viability testing of HEK293T and Huh-7 cells grown in media with or without serum.

The viability of HEK293T and Huh-7 cells grown in complete media (CM) and SFM was determined using a MTT test. Cells (1 x 10^4) were seeded into 8 wells of a PDL-coated 96 well-plate in CM for 24 h before being washed and the media changed to either SFM or SFM containing 10% FBS. After incubation in the respective media for 48 and 30 h for HEK293T and Huh-7 cells, respectively, the cell viability was tested using an MTT assay. Data are presented as the mean ± SEM. A two sample Student's *t-test* was used to compare the difference between the 2 groups. There was no statistically significant difference between cells grown in SFM containing 10 % FBS and SFM, (P-values of 0.20 and 0.33 for HEK293T and Huh-7 cells, respectively).

3.4 Detection of proteins in concentrated cell culture supernatants by SYPRO Ruby staining and LC-MS/MS.

The optimisation experiments showed that conditions had been established to produce cell culture supernatant samples for secretome analysis using SFM, with minimal effects on cell viability or virus infection efficiency, but with a large reduction in the protein/s derived from CM. However, after these procedures, proteins could not be detected in the concentrated supernatant samples by Coomassie blue staining (Figure 3.2). The more sensitive stain SYPRO Ruby was therefore used for protein detection. HEK293T and REP cells were seeded and grown in CM for 24 h. The HEK293T cells were then infected with DENV-2 (at MOI of 5) or mock infected. After infection, all cells were washed five times with warm PBS and further grown in SFM for 48 h. The cell culture supernatants (5 ml each) were collected and concentrated by TCA precipitation to a final volume of 80 µl (as described in section 2.3.1). Finally, the proteins in the concentrated supernatants (10 µl each) were analysed by 10% SDS PAGE followed by SYPRO Ruby staining (as described in section 2.3.5) as shown in Figure 3.4. The results showed the presence of proteins in the concentrated supernatants with a predominant protein with a size of ~ 69 kDa, most likely BSA.

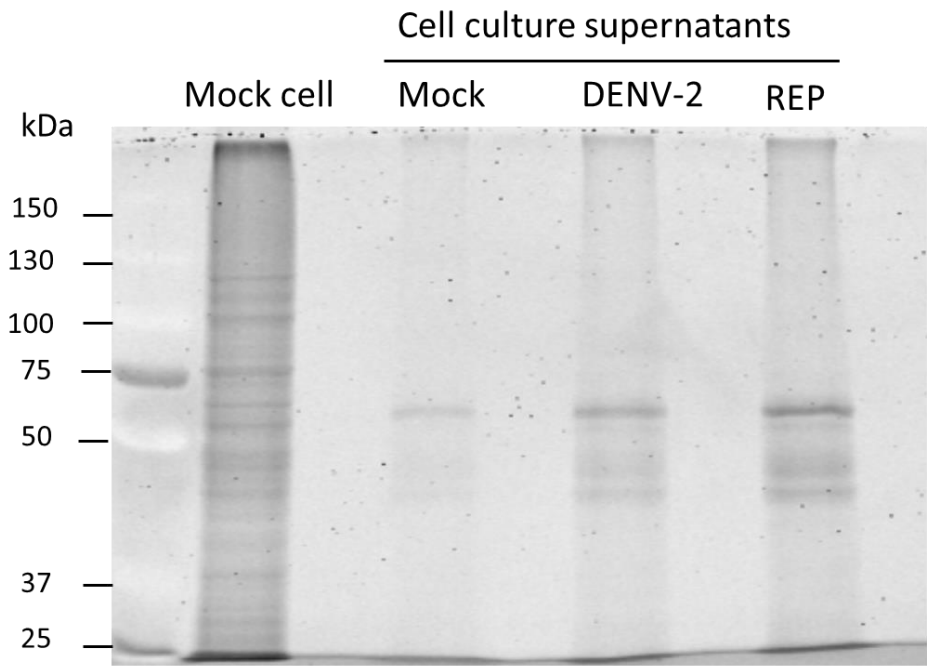

Figure 3.4 Analysis of concentrated cell culture supernatants from mock and DENV-2 infected HEK293T and REP cells.

HEK293T and REP cells were seeded and grown in CM for 24 h until reaching 80% confluency. The HEK293T cells then were DENV-2 (at MOI 5) or mock infected. After infection, all cells were washed five times with warm PBS and further grown in SFM. At 48 hpi, the cell culture supernatants were collected and concentrated by TCA precipitation. Twenty µg of mock infected HEK293T cells was used as control. Equal amounts (10 µl) of the concentrated culture supernatants were analysed by 10% SDS-PAGE and SYPRO Ruby staining. The molecular masses (in kDa) of protein markers are shown on the figure.

To determine whether the protocol established was suitable for the detection of proteins in the culture supernatants by LC-MS/MS, preliminary LC-MS/MS secretome analysis was performed using HEK293T cells. The cells were initially grown in a PDL coated flask in CM for 24 h, followed by PBS washing before further growth in SFM for 48 h. The cell culture supernatant was harvested and concentrated ~ 40X and then a sample (20 µl) analysed by LC-MS/MS. The MS/MS spectral files were searched against a list of bovine and human proteins, resulting in the identification of 1567 proteins. Of these proteins, 963 were identified by ≥2 peptides, there were 773 human proteins and 190 bovine proteins including BSA (Supplementary Table S 3.1).

The human proteins detected in secretome from HEK293T cells were analysed using the program STRING, to determine whether the proteins detected were typical of secreted proteins. The human proteins detected in secretome from HEK293T cells were significantly enriched in the GOBP terms "secretion by cell" (GO:0032940), "vesicle-mediated transport" (GO:0016192) and "cell activation involved in immune response" (GO:0002263) (Figure 3.5).

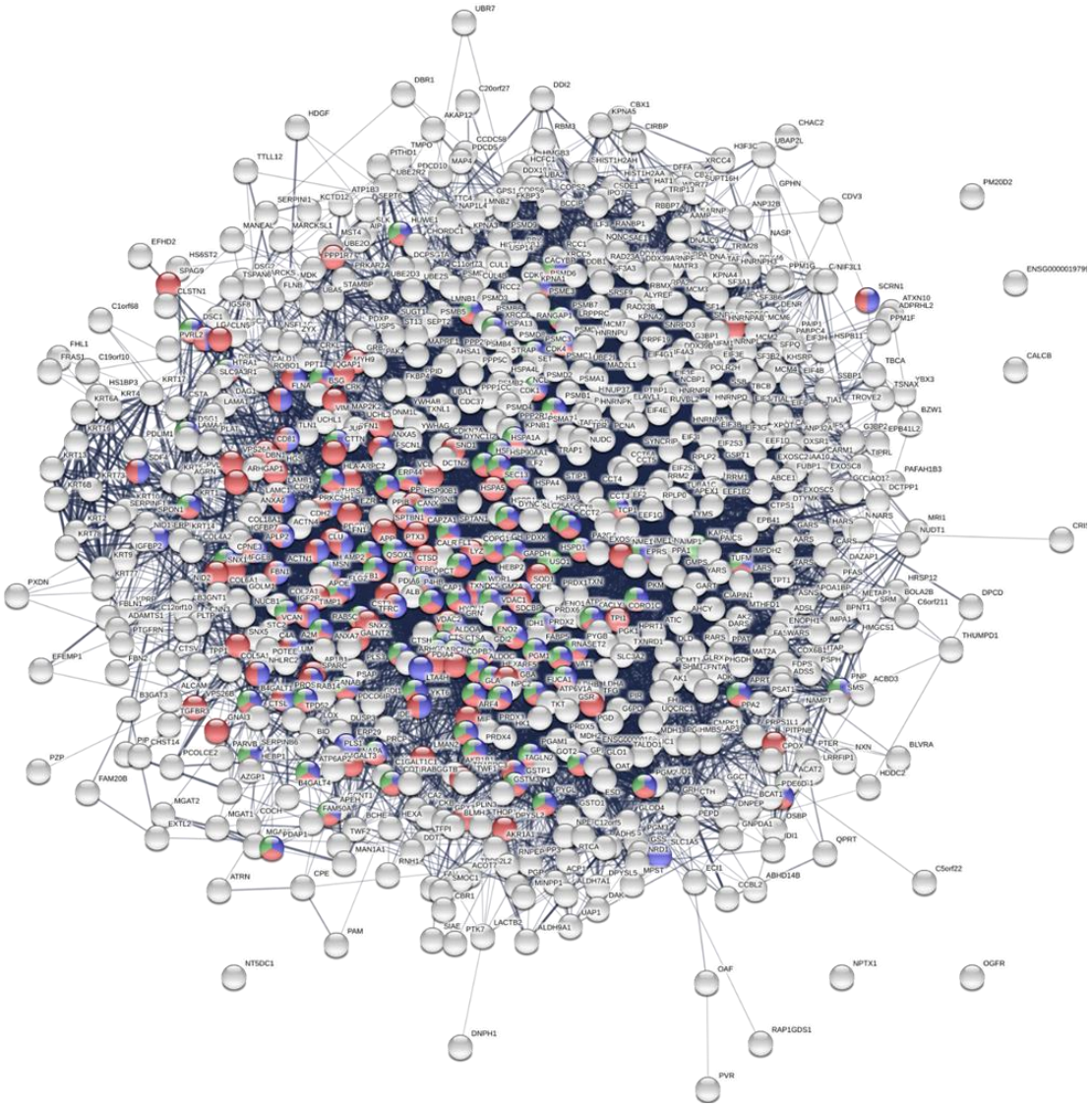

GO term/ pathway	Description	Count in gene set	FDR
GO:0032940	secretion by cell	122 of 959	1.47E-25
GO:0016192	vesicle-mediated transport	169 of 1699	3.67E-25
GO:0002263	cell activation involved in immune response	94 of 620	4.15E-24

Figure 3.5 STRING analysis of human proteins detected in the secretome of HEK293T cells.

The STRING database was searched to analyse human proteins detected in the secretome of HEK293T cells by LC-MS/MS. Nodes representing proteins associated with the significantly enriched GOBP terms "secretion by cell", "vesicle-mediated transport" and "cell activation involved in immune response" are shaded in blue, red and green, respectively. The number of coloured nodes/total proteins involved for each term and the FDR of each GO term are listed in the table.

Finally, to determine whether DENV infection had any major effect on the final yield of proteins using the protocol established, the protein amounts in the supernatants from mock and DENV-2 infected HEK293T and Huh-7 cells were estimated using a BCA assay (Figure 3.6). The estimate was performed for six samples in each group. For HEK293T cells, the amounts of protein in the concentrated supernatants from mock and DENV-2 infected cells were similar, with an average of 1761.7 and 1789.9 µg/ml, respectively (P-value= 0.93). Although the average amount of protein in the concentrated supernatants from mock infected Huh-7 cells was slightly higher than that from DENV-2 infected cells, this difference was not statistically significant (2762.2 and 2456.7 µg/ml, P-value = 0.61).

Supplementary Table

Table S 3.1 Preliminary LC-MS/MS analysis of the secretome from HEK293T cells

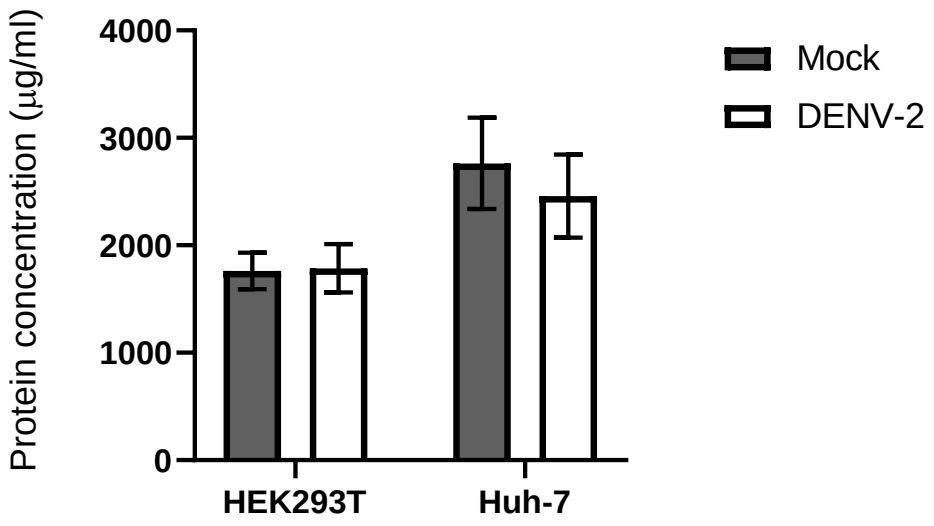

Figure 3.6 Determination of protein amounts in concentrated supernatants from DENV-2 and mock infected HEK293T and Huh-7 cells.

HEK293T and Huh-7 cells were grown in CM for 24 h before mock and DENV-2 (at MOI 5) infection. After infection cells were extensively washed and media was changed to SFM. At 48 and 30 hpi for HEK293T and Huh-7 cells respectively, cell culture supernatants were collected and concentrated ~ 40X with ultrafiltration technique. The protein amounts in concentrated supernatants were measured by BCA assay, n=6 in each group. Data are presented as the mean ± SEM. A two sample Student's *t-test* was used to compare the difference between the mock and DENV-2 group. The results showed no significant difference in protein amount between supernatants derived from mock and DENV-2 cells in both cell types, P-values of 0.93 and 0.61 for HEK293T and Huh-7 cells, respectively.

3.5 Discussion

This chapter describes the development of an optimised protocol that can now be used for secretome analysis by LC-MS/MS and Western blotting. In brief, cells were seeded in PDL-coated flasks and grown in CM for 24 h. After DENV infection, the cells were extensively washed with PBS and further incubated in SFM. At the time of harvest, the cell culture supernatants were collected and the supernatants were then concentrated by ultrafiltration. Furthermore, the cells remaining after removal of the culture supernatants can also be harvested and used to prepare cell lysates using standard methods, to allow simultaneous analysis of the proteome and secretome of DENV infected cells.

Reports in the literature of comprehensive proteomic studies analysing both the cellular proteome and secretome are limited, and there are none for DENV. A previous study which investigated the subcellular proteome and secretome of influenza A virus infected human primary macrophages analysed cell lysates grown in CM whilst the secretomes were separately prepared using SFM conditions (Lietzen *et al*., 2011). In contrast, this study was designed to analyse cell lysates and secretomes from cells grown under the same experimental conditions to better correlate any changes in the proteome and associated secretome. Thus, the cells were grown under SFM conditions. The viability of HEK293T and Huh-7 cells grown under in CM and then abruptly exchanged into SFM conditions, rather than undergoing a slower adaptation process (Beltran Paschoal *et al*, 2014) has not been reported. Therefore, the viability of cells grown under the established protocol were verified using an MTT assay, which is more sensitive than trypan blue staining. Furthermore, growth of the cells in SFM had no obvious effect on the efficiency of DENV at high MOI as determined by IFA. In a previous study, which analysed DENV-2 infected HepG2 cells, the effect of SFM on cell growth was also verified using both trypan blue staining and a MTT assay (Higa *et al*., 2008). However, Higa's study used a low MOI (MOI of 1) for DENV-2 infection and did not describe the effect of the SFM cell growth conditions on infection.

The proteins present in the concentrated supernatants from HEK293T and Huh-7 cells could not be detected by Ponceau and/or Coomassie blue staining. Thus, the more sensitive SYPRO Ruby staining method was used, which demonstrated that proteins were

present in the prepared samples. Finally, a preliminary LC-MS/MS analysis was done to confirm the presence of proteins in the secretome prepared with the optimised protocol. Although the cells were extensively washed before changing to SFM, some bovine proteins were still detectable by LC-MS/MS results. However, a much greater number of human proteins were detected than bovine proteins, which could also be discriminated as contaminants by the analysis. The residual bovine proteins detected may be due to binding of the bovine proteins to cells, as the PDL coating did not appear to result in binding of bovine proteins to the culture vessel (Figure 3.1B). Furthermore, many of the human proteins detected in secretome of HEK293T cells were associated with the GOBP terms "secretion by cell" and "vesicle-mediated transport", ensuring that the protocol resulted in the detection of secreted proteins.

The preliminary secretome results were compared with the results of a previous study which analysed the secretome of HEK293T cells. In the study of Kuhn *et al*., (Kuhn *et al*., 2015) the secretome of HEK293T cells that either overexpressed or were depleted of signal peptide peptidase-like 3 (SPPL3), were analysed by label free LC-MS/MS. A total of 428 proteins were reliably identified, compared with 963 human proteins in the preliminary MS analysis (a comprehensive analysis of the proteins identified in each study is described in Chapter 4). In Kuhn's study (Kuhn *et al*., 2015) the HEK293T cells were grown in CM. The cell culture supernatants were then concentrated by ultrafiltration and depleted of ALB; however, this approach did not effectively remove all bovine proteins which may have led to a lower number of identifications by LC-MS/MS analysis. Overall, the results obtained in the preliminary analysis demonstrated that the protocol established in this study had the sensitivity required for a full-scale analysis.

There are lots of challenges in secretomic analysis that need to be considered and potentially improved. Firstly, the best way to minimise contamination with bovine proteins. The abundance of these proteins, if not removed, will interfere with the LC-MS/MS analysis. Growing cells in SFM may affect cell growth and metabolism. Starvation of FBS may skew normal cell metabolic processes, especially energy metabolism, and may affect the levels of proteins involved in these processes. There might be more protein and/or fatty acid break down in order to produce more energy. In contrast, growing cells in CM and

followed by ALB depletion would maintain normal cell growth and metabolism but could still lead to excessive amounts of BSA and other bovine serum proteins as mentioned before. A second consideration is the method of concentration. Ultrafiltration provides the best results for protein concentration but can lead to a loss of low molecular weight and hydrophilic proteins (Cao J *et al*., 2011). Finally, validation after LC-MS/MS analysis is still a problem in secretome studies as depending on the cell type, the secreted proteins may be present in low amounts in the cell culture supernatants. Additionally, unlike the analysis of intracellular proteins, there are no standard loading controls for secretome analysis. The results presented in this chapter (Figure 3.6) imply that equal volumes of concentrated supernatants could be used for validation by Western blotting because they contained equal total amounts of protein. However, even small amounts of residual bovine serum proteins have the potential to skew the results.

In summary, a protocol for the analysis of the secretome derived from DENV-2 infected cells was established, based on the growth of cells in SFM. This protocol can now be combined with intracellular protein analysis to undertake a simultaneous proteomic and secretomic analysis of DENV infected cell by high-throughput LC-MS/MS, as described in Chapters 4 and 5.

CHAPTER 4. HIGH THROUGHPUT PROTEOMIC ANALYSIS OF THE PROTEOME AND SECRETOME OF DENV INFECTED AND DENV REPLICON CONTANING HEK293T CELLS

4.1 Introduction

Similar to other RNA viruses, DENV replication relies heavily on the subversion of normal host cell processes, resulting in the dysregulation of host gene expression and protein amounts. Thus, investigations aiming to define the changes that occur in the host proteome in response to DENV infection have the potential to identify key host proteins and processes required for viral replication. However, limited studies have been done on the effects of DENV replication on proteins secreted from cells, known as the host cell secretome; these proteins function in cell-cell signal transduction and play key roles in the host immune response. Therefore, studying the effects of DENV replication on the proteome and secretomes of different cell populations will not only identify intracellular targets for antiviral strategies but will increase our understanding of how infection disrupts communication between cells, ultimately resulting in DEN pathogenesis. A number of studies have previously analysed changes in cellular protein amounts in response to DENV infection *in vitro* (reviewed in Chapter 1, Table 1.2), however few of these studies used high throughput proteomic approaches (Pando-Robles *et al*., 2014; Chiu *et al*., 2014; Miao *et a*l., 2019). Moreover, to date, no integrated analysis of the effect of DENV replication on both the cellular proteome and secretome has been done, either by traditional low throughput (2D SDS-PAGE) or high throughput LC-MS/MS based analysis.

Flavivirus replicon systems have been widely used to study flavivirus molecular biology and as platforms for antiviral screening. These replicons are virus subgenomic RNAs in which the virus structural genes have been deleted (either C-prM-E or prM-E) by reverse genetics whilst retaining the viral 5′ and 3′ UTRs and the non-structural genes essential for virus genome replication. The introduction of replicons into cell lines

permissive for virus replication results in autonomous replication of the replicon subgenome but does not result in the release of infectious virus particles. Replicons therefore provide a biosafe system for studying many aspects of virus replication. Replicons may be either transiently expressed in cell lines permissive for virus replication or continuously expressed. In the latter case, drug resistance markers and reporter genes are introduced into the viral genome in place of the structural genes, allowing selection and identification of cells containing the replicons (Ward and Davidson, 2008). Although replicon systems have been used to validate the results of proteomic and interactomic studies (Khadka *et al*, 2011), only limited studies have analysed changes in the proteome of replicon containing cell lines. Recently, Hafirassou and colleagues characterised the host protein-NS1 interactome using DENV replicons expressing FLAG and HA tagged NS1 proteins in three different cell lines (HeLa, Raji and HAP1) and a two-step co-IP approach followed by LC-MS/MS analysis (Hafirassou *et al*, 2017).

Although DENV replicons have widely been used as a biosafe platform for screening antiviral compounds (Ng *et al*., 2007), changes in the host cell, in response to replicon replication in comparison to viral infection have not been well characterised. A study directly comparing the proteomic changes that occur in a replicon cell line with the corresponding cell line that is DENV infected would fill this gap and provide more information on how specific viral processes effect the host response. To compare a replicon system with DENV infected cells, HEK293T cells stably expressing a DENV-2 subgenomic replicon (HEK293T-DV-Rep; REP) was used, this replicon represented the only available DENV replicon system in the laboratory at the commencement of this study.

The HEK293 cells and derivatives including HEK293T cells are widely used for transient gene expression studies as they have a high transfection efficiency. HEK293 cells are also widely used for recombinant protein production (Thomas and Smart, 2005; Petiot *et al*., 2015). As HEK293 cells are permissive for DENV infection, they have also been used for DENV infection experiments especially when coupled with transient gene expression studies (Hannemann *et al*., 2013; Tongluan *et al*., 2017). Furthermore, HEK293 cells were found to provide a good *in vitro* model for DENV-induced chemokine studies (Medin *et al*., 2005).

The investigations described in this chapter aimed to determine the effect of DENV replication on the cellular proteome and secretome of HEK293T cells, either during DENV-2 infection or using REP cells, compared to mock infected cells. The results were subjected to bioinformatic analysis to explore the effect of DENV infection and viral replication on host biological processes and to identify similarities and differences in host protein dysregulation between DENV infected and replicon containing cells.

Results

4.2 Preparation of cell lysates and concentrated cell culture supernatants from DENV-2 and mock infected HEK293T cells and REP cells for proteomic analysis.

To analyse the effects of DENV-2 on the proteome and secretome of HEK293T cells, these cells were infected with DENV-2 at MOI of 5 or mock infected. Before infection, the cells were grown in CM. After infection the cells were washed extensively with PBS and then grown in SFM for 48 h, at which time the culture supernatants and cells were harvested. REP cells were also prepared at the same time using the same conditions (except for infection). At 48 hpi, the cell culture supernatants were harvested and concentrated and the corresponding cells were harvested in RIPA buffer to produce cell lysates (Figure 4.1). The infection rate was estimated to be 95%-100% by IFA (Figure 4.2A) and the presence of the replicon in the REP cells was verified by the detection of GFP and the DENV NS1 protein by IFA (Figure 4.2B). The experiments were performed independently in triplicate. The amount of protein in the concentrated supernatants and cell lysates was measured by BCA assay and samples containing equal amounts of protein were then sent for TMT labelling and LC-MS/MS analysis at the Faculty Proteomics facility (done by Dr Kate Heesom and co-workers).

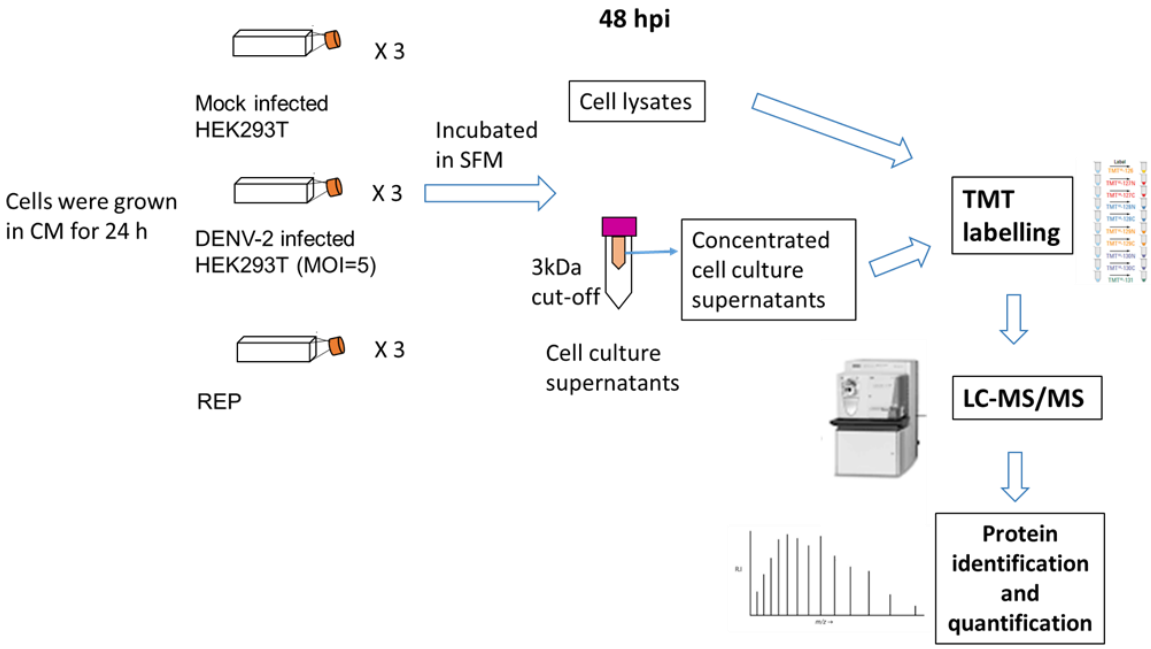

Figure 4.1 Diagram of workflow to analyse the proteomes and secretomes of DENV-2 infected HEK293T cells and REP cells.

In brief, HEK293T and REP cells were grown in CM for 24 h, then infected with DENV-2 or mock infected. After infection, the cells were extensively washed with PBS and further grown in SFM for 48 h. At 48 hpi, the cells were harvested and used to produce lysates and the cell culture supernatants were concentrated by centrifugation. Experiments were done in triplicate. Cell lysates and concentrated supernatants were TMT labelled and analysed by LC-MS/MS.

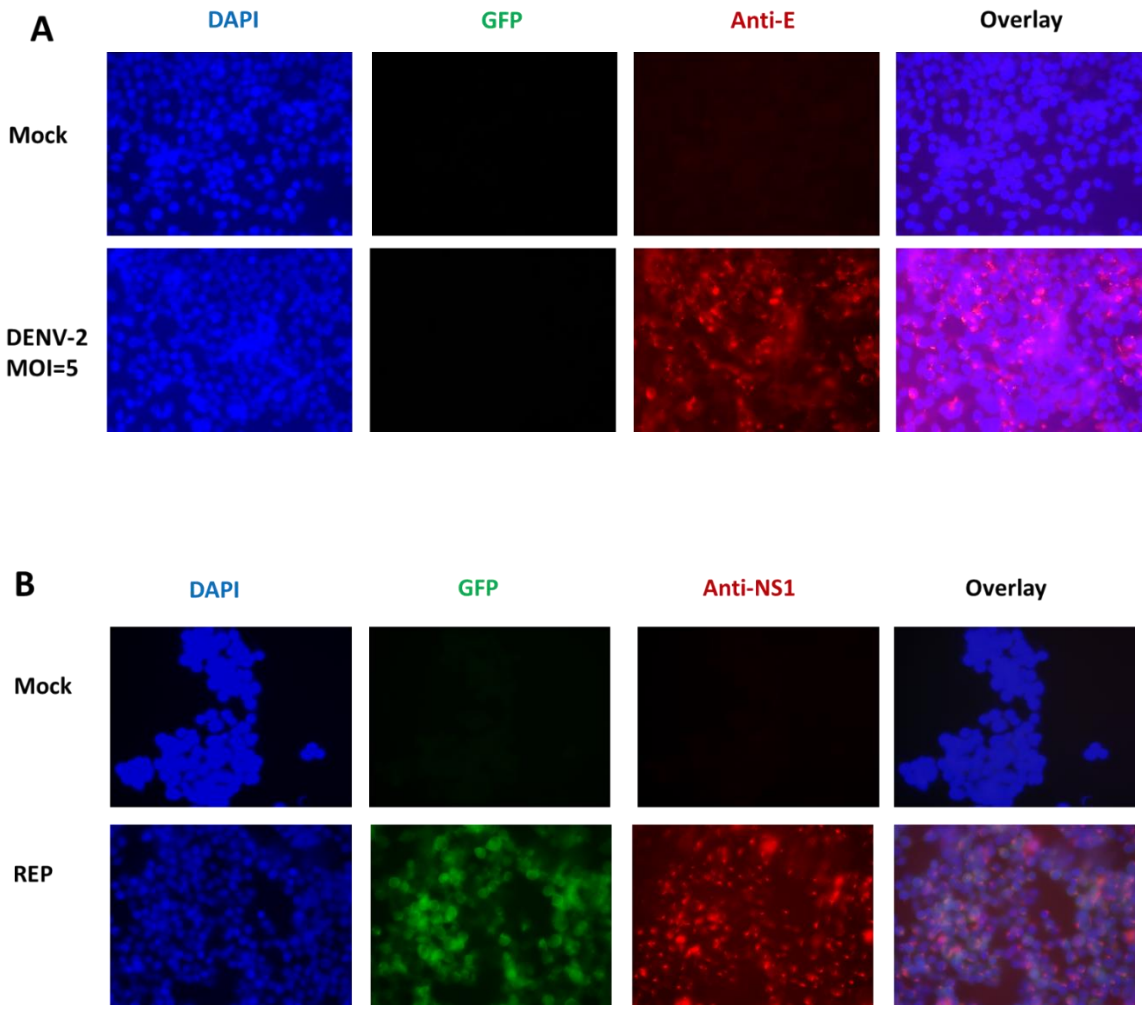

Figure 4.2 IFA analysis of HEK293T cells infected with DENV-2 or mock infected, and REP cells.

(A) HEK293T cells were infected with DENV-2 or mock infected. After 48 h of incubation in SFM, the cells were fixed with ice cold methanol and immunostained with an antibody against the DENV-2 E protein (Anti-E, red), nuclear DNA was visualised with DAPI (blue). (B) REP cells, after 48 h of incubation in SFM, were fixed with ice cold methanol and immunostained with an antibody against the DENV-2 NS1 protein (Anti-NS1, red). Cells were examined for the presence of GFP (green), nuclear DNA was visualised with DAPI (blue). Images were taken using a Leica widefield microscope with 40X magnification.

4.3 Quantitative LC-MS/MS analysis

The spectral files from the LC-MS/MS analysis of the cell lysates and concentrated supernatants from DENV and mock infected HEK293T cells and the REP cells were analysed using Proteome Discoverer 2.1 to identify and quantify proteins. The human Uniprot list, common contaminant list as well as the individual proteins and complete polyprotein encoded by DENV-2 were used as the protein search lists. The proteins identified and quantitated in the cell lysates and concentrated cell culture supernatants are hereafter referred to as the "proteome" and "secretome", respectively. For the proteomes, a total of 8,139 proteins were identified. Of these proteins, 7,540 were reliably identified and quantified based on a ratio determined using ≥ 2 peptides. Subsequently, 7,250 proteins were processed for statistical analysis using the Perseus program; inclusion of proteins in this group required that they were quantified in at least two of the three experiments in each group. The significance of the change in protein abundance was determined over the three experiments using an unpaired two-sided Student's *t-test* and a significant change defined as $p < 0.05$. Finally, the non-human contaminant proteins were excluded, leaving 7,217 human proteins for further bioinformatic analysis.

For the secretomes, a total of 5,369 proteins were identified, of which 4,579 proteins were reliably identified and quantified based on a ratio determined using ≥ 2 peptides. 3,960 proteins that were quantified in at least two of the three experiments in each group were processed by statistical analysis as described above. After excluding non-human proteins, there were 3,867 human proteins that were used for further bioinformatic analysis.

The protein abundance in the proteomes and secretomes from DENV-2 infected and REP cells were compared with their abundance in mock infected cells (Supplementary Tables S4.1-4.2). The number of proteins in the proteomes and secretomes that increased or decreased in abundance with fold change cut-off values of ≥ 2, ≥ 1.5 and ≥ 1.3 in each of the conditions are summarised in Tables 4.1 and 4.2.

Table 4.1 The number of host *p*roteins that changed in abundance in the <u>proteome</u>s of DENV-2 infected HEK293T and REP cells compared with mock infected cells.

	Number of proteins changed in abundance		Number of proteins significantly changed in abundance (P-value < 0.05)	
	DENV-2 /Mock	REP/Mock	DENV-2 /Mock	REP/Mock
Increased ≥ 2 fold	14	181	3	159
Increased ≥ 1.5 fold	335	789	168	616
Increased ≥ 1.3 fold	1159	1577	422	1203
Decreased ≥ 2 fold	16	301	1	283
Decreased ≥ 1.5 fold	145	852	31	752
Decreased ≥ 1.3 fold	683	1480	115	1118

Table 4.2 The number of host proteins that changed in abundance in the <u>secretomes</u> from DENV-2 infected HEK293T and REP cells compared with mock infected cells.

	Number of proteins changed in abundance		Number of proteins significantly changed in abundance (P-value < 0.05)	
	DENV-2 /Mock	REP/Mock	DENV- /Mock	REP/Mock
Increased ≥ 2 fold	12	267	5	164
Increased ≥ 1.5 fold	129	599	29	368
Increased ≥ 1.3 fold	445	899	82	490
Decreased ≥ 2 fold	12	256	2	209
Decreased ≥ 1.5 fold	119	662	23	472
Decreased ≥ 1.3 fold	391	1065	50	638

By MS analysis, all DENV-2 structural and NS proteins and NS proteins only were detected in the proteome of DENV-2 infected and REP cells respectively by MS analysis, respectively. While all structural proteins, NS1, NS4B and NS5 and NS1, NS4B and NS5 were detected in secretomes of DENV-2 infected and REP cells, respectively. The % coverage, number of peptides, unique peptides and peptide-to-spectrum match (PSMs) of DENV-2 proteins detected in the proteomes/secretomes of DENV-2 infected HEK293T and REP cells are summarised in Table 4.3.

Table 4.3 DENV-2 proteins detected in DENV-2 infected HEK293T and REP cells.

Description	MW (kDa)	Proteomes				Secretomes			
		% coverage	Peptides	Unique Peptides	PSMs	% coverage	Peptides	Unique Peptides	PSMs
C*	13.2	44.74	6	6	10	15.79	2	2	2
E*	54.3	30.91	14	14	60	22.63	11	11	16
pr*	18.7	20.61	3	3	6	9.09	1	1	1
NS1	39.9	50.28	19	2	62	53.13	24	3	144
NS2A	23.7	11.47	2	2	3	ND	ND	ND	ND
NS2B	14	16.15	2	2	4	ND	ND	ND	ND
NS3	69.3	66.67	42	35	88	ND	ND	ND	ND
NS4A	14	19.69	2	2	3	ND	ND	ND	ND
NS4B	26.8	6.05	2	1	4	3.23	1	1	3
NS5	103.1	51.44	47	41	83	2.11	2	2	2

* detected in DENV-2 but not REP cells at a > 2 fold change compared to mock infected cells.

ND = not detected

Overall, the number of proteins that changed in abundance in the proteome and secretome of DENV-2 infected cells compared with mock infected cells increased rather than decreased (Tables 4.1 and 4.2). Moreover, there were a greater number of proteins that significantly changed in abundance in both the proteome and secretome of REP cells than those of DENV-2 infected cells.

Proteins that significantly changed in abundance in the proteomes/secretomes of DENV-2 infected and REP cells compared with mock infected cells, with a fold change in abundance cut-off of ≥ 1.5, were selected for further downstream bioinformatics analysis. The proteins that met this cut-off in the proteomes and secretomes from DENV-2 infected cells compared with mock infected cells are listed in Tables 4.4 and 4.5, respectively. The proteins that significantly changed in the proteomes and secretome of REP cells compared to mock infected cells are listed in Supplementary Table S4.1.

Table 4.4 Proteins that significantly changed ≥ 1.5 fold in abundance in <u>proteomes</u> of DENV-2 infected HEK293T cells compared to mock infected cells.

Accession	Description	Gene	Fold change DENV-2/Mock	P-value
Significantly increased ≥1.5 fold in proteome of DENV-2 infected HEK293T				
P56199	Integrin alpha-1	*ITGA1*	2.24	4.43E-02
Q9P2F9	Zinc finger protein 319	*ZNF319*	2.17	8.78E-03
Q6IAQ2	SDHC protein	*SDHC*	2.10	4.82E-02
Q5T8I3	Protein FAM102B	*FAM102B*	1.90	1.80E-02
Q9NX18	Succinate dehydrogenase assembly factor 2, mitochondrial	*SDHAF2*	1.88	9.91E-03
H3BQT6	Tyrosine-protein phosphatase	*PTPN9*	1.87	3.41E-02
Q9UEI6	Polio virus related protein 2, alpha isoform	N/A	1.82	4.04E-02
A0A024R5K5	Alpha-1,3-glucosyltransferase	*ALG8*	1.81	2.53E-02
Q9HB66	Alternative protein MKKS	*MKKS*	1.79	1.06E-02
E9PJL9	NADH dehydrogenase [ubiquinone] flavoprotein 1, mitochondrial	*NDUFV1*	1.78	4.54E-02
Q15651	High mobility group nucleosome-binding domain-containing protein 3	*HMGN3*	1.76	2.87E-02
J3QL06	Hypoxia up-regulated protein 1	*HYOU1*	1.75	1.19E-04
B2R749	Cell division cycle associated 3	CDCA3	1.75	1.36E-02
B7Z2V6	Vacuolar ATP synthase catalytic subunit A, ubiquitous isoform	*ATP6V1A*	1.75	2.20E-02
Q9Y5J6	Mitochondrial import inner membrane translocase subunit Tim10 B	*TIMM10B*	1.75	3.38E-02
H0Y9Z5	CCR4-NOT transcription complex subunit 6-like (Fragment)	*CNOT6L*	1.74	3.66E-02
O14548	Cytochrome c oxidase subunit 7A-related protein, mitochondrial	*COX7A2L*	1.73	2.13E-02
D6RB85	Calnexin	*CANX*	1.73	6.11E-03
P04179	Superoxide dismutase [Mn], mitochondrial	*SOD2*	1.72	3.92E-02
Q69YU5	Uncharacterized protein C12orf73	*C12orf73*	1.71	2.07E-02
Q496I0	COX7A2 protein	*COX7A2*	1.71	3.33E-02
Q9NX40	OCIA domain-containing protein 1	*OCIAD1*	1.71	4.22E-03
P05114	Non-histone chromosomal protein HMG-14	*HMGN1*	1.71	1.83E-02
A0A024R9G3	Derlin	*DERL1*	1.70	2.64E-02
Q9NUJ1	Mycophenolic acid acyl-glucuronide esterase, mitochondrial	*ABHD10*	1.69	4.01E-02
A8K7T4	Lectin, mannose-binding 2 (LMAN2), mRNA	*N/A*	1.68	1.87E-02

P15954	Cytochrome c oxidase subunit 7C, mitochondrial	*COX7C*	1.68	8.53E-03
A0A2P9AUF2	Pyruvate carboxylase	*pyc*	1.66	1.25E-02
A0A024RC97	Phosphatidylserine synthase 2, isoform	*PTDSS2*	1.66	1.22E-02
Q9BQE4	Selenoprotein S	*SELENOS*	1.66	1.88E-02
B2R761	Sterol carrier protein 2 (SCP2), mRNA	*N/A*	1.66	3.81E-02
Q92520	Protein FAM3C	*FAM3C*	1.66	3.06E-02
P48380	Transcription factor RFX3	*RFX3*	1.66	4.39E-02
Q7Z4X2	Neuronal protein	*N/A*	1.66	3.65E-02
Q0IIN1	Keratin 77	*KRT77*	1.65	1.74E-02
P53370	Nucleoside diphosphate-linked moiety X motif 6	*NUDT6*	1.65	2.75E-02
Q6DKI0	Raptor protein (Fragment)	*raptor*	1.65	3.40E-02
Q6IB54	ATP synthase-coupling factor 6, mitochondrial	*ATP5J*	1.65	2.56E-02
D6W551	Chromosome 2 open reading frame 28, isoform	*C2orf28*	1.64	7.17E-03
Q4KWH8	1-phosphatidylinositol 4,5-bisphosphate phosphodiesterase eta-1	*PLCH1*	1.64	7.91E-03
O60637	Tetraspanin-3	*TSPAN3*	1.64	2.43E-02
Q6P587	Acylpyruvase FAHD1, mitochondrial	*FAHD1*	1.64	3.39E-02
Q92526	T-complex protein 1 subunit zeta-2	*CCT6B*	1.64	3.37E-02
H9STE0	Cytochrome c oxidase subunit 2	*COX2*	1.64	3.79E-02
B2R673	Dihydrolipoamide acetyltransferase component of pyruvate dehydrogenase complex	N/A	1.64	4.57E-02
H0YIC4	Citrate synthase (Fragment)	*CS*	1.63	4.83E-02
B9ECT5	NADH-ubiquinone oxidoreductase chain 4	*NADH4*	1.63	5.01E-02
A0A024R6A0	Arginase	*ARG2*	1.63	2.04E-02
P08962	CD63 antigen	*CD63*	1.62	3.59E-02
O95169	NADH dehydrogenase [ubiquinone] 1 beta subcomplex subunit 8, mitochondrial	*NDUFB8*	1.62	2.56E-02
P62072	Mitochondrial import inner membrane translocase subunit Tim10	*TIMM10*	1.62	3.55E-02
Q86U75	Dihydropyrimidinase-like 2	N/A	1.62	1.68E-02
A8K5D4	Myelin protein zero-like 1, isoform	*MPZL1*	1.61	2.94E-02
A0A024R8T9	Synaptogyrin	*SYNGR2*	1.61	1.75E-02
Q9BSF4	Mitochondrial import inner membrane translocase subunit Tim29	*TIMM29*	1.61	4.03E-02
B1Q2B0	URCC5	*URCC5*	1.60	5.11E-03
D3DP46	Signal peptidase complex subunit 3	*SPCS3*	1.60	2.66E-02

B2R6N9	Signal sequence receptor, alpha (translocon-associated protein alpha) (SSR1)	N/A	1.60	1.39E-02
Q9H490	Phosphatidylinositol glycan anchor biosynthesis class U protein	*PIGU*	1.60	4.17E-02
Q9NVV0	Trimeric intracellular cation channel type B	*TMEM38B*	1.60	2.10E-02
A0A024RCB3	Tetraspanin	*CD151*	1.59	2.36E-02
Q6IBA0	NADH dehydrogenase (Ubiquinone) Fe-S protein 5, 15kDa (NADH-coenzyme Q reductase)	*NDUFS5*	1.59	4.04E-02
Q9NX24	H/ACA ribonucleoprotein complex subunit 2	*NHP2*	1.59	2.62E-02
P36957	Dihydrolipoyllysine-residue succinyltransferase component of 2-oxoglutarate dehydrogenase complex, mitochondrial	*DLST*	1.59	2.76E-02
A0A1B0GW05	Probable C-mannosyltransferase DPY19L1	*DPY19L1*	1.58	2.37E-02
A0A0S2Z3G4	Frataxin isoform 1 (Fragment)	*FXN*	1.58	2.88E-02
G3V556	ATP synthase membrane subunit 6.8PL	*ATP5MPL*	1.58	2.67E-02
A4D1U3	Single-stranded DNA binding protein 1,	*SSBP1*	1.58	2.34E-02
B4DLN7	Cytochrome P450, family 20, subfamily A, polypeptide 1, transcript variant 1	N/A	1.58	4.73E-02
V9HWB4	Endoplasmic reticulum chaperone BiP	*HSPA5*	1.58	2.29E-02
Q59GX2	Solute carrier family 2 (Facilitated glucose transporter), member 1 variant	N/A	1.57	2.59E-02
A0A0R4J2F2	Claudin domain-containing protein 1	*CLDND1*	1.57	2.90E-03
A0A024RBY9	Cytochrome c heme lyase	*HCCS*	1.57	4.73E-03
P35914	Hydroxymethylglutaryl-CoA lyase, mitochondrial	*HMGCL*	1.56	2.83E-02
Q4QQP8	PTGFRN protein (Fragment)	*PTGFRN*	1.56	1.72E-02
P62487	DNA-directed RNA polymerase II subunit RPB7	*POLR2G*	1.56	4.28E-02
B3KQB4	PRA1 family protein	N/A	1.56	3.26E-02
O75381	Peroxisomal membrane protein PEX14	*PEX14*	1.56	3.33E-02
E5KSU5	Mitochondrial transcription factor A	*TFAM*	1.56	3.84E-02
Q9H173	Nucleotide exchange factor SIL1	*SIL1*	1.56	2.06E-02
E9PIE4	Mitochondrial carrier homolog 2 (Fragment)	*MTCH2*	1.56	1.69E-02
Q15907	Ras-related protein Rab-11B	*RAB11B*	1.56	3.84E-02
O60783	28S ribosomal protein S14, mitochondrial	*MRPS14*	1.56	2.43E-02
O75947	ATP synthase subunit d, mitochondrial	*ATP5PD*	1.56	4.74E-02

Q9BV79	Enoyl-[acyl-carrier-protein] reductase, mitochondrial	*MECR*	1.56	4.04E-02
B4DDK9	Alpha-1,6-mannosyl-glycoprotein2-beta-N- acetylglucosaminyltransferase	N/A	1.56	4.04E-02
Q9C0E8	Endoplasmic reticulum junction formation protein lunapark	*LNPK*	1.55	2.63E-02
O43181	NADH dehydrogenase [ubiquinone] iron-sulfur protein 4, mitochondrial	*NDUFS4*	1.55	3.32E-02
P11117	Lysosomal acid phosphatase	*ACP2*	1.55	3.19E-02
Q5RI15	Cytochrome c oxidase assembly protein COX20, mitochondrial	*COX20*	1.55	4.60E-02
Q9Y320	Thioredoxin-related transmembrane protein 2	*TMX2*	1.55	4.66E-02
Q9UII2	ATPase inhibitor, mitochondrial	*ATP5IF1*	1.55	2.93E-02
O00479	High mobility group nucleosome-binding domain-containing protein 4	*HMGN4*	1.55	3.52E-02
Q92791	Endoplasmic reticulum protein SC65	*P3H4*	1.55	2.58E-02
A0A024R9D2	Metadherin, isoform	*MTDH*	1.55	3.07E-02
A0A024R8S5	Protein disulfide-isomerase	*P4HB*	1.55	4.89E-02
Q68D91	Metallo-beta-lactamase domain-containing protein 2	*MBLAC2*	1.55	2.98E-02
Q9NWQ8	Phosphoprotein associated with glycosphingolipid-enriched microdomains 1	*PAG1*	1.55	3.72E-02
Q9HDC9	Adipocyte plasma membrane-associated protein	*APMAP*	1.55	3.85E-02
Q9HB40	Retinoid-inducible serine carboxypeptidase	*SCPEP1*	1.55	1.77E-02
Q9NPL8	Complex I assembly factor TIMMDC1, mitochondrial	*TIMMDC1*	1.54	3.61E-02
Q6ZMG9	Ceramide synthase 6	*CERS6*	1.54	2.85E-02
P30049	ATP synthase subunit delta, mitochondrial	*ATP5F1D*	1.54	3.19E-02
V9GYT7	PC4 and SFRS1-interacting protein (Fragment)	*PSIP1*	1.54	3.29E-02
O75380	NADH dehydrogenase [ubiquinone] iron-sulfur protein 6, mitochondrial	*NDUFS6*	1.54	4.16E-02
E9PKU7	Neutral alpha-glucosidase AB	*GANAB*	1.54	2.98E-02
O75844	CAAX prenyl protease 1 homolog	*ZMPSTE24*	1.54	3.58E-02
Q6P1L8	39S ribosomal protein L14, mitochondrial	*MRPL14*	1.54	4.07E-02
B2R9T9	Transmembrane protein 109	TMEM109	1.54	1.59E-02
B3KN15	Heparan sulfate 2-O-sulfotransferase 1	*HS2ST1*	1.53	4.02E-02
A0A0S2Z5H0	Mitochondrial ribosomal protein S28 isoform 2 (Fragment)	*MRPS28*	1.53	2.05E-02
A8K337	Catechol-O-methyltransferase domain containing 1 (COMTD1), mRNA	COMTD1	1.53	1.44E-02

Q5T6U8	High mobility group AT-hook 1	*HMGA1*	1.53	3.75E-02
Q5T1C6	Acyl-coenzyme A thioesterase THEM4	*THEM4*	1.53	4.35E-02
O43493	Trans-Golgi network integral membrane protein 2	*TGOLN2*	1.53	2.64E-02
Q9UDW1	Cytochrome b-c1 complex subunit 9	*UQCR10*	1.53	2.99E-02
A0A024RBE7	Thymopoietin, isoform	*TMPO*	1.53	4.49E-02
A0A024R4K3	Malate dehydrogenase	*MDH2*	1.53	4.81E-02
Q9H6E4	Coiled-coil domain-containing protein 134	*CCDC134*	1.52	4.44E-02
Q05DH5	EXTL2 protein (Fragment)	*EXTL2*	1.52	2.59E-02
P14927	Cytochrome b-c1 complex subunit 7	*UQCRB*	1.52	4.64E-02
Q5JTV8	Torsin-1A-interacting protein 1	*TOR1AIP1*	1.52	4.38E-02
E9PCR7	2-oxoglutarate dehydrogenase, mitochondrial	*OGDH*	1.52	4.62E-02
Q8N4H5	Mitochondrial import receptor subunit TOM5 homolog	*TOMM5*	1.52	1.39E-02
Q8NFQ8	Torsin-1A-interacting protein 2	*TOR1AIP2*	1.52	1.31E-02
H3BNX8	Cytochrome c oxidase subunit 5A, mitochondrial	*COX5A*	1.52	3.66E-02
A0A090N8Y2	Protein disulfide-isomerase A4	*ERP70*	1.52	4.31E-02
Q96BP2	Coiled-coil-helix-coiled-coil-helix domain-containing protein 1	*CHCHD1*	1.52	4.09E-02
Q09328	Alpha-1,6-mannosylglycoprotein 6-beta-N-acetylglucosaminyltransferase A	*MGAT5*	1.52	4.46E-02
Q3ZAQ7	Vacuolar ATPase assembly integral membrane protein VMA21	*VMA21*	1.52	1.22E-02
L0R6Q1	SLC35A4 upstream open reading frame protein	*SLC35A4*	1.52	4.83E-02
Q96AY3	Peptidyl-prolyl cis-trans isomerase FKBP10	*FKBP10*	1.52	1.48E-02
A0A087WSV8	Nucleobindin 2, isoform	*NUCB2*	1.52	4.94E-02
Q8N766	ER membrane protein complex subunit 1	*EMC1*	1.51	4.28E-02
P35609	Alpha-actinin-2	*ACTN2*	1.51	2.55E-02
Q13443	Disintegrin and metalloproteinase domain-containing protein 9	*ADAM9*	1.51	4.78E-02
V9HWF6	Alpha-1-acid glycoprotein	*ORM1*	1.51	1.03E-02
P51970	NADH dehydrogenase [ubiquinone] 1 alpha subcomplex subunit 8	*NDUFA8*	1.51	3.43E-02
A8K4V4	Mitochondrial ribosomal protein L43 (MRPL43), transcript variant 1	*MRPL43*	1.51	3.72E-02
E7EPT4	NADH dehydrogenase [ubiquinone] flavoprotein 2, mitochondrial	*NDUFV2*	1.51	1.74E-02

P61803	Dolichyl-diphosphooligosaccharide--protein glycosyltransferase subunit DAD1	*DAD1*	1.51	4.59E-02
Q9NPJ3	Acyl-coenzyme A thioesterase 13	*ACOT13*	1.51	3.05E-02
O95881	Thioredoxin domain-containing protein 12	*TXNDC12*	1.51	3.50E-02
B2R4A2	Cytochrome b-c1 complex subunit 7	N/A	1.51	3.88E-02
A0A024R8Q1	Glucosidase, alpha acid (Pompe disease, glycogen storage disease type II)	*GAA*	1.51	9.26E-03
Q99720	Sigma non-opioid intracellular receptor 1	*SIGMAR1*	1.51	4.90E-02
Q15084	Protein disulfide-isomerase A6	*PDIA6*	1.51	2.58E-02
A0A024RBS4	Scavenger receptor class B, member 1, isoform	*SCARB1*	1.51	3.11E-02
Q96EL3	39S ribosomal protein L53, mitochondrial	*MRPL53*	1.51	1.87E-02
A8K769	Secretory carrier-associated membrane protein	N/A	1.51	4.61E-02
A0A087WZE9	High mobility group nucleosome-binding domain-containing protein 3	*HMGN3*	1.50	3.80E-02
Q96HE7	ERO1-like protein alpha	*ERO1A*	1.50	2.67E-02
Q53GR7	Solute carrier family 25, member 13 (Citrin) variant (Fragment)	N/A	1.50	4.30E-02
Q9UKU7	Isobutyryl-CoA dehydrogenase, mitochondrial	*ACAD8*	1.50	4.12E-02
Q14165	Malectin	*MLEC*	1.50	4.87E-02
P16104	Histone H2AX	*H2AFX*	1.50	4.32E-02
P60468	Protein transport protein Sec61 subunit beta	*SEC61B*	1.50	2.39E-02
Q59E90	Alpha-mannosidase (Fragment)	N/A	1.50	4.07E-02
A8K2Q6	Peptidyl-prolyl cis-trans isomerase	N/A	1.50	2.09E-02
A0A2S1PH31	Methylmalonyl-CoA mutase variant	*MUT*	1.50	4.94E-02
B0QYW5	Peroxisomal membrane protein PMP34	*SLC25A17*	1.50	2.95E-02
B2R6X6	Peptidyl-prolyl cis-trans isomerase	N/A	1.50	4.29E-02
A0A024RDY3	Lysosomal-associated membrane protein 1	*LAMP1*	1.50	3.83E-02
B4E2S3	RFTN1 protein	*RFTN1*	1.50	2.73E-02
Q9BRX8	Redox-regulatory protein FAM213A	*PRXL2A*	1.50	3.35E-02
Q2M1J6	Oxidase (Cytochrome c) assembly 1-like	*OXA1L*	1.50	3.67E-02
A0A024R3C4	KDEL (Lys-Asp-Glu-Leu) containing 2, isoform	*KDELC2*	1.50	3.74E-02
Q5HYK3	2-methoxy-6-polyprenyl-1,4-benzoquinol methylase, mitochondrial	*COQ5*	1.50	2.89E-02
Significantly decreased ≥1.5 fold in proteome of DENV-2 infected HEK293T cells				
Q6FIC5	Chloride intracellular channel protein	*CLIC4*	0.67	3.35E-02
A8K646	Osteoclast stimulating factor 1 (OSTF1)	*OSTF1*	0.67	3.71E-02
Q12933	TNF receptor-associated factor 2	*TRAF2*	0.67	3.18E-02
H7C3M7	FERM, ARHGEF and pleckstrin domain-containing protein 2 (Fragment)	*FARP2*	0.67	3.63E-02

A0A024R6Q1	Eukaryotic translation initiation factor 5, isoform	*EIF5*	0.66	3.48E-02
F2Z2X4	Exportin-4	*XPO4*	0.66	1.49E-02
P43490	Nicotinamide phosphoribosyltransferase	*NAMPT*	0.65	3.50E-02
Q9C0D3	Protein zyg-11 homolog B	*ZYG11B*	0.65	3.02E-02
P30291	Wee1-like protein kinase	*WEE1*	0.65	1.72E-04
Q6FI81	Anamorsin	*CIAPIN1*	0.65	3.74E-02
O76064	E3 ubiquitin-protein ligase RNF8	*RNF8*	0.65	3.50E-02
O43639	Cytoplasmic protein NCK2	*NCK2*	0.64	3.64E-02
Q96D05	Uncharacterized protein FAM241B	*FAM241B*	0.64	1.59E-02
A0A024QZ45	BRCA1 interacting protein C-terminal helicase 1, isoform	*BRIP1*	0.64	2.69E-03
Q59FS2	ZNF589 protein variant (Fragment)	N/A	0.64	2.68E-02
A6NCF6	Putative MAGE domain-containing protein MAGEA13P	*MAGEA13P*	0.62	7.13E-03
O75953	DnaJ homolog subfamily B member 5	*DNAJB5*	0.61	2.40E-02
B4DUT8	Calponin	*CNN2*	0.61	1.99E-02
P31629	Transcription factor HIVEP2	*HIVEP2*	0.61	1.98E-02
Q8IXQ3	Uncharacterized protein C9orf40	*C9orf40*	0.60	3.98E-02
Q00534	Cyclin-dependent kinase 6	*CDK6*	0.60	2.96E-02
X6RLX0	ELKS/Rab6-interacting/CAST family member 1	*ERC1*	0.59	2.07E-02
Q8N9N8	Probable RNA-binding protein EIF1AD	*EIF1AD*	0.59	3.13E-02
P42677	40S ribosomal protein S27	*RPS27*	0.58	2.75E-02
O15541	RING finger protein 113A	*RNF113A*	0.58	3.07E-02
Q66K64	DDB1- and CUL4-associated factor 15	*DCAF15*	0.57	5.00E-02
B7ZLK1	KIAA0528 protein	*KIAA0528*	0.56	3.60E-02
P52788	Spermine synthase	*SMS*	0.56	7.80E-03
A0A024R2T2	KIAA1143, isoform	*KIAA1143*	0.55	3.00E-02
P02533	Keratin, type I cytoskeletal 14	*KRT14*	0.53	1.59E-02
Q8N612	FTS and Hook-interacting protein	*FAM160A2*	0.50	3.05E-02

Table 4.5 Proteins that significantly changed ≥ 1.5 fold in abundance in <u>secretomes</u> from DENV-2 infected HEK293T cells compared to mock infected cells.

Accession	Description	Gene	Fold change DENV-2 /Mock	P-value
Significantly increased ≥1.5 fold in secretome of DENV-2 infected HEK293T				
H3BMS5	PH domain leucine-rich repeat-containing protein phosphatase 2	*PHLPP2*	13.46	2.62E-03
B2R4R0	Histone H4	*HIST1H4L*	2.97	1.87E-02
Q12797	Aspartyl/asparaginyl beta-hydroxylase	*ASPH*	2.74	8.80E-04
Q7L5D6	Golgi to ER traffic protein 4 homolog	*GET4*	2.10	3.27E-02
Q15008	26S proteasome non-ATPase regulatory subunit 6	*PSMD6*	2.02	3.46E-02
Q9HBI1	Beta-parvin	*PARVB*	1.98	4.78E-02
O43345	Zinc finger protein 208	*ZNF208*	1.97	7.00E-03
P51784	Ubiquitin carboxyl-terminal hydrolase 11	*USP11*	1.81	2.30E-02
F8W8D3	Histone RNA hairpin-binding protein	*SLBP*	1.80	3.46E-02
Q9Y657	Spindlin-1	*SPIN1*	1.74	1.80E-02
A8K061	Angiopoietin-like 3, mRNA	N/A	1.69	4.81E-02
P22059	Oxysterol-binding protein 1	*OSBP*	1.67	5.04E-03
A0A024R1Z6	Vesicle amine transport protein 1 homolog	*VAT1*	1.64	1.52E-02
A8K5Y7	Exportin 5	*XPO5*	1.62	3.51E-02
E5KLL9	Mitochondrial dynamin-like 120 kDa protein	N/A	1.60	4.70E-02
P61225	Ras-related protein Rap-2b	*RAP2B*	1.60	4.84E-02
B5BU08	U2 small nuclear RNA auxillary factor 1 isoform a	*U2AF1*	1.59	3.56E-02
O60568	Procollagen-lysine,2-oxoglutarate 5-dioxygenase 3	*PLOD3*	1.58	1.88E-02
Q9BZX2	Uridine-cytidine kinase 2	*UCK2*	1.58	3.17E-02
O14929	Histone acetyltransferase type B catalytic subunit	*HAT1*	1.57	3.03E-02
P26599	Polypyrimidine tract-binding protein 1	*PTBP1*	1.56	4.52E-02
Q13162	Peroxiredoxin-4	*PRDX4*	1.56	5.42E-04
Q9BV44	THUMP domain-containing protein 3	*THUMPD3*	1.55	8.68E-03
Q86XP3	ATP-dependent RNA helicase DDX42	*DDX42*	1.54	3.97E-02
A0A023T6R1	Mago nashi protein	*FLJ10292*	1.54	2.50E-02
P25490	Transcriptional repressor protein YY1	*YY1*	1.53	4.23E-02
A0A024RC37	Uncharacterized protein	*P15RS*	1.50	1.31E-02
P13010	X-ray repair cross-complementing protein 5	*XRCC5*	1.50	2.54E-02

P48556	26S proteasome non-ATPase regulatory subunit 8	*PSMD8*	1.49	1.31E-02
Significantly decreased ≥1.5 fold in secreteome of DENV-2 infected HEK293T				
Q96BK5	PIN2/TERF1-interacting telomerase inhibitor 1	*PINX1*	0.66	2.48E-02
Q6IAX2	RPL21 protein	*RPL21*	0.66	1.92E-02
B2RDV7	tRNA-dihydrouridine(47) synthase	N/A	0.66	2.14E-02
Q03701	CCAAT/enhancer-binding protein zeta	*CEBPZ*	0.64	3.01E-02
B3KNS8	Surfeit locus protein 6	*SURF6*	0.64	2.28E-03
A0A024R0Z3	DEAD (Asp-Glu-Ala-Asp) box polypeptide 23	*DDX23*	0.64	1.85E-02
Q03164	Histone-lysine N-methyltransferase 2A	*KMT2A*	0.64	3.51E-02
O95292	Vesicle-associated membrane protein-associated protein B/C	*VAPB*	0.63	2.88E-02
A5D8W8	Gamma-glutamyltransferase 7	*GGT7*	0.63	4.46E-02
Q9Y4W2	Ribosomal biogenesis protein LAS1L	*LAS1L*	0.63	2.04E-02
A0A087WYZ4	Glycoprotein hormones alpha chain	*CGA*	0.62	1.26E-02
Q9UPN4	Centrosomal protein of 131 kDa	*CEP131*	0.61	3.88E-02
A0A0X1KG71	Negative elongation factor B	*NELFB*	0.58	2.95E-02
Q86UE8	Serine/threonine-protein kinase tousled-like 2	*TLK2*	0.55	1.97E-03
Q9Y4C8	Probable RNA-binding protein 19	*RBM19*	0.55	4.78E-02
Q15059	Bromodomain-containing protein 3	*BRD3*	0.55	4.77E-02
P49916	DNA ligase 3	*LIG3*	0.55	4.65E-02
Q6P1M0	Long-chain fatty acid transport protein 4	*SLC27A4*	0.55	4.38E-02
G5EA30	CUG triplet repeat, RNA binding protein 1	*CELF1*	0.54	3.88E-02
A0A0A0MQX1	Unconventional myosin-X	*MYO10*	0.54	1.64E-02
B2R5U7	CCAAT-box-binding transcription factor (CBF2)	N/A	0.53	1.22E-02
Q99442	Translocation protein SEC62	*SEC62*	0.43	8.22E-03
A0A0J9YXC7	LIM and senescent cell antigen-like-containing domain protein	*LIMS4*	0.43	4.50E-02

An integrated analysis of the proteins that significantly changed in both the proteomes and secretomes from DENV-2 infected HEK293T and REP cells compared to mock infected cells was done to determine the relationship of intracellular and secreted proteins (Figure 4.3A). There were 2,984 proteins that were commonly identified in both the proteomes and secretomes.

A less stringent cut-off (compared to the ≥ 1.5 fold cut-off used for the analysis of either data set alone) of a ≥ 1.3 fold change in abundance was applied for combined data analysis, to allow for proteins that altered in one data set but not to the threshold of 1.5 fold in the other dataset. The number of proteins that significantly changed ≥1.3 fold in amount in both the proteomes and secretomes from DENV-2 infected HEK293T and REP cells compared to mock infected cells are summarised in Figures 4.3B and 4.3C, respectively. There were only 5 common proteins that were significantly altered ≥1.3 fold in amount in the proteomes and secretomes from DENV-2 infected HEK293T cells compared to mock infected cells (listed in Table 4.6). Whereas, there were 309 common proteins that were significantly altered ≥1.3 fold in amount in the proteome and secretome of REP cells compared to mock infected cells (Figure 4.3C). Half of these proteins (150 of 309 proteins) were significantly decreased in both the proteomes and secretomes.

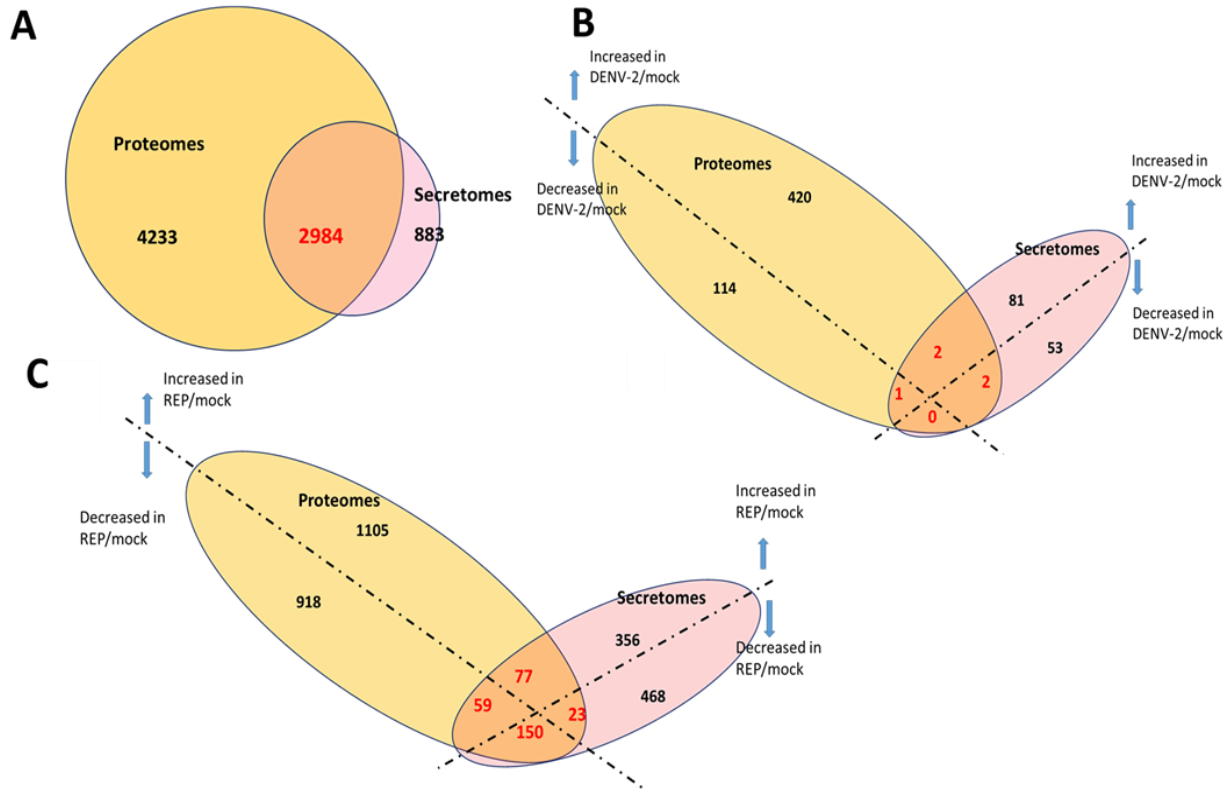

Figure 4.3 Overlap between proteins detected in proteomes and secretomes of DENV-2 infection and in REP cells.

(A) Venn diagram shows the number of proteins that were detected in either the proteomes or secretomes of DENV-2 infected HEK293T and REP cells, as well as those detected in both. **(B-C)** Venn diagram shows the number of proteins that significantly (P-value < 0.05) increased and decreased (≥1.3 fold) in the proteomes and secretomes from DENV-2 infected HEK293T **(B)** and REP **(C)** cells compared to mock infected cells.

Table 4.6 Host proteins that were significantly changed ≥ 1.3 fold in amount in both the proteomes and secretomes from DENV-2 infected HEK293T cells compared to mock infected cells.

Accession	Description	Gene	Proteome		Secretome	
			Fold change DENV-2/Mock	P-value	Fold change DENV-2/Mock	P-value
Increased in both cell lysates and secretomes						
Q8NFH4	Nucleoporin Nup37	*NUP37*	1.39	9.80E-03	1.45	4.09E-02
A0A024R9B7	Cytochrome c oxidase subunit VIc	*COX6C*	1.46	4.63E-02	1.45	3.55E-02
Increased in cell lysates but decrease in secretomes						
Q96KC8	DnaJ homolog subfamily C member 1	*DNAJC1*	1.30	2.30E-02	0.76	4.30E-02
O95292	Vesicle-associated membrane protein-associated protein B/C	*VAPB*	1.47	4.18E-02	0.63	2.88E-02
Decreased in cell lysates but increase in secretomes						
A8K646	Osteoclast stimulating factor 1	*OSTF1*	0.67	3.71E-02	1.47	2.83E-03

Proteins that were commonly altered in amount (increased and decreased) in proteomes and secretomes of DENV-2 infected and REP cells compared to mock infected cells were also identified (Figure 4.4). The proteins that were significantly altered ≥ 1.3 fold in the proteomes (n=304) and secretomes (n=56) from both DENV-2 infected and REP cells compared to mock infected cells are listed in Tables 4.7 and 4.8, respectively. Interestingly, nucleoporin Nup37 (NUP37) was the only protein that significantly increased ≥1.3 fold in the proteome and secretome of both DENV-2 infected and REP cells compared to mock infected cells.

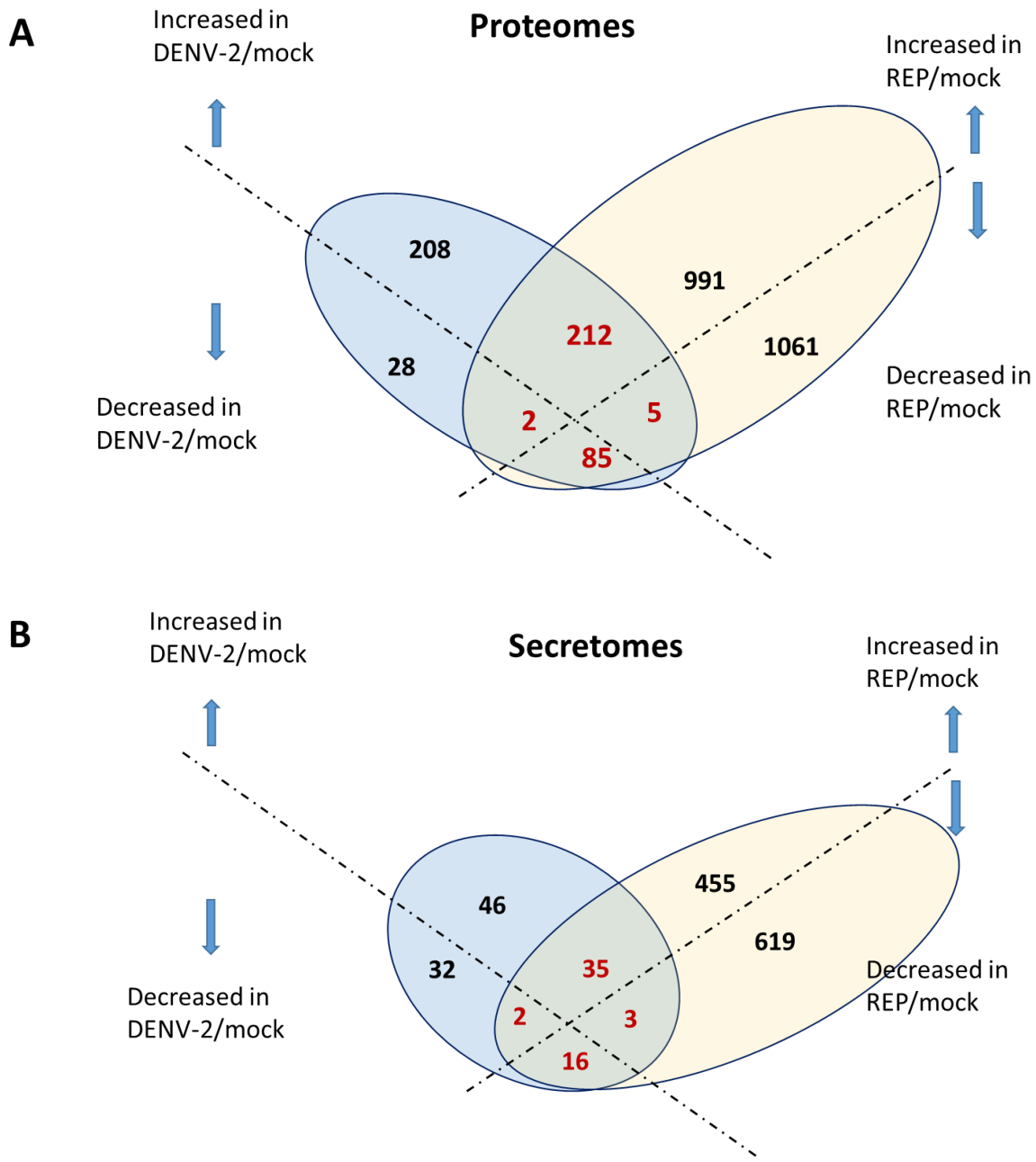

Figure 4.4 Overlap between proteins commonly altered (≥ 1.3 fold) in both proteomes and secretomes of DENV-2 infected HEK293T and REP cells compared to mock infected cells.

Venn diagram shows the number of common proteins that significantly (P-value < 0.05) increased and decreased (≥1.3 fold) in proteomes **(A)** and secretomes **(B)** from DENV-2 infected HEK293T cells and REP cells compared to mock infected cells.

Table 4.7 List of common proteins that were significantly altered ≥ 1.3 fold in amount in proteomes of both DENV-2 infected HEK293T and REP cells compared to mock infected cells.

Accession	Description	Gene	Fold change DENV-2 /Mock	P-value	Fold change REP /Mock	P-value
Increased in proteome of both DENV-2 and REP cells						
Q9P2F9	Zinc finger protein 319	*ZNF319*	2.17	8.78E-03	2.29	6.17E-04
Q5T8I3	Protein FAM102B	*FAM102B*	1.90	1.80E-02	2.02	2.37E-02
Q9NX18	Succinate dehydrogenase assembly factor 2	*SDHAF2*	1.88	9.91E-03	1.77	2.83E-02
H3BQT6	Tyrosine-protein phosphatase	*PTPN9*	1.87	3.41E-02	2.87	7.49E-03
Q9HB66	Alternative protein MKKS	*MKKS*	1.79	1.06E-02	1.67	3.16E-02
B7Z2V6	Vacuolar ATP synthase catalytic subunit A, ubiquitous	*N/A*	1.75	2.20E-02	2.29	5.30E-03
H0Y9Z5	CCR4-NOT transcription complex subunit 6-like	*CNOT6L*	1.74	3.66E-02	3.00	6.19E-03
Q69YU5	Uncharacterized protein C12orf73	*C12orf73*	1.71	2.07E-02	1.64	3.31E-02
Q496I0	COX7A2 protein	*COX7A2*	1.71	3.33E-02	1.47	1.82E-02
Q9NX40	OCIA domain-containing protein 1	*OCIAD1*	1.71	4.22E-03	1.52	3.50E-02
Q9NUJ1	Mycophenolic acid acyl-glucuronide esterase, mitochondrial	*ABHD10*	1.69	4.01E-02	1.53	4.60E-02
A0A024RC97	Phosphatidylserine synthase 2, isoform CRA_a	*PTDSS2*	1.66	1.22E-02	1.77	5.47E-03
B2R761	Sterol carrier protein 2 (SCP2), mRNA	*N/A*	1.66	3.81E-02	1.56	3.18E-02
Q92520	Protein FAM3C	*FAM3C*	1.66	3.06E-02	2.11	8.88E-03
Q7Z4X2	Neuronal protein	*N/A*	1.66	3.65E-02	1.41	3.92E-02
Q0IIN1	Keratin 77	*KRT77*	1.65	1.74E-02	1.52	6.55E-04
Q6IB54	ATP synthase-coupling factor 6, mitochondrial	*ATP5J*	1.65	2.56E-02	1.59	1.55E-02
Q4KWH8	1-phosphatidylinositol 4,5-bisphosphate phosphodiesterase eta-1	*PLCH1*	1.64	7.91E-03	1.39	3.29E-02
Q6P587	Acylpyruvase FAHD1, mitochondrial	*FAHD1*	1.64	3.39E-02	2.36	4.03E-03

Q92526	T-complex protein 1 subunit zeta-2	*CCT6B*	1.64	3.37E-02	1.35	4.39E-02
H9STE0	Cytochrome c oxidase subunit 2	*COX2*	1.64	3.79E-02	1.38	3.16E-02
B2R673	Dihydrolipoamide acetyltransferase component of pyruvate dehydrogenase complex	*N/A*	1.64	4.57E-02	1.96	6.18E-03
O95169	NADH dehydrogenase [ubiquinone] 1 beta subcomplex subunit 8, mitochondrial	*NDUFB8*	1.62	2.56E-02	1.65	6.58E-03
P62072	Mitochondrial import inner membrane translocase subunit Tim10	*TIMM10*	1.62	3.55E-02	1.45	2.90E-02
A8K5D4	Myelin protein zero-like 1, isoform CRA_b	*MPZL1*	1.61	2.94E-02	1.66	1.71E-02
Q9BSF4	Mitochondrial import inner membrane translocase subunit Tim29	*TIMM29*	1.61	4.03E-02	1.54	5.25E-03
B1Q2B0	URCC5	*URCC5*	1.60	5.11E-03	2.20	1.52E-04
B2R6N9	Signal sequence receptor, alpha (translocon-associated protein alpha) (SSR1), mRNA	*SSR1*	1.60	1.39E-02	1.33	2.75E-02
A0A024RCB3	Tetraspanin	*CD151*	1.59	2.36E-02	2.14	4.12E-03
Q6IBA0	NADH dehydrogenase (Ubiquinone) Fe-S protein 5, 15kDa	*NDUFS5*	1.59	4.04E-02	1.37	1.67E-02
Q9NX24	H/ACA ribonucleoprotein complex subunit 2	*NHP2*	1.59	2.62E-02	2.36	9.39E-04
P36957	Dihydrolipoyllysine-residue succinyltransferase component of 2-oxoglutarate dehydrogenase complex, mitochondrial	*DLST*	1.59	2.76E-02	1.67	8.36E-03
A0A0S2Z3G4	Frataxin isoform 1	*FXN*	1.58	2.88E-02	1.36	4.76E-02
A4D1U3	Single-stranded DNA binding protein 1, isoform CRA_a	*SSBP1*	1.58	2.34E-02	1.88	3.39E-03
B4DLN7	Cytochrome P450, family 20, subfamily A, polypeptide 1, transcript variant 1, mRNA		1.58	4.73E-02	1.80	7.65E-03
A0A0R4J2F2	Claudin domain-containing protein 1	*CLDND1*	1.57	2.90E-03	1.48	9.02E-03
P35914	Hydroxymethylglutaryl-CoA lyase, mitochondrial	*HMGCL*	1.56	2.83E-02	1.48	8.96E-03

Q4QQP8	PTGFRN protein (Fragment)	*PTGFRN*	1.56	1.72E-02	3.70	8.02E-04
P62487	DNA-directed RNA polymerase II subunit RPB7	*POLR2G*	1.56	4.28E-02	1.71	1.24E-02
B3KQB4	PRA1 family protein	*N/A*	1.56	3.26E-02	1.59	3.57E-03
O75381	Peroxisomal membrane protein PEX14	*PEX14*	1.56	3.33E-02	1.54	2.34E-02
E5KSU5	Mitochondrial transcription factor A	*TFAM*	1.56	3.84E-02	2.47	1.03E-03
E9PIE4	Mitochondrial carrier homolog 2 (Fragment)	*MTCH2*	1.56	1.69E-02	1.70	4.64E-03
Q15907	Ras-related protein Rab-11B	*RAB11B*	1.56	3.84E-02	1.50	3.82E-02
O60783	28S ribosomal protein S14, mitochondrial	*MRPS14*	1.56	2.43E-02	1.79	6.79E-03
O75947	ATP synthase subunit d, mitochondrial	*ATP5PD*	1.56	4.74E-02	1.67	1.24E-02
Q9BV79	Enoyl-[acyl-carrier-protein] reductase, mitochondrial	*MECR*	1.56	4.04E-02	2.23	2.75E-03
B4DDK9	Alpha-1,6-mannosyl-glycoprotein2-beta-N-acetylglucosaminyltransferase	*N/A*	1.56	4.04E-02	1.65	3.55E-02
O43181	NADH dehydrogenase [ubiquinone] iron-sulfur protein 4, mitochondrial	*NDUFS4*	1.55	3.32E-02	1.42	2.90E-02
Q5RI15	Cytochrome c oxidase assembly protein COX20, mitochondrial	*COX20*	1.55	4.60E-02	1.63	2.26E-02
Q9UII2	ATPase inhibitor, mitochondrial	*ATP5IF1*	1.55	2.93E-02	1.53	2.70E-02
O00479	High mobility group nucleosome-binding domain-containing protein 4	*HMGN4*	1.55	3.52E-02	1.53	2.78E-02
Q9HB40	Retinoid-inducible serine carboxypeptidase	*SCPEP1*	1.55	1.77E-02	1.53	1.23E-02
Q9NPL8	Complex I assembly factor TIMMDC1, mitochondrial	*TIMMDC1*	1.54	3.61E-02	1.55	8.51E-03
Q6ZMG9	Ceramide synthase 6	*CERS6*	1.54	2.85E-02	1.70	2.27E-02
V9GYT7	PC4 and SFRS1-interacting protein (Fragment)	*PSIP1*	1.54	3.29E-02	1.72	1.77E-02
O75380	NADH dehydrogenase [ubiquinone] iron-sulfur protein 6, mitochondrial	*NDUFS6*	1.54	4.16E-02	1.32	2.45E-02
O75844	CAAX prenyl protease 1 homolog	*ZMPSTE24*	1.54	3.58E-02	1.54	2.29E-02

Q6P1L8	39S ribosomal protein L14, mitochondrial	*MRPL14*	1.54	4.07E-02	1.43	2.90E-02
B2R9T9	Transmembrane protein 109	*N/A*	1.54	1.59E-02	1.66	1.57E-02
B3KN15	Heparan sulfate 2-O-sulfotransferase 1	*N/A*	1.53	4.02E-02	1.93	9.38E-03
A0A0S2Z5H0	Mitochondrial ribosomal protein S28 isoform 2	*MRPS28*	1.53	2.05E-02	1.68	1.28E-02
A8K337	Catechol-O-methyltransferase domain containing 1 (COMTD1)	*N/A*	1.53	1.44E-02	1.51	3.22E-03
Q5T1C6	Acyl-coenzyme A thioesterase THEM4	*THEM4*	1.53	4.35E-02	1.42	2.73E-02
O43493	Trans-Golgi network integral membrane protein 2	*TGOLN2*	1.53	2.64E-02	2.61	9.49E-03
A0A024RBE7	Thymopoietin	*TMPO*	1.53	4.49E-02	1.79	5.92E-03
A0A024R4K3	Malate dehydrogenase	*MDH2*	1.53	4.81E-02	1.63	2.16E-02
Q9H6E4	Coiled-coil domain-containing protein 134	*CCDC134*	1.52	4.44E-02	1.70	2.16E-02
Q05DH5	EXTL2 protein	*EXTL2*	1.52	2.59E-02	3.07	5.22E-04
Q5JTV8	Torsin-1A-interacting protein 1	*TOR1AIP1*	1.52	4.38E-02	1.58	1.41E-02
Q8NFQ8	Torsin-1A-interacting protein 2	*TOR1AIP2*	1.52	1.31E-02	1.35	1.63E-02
H3BNX8	Cytochrome c oxidase subunit 5A, mitochondrial	*COX5A*	1.52	3.66E-02	1.37	3.36E-02
Q96BP2	Coiled-coil-helix-coiled-coil-helix domain-containing protein 1	*CHCHD1*	1.52	4.09E-02	1.52	9.30E-03
Q3ZAQ7	Vacuolar ATPase assembly integral membrane protein VMA21	*VMA21*	1.52	1.22E-02	1.53	6.96E-03
L0R6Q1	SLC35A4 upstream open reading frame protein	*SLC35A4*	1.52	4.83E-02	1.32	1.72E-02
P35609	Alpha-actinin-2	*ACTN2*	1.51	2.55E-02	1.61	3.69E-03
Q13443	Disintegrin and metalloproteinase domain-containing protein 9	*ADAM9*	1.51	4.78E-02	1.59	1.03E-02
A8K4V4	Mitochondrial ribosomal protein L43 (MRPL43), transcript variant 1	*N/A*	1.51	3.72E-02	1.49	6.22E-03
E7EPT4	NADH dehydrogenase [ubiquinone] flavoprotein 2, mitochondrial	*NDUFV2*	1.51	1.74E-02	1.34	2.78E-02
Q9NPJ3	Acyl-coenzyme A thioesterase 13	*ACOT13*	1.51	3.05E-02	1.39	3.56E-02

O95881	Thioredoxin domain-containing protein 12	*TXNDC12*	1.51	3.50E-02	1.73	1.16E-02
A0A024R8Q1	Glucosidase, alpha acid (Pompe disease, glycogen storage disease type II)	*GAA*	1.51	9.26E-03	1.43	1.58E-02
A0A024RBS4	Scavenger receptor class B, member 1, isoform CRA_b	*SCARB1*	1.51	3.11E-02	1.67	2.52E-02
Q96EL3	39S ribosomal protein L53, mitochondrial	*MRPL53*	1.51	1.87E-02	1.55	4.36E-02
A8K769	Secretory carrier-associated membrane protein	*N/A*	1.51	4.61E-02	1.53	3.64E-02
A0A087WZE9	High mobility group nucleosome-binding domain-containing protein 3	*HMGN3*	1.50	3.80E-02	1.73	7.67E-03
Q96HE7	ERO1-like protein alpha	*ERO1*	1.50	2.67E-02	1.57	2.04E-02
Q9UKU7	Isobutyryl-CoA dehydrogenase, mitochondrial	*ACAD8*	1.50	4.12E-02	1.94	9.68E-04
Q14165	Malectin	*MLEC*	1.50	4.87E-02	1.89	7.09E-04
P16104	Histone H2AX	*H2AFX*	1.50	4.32E-02	2.02	5.81E-03
A0A2S1PH31	Methylmalonyl-CoA mutase variant	*MUT*	1.50	4.94E-02	1.39	1.94E-02
B2R6X6	Peptidyl-prolyl cis-trans isomerase	*N/A*	1.50	4.29E-02	1.60	1.35E-02
A0A024RDY3	Lysosomal-associated membrane protein 1, isoform CRA_a	*N/A*	1.50	3.83E-02	2.21	3.33E-03
Q5HYK3	2-methoxy-6-polyprenyl-1,4-benzoquinol methylase, mitochondrial	*N/A*	1.50	2.89E-02	1.49	2.50E-02
Q13232	Nucleoside diphosphate kinase 3	*NME3*	1.49	1.01E-02	1.39	3.01E-02
Q7LD69	NADH-ubiquinone oxidoreductase Fe-S protein 7 variant	*N/A*	1.49	4.10E-02	1.48	7.51E-03
A0A024RB75	Citrate synthase	*CS*	1.49	2.86E-02	1.51	1.20E-02
B4DEF8	39S ribosomal protein L45, mitochondrial	*N/A*	1.48	4.62E-02	1.37	2.10E-02
Q96DP0	NADH-UBIQUINONE OXIDOREDUCTASE 9 KD SUBUNIT	*N/A*	1.48	3.23E-02	1.33	4.76E-02
A0A087WWD4	Neural cell adhesion molecule 1	*NCAM1*	1.48	5.02E-02	2.16	4.38E-04

O95202	Mitochondrial proton/calcium exchanger protein	*LETM1*	1.48	3.81E-02	1.40	4.29E-02
Q6P1N1	PPM2C protein (Fragment)	*PPM2C*	1.48	2.75E-02	1.75	8.08E-03
P24752	Acetyl-CoA acetyltransferase, mitochondrial	*ACAT1*	1.47	3.64E-02	1.62	1.79E-02
J3QLS3	28S ribosomal protein S7, mitochondrial	*MRPS7*	1.47	3.17E-02	1.61	1.35E-02
Q8IXM3	39S ribosomal protein L41, mitochondrial	*MRPL41*	1.47	2.22E-02	1.45	3.39E-02
O15446	DNA-directed RNA polymerase I subunit RPA34	*CD3EAP*	1.47	4.30E-02	2.31	4.36E-03
Q3KRB4	MRPS33 protein	*MRPS33*	1.47	4.57E-02	1.65	7.40E-03
O43678	NADH dehydrogenase [ubiquinone] 1 alpha subcomplex subunit 2	*NDUFA2*	1.47	3.63E-02	1.32	2.82E-02
A0A0S2Z4C3	Fumarate hydratase isoform 1 (Fragment)	*FH*	1.47	4.14E-02	1.69	2.36E-02
O94919	Endonuclease domain-containing 1 protein	*ENDOD1*	1.47	1.99E-02	1.69	5.28E-03
Q9NYU2	UDP-glucose:glycoprotein glucosyltransferase 1	*UGGT1*	1.46	4.88E-02	1.46	2.92E-02
P83876	Thioredoxin-like protein 4A	*TXNL4A*	1.46	2.11E-02	1.73	2.14E-03
A0A024R3D8	Acetyltransferase component of pyruvate dehydrogenase complex	*DLAT*	1.46	4.12E-02	1.32	3.44E-02
Q4U2R6	39S ribosomal protein L51, mitochondrial	*MRPL51*	1.46	3.87E-02	1.37	3.70E-02
A0A024R9B7	Cytochrome c oxidase subunit VIc, isoform CRA_a	*COX6C*	1.46	4.63E-02	1.53	3.56E-02
Q9HC06	Cd002 protein	*N/A*	1.45	4.02E-02	1.80	4.13E-02
A8K0M6	cDNA FLJ76697	*MRPL37*	1.45	4.99E-02	2.03	7.60E-04
Q9BZE1	39S ribosomal protein L37, mitochondrial	*MRPL37*	1.45	1.75E-02	1.30	4.48E-03
A0A090N8G7	Similar to RP9 protein	*LOC402478*	1.45	4.57E-04	1.67	2.10E-02
Q14696	LRP chaperone MESD	*MESD*	1.45	2.82E-02	1.62	1.04E-02
E9LUH4	Methyl-CpG-binding protein 2	*MECP2*	1.45	4.74E-02	1.78	8.11E-03
Q8N183	NADH dehydrogenase [ubiquinone] 1 alpha subcomplex assembly factor 2	*NDUFAF2*	1.45	3.85E-02	1.60	6.18E-03

A0A024R745	NADH dehydrogenase (Ubiquinone) 1 alpha subcomplex, 5, 13kDa, isoform CRA_b	*NDUFA5*	1.45	3.89E-02	1.42	9.92E-03
Q05DF2	SF3A2 protein (Fragment)	*SF3A2*	1.45	3.77E-02	1.45	2.63E-02
Q9BVK6	Transmembrane emp24 domain-containing protein 9	*TMED9*	1.44	3.95E-02	1.41	1.51E-02
A0A024R2P4	Chromosome 3 open reading frame 39, isoform CRA_a	*C3orf39*	1.44	4.16E-02	1.39	1.67E-02
Q9Y385	Ubiquitin-conjugating enzyme E2 J1	*UBE2J1*	1.44	3.52E-03	1.69	1.71E-04
Q9Y3B7	39S ribosomal protein L11, mitochondrial	*MRPL11*	1.44	3.37E-02	1.54	1.61E-02
A0A0S2Z5M1	SEC63-like (S. cerevisiae) (Fragment)	*SEC63*	1.44	4.29E-02	1.99	2.16E-03
A0A024QZ86	T-box 2, isoform CRA_a	*TBX2*	1.44	2.06E-02	1.86	3.55E-02
Q9BSR8	Protein YIPF4	*YIPF4*	1.44	1.77E-02	2.01	1.88E-03
Q96A33	Coiled-coil domain-containing protein 47	*CCDC47*	1.44	3.62E-02	1.46	2.23E-02
P16402	Histone H1.3	*HIST1H1D*	1.43	1.09E-02	3.34	1.28E-04
A2A274	Aconitate hydratase, mitochondrial	*ACO2*	1.43	4.75E-02	1.45	3.76E-02
A0A024RBC5	N-acetylglucosamine-6-sulfatase	*GNS*	1.43	2.59E-02	1.55	1.23E-02
P11177	Pyruvate dehydrogenase E1 component subunit beta, mitochondrial	*PDHB*	1.43	3.17E-02	1.45	2.30E-02
O00469	Procollagen-lysine,2-oxoglutarate 5-dioxygenase 2	*PLOD2*	1.43	2.55E-02	2.05	1.21E-03
B7Z6S9	Glucosylceramidase	*N/A*	1.43	4.16E-02	2.12	3.59E-03
O75489	NADH dehydrogenase [ubiquinone] iron-sulfur protein 3, mitochondrial	*NDUFS3*	1.43	3.11E-02	1.40	7.95E-03
V9HW88	Calreticulin, isoform CRA_b	*HEL-S-99n*	1.43	4.08E-02	1.51	4.34E-03
A0A024RDQ7	Mitochondrial translational initiation factor 3, isoform CRA_a	*MTIF3*	1.43	4.26E-02	1.47	4.08E-02
M0QXB5	Persulfide dioxygenase ETHE1, mitochondrial	*ETHE1*	1.43	4.32E-02	1.49	4.68E-02
Q6PUJ7	Epididymis luminal protein 215	*HEL-215*	1.42	3.35E-02	1.39	6.25E-03
Q8IY95	Transmembrane protein 192	*TMEM192*	1.42	2.83E-02	1.43	6.43E-03

P52815	39S ribosomal protein L12, mitochondrial	*MRPL12*	1.42	4.64E-02	1.49	2.97E-02
Q9H2W6	39S ribosomal protein L46, mitochondrial	*MRPL46*	1.42	4.26E-02	1.55	1.28E-03
P84090	Enhancer of rudimentary homolog	*ERH*	1.42	3.81E-02	1.50	2.69E-02
Q7Z4Y4	GTP:AMP phosphotransferase AK3, mitochondrial	*AK3*	1.42	4.11E-02	2.01	2.34E-03
Q9H2J9	DC39	*N/A*	1.41	4.76E-02	1.93	1.42E-02
Q96S66	Chloride channel CLIC-like protein 1	*CLCC1*	1.41	2.56E-02	1.43	3.79E-02
Q07021	Complement component 1 Q subcomponent-binding protein, mitochondrial	*C1QBP*	1.41	4.54E-02	1.51	1.19E-02
Q96A35	39S ribosomal protein L24, mitochondrial	*MRPL24*	1.41	3.66E-02	1.40	1.65E-02
Q86VR2	Reticulophagy regulator 3	*RETREG3*	1.40	3.84E-02	1.46	3.18E-02
P50151	Guanine nucleotide-binding protein G(I)/G(S)/G(O) subunit gamma-10	*GNG10*	1.40	3.19E-02	1.42	1.27E-02
Q9H1K1	Iron-sulfur cluster assembly enzyme ISCU, mitochondrial	*ISCU*	1.40	4.79E-02	1.31	4.52E-02
A0A024R313	Glycosyltransferase 8 domain containing 1, isoform CRA_a	*GLT8D1*	1.40	4.15E-03	1.51	1.24E-02
Q59EK0	Epsilon isoform of regulatory subunit B56, protein phosphatase 2A variant	*N/A*	1.40	2.36E-02	1.47	2.85E-02
Q9BYC9	39S ribosomal protein L20, mitochondrial	*MRPL20*	1.40	4.12E-02	1.33	2.17E-02
Q13405	39S ribosomal protein L49, mitochondrial	*MRPL49*	1.39	4.35E-02	1.38	2.90E-02
Q16630	Cleavage and polyadenylation specificity factor subunit 6	*CPSF6*	1.39	3.72E-02	1.43	4.61E-02
Q8NFH4	Nucleoporin Nup37	*NUP37*	1.39	9.80E-03	1.35	7.80E-03
B4E2B5	MICOS complex subunit MIC60	*N/A*	1.39	1.64E-02	1.70	1.90E-02
Q59GR1	Niemann-Pick disease, type C1 variant (Fragment)	*N/A*	1.39	2.87E-02	1.56	1.36E-02
A0A024RD07	Trinucleotide repeat containing 5, isoform CRA_c	*TNRC5*	1.39	3.59E-02	1.48	2.18E-02

P17693	HLA class I histocompatibility antigen, alpha chain G	*HLA-G*	1.39	4.57E-02	1.59	2.60E-02
B4DRS6	Sideroflexin	*N/A*	1.38	3.13E-02	1.47	3.51E-02
Q8NDZ4	Deleted in autism protein 1	*DIPK2A*	1.38	2.60E-02	1.50	3.05E-02
Q9BQ95	Evolutionarily conserved signaling intermediate in Toll pathway, mitochondrial	*ECSIT*	1.38	4.43E-02	1.69	2.09E-03
P62875	DNA-directed RNA polymerases I, II, and III subunit RPABC5	*POLR2L*	1.38	1.05E-03	1.41	2.75E-02
P31327	Carbamoyl-phosphate synthase [ammonia], mitochondrial	*CPS1*	1.38	4.92E-02	1.42	2.51E-03
Q16795	NADH dehydrogenase [ubiquinone] 1 alpha subcomplex subunit 9, mitochondrial	*NDUFA9*	1.38	4.57E-02	1.37	2.66E-02
D3DSQ1	N-acylsphingosine amidohydrolase (Acid ceramidase) 1, isoform CRA_c	*ASAH1*	1.38	1.12E-03	2.24	1.19E-03
Q969X5	Endoplasmic reticulum-Golgi intermediate compartment protein 1	*ERGIC1*	1.37	4.77E-02	1.63	1.84E-03
Q8NCN5	Pyruvate dehydrogenase phosphatase regulatory subunit, mitochondrial	*PDPR*	1.37	3.87E-02	1.61	9.84E-03
J3KTA1	F-box and leucine-rich repeat protein 20, isoform CRA_a	*FBXL20*	1.37	3.85E-03	1.47	7.30E-03
T2C6S4	WWC family member 3	*WWC3*	1.37	4.14E-02	1.56	3.69E-02
Q6P4F2	Ferredoxin-2, mitochondrial	*FDX2*	1.37	4.71E-02	1.69	4.39E-02
Q8WWV3	Reticulon-4-interacting protein 1, mitochondrial	*RTN4IP1*	1.37	2.69E-03	1.66	1.00E-02
Q9NQ50	39S ribosomal protein L40, mitochondrial	*MRPL40*	1.36	4.99E-02	1.31	4.48E-02
A8KAL2	Golgi autoantigen, golgin subfamily a, 5 (GOLGA5), mRNA	*N/A*	1.36	2.03E-02	1.38	4.69E-02
A0A2R8Y5P7	Probable histidine--tRNA ligase, mitochondrial	*HARS2*	1.36	2.14E-02	1.55	1.32E-03
Q96HY6	DDRGK domain-containing protein 1	*DDRGK1*	1.36	2.61E-02	1.34	1.94E-02
Q6ZXV5	Transmembrane and TPR repeat-containing protein 3	*TMTC3*	1.35	3.10E-02	1.32	3.87E-02

V9HWD3	Epididymis luminal protein 117	*HEL117*	1.35	2.97E-02	1.77	6.28E-03
Q8NBX0	Saccharopine dehydrogenase-like oxidoreductase	*SCCPDH*	1.35	4.48E-02	1.67	1.70E-02
Q5T2R2	Decaprenyl-diphosphate synthase subunit 1	*PDSS1*	1.35	2.61E-02	1.47	1.32E-02
A5YM53	ITGAV protein	*ITGAV*	1.35	4.82E-02	1.47	3.43E-02
K7EMG5	AP-1 complex subunit mu-2 (Fragment)	*AP1M2*	1.35	4.44E-02	1.38	3.81E-03
Q96EY7	Pentatricopeptide repeat domain-containing protein 3, mitochondrial	*PTCD3*	1.34	4.65E-02	1.39	2.98E-02
A0A024RDW4	Uncharacterized protein	*FLJ10154*	1.34	4.69E-02	1.33	1.29E-02
Q7L0Y3	tRNA methyltransferase 10 homolog C	*TRMT10C*	1.34	3.81E-02	1.79	5.14E-03
A0A0G2JJD3	HLA-B associated transcript 5, isoform CRA_b	*ABHD16A*	1.34	4.48E-02	1.53	1.10E-02
Q53EU6	Glycerol-3-phosphate acyltransferase 3	*GPAT3*	1.34	3.05E-02	1.75	1.23E-02
Q05048	Cleavage stimulation factor subunit 1	*CSTF1*	1.34	4.38E-02	1.32	5.93E-03
Q9NY12	H/ACA ribonucleoprotein complex subunit 1	*GAR1*	1.34	4.38E-02	1.67	3.64E-03
Q6IQ19	Centriole, cilia and spindle-associated protein	*CCSAP*	1.34	3.88E-02	1.51	6.11E-03
Q96F25	UDP-N-acetylglucosamine transferase subunit ALG14 homolog	*ALG14*	1.33	2.30E-02	1.76	1.61E-03
Q7Z3D4	LysM and putative peptidoglycan-binding domain-containing protein 3	*LYSMD3*	1.33	3.17E-02	1.36	7.63E-03
Q92575	UBX domain-containing protein 4	*UBXN4*	1.33	3.83E-02	1.44	3.01E-02
Q8TA92	Similar to AFG3 ATPase family gene 3-like 2	*N/A*	1.32	4.74E-02	1.37	1.66E-02
I3L0E3	HCG1984214, isoform CRA_a	*hCG_1984214*	1.32	4.86E-02	1.51	3.45E-03
P82912	28S ribosomal protein S11, mitochondrial	*MRPS11*	1.32	3.84E-02	1.49	1.55E-02
Q9NUQ2	1-acyl-sn-glycerol-3-phosphate acyltransferase epsilon	*AGPAT5*	1.32	4.88E-02	1.94	4.03E-04
A8K1K8	Chromosome 18 open reading frame 55, isoform CRA_b	*C18orf55*	1.31	1.75E-02	1.52	1.78E-02

B4E3G8	cDNA FLJ61576, highly similar to Mitochondrial fission regulator 1	*PON2*	1.31	1.10E-04	1.34	1.18E-02
A0A0J9YXF2	Paraoxonase 2, isoform CRA_a	*SP1*	1.31	4.69E-02	1.91	7.51E-05
P08047	Transcription factor Sp1	*UGT8*	1.31	4.41E-03	1.35	1.37E-02
Q16880	2-hydroxyacylsphingosine 1-beta-galactosyltransferase	*DNAH17*	1.31	5.82E-03	1.41	2.33E-02
Q9UFH2	Dynein heavy chain 17, axonemal	*PWWP2A*	1.31	1.22E-03	1.41	1.33E-03
Q96N64	PWWP domain-containing protein 2A		1.30	1.27E-02	1.43	1.38E-02
Increased in proteome of DENV-2 but decreased in those of REP cells						
Q16762	Thiosulfate sulfurtransferase	*TST*	1.48	3.99E-02	0.73	1.07E-02
P35612	Beta-adducin	*ADD2*	1.40	7.69E-03	0.72	1.36E-02
G3V3D1	NPC intracellular cholesterol transporter 2 (Fragment)	*NPC2*	1.38	4.12E-02	0.73	2.20E-02
E9PGC8	Microtubule-associated protein 1A	*MAP1A*	1.31	4.55E-02	0.42	1.98E-03
A0A024R871	Solute carrier family 2, (Facilitated glucose transporter) member 8, isoform CRA_a	*SLC2A8*	1.30	4.50E-03	0.72	3.32E-02
Decreased in proteome of DENV-2 but increased in those of REP cells						
P85298	Rho GTPase-activating protein 8	*ARHGAP8*	0.72	4.91E-02	1.44	1.88E-03
Q8WUU5	GATA zinc finger domain-containing protein 1	*GATAD1*	0.69	1.01E-02	1.39	6.57E-03
Decreased in proteomes of both DENV-2 and REP cells						
Q9UBC2	Epidermal growth factor receptor substrate 15-like 1	*EPS15L1*	0.77	3.54E-02	0.59	8.63E-04
Q9ULH1	Arf-GAP with SH3 domain, ANK repeat and PH domain-containing protein 1	*ASAP1*	0.77	4.07E-02	0.64	6.91E-03
Q5T6F2	Ubiquitin-associated protein 2	*UBAP2*	0.76	4.78E-02	0.69	1.95E-03
Q9UBV8	Peflin	*PEF1*	0.76	4.14E-02	0.62	8.64E-03
D3DWY7	Prefoldin subunit 3	*VBP1*	0.76	3.06E-03	0.66	1.87E-03
Q14687	Genetic suppressor element 1	*GSE1*	0.76	2.71E-02	0.44	2.54E-04
Q7KZ85	Transcription elongation factor SPT6	*SUPT6H*	0.76	4.65E-02	0.71	7.77E-03

Q96C86	m7GpppX diphosphatase	*DCPS*	0.76	1.98E-02	0.70	1.01E-02
Q8IWV8	E3 ubiquitin-protein ligase UBR2	*UBR2*	0.76	4.01E-02	0.70	3.61E-03
Q96Q83	Alpha-ketoglutarate-dependent dioxygenase alkB homolog 3	*ALKBH3*	0.76	4.92E-02	0.74	3.81E-02
Q9Y2Z0	Protein SGT1 homolog	*SUGT1*	0.76	3.60E-02	0.65	1.28E-03
Q7Z7A4	PX domain-containing protein kinase-like protein	*PXK*	0.76	2.14E-02	0.62	1.86E-04
A0A2R8YE63	Epidermal growth factor receptor kinase substrate 8	*EPS8*	0.75	3.07E-02	0.74	2.13E-02
P11802	Cyclin-dependent kinase 4	*CDK4*	0.75	3.91E-02	0.70	3.31E-02
Q5U0F4	Eukaryotic translation initiation factor 3 subunit I	*EIF3S2*	0.75	3.50E-02	0.75	3.31E-02
A0A024R1K7	Tyrosine 3-monooxygenase/tryptophan 5-monooxygenase activation protein, eta polypeptide, isoform CRA_b	*YWHAH*	0.75	4.13E-02	0.46	5.12E-04
D3DUW5	Dynamin 1-like, isoform CRA_c	*DNM1L*	0.74	2.42E-02	0.68	9.45E-03
A0A068F7M9	FH1/FH2 domain-containing protein 1 variant	*FHOD1*	0.74	2.06E-02	0.42	6.28E-04
Q9NZ63	Telomere length and silencing protein 1 homolog	*C9orf78*	0.74	2.62E-02	0.57	9.86E-04
P50479	PDZ and LIM domain protein 4	*PDLIM4*	0.74	6.36E-03	0.54	6.90E-03
Q99622	Protein C10	*C12orf57*	0.74	2.56E-02	0.69	7.20E-03
Q96PU5	E3 ubiquitin-protein ligase NEDD4-like	*NEDD4L*	0.73	2.07E-02	0.60	3.34E-02
Q147X3	N-alpha-acetyltransferase 30	*NAA30*	0.73	4.42E-02	0.56	2.15E-02
Q9BUA3	Spindlin interactor and repressor of chromatin-binding protein	*SPINDOC*	0.73	2.33E-02	0.66	2.72E-03
J3KNN3	Phosphorylase b kinase gamma catalytic chain, liver/testis isoform	*PHKG2*	0.73	4.36E-02	0.67	1.36E-03
A0A2R8YEL6	Glutamate--cysteine ligase catalytic subunit (Fragment)	*GCLC*	0.73	3.15E-02	0.53	2.55E-03
Q15814	Tubulin-specific chaperone C	*TBCC*	0.73	2.96E-02	0.69	1.37E-03
Q9BZI7	Regulator of nonsense transcripts 3B	*UPF3B*	0.73	2.92E-02	0.64	1.13E-02

Q71RG4	Transmembrane and ubiquitin-like domain-containing protein 2	*TMUB2*	0.72	3.51E-02	0.47	9.93E-03
Q2NL82	Pre-rRNA-processing protein TSR1 homolog	*TSR1*	0.72	4.74E-02	0.62	2.81E-03
B0QZ18	Copine-1	*CPNE1*	0.72	2.03E-02	0.72	2.63E-02
P17707	S-adenosylmethionine decarboxylase proenzyme	*AMD1*	0.72	1.08E-02	0.68	3.01E-03
A8K486	Peptidyl-prolyl cis-trans isomerase	*N/A*	0.72	5.04E-03	0.64	7.71E-03
A0A140VJZ4	Ubiquitin carboxyl-terminal hydrolase	*N/A*	0.71	3.23E-02	0.37	1.59E-03
Q9NP79	Vacuolar protein sorting-associated protein VTA1 homolog	*VTA1*	0.71	1.80E-03	0.64	2.51E-04
A0A0B4J2C3	Translationally-controlled tumor protein	*TPT1*	0.71	2.46E-02	0.54	1.41E-02
O75132	Zinc finger BED domain-containing protein 4	*ZBED4*	0.71	3.65E-02	0.70	1.00E-02
A0A0S2Z462	ArfGAP with FG repeats 1 isoform 2 (Fragment)	*AGFG1*	0.71	1.53E-02	0.56	4.14E-04
Q15369	Elongin-C	*ELOC*	0.71	4.21E-02	0.58	7.69E-03
A8K2A8	Importin 13 (IPO13), mRNA	*N/A*	0.71	2.53E-02	0.53	3.86E-03
B3KSH8	Inositol polyphosphate 1-phosphatase	*N/A*	0.71	7.62E-03	0.30	6.53E-04
V9HW44	Epididymis secretory protein Li 303	*HEL-S-303*	0.70	6.64E-03	0.44	5.87E-05
Q9NP77	RNA polymerase II subunit A C-terminal domain phosphatase SSU72	*SSU72*	0.70	4.18E-02	0.63	1.52E-02
Q9NRN7	L-aminoadipate-semialdehyde dehydrogenase-phosphopantetheinyl transferase	*AASDHPPT*	0.70	4.28E-02	0.51	3.14E-03
A0A024RBB7	Nucleosome assembly protein 1-like 1, isoform CRA_a	*NAP1L1*	0.70	4.09E-02	0.55	8.06E-03
Q8TE76	MORC family CW-type zinc finger protein 4	*MORC4*	0.70	1.82E-02	0.70	1.81E-02
Q96CW6	Probable RNA polymerase II nuclear localization protein SLC7A6OS	*SLC7A6OS*	0.70	4.95E-02	0.57	4.43E-03
Q9Y508	E3 ubiquitin-protein ligase RNF114	*RNF114*	0.70	1.69E-02	0.59	6.89E-03
O95433	Activator of 90 kDa heat shock protein ATPase homolog 1	*AHSA1*	0.70	3.05E-02	0.57	1.80E-03

O43296	Zinc finger protein 264	*ZNF264*	0.70	4.02E-02	0.64	3.04E-03
Q86U44	N6-adenosine-methyltransferase catalytic subunit	*METTL3*	0.69	1.68E-02	0.49	9.57E-04
P34896	Serine hydroxymethyltransferase, cytosolic	*SHMT1*	0.69	3.75E-02	0.55	4.93E-03
P49327	Fatty acid synthase	*FASN*	0.69	4.42E-02	0.35	5.02E-04
B4DPD5	Ubiquitin thioesterase	*N/A*	0.69	4.94E-02	0.56	3.38E-03
Q15417	Calponin-3	*CNN3*	0.69	2.10E-02	0.35	5.60E-04
A8K0J3	cDNA FLJ76732, highly similar to Homo sapiens TAO kinase 3 (TAOK3), mRNA	*N/A*	0.69	3.38E-02	0.73	4.50E-02
P47813	Eukaryotic translation initiation factor 1A, X-chromosomal	*EIF1AX*	0.69	1.17E-02	0.57	4.50E-04
Q5T9B7	Adenylate kinase isoenzyme 1	*AK1*	0.69	3.87E-02	0.56	1.10E-03
Q8N543	Prolyl 3-hydroxylase OGFOD1	*OGFOD1*	0.68	1.11E-02	0.40	2.44E-03
Q9BVA1	Tubulin beta-2B chain	*TUBB2B*	0.68	3.49E-03	0.32	5.66E-04
O60763	General vesicular transport factor p115	*USO1*	0.68	3.41E-02	0.42	1.43E-04
A8KA19	Exportin, tRNA (nuclear export receptor for tRNAs) (XPOT), mRNA	*N/A*	0.68	4.65E-02	0.47	2.38E-03
Q9NQT8	Kinesin-like protein KIF13B	*KIF13B*	0.67	1.73E-02	0.75	3.57E-02
Q6FIC5	Chloride intracellular channel protein	*CLIC4*	0.67	3.35E-02	0.55	1.39E-03
A8K646	Osteoclast stimulating factor 1 (OSTF1), mRNA	*N/A*	0.67	3.71E-02	0.40	1.10E-04
Q12933	TNF receptor-associated factor 2	*TRAF2*	0.67	3.18E-02	0.47	2.49E-03
A0A024R6Q1	Eukaryotic translation initiation factor 5, isoform CRA_b	*EIF5*	0.66	3.48E-02	0.56	1.17E-03
F2Z2X4	Exportin-4	*XPO4*	0.66	1.49E-02	0.52	2.14E-04
P43490	Nicotinamide phosphoribosyltransferase	*NAMPT*	0.65	3.50E-02	0.39	2.82E-03
Q9C0D3	Protein zyg-11 homolog B	*ZYG11B*	0.65	3.02E-02	0.40	1.88E-03
P30291	Wee1-like protein kinase	*WEE1*	0.65	1.72E-04	0.74	7.64E-05
Q6FI81	Anamorsin	*CIAPIN1*	0.65	3.74E-02	0.41	3.70E-04
O76064	E3 ubiquitin-protein ligase RNF8	*RNF8*	0.65	3.50E-02	0.69	4.10E-02
O43639	Cytoplasmic protein NCK2	*NCK2*	0.64	3.64E-02	0.43	9.50E-04

Q96D05	Uncharacterized protein FAM241B	*FAM241B*	0.64	1.59E-02	0.21	3.12E-04
P31629	Transcription factor HIVEP2	*HIVEP2*	0.61	1.98E-02	0.61	3.72E-02
Q8IXQ3	Uncharacterized protein C9orf40	*C9orf40*	0.60	3.98E-02	0.23	2.59E-02
Q00534	Cyclin-dependent kinase 6	*CDK6*	0.60	2.96E-02	0.31	2.17E-04
Q8N9N8	Probable RNA-binding protein EIF1AD	*EIF1AD*	0.59	3.13E-02	0.59	1.99E-03
P42677	40S ribosomal protein S27	*RPS27*	0.58	2.75E-02	0.45	3.78E-02
O15541	RING finger protein 113A	*RNF113A*	0.58	3.07E-02	0.29	2.51E-04
Q66K64	DDB1- and CUL4-associated factor 15	*DCAF15*	0.57	5.00E-02	0.34	4.23E-04
B7ZLK1	KIAA0528 protein	*KIAA0528*	0.56	3.60E-02	0.52	1.12E-02
P52788	Spermine synthase	*SMS*	0.56	7.80E-03	0.51	4.82E-03
A0A024R2T2	KIAA1143, isoform CRA_a	*KIAA1143*	0.55	3.00E-02	0.36	6.80E-03

Table 4.8 List of common proteins that were significantly altered ≥ 1.3 fold in amount in secretomes from both DENV-2 infected HEK293T and REP cells compared to mock infected cells.

Accession	Description	Gene	Fold change DENV-2/Mock	P-value	Fold change Rep/Mock	P-value
Increased in secretomes of both DENV-2 and REP cells						
H3BMS5	PH domain leucine-rich repeat-containing protein phosphatase 2	*PHLPP2*	13.46	2.62E-03	24.54	2.84E-05
B2R4R0	Histone H4	*HIST1H4L*	2.97	1.87E-02	2.97	2.13E-02
Q12797	Aspartyl/asparaginyl beta-hydroxylase	*ASPH*	2.74	8.80E-04	13.37	2.21E-05
Q7L5D6	Golgi to ER traffic protein 4 homolog	*GET4*	2.10	3.27E-02	2.14	3.21E-02
Q15008	26S proteasome non-ATPase regulatory subunit 6	*PSMD6*	2.02	3.46E-02	2.92	2.80E-03
O43345	Zinc finger protein 208	*ZNF208*	1.97	7.00E-03	1.98	5.81E-03
A8K061	Angiopoietin-like 3, mRNA	*ANGPTL3*	1.69	4.81E-02	2.33	1.15E-02
A0A024R1Z6	Vesicle amine transport protein 1 homolog (T californica)	*VAT1*	1.64	1.52E-02	1.56	1.11E-02
A8K5Y7	Exportin 5	*XPO5*	1.62	3.51E-02	1.45	3.42E-02
P61225	Ras-related protein Rap-2b	*RAP2B*	1.60	4.84E-02	2.46	6.15E-03
O14929	Histone acetyltransferase type B catalytic subunit	*HAT1*	1.57	3.03E-02	1.39	2.53E-02
P26599	Polypyrimidine tract-binding protein 1	*PTBP1*	1.56	4.52E-02	1.58	3.44E-02
Q86XP3	ATP-dependent RNA helicase DDX42	*DDX42*	1.54	3.97E-02	1.54	3.25E-02
A0A023T6R1	Mago nashi protein	*FLJ10292*	1.54	2.50E-02	1.90	2.14E-03
P25490	Transcriptional repressor protein YY1	*YY1*	1.53	4.23E-02	2.01	6.03E-03
P48556	26S proteasome non-ATPase regulatory subunit 8	*PSMD8*	1.49	1.31E-02	1.44	6.51E-03
P16298	Serine/threonine-protein phosphatase 2B catalytic subunit beta isoform	*PPP3CB*	1.46	3.27E-02	1.48	2.17E-02
A0A2P9AAR3	Uncharacterized protein	*BQ8482_110136*	1.46	3.92E-02	1.58	2.97E-02
Q14686	Nuclear receptor coactivator 6	*NCOA6*	1.46	2.22E-02	1.46	1.69E-02
Q8NFH4	Nucleoporin Nup37	*NUP37*	1.45	4.09E-02	1.71	2.14E-02
A8K245	Vaccinia related kinase 1	*VRK1*	1.43	4.28E-02	2.01	2.53E-03
P21283	V-type proton ATPase subunit C 1	*ATP6V1C1*	1.42	4.43E-03	1.36	2.00E-02
B7Z2U5	Heparan-sulfate 6-O-sulfotransferase	*HS6ST2*	1.42	3.77E-02	2.09	8.09E-04

O00148	ATP-dependent RNA helicase DDX39A	*DDX39A*	1.42	3.86E-02	1.71	1.55E-02
Q6FG99	RPLP1 protein	*RPLP1*	1.41	3.87E-02	1.40	4.62E-02
B2R6D4	Phosphomannomutase	*REEP5*	1.41	1.65E-02	1.84	2.33E-03
Q00765	Receptor expression-enhancing protein 5	*VPS25*	1.37	1.20E-02	1.50	1.71E-02
Q9BRG1	Vacuolar protein-sorting-associated protein 25	*TK1*	1.37	3.95E-02	1.43	3.02E-02
A0A024R8N6	Thymidine kinase sapiens	*FAM50A*	1.37	3.85E-02	1.43	5.93E-03
Q14320	Protein FAM50A	*CKMT1A*	1.37	4.44E-03	1.47	1.19E-02
P12532	Creatine kinase U-type, mitochondrial	*CKMT1B*	1.35	1.62E-02	2.39	1.74E-03
G8JLB6	Heterogeneous nuclear ribonucleoprotein H	*HNRNPH1*	1.32	3.42E-02	1.32	1.46E-02
V9HWP2	Epididymis luminal protein 35	*HSP90B1*	1.32	2.72E-02	1.67	7.53E-03
Increased in secretomes of DENV-2 cells but decreased in those of REP cells						
O60568	Procollagen-lysine,2-oxoglutarate 5-dioxygenase 3	*PLOD3*	1.58	0.01878	0.39	2.78E-02
Q8WVF1	Protein OSCP1	*OSCP1*	1.42	0.025136	0.58	4.77E-02
B3KN55	RBR-type E3 ubiquitin transferase	*RNF14*	1.34	0.024722	0.67	5.71E-03
Decreased in secretomes of DENV-2 cells but increased in those of REP cells						
Q86UE8	Serine/threonine-protein kinase tousled-like 2	N/A	0.55	0.001965	1.70	1.56E-03
Q9Y4W2	Ribosomal biogenesis protein LAS1L	*LAS1L*	0.63	0.020365	1.59	2.89E-02
Decreased in secretomes of both DENV-2 and REP cells						
Q96KC8	DnaJ homolog subfamily C member 1	*DNAJC1*	0.76	0.042957	0.66	1.49E-02
P23284	Peptidyl-prolyl cis-trans isomerase B	*PPIB*	0.76	0.028982	0.70	3.15E-03
A0A087WX97	Bcl-2-like protein 13	*BCL2L13*	0.75	0.014139	0.43	7.11E-03
O95104	Splicing factor, arginine/serine-rich 15	*SCAF4*	0.73	0.030422	0.72	4.47E-02
Q99549	M-phase phosphoprotein 8	*MPHOSPH8*	0.73	0.027138	0.52	5.59E-04
Q96ST2	Protein IWS1 homolog	*IWS1*	0.73	0.03852	0.70	3.14E-02
A0A0D9SF53	ATP-dependent RNA helicase DDX3X	*DDX3X*	0.71	0.047945	0.56	1.51E-02
A0A0A0MT49	Transcription activator BRG1	*SMARCA4*	0.70	0.022724	0.75	7.74E-03
Q3KQU3	MAP7 domain-containing protein 1	*MAP7D1*	0.70	0.005772	0.60	1.84E-02
A0A024R0L4	Ets2 repressor factor, isoform	*ERF*	0.69	0.029911	0.70	1.77E-02
Q9P0B6	Coiled-coil domain-containing protein 167	*CCDC167*	0.68	0.00123	0.40	1.01E-02
B2RDV7	tRNA-dihydrouridine(47) synthase	*DUS3L*	0.66	0.021352	0.60	4.60E-03
B3KNS8	Surfeit locus protein 6	*SURF6*	0.64	0.002283	0.72	1.21E-02
A0A087WYZ4	Glycoprotein hormones alpha	*CGA*	0.62	0.012637	0.62	1.54E-02
Q6P1M0	Long-chain fatty acid transport protein 4	*SLC27A4*	0.55	0.043769	0.59	3.29E-02
B2R5U7	CCAAT-box-binding transcription factor (CBF2)	*CBF2*	0.53	0.012229	0.69	2.27E-02

To examine the effect of the DENV structural proteins and virus particle secretion on host cell protein amounts, the cellular and secreted proteins that were significantly altered (≥1.3 fold) in only DENV-2 infected HEK293T cells but not significantly changed in REP cells (< 1.3 fold or not significant) compared to mock infected cells were identified (Tables 4.9-4.10). All the groups of proteins identified above were subjected to downstream bioinformatic analysis.

Table 4.9 List of proteins significantly altered (≥1.3 fold) in proteome of DENV-2 infected HEK293T cells but not in REP cells (< 1.3 fold or not significant).

Accession	Description	Gene	Fold change DENV-2/Mock	P-value	Fold change REP/Mock	P-value
P56199	Integrin alpha-1	ITGA1	2.24	4.43E-02	2.37	5.10E-02
Q6IAQ2	SDHC protein	SDHC	2.10	4.82E-02	2.02	5.05E-02
Q9UEI6	Polio virus related protein 2, alpha isoform	N/A	1.82	4.04E-02	1.55	7.40E-02
A0A024R5K5	Alpha-1,3-glucosyltransferase	ALG8	1.81	2.53E-02	0.84	6.56E-01
E9PJL9	NADH dehydrogenase [ubiquinone] flavoprotein 1, mitochondrial	NDUFV1	1.78	4.54E-02	1.57	4.20E-01
Q15651	High mobility group nucleosome-binding domain-containing protein 3	HMGN3	1.76	2.87E-02	1.35	1.62E-01
J3QL06	Hypoxia up-regulated protein 1	HYOU1	1.75	1.19E-04	1.07	7.91E-01
B2R749	Cell division cycle associated 3 (CDCA3), mRNA	N/A	1.75	1.36E-02	1.40	8.47E-02
Q9Y5J6	Mitochondrial import inner membrane translocase subunit Tim10 B	TIMM10B	1.75	3.38E-02	1.32	1.43E-01
O14548	Cytochrome c oxidase subunit 7A-related protein, mitochondrial	COX7A2L	1.73	2.13E-02	0.93	5.51E-01
D6RB85	Calnexin	CANX	1.73	6.11E-03	1.40	3.49E-01
P04179	Superoxide dismutase [Mn], mitochondrial	SOD2	1.72	3.92E-02	1.21	2.95E-01
P05114	Non-histone chromosomal protein HMG-14	HMGN1	1.71	1.83E-02	1.05	5.17E-01
A0A024R9G3	Derlin	DERL1	1.70	2.64E-02	1.73	3.63E-01
A8K7T4	Mannose-binding 2 (LMAN2), mRNA	N/A	1.68	1.87E-02	1.01	9.30E-01
P15954	Cytochrome c oxidase subunit 7C, mitochondrial	COX7C	1.68	8.53E-03	1.26	9.69E-02
A0A2P9AUF2	Pyruvate carboxylase	pyc	1.66	1.25E-02	1.76	6.96E-02
Q9BQE4	Selenoprotein S	SELENOS	1.66	1.88E-02	1.28	8.09E-02
P48380	Transcription factor RFX3	RFX3	1.66	4.39E-02	0.98	9.35E-01
P53370	Nucleoside diphosphate-linked moiety X motif 6	NUDT6	1.65	2.75E-02	1.01	9.55E-01

Q6DKI0	Raptor protein (Fragment)	raptor	1.65	3.40E-02	1.16	1.87E-01
D6W551	Chromosome 2 open reading frame 28, isoform CRA_d	C2orf28	1.64	7.17E-03	1.24	1.75E-02
O60637	Tetraspanin-3	TSPAN3	1.64	2.43E-02	1.26	6.83E-02
H0YIC4	Citrate synthase (Fragment)	CS	1.63	4.83E-02	1.51	8.63E-02
B9ECT5	NADH-ubiquinone oxidoreductase chain 4	NADH4	1.63	5.01E-02	1.12	7.05E-01
A0A024R6A0	Arginase	ARG2	1.63	2.04E-02	1.42	6.01E-02
P08962	CD63 antigen	CD63	1.62	3.59E-02	0.87	1.01E-01
Q86U75	Dihydropyrimidinase-like 2	N/A	1.62	1.68E-02	0.94	6.79E-01
A0A024R8T9	Synaptogyrin	SYNGR2	1.61	1.75E-02	0.75	2.36E-01
D3DP46	Signal peptidase complex subunit 3	SPCS3	1.60	2.66E-02	1.21	4.55E-01
Q9H490	Phosphatidylinositol glycan anchor biosynthesis class U protein	PIGU	1.60	4.17E-02	1.29	2.88E-01
Q9NVV0	Trimeric intracellular cation channel type B	TMEM38B	1.60	2.10E-02	1.10	6.31E-01
A0A1B0GW05	Probable C-mannosyltransferase DPY19L1	DPY19L1	1.58	2.37E-02	1.44	5.19E-02
G3V556	ATP synthase membrane subunit 6.8PL	ATP5MPL	1.58	2.67E-02	1.33	1.14E-01
V9HWB4	Endoplasmic reticulum chaperone BiP	HSPA5	1.58	2.29E-02	1.23	1.08E-01
Q59GX2	Solute carrier family 2 (Facilitated glucose transporter), member 1 variant	N/A	1.57	2.59E-02	1.64	6.39E-02
A0A024RBY9	Cytochrome c heme lyase	HCCS	1.57	4.73E-03	0.99	9.54E-01
Q9H173	Nucleotide exchange factor SIL1	SIL1	1.56	2.06E-02	1.22	2.36E-01
Q9C0E8	Endoplasmic reticulum junction formation protein lunapark	LNPK	1.55	2.63E-02	1.75	5.38E-02
P11117	Lysosomal acid phosphatase	ACP2	1.55	3.19E-02	1.21	1.16E-01
Q9Y320	Thioredoxin-related transmembrane protein 2	TMX2	1.55	4.66E-02	0.96	7.37E-01
Q92791	Endoplasmic reticulum protein SC65	P3H4	1.55	2.58E-02	1.32	2.03E-01
A0A024R9D2	Metadherin, isoform CRA_a	MTDH	1.55	3.07E-02	1.29	9.97E-02
A0A024R8S5	Protein disulfide-isomerase	P4HB	1.55	4.89E-02	1.32	6.33E-02
Q68D91	Metallo-beta-lactamase domain-containing protein 2	MBLAC2	1.55	2.98E-02	0.90	4.50E-01
Q9NWQ8	Phosphoprotein associated with glycosphingolipid-enriched microdomains 1	PAG1	1.55	3.72E-02	0.91	5.30E-01
Q9HDC9	Adipocyte plasma membrane-associated protein	APMAP	1.55	3.85E-02	1.41	9.07E-02

P30049	ATP synthase subunit delta, mitochondrial	ATP5F1D	1.54	3.19E-02	1.36	8.36E-02
E9PKU7	Neutral alpha-glucosidase AB	GANAB	1.54	2.98E-02	1.10	4.89E-01
Q5T6U8	High mobility group AT-hook 1	HMGA1	1.53	3.75E-02	1.09	4.86E-01
Q9UDW1	Cytochrome b-c1 complex subunit 9	UQCR10	1.53	2.99E-02	1.02	8.58E-01
P14927	Cytochrome b-c1 complex subunit 7	UQCRB	1.52	4.64E-02	0.80	7.35E-02
E9PCR7	2-oxoglutarate dehydrogenase, mitochondrial	OGDH	1.52	4.62E-02	1.27	5.09E-02
Q8N4H5	Mitochondrial import receptor subunit TOM5 homolog	TOMM5	1.52	1.39E-02	1.28	3.39E-02
A0A090N8Y2	Protein disulfide-isomerase A4	ERP70	1.52	4.31E-02	1.29	4.08E-02
Q09328	Alpha-1,6-mannosylglycoprotein 6-beta-N-acetylglucosaminyltransferase A	MGAT5	1.52	4.46E-02	1.19	1.54E-01
Q96AY3	Peptidyl-prolyl cis-trans isomerase FKBP10	FKBP10	1.52	1.48E-02	1.10	4.05E-01
A0A087WSV8	Nucleobindin 2, isoform CRA_b	NUCB2	1.52	4.94E-02	1.18	1.52E-01
Q8N766	ER membrane protein complex subunit 1	EMC1	1.51	4.28E-02	1.13	2.25E-01
V9HWF6	Alpha-1-acid glycoprotein	HEL-S-153w	1.51	1.03E-02	1.05	8.54E-01
P51970	NADH dehydrogenase [ubiquinone] 1 alpha subcomplex subunit 8	NDUFA8	1.51	3.43E-02	1.25	6.43E-02
P61803	Dolichyl-diphosphooligosaccharide--protein glycosyltransferase subunit DAD1	DAD1	1.51	4.59E-02	1.52	6.95E-02
B2R4A2	Cytochrome b-c1 complex subunit 7	N/A	1.51	3.88E-02	0.92	4.95E-01
Q99720	Sigma non-opioid intracellular receptor 1	SIGMAR1	1.51	4.90E-02	1.15	4.63E-01
Q15084	Protein disulfide-isomerase A6	PDIA6	1.51	2.58E-02	1.34	1.42E-01
Q53GR7	Solute carrier family 25, member 13 (Citrin) variant (Fragment)	N/A	1.50	4.30E-02	1.06	5.49E-01
P60468	Protein transport protein Sec61 subunit beta	SEC61B	1.50	2.39E-02	0.89	5.53E-01
Q59E90	Alpha-mannosidase (Fragment)	N/A	1.50	4.07E-02	1.15	2.70E-01
A8K2Q6	Peptidyl-prolyl cis-trans isomerase	N/A	1.50	2.09E-02	1.55	5.71E-02
B0QYW5	Peroxisomal membrane protein PMP34	SLC25A17	1.50	2.95E-02	1.00	9.93E-01
B4E2S3	cDNA FLJ56561		1.50	2.73E-02	1.07	2.51E-01
Q9BRX8	Redox-regulatory protein FAM213A	PRXL2A	1.50	3.35E-02	0.92	4.47E-01

Q2M1J6	Oxidase (Cytochrome c) assembly 1-like	OXA1L	1.50	3.67E-02	1.42	9.73E-02
A0A024R3C4	KDEL (Lys-Asp-Glu-Leu) containing 2, isoform CRA_a	KDELC2	1.50	3.74E-02	1.35	7.64E-02
Q96ET8	Golgi apparatus membrane protein TVP23 homolog C	TVP23C	1.49	2.91E-02	1.38	6.40E-02
B7Z1V4	4-aminobutyrate aminotransferase, mitochondrial	N/A	1.49	2.45E-02	1.03	5.42E-01
Q14197	Peptidyl-tRNA hydrolase ICT1, mitochondrial	MRPL58	1.49	4.78E-02	1.32	7.87E-02
O75052	Carboxyl-terminal PDZ ligand of neuronal nitric oxide synthase protein	NOS1AP	1.49	2.02E-02	1.11	4.74E-01
P48723	Heat shock 70 kDa protein 13	HSPA13	1.48	1.99E-02	0.73	6.10E-02
Q53YE2	Syntaxin 3A, isoform CRA_c	STX3A	1.48	3.82E-02	1.01	9.43E-01
Q9BWH2	FUN14 domain-containing protein 2	FUNDC2	1.48	4.85E-02	1.35	6.60E-02
Q9BS26	Endoplasmic reticulum resident protein 44	ERP44	1.48	1.34E-02	1.09	4.67E-01
Q9BXK5	Bcl-2-like protein 13	BCL2L13	1.48	1.57E-02	0.85	1.34E-01
A0A140VJG8	Testicular tissue protein Li 42	N/A	1.47	3.94E-02	1.16	2.25E-01
P10606	Cytochrome c oxidase subunit 5B, mitochondrial	COX5B	1.47	3.44E-02	1.33	9.16E-02
A0A2P9A9L1	Transcription-repair-coupling factor	mfd	1.47	3.32E-02	1.13	8.28E-01
Q7KYR7	Butyrophilin subfamily 2 member A1	BTN2A1	1.47	4.00E-02	1.18	2.50E-01
Q8NF37	Lysophosphatidylcholine acyltransferase 1	LPCAT1	1.47	2.77E-02	1.09	5.60E-01
Q53GQ0	Very-long-chain 3-oxoacyl-CoA reductase	HSD17B12	1.47	3.98E-02	0.93	5.82E-01
P27824	Calnexin	CANX	1.47	3.10E-02	1.21	4.59E-02
B2R694	Terpene cyclase/mutase family member	N/A	1.47	4.76E-02	1.12	3.01E-01
P07686	Beta-hexosaminidase subunit beta	HEXB	1.47	2.91E-02	1.18	1.66E-01
Q9BQA9	Cytochrome b-245 chaperone 1	CYBC1	1.47	2.08E-02	0.76	8.93E-02
Q9NS69	Mitochondrial import receptor subunit TOM22 homolog	TOMM22	1.47	2.55E-02	1.14	3.43E-01
O95292	Vesicle-associated membrane protein-associated protein B/C	VAPB	1.47	4.18E-02	1.17	3.56E-01
A8K335	Gamma-glutamyl hydrolase	N/A	1.46	4.31E-02	1.34	1.07E-01
Q8WUY8	N-acetyltransferase 14	NAT14	1.46	2.39E-02	1.51	5.14E-02
Q8N353	TMEM106B protein	TMEM106B	1.46	4.73E-02	1.28	1.10E-01

O15173	Membrane-associated progesterone receptor component 2	PGRMC2	1.46	4.61E-02	1.32	7.30E-02
P47985	Cytochrome b-c1 complex subunit Rieske, mitochondrial	UQCRFS1	1.46	3.11E-02	1.10	3.68E-01
Q96A26	Protein FAM162A	FAM162A	1.46	2.84E-02	1.26	9.85E-02
H7BZJ3	Protein disulfide-isomerase A3 (Fragment)	PDIA3	1.46	4.53E-02	1.36	9.97E-02
A0A024R1E4	Mitochondrial protein 18 kDa, isoform CRA_a	MTP18	1.46	4.97E-02	1.17	1.32E-01
Q93050	V-type proton ATPase 116 kDa subunit a isoform 1	ATP6V0A1	1.45	4.64E-02	1.16	2.21E-01
A8K032	Translocating chain-associated membrane protein	N/A	1.45	4.52E-02	1.08	3.52E-01
A4D1E9	GTP-binding protein 10	GTPBP10	1.45	5.18E-04	1.68	5.58E-02
A0A140VJK2	Glycerol-3-phosphate dehydrogenase	N/A	1.45	3.43E-02	0.79	6.86E-02
Q9BZE1	39S ribosomal protein L37, mitochondrial	MRPL37	1.45	1.75E-02	1.30	4.48E-03
A0A087WUM0	SYNJ2BP-COX16 readthrough (Fragment)	SYNJ2BP-COX16	1.45	3.02E-02	1.05	6.38E-01
M0R2A0	ER membrane protein complex subunit 10	EMC10	1.45	1.80E-02	0.90	3.51E-01
A0A024R2K1	RAB5A, member RAS oncogene family, isoform CRA_a	RAB5A	1.45	1.85E-02	1.16	2.98E-01
Q8NHP8	Putative phospholipase B-like 2	PLBD2	1.44	1.35E-02	1.23	1.85E-01
P17568	NADH dehydrogenase [ubiquinone] 1 beta subcomplex subunit 7	NDUFB7	1.44	3.65E-02	1.20	6.31E-02
A0A0S2Z4J1	Hydroxysteroid (17-beta) dehydrogenase 4, isoform CRA_b (Fragment)	HSD17B4	1.44	4.14E-02	1.26	7.68E-02
P50749	Ras association domain-containing protein 2	RASSF2	1.44	3.83E-02	1.30	1.10E-01
Q8NBS9	Thioredoxin domain-containing protein 5	TXNDC5	1.44	2.94E-02	1.27	1.57E-01
B2R728	Solute carrier family 7 (cationic amino acidtransporter, y+ system), member 1	N/A	1.44	2.46E-02	0.98	8.72E-01
Q96GC5	39S ribosomal protein L48, mitochondrial	MRPL48	1.44	4.63E-02	1.27	7.45E-02
E9PBY3	N-acetylgalactosaminyltransferase 7	GALNT7	1.44	3.31E-02	0.89	4.27E-01
Q8WY22	BRI3-binding protein	BRI3BP	1.44	3.71E-02	1.31	1.17E-01
P84157	Matrix-remodeling-associated protein 7	MXRA7	1.44	3.00E-02	0.93	5.94E-01

Q96DX4	RING finger and SPRY domain-containing protein 1	RSPRY1	1.43	9.01E-03	1.64	9.49E-02
Q96AJ9	Vesicle transport through interaction with t-SNAREs homolog 1A	VTI1A	1.43	1.47E-02	1.32	7.94E-02
A0A218KGN3	Presenilin	PSEN1	1.43	1.57E-02	1.13	2.37E-01
Q9Y3E0	Vesicle transport protein GOT1B	GOLT1B	1.43	4.82E-02	1.03	8.54E-01
A0A024R008	Solute carrier family 35, member B3, isoform CRA_c	SLC35B3	1.43	1.45E-02	1.25	1.90E-01
P37108	Signal recognition particle 14 kDa protein	SRP14	1.42	4.32E-02	1.23	2.39E-01
P48047	ATP synthase subunit O, mitochondrial	ATP5PO	1.42	2.52E-02	1.32	7.77E-02
Q96H44	GTPBP3 protein (Fragment)	GTPBP3	1.42	7.96E-03	1.19	3.80E-02
B7ZKQ8	Podocalyxin	PODXL	1.42	4.95E-02	0.91	5.04E-01
Q16698	2,4-dienoyl-CoA reductase, mitochondrial	DECR1	1.42	5.01E-02	0.92	3.29E-01
Q9BYV8	Centrosomal protein of 41 kDa	CEP41	1.42	2.73E-02	0.95	9.01E-01
Q9HBL7	Plasminogen receptor (KT)	PLGRKT	1.42	4.07E-02	1.21	2.08E-01
P51572	B-cell receptor-associated protein 31	BCAP31	1.42	3.59E-02	1.08	4.01E-01
H0YCZ6	Transcriptional enhancer factor TEF-1 (Fragment)	TEAD1	1.42	2.81E-02	1.24	5.42E-02
P02654	Apolipoprotein C-I	APOC1	1.41	1.51E-02	0.93	5.07E-01
Q9UBS4	DnaJ homolog subfamily B member 11	DNAJB11	1.41	3.92E-02	1.17	2.81E-01
B2RE48	Candidate tumor suppressor protein (LOC57107), mRNA	N/A	1.41	1.64E-02	1.25	9.24E-02
P23458	Tyrosine-protein kinase JAK1	JAK1	1.41	3.19E-02	1.32	6.42E-02
A0A087WZQ7	Beta-soluble NSF attachment protein	NAPB	1.40	8.78E-05	1.22	1.36E-02
X6R8A1	Carboxypeptidase	CTSA	1.40	4.48E-02	1.24	1.31E-01
O95873	Uncharacterized protein C6orf47	C6orf47	1.40	4.63E-02	1.21	1.44E-01
Q6IB11	PGRMC1 protein	PGRMC1	1.40	3.87E-02	1.09	3.41E-01
Q7Z5P9	Mucin-19	MUC19	1.40	1.11E-02	1.27	1.15E-01
Q9Y4L1	Hypoxia up-regulated protein 1	HYOU1	1.40	2.44E-02	1.15	9.57E-02
Q9H6R6	Palmitoyltransferase ZDHHC6	ZDHHC6	1.39	1.26E-02	1.16	8.73E-02
I6L975	Hydroxysteroid dehydrogenase like 1	HSDL1	1.39	2.27E-02	0.89	2.11E-01
P13473	Lysosome-associated membrane glycoprotein 2	LAMP2	1.39	4.51E-02	1.07	4.47E-01
O00400	Acetyl-coenzyme A transporter 1	SLC33A1	1.39	3.55E-02	1.12	3.25E-01

P49821	NADH dehydrogenase [ubiquinone] flavoprotein 1, mitochondrial	NDUFV1	1.39	4.16E-02	1.24	1.54E-02
Q9P0S3	ORM1-like protein 1	ORMDL1	1.39	4.86E-02	1.08	4.88E-01
V9HVY3	Protein disulfide-isomerase	HEL-S-269	1.39	3.28E-02	1.26	5.48E-02
Q68CN5	Uncharacterized protein DKFZp686D17136	DKFZp686D17136	1.39	2.68E-02	1.07	5.56E-01
P20226	TATA-box-binding protein	TBP	1.38	3.54E-02	1.28	1.76E-01
B4DKM0	Mitochondrial 39S ribosomal protein L3		1.38	4.23E-02	1.18	1.23E-01
Q8TDB4	Protein MGARP	MGARP	1.38	1.52E-02	1.63	7.89E-02
Q15836	Vesicle-associated membrane protein 3	VAMP3	1.38	3.63E-02	1.07	5.07E-01
O95772	STARD3 N-terminal-like protein	STARD3NL	1.38	3.32E-02	1.24	2.30E-01
A0A024R8L7	Acyl-coenzyme A oxidase	ACOX1	1.38	4.90E-02	1.06	5.14E-01
Q9HBH5	Retinol dehydrogenase 14	RDH14	1.37	2.96E-02	1.23	4.38E-02
P51149	Ras-related protein Rab-7a	RAB7A	1.37	4.18E-02	1.15	2.55E-01
Q9NZT2	Opioid growth factor receptor	OGFR	1.37	3.65E-02	1.08	4.20E-01
Q9BVT8	Transmembrane and ubiquitin-like domain-containing protein 1	TMUB1	1.37	1.66E-03	0.89	9.68E-02
P05556	Integrin beta-1	ITGB1	1.37	1.27E-02	1.28	4.31E-02
A0A024R7F4	Deoxyribonuclease II, lysosomal, isoform CRA_a	DNASE2	1.37	1.95E-02	1.22	1.68E-01
A0A0S2Z5B0	Atlastin GTPase 1 isoform 1	ATL1	1.36	2.60E-02	1.41	1.86E-01
B4DV59	REST corepressor 3	RCOR3	1.36	2.64E-02	1.41	1.22E-01
Q86T03	Type 1 phosphatidylinositol 4,5-bisphosphate 4-phosphatase	PIP4P1	1.36	8.32E-03	1.16	4.60E-02
B3KTR4	ARF-related protein 1	N/A	1.36	2.61E-02	1.23	6.81E-02
P51398	28S ribosomal protein S29, mitochondrial	DAP3	1.35	4.44E-02	1.29	3.21E-02
Q6MZM3	Uncharacterized protein DKFZp686C21148	DKFZp686C21148	1.35	1.90E-02	0.92	6.94E-01
Q96ER9	Coiled-coil domain-containing protein 51	CCDC51	1.35	4.37E-02	1.12	3.82E-01
Q86SX6	Glutaredoxin-related protein 5, mitochondrial	GLRX5	1.35	1.96E-02	1.38	8.48E-02
G8JLH6	Tetraspanin	CD9	1.35	3.45E-02	1.15	2.05E-01
A0A024R1U4	RAB5C, member RAS oncogene family, isoform CRA_a	RAB5C	1.34	3.41E-02	1.05	6.21E-01
Q13563	Polycystin-2	PKD2	1.34	2.45E-02	1.39	7.76E-02
Q9H6R3	Acyl-CoA synthetase short-chain family member 3, mitochondrial	ACSS3	1.34	4.97E-02	1.13	1.89E-01

J3KQY1	39S ribosomal protein L22, mitochondrial	MRPL22	1.34	4.49E-02	1.18	3.23E-02
Q9Y6X4	Soluble lamin-associated protein of 75 kDa	FAM169A	1.34	2.54E-02	1.01	9.26E-01
Q9UBI6	Guanine nucleotide-binding protein G(I)/G(S)/G(O) subunit gamma-12	GNG12	1.34	4.44E-02	1.29	4.80E-02
P09661	U2 small nuclear ribonucleoprotein A'	SNRPA1	1.34	4.30E-02	1.26	6.07E-02
B2RE36	cDNA, FLJ96903	N/A	1.34	3.46E-02	1.23	1.31E-01
O15400	Syntaxin-7	STX7	1.34	1.69E-02	0.92	4.88E-01
P38646	Stress-70 protein, mitochondrial	HSPA9	1.34	3.39E-02	1.27	3.35E-02
A1L172	Acyl-CoA thioesterase 1	ACOT1	1.34	2.64E-02	0.99	9.12E-01
A0A024R2Y2	Testicular tissue protein Li 201	TMEM115	1.33	3.89E-02	1.15	1.63E-01
A0A024QZN7	Chromosome 10 open reading frame 70, isoform CRA_b	C10orf70	1.33	2.68E-02	1.09	3.94E-01
Q13948	Protein CASP	CUX1	1.33	1.77E-02	1.41	6.04E-02
P62318	Small nuclear ribonucleoprotein Sm D3	SNRPD3	1.33	4.70E-02	1.15	1.38E-01
Q6UW63	KDEL motif-containing protein 1	POGLUT2	1.33	3.61E-02	1.13	1.07E-01
Q8IXB1	DnaJ homolog subfamily C member 10	DNAJC10	1.32	2.09E-02	1.16	1.77E-01
G0XQ39	STIM1L	STIM1	1.32	4.23E-02	1.23	5.91E-02
P30044	Peroxiredoxin-5, mitochondrial	PRDX5	1.32	4.70E-02	1.30	6.01E-02
A8K644	Splicing factor, arginine/serine-rich 4, isoform CRA_b	SFRS4	1.32	9.30E-03	1.12	2.67E-01
B2R6S9	Low density lipoprotein receptor-related protein associated protein 1 (LRPAP1), mRNA	LRPAP1	1.32	2.71E-02	0.98	7.38E-01
Q96HQ2	CDKN2AIP N-terminal-like protein	CDKN2AIPNL	1.32	3.98E-03	1.18	5.14E-02
A0A024R006	Family with sequence similarity 8, member A1, isoform CRA_a	FAM8A1	1.32	4.13E-02	1.22	2.34E-01
O95822	Malonyl-CoA decarboxylase, mitochondrial	MLYCD	1.32	2.61E-02	1.29	3.32E-02
Q7L5N7	Lysophosphatidylcholine acyltransferase 2	LPCAT2	1.31	3.53E-02	1.33	5.27E-02
A7BI36	p180/ribosome receptor	RRBP1	1.31	1.57E-02	1.24	1.72E-02
A8K6M4	Vesicle transport through interaction with t-SNAREs homolog 1B (yeast) (VTI1B), mRNA	N/A	1.31	4.29E-02	0.99	8.82E-01
E9PK54	Heat shock cognate 71 kDa protein	HSPA8	1.31	6.99E-03	0.91	6.09E-01
A0A024R7G7	Solute carrier family 35, member E1, isoform CRA_c	SLC35E1	1.31	2.98E-02	1.23	2.02E-01

O75167	Phosphatase and actin regulator 2	PHACTR2	1.30	4.06E-02	1.03	7.49E-01
Q9BYD2	39S ribosomal protein L9, mitochondrial	MRPL9	1.30	4.19E-02	1.15	1.22E-01
Q96KC8	DnaJ homolog subfamily C member 1	DNAJC1	1.30	2.30E-02	1.02	8.78E-01
Q16629	Serine/arginine-rich splicing factor 7	SRSF7	1.30	3.07E-02	1.27	5.57E-03
Q16775	Hydroxyacylglutathione hydrolase, mitochondrial	HAGH	1.30	3.18E-02	0.82	2.21E-02
B2RDT8	Sorting nexin 8 (SNX8), mRNA	N/A	0.77	1.64E-02	0.91	1.95E-01
Q86WR7	Proline and serine-rich protein 2	PROSER2	0.76	3.13E-02	0.86	1.74E-01
P55210	Caspase-7	CASP7	0.76	2.61E-02	1.04	7.66E-01
Q8IYR2	SET and MYND domain-containing protein 4	SMYD4	0.76	2.77E-02	1.02	8.29E-01
Q9Y2K3	Myosin-15	MYH15	0.76	1.53E-03	1.13	1.56E-02
Q59EE8	Nuclear receptor coactivator 3 isoform a variant	N/A	0.76	4.22E-02	1.05	5.53E-01
A8K1Z3	Neural cell expressed,developmentally down-regulated gene 1	N/A	0.76	3.92E-02	1.13	2.25E-01
F8VRH0	Poly(rC)-binding protein 2 (Fragment)	PCBP2	0.75	2.12E-02	0.86	1.43E-01
K7ENW2	Zinc finger protein 286A	ZNF286A	0.74	4.44E-02	0.85	2.13E-01
Q9Y3P9	Rab GTPase-activating protein 1	RABGAP1	0.74	3.00E-02	0.83	4.48E-02
O95376	E3 ubiquitin-protein ligase ARIH2	ARIH2	0.74	2.19E-02	0.81	1.84E-01
Q5JTD0	Tight junction-associated protein 1	TJAP1	0.73	3.18E-02	0.77	1.82E-01
Q96E14	RecQ-mediated genome instability protein 2	RMI2	0.73	6.35E-03	0.92	3.58E-01
Q15654	Thyroid receptor-interacting protein 6	TRIP6	0.73	3.15E-02	0.72	6.54E-02
Q712K3	Ubiquitin-conjugating enzyme E2 R2	UBE2R2	0.72	4.33E-02	0.93	6.28E-01
P78356	Phosphatidylinositol 5-phosphate 4-kinase type-2 beta	PIP4K2B	0.69	8.26E-03	1.04	7.13E-01
A0A024QZB4	Sulfotransferase	hCG_1993905	0.69	2.91E-02	0.67	1.68E-01
Q86SE9	Polycomb group RING finger protein 5	PCGF5	0.69	1.83E-02	0.84	1.69E-01
Q9BRX2	Protein pelota homolog	PELO	0.67	1.12E-03	1.25	4.97E-01
H7C3M7	FERM, ARHGEF and pleckstrin domain-containing protein 2	FARP2	0.67	3.63E-02	0.84	2.06E-01

A0A024QZ45	BRCA1 interacting protein C-terminal helicase 1, isoform CRA_a	N/A	0.64	2.69E-03	1.00	9.87E-01
Q59FS2	ZNF589 protein variant	ZNF589	0.64	2.68E-02	0.94	3.20E-01
A6NCF6	Putative MAGE domain-containing protein MAGEA13P	MAGEA13P	0.62	7.13E-03	0.32	1.23E-01
O75953	DnaJ homolog subfamily B member 5	DNAJB5	0.61	2.40E-02	0.72	6.89E-02
B4DUT8	Calponin	CNN2	0.61	1.99E-02	0.78	1.43E-01
X6RLX0	ELKS/Rab6-interacting/CAST family member 1	ERC1	0.59	2.07E-02	0.81	7.84E-02
P02533	Keratin, type I cytoskeletal 14	KRT14	0.53	1.59E-02	0.78	6.29E-01
Q8N612	FTS and Hook-interacting protein	FAM160A2	0.50	3.05E-02	0.24	6.80E-02

Table 4.10 List of proteins significantly altered (≥1.3 fold) in the secretomes of DENV-2 infected HEK293T cells but not in those of REP cells (< 1.3 fold or not significant).

Accession	Description	Gene	Fold change DENV-2/Mock	P-value	Fold change REP/Mock	P-value
Q9HBI1	Beta-parvin	*PARVB*	1.98	4.78E-02	1.44	1.34E-01
P51784	Ubiquitin carboxyl-terminal hydrolase	*USP11*	1.81	2.30E-02	0.79	6.04E-01
F8W8D3	Histone RNA hairpin-binding protein	*SLBP*	1.80	3.46E-02	1.36	2.87E-01
Q9Y657	Spindlin-1	*SPIN1*	1.74	1.80E-02	1.43	1.31E-01
P22059	Oxysterol-binding protein 1	*OSBP*	1.67	5.04E-03	1.34	7.39E-02
E5KLL9	Mitochondrial dynamin-like 120 kDa protein	*N/A*	1.60	4.70E-02	0.92	7.21E-01
B5BU08	U2 small nuclear RNA auxillary factor 1 isoform a	*U2AF1*	1.59	3.56E-02	1.30	1.26E-01
Q9BZX2	Uridine-cytidine kinase 2	*UCK2*	1.58	3.17E-02	1.36	1.72E-01
Q13162	Peroxiredoxin-4	*PRDX4*	1.56	5.42E-04	1.35	8.04E-02
Q9BV44	THUMP domain-containing protein 3	*THUMPD3*	1.55	8.68E-03	0.93	4.98E-01
A0A024RC37	Uncharacterized protein	*P15RS*	1.50	1.31E-02	1.26	2.53E-01
P13010	X-ray repair cross-complementing protein 5	*XRCC5*	1.50	2.54E-02	1.35	1.05E-01
Q96RS6	NudC domain-containing protein 1	*NUDCD1*	1.47	3.30E-02	1.49	6.35E-02
B3KM36	BAG family molecular chaperone regulator 2	*N/A*	1.47	2.34E-02	1.40	1.07E-01
A8K646	Osteoclast stimulating factor 1 (OSTF1), mRNA	*OSTF1*	1.47	2.83E-03	0.74	8.17E-02
P30050	60S ribosomal protein L12	*RPL12*	1.46	2.66E-02	1.09	3.97E-01
Q6NXE6	Armadillo repeat-containing protein 6	*ARMC6*	1.46	1.52E-02	1.16	7.50E-02
A0A024R9B7	Cytochrome c oxidase subunit VIc, isoform CRA_a	*COX6C*	1.45	3.55E-02	1.11	7.11E-01
A8JZZ5	CHK2 checkpoint homolog (S. pombe) (CHEK2), transcript variant 1	*N/A*	1.45	6.10E-03	1.18	1.71E-01
E9PGZ1	Caldesmon	*CALD1*	1.44	1.36E-02	1.14	1.06E-01
A0A087WW40	Endophilin-B1	*SH3GLB1*	1.44	4.53E-02	1.05	5.82E-01
Q14566	DNA replication licensing factor MCM6	*MCM6*	1.43	4.19E-02	1.29	8.96E-02

Q59HH3	Trifunctional purine biosynthetic protein adenosine-3	*N/A*	1.42	2.68E-02	1.25	5.90E-02
E5KT65	DNA-directed RNA polymerase subunit RPABC1	*N/A*	1.41	2.24E-02	1.35	3.04E-01
Q7Z4Q2	HEAT repeat-containing protein 3	*HEATR 3*	1.41	1.89E-02	1.29	1.16E-01
P05412	Transcription factor AP-1	*JUN*	1.41	4.21E-02	1.23	2.21E-01
D3DSW3	Pyridoxal phosphate homeostasis protein	*PROSC*	1.41	2.22E-02	1.15	2.49E-01
P08754	Guanine nucleotide-binding protein G(k) subunit alpha	*GNAI3*	1.40	4.55E-02	1.05	8.74E-01
Q9UK59	Lariat debranching enzyme	*DBR1*	1.40	3.15E-02	1.15	5.57E-01
P12956	X-ray repair cross-complementing protein 6	*XRCC6*	1.40	3.98E-02	1.35	1.17E-01
A0A0S2PZM4	Bifunctional arginine demethylase and lysyl-hydroxylase	*JMJD6*	1.40	3.74E-02	1.04	7.84E-01
Q13596	Sorting nexin-1	*SNX1*	1.38	2.91E-02	1.02	8.66E-01
Q96RU3	Formin-binding protein 1	*FNBP1*	1.37	3.52E-02	1.08	4.24E-01
Q9BUB5	MAP kinase-interacting serine/threonine-protein kinase 1	*MKNK1*	1.36	5.65E-03	1.09	2.27E-01
Q6QNY1	Biogenesis of lysosome-related organelles complex 1 subunit 2	*BLOC1 S2*	1.36	2.08E-02	0.86	2.82E-01
O75794	Cell division cycle protein 123 homolog	*CDC12 3*	1.35	3.61E-02	0.99	9.11E-01
P0DI82	Trafficking protein particle complex subunit 2B	*TRAPPC 2B*	1.34	3.73E-02	0.99	9.64E-01
A0A024R2H7	tRNA nucleotidyl transferase, CCA-adding, 1, isoform CRA_b	*TRNT1*	1.34	4.52E-02	1.25	2.28E-01
B4DSS8	Polypyrimidine tract-binding protein 2	*N/A*	1.34	3.76E-02	1.07	4.21E-01
E5KN59	Peptidyl-prolyl cis-trans isomerase D	*N/A*	1.33	1.62E-03	1.11	9.61E-04
Q96K21	Abscission/NoCut checkpoint regulator	*ZFYVE1 9*	1.32	7.66E-04	1.12	8.72E-01
Q15185	Prostaglandin E synthase 3	*PTGES3*	1.32	1.73E-02	1.21	2.64E-01
Q9BRP1	Programmed cell death protein 2-like	*PDCD2 L*	1.32	3.06E-02	0.94	9.07E-02
P48507	Glutamate--cysteine ligase regulatory subunit	*GCLM*	1.31	2.81E-02	1.18	2.64E-01
O95295	SNARE-associated protein Snapin	*SNAPI N*	1.31	4.07E-03	0.93	3.33E-01
B1AHD1	NHP2-like protein 1	*SNU13*	1.30	3.43E-02	1.02	8.64E-01
Q8IUH2	Protein CREG2	*CREG2*	0.77	3.75E-03	0.15	1.51E-01
Q9BY77	Polymerase delta-interacting protein 3	*POLDI P3*	0.77	3.60E-02	0.89	4.51E-01

Q96PY6	Serine/threonine-protein kinase Nek1	*NEK1*	0.76	1.42E-02	0.90	4.61E-01
Q9NWK9	Box C/D snoRNA protein 1 O	*ZNHIT6*	0.75	3.40E-02	0.88	9.84E-02
Q5SSJ5	Heterochromatin protein 1-binding protein 3	*HP1BP3*	0.74	8.89E-03	1.40	1.78E-01
Q9NZB2	Constitutive coactivator of PPAR-gamma-like protein 1	*FAM120A*	0.72	1.24E-02	0.75	1.70E-01
A8K492	Methionine-tRNA synthetase (MARS), mRNA	*MARS*	0.71	4.93E-02	0.88	4.18E-01
A8K7E0	Biglycan	*BGN*	0.70	3.38E-02	1.32	1.79E-01
A8K5Q1	Bin3, bicoid-interacting 3, homolog (Drosophila) (BCDIN3)	*N/A*	0.70	2.19E-02	0.77	1.44E-01
Q96IZ7	Serine/Arginine-related protein 53	*RSRC1*	0.70	2.39E-02	0.78	1.41E-01
A0A0S2Z4Z0	RNA binding motif protein 14 isoform 1	*RBM14*	0.69	3.82E-02	0.77	1.35E-01
H7C2Q8	EBNA1 binding protein 2	*EBNA1BP2*	0.68	4.09E-02	0.92	6.54E-01
W5ZR30	Transcription factor 20 (AR1), isoform CRA_b	*TCF20*	0.68	8.50E-03	0.91	2.50E-01
B4DUT2	Protein KRI1 homolog	*KRI1*	0.68	3.27E-02	0.91	6.47E-01
Q15149	Plectin	*PLEC*	0.68	1.72E-02	1.05	9.03E-01
Q8ND82	Zinc finger protein 280C	*ZNF280C*	0.67	3.60E-02	0.73	1.43E-01
Q96BK5	PIN2/TERF1-interacting telomerase inhibitor 1	*PINX1*	0.66	2.48E-02	0.72	1.47E-01
Q6IAX2	RPL21 protein	*RPL21*	0.66	1.92E-02	0.78	7.44E-02
Q03701	CCAAT/enhancer-binding protein zeta	*CEBPZ*	0.64	3.01E-02	1.15	4.84E-01
A0A024R0Z3	DEAD (Asp-Glu-Ala-Asp) box polypeptide 23	*DDX23*	0.64	1.85E-02	0.65	5.41E-02
Q03164	Histone-lysine N-methyltransferase 2A	*KMT2A*	0.64	3.51E-02	0.91	6.21E-01
O95292	Vesicle-associated membrane protein-associated protein B/C	*VAPB*	0.63	2.88E-02	1.21	3.52E-01
A5D8W8	Gamma-glutamyltransferase 7	*GGT7*	0.63	4.46E-02	0.95	7.95E-01
Q9UPN4	Centrosomal protein of 131 kDa	*CEP131*	0.61	3.88E-02	0.36	6.86E-02
A0A0X1KG71	Negative elongation factor B	*NELFB*	0.58	2.95E-02	0.73	4.62E-01
Q9Y4C8	Probable RNA-binding protein 19	*RBM19*	0.55	4.78E-02	0.60	1.47E-01
Q15059	Bromodomain-containing protein 3	*BRD3*	0.55	4.77E-02	0.69	2.62E-01
P49916	DNA ligase 3	*LIG3*	0.55	4.65E-02	0.67	4.36E-01
G5EA30	CUG triplet repeat, RNA binding protein 1	*CELF1*	0.54	3.88E-02	1.12	6.30E-01
Q99442	Translocation protein SEC62	*SEC62*	0.43	8.22E-03	0.68	1.38E-01
A0A0J9YXC7	LIM and senescent cell antigen-like-containing domain protein	*LIMS4*	0.43	4.50E-02	0.93	6.59E-01

4.4 Bioinformatic analysis of cellular and secreted proteins altered in abundance in response to DENV-2 infection

4.4.1 Bioinformatic analysis of cellular proteins altered in abundance in response to DENV-2 infection.

The 171 and 31 proteins (listed in Table 4.4) that significantly increased and decreased ≥ 1.5 fold, respectively, in DENV-2 cells compared to mock infected cells were subjected to gene enrichment and network analysis using the DAVID and STRING analysis programs (Figures 4.5-4.6 and supplementary Table S4.2).

DAVID analysis showed that the proteins that significantly increased in response to DENV infection included 14 enriched clusters of proteins (Figure 4.5). The top three were associated with the GOCC terms "integral component of membrane", (GO:0016021) followed by "mitochondrion" (GO:0005739) and the Uniprot (UP) keyword "glycoprotein". Other significantly enriched GO terms that are related to DENV infection included the GOBP term "endoplasmic reticulum unfolded protein response" (GO:0030968). The top enriched KEGG pathway was "oxidative phosphorylation" (hsa00190: P-value = 9.30E-09) (data not shown). However, the proteins that significantly decreased in response to DENV infection were not associated with any specific GO term.

STRING analysis revealed that proteins increased in response to DENV infection were significantly associated with the GOBP terms "generation of precursor metabolites and energy", "cellular respiration" and "ATP metabolic process" (Figure 4.6). An enrichment of proteins associated with the GOCC terms "mitochondrion" and KEGG pathway of "oxidative phosphorylation" were also observed. Whereas the proteins that decreased in response to infection were associated with only the UP keyword "phosphoprotein".

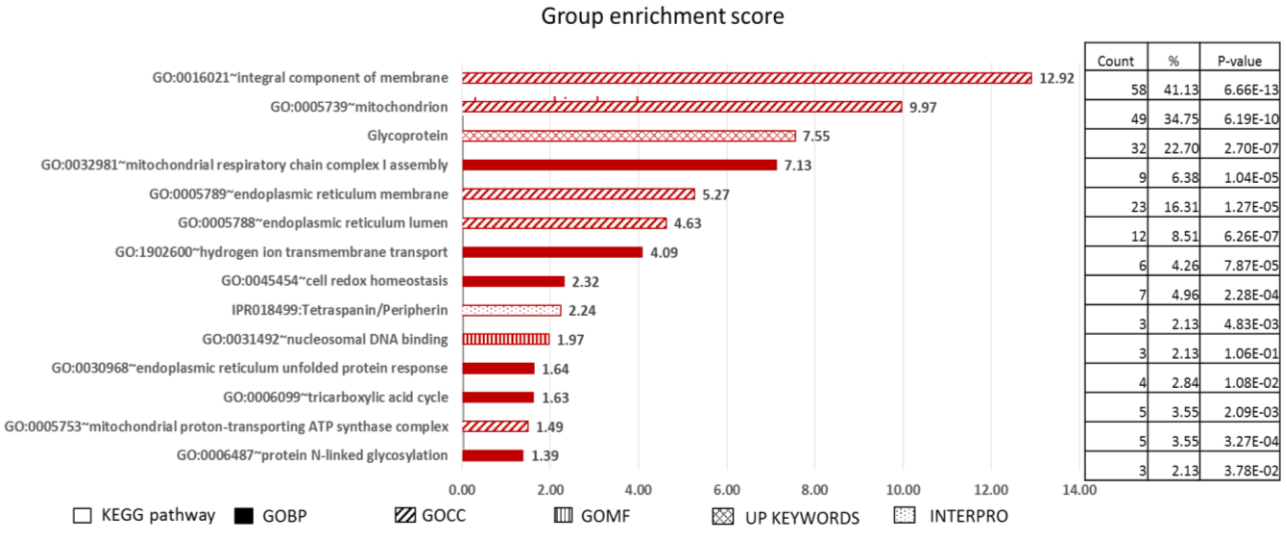

Figure 4.5 DAVID analysis of cellular proteins that were altered in abundance in DENV-2 infected HEK293T cells, compared to mock infected cells.

Proteins that were significantly (P-value < 0.05) altered in amount by ≥ 1.5 fold in DENV-2 infected HEK293T cells compared to mock infected cells were analysed using the DAVID database. The GO accession numbers/terms that were significantly enriched and the properties of the corresponding protein clusters are shown. The GES of significantly enriched GO terms are plotted as bar graphs (red) with the corresponding GES score shown. The shading shows the type of GO term (GOBP, GOCC or GOMF), UP keywords, Interpro term or KEGG pathway. The number of proteins in each cluster (count), number of proteins associated with each GO term/total number of proteins in the dataset (%) and P-value for each of the annotation terms are listed in the table.

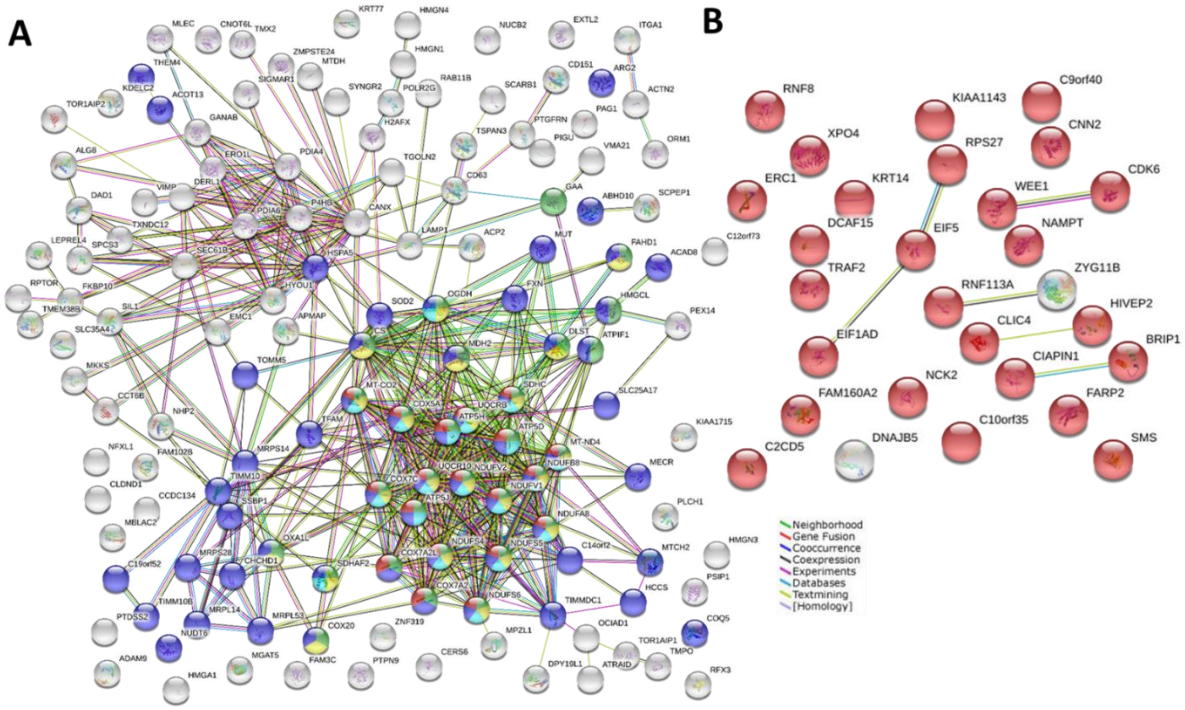

GO term/ pathway	description	count in gene set	FDR
GO:0006091	generation of precursor metabolites and energy	30 of 388	2.50E-18
GO:0045333	cellular respiration	22 of 153	2.77E-18
GO:0046034	ATP metabolic process	19 of 190	1.79E-13
GO:0005739	mitochondrion	57 of 1531	3.53E-24
hsa00190	Oxidative phosphorylation	19 of 131	1.25E-16

GO term/ pathway	description	count in gene set	FDR
KW-0597	Phosphoprotein	26 of 8066	1.33e-06

Figure 4.6STRING analysis of cellular proteins that were altered in abundance in DENV-2 infected HEK293T cells, compared to mock infected cells.

The STRING database was searched to analyse cellular proteins that significantly (P-value < 0.05) increased **(A)** and decreased **(B)** ≥ 1.5 fold in response to DENV-2 infection. **(A)** Nodes representing proteins associated with the significantly enriched GO terms "generation of precursor metabolites and energy", "cellular respiration", "ATP metabolic process" and "mitochondrion" as well as the KEGG pathway "Oxidative phosphorylation" are shaded in green, yellow, light blue, blue, and red, respectively. (**B**) Nodes representing proteins associated with the significantly enriched UP keyword term "phosphoprotein" are shaded in red. The number of coloured nodes/ total proteins involved for each term and the FDR of each GO term are listed in the table.

4.4.2 Bioinformatic analysis of the secretomes from DENV-2 infected HEK293T cells

The 31 and 23 host proteins (listed in Table 4.5) that significantly increased and decreased ≥ 1.5 fold, respectively, in the secretomes from DENV-2 cells, compared to mock infected cells, were also analysed using the DAVID and STRING analysis programs. These secreted proteins were not significantly associated with any GO term by DAVID analysis. In contrast, STRING analysis showed that for proteins that increased in amount, there was an enrichment of proteins that were associated with the GO terms “metabolic process”, “gene expression”, “mRNA splicing, via spliceosome”, “proteasome regulatory particle” and “secretory granule" (Figure 4.7A). The secreted proteins that decreased in amount in response to DENV-2 infection were associated with the GOCC term “intracellular membrane-bounded organelle” and the UP keyword “phosphoprotein” similar to the proteins that decreased in abundance in the proteome (Figure 4.7B).

4.4.3 Bioinformatic analysis of proteins that significantly changed in both the proteome and secretome of HEK293T cells in response to DENV infection.

The five proteins that significantly changed (≥1.3 fold, both increased and decreased) in both the cellular proteome and secretome (Table 4.6) were analysed using STRING. Three of five proteins (NUP37, COX6C and DNAJC1) were associated with the GOCC term “organelle envelope” (GO:0031967; 3 of 1146 proteins, FDR= 4.79E-02).

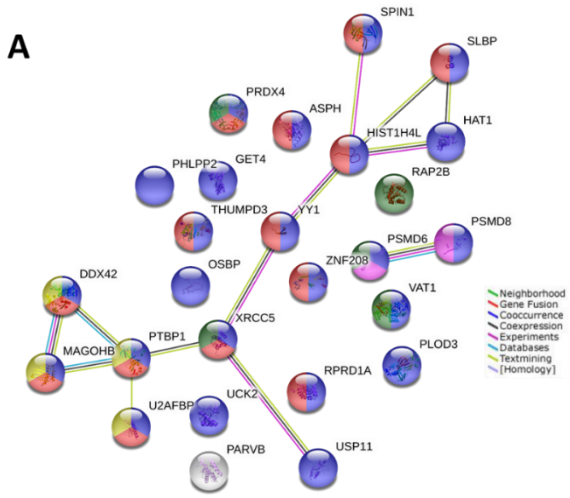

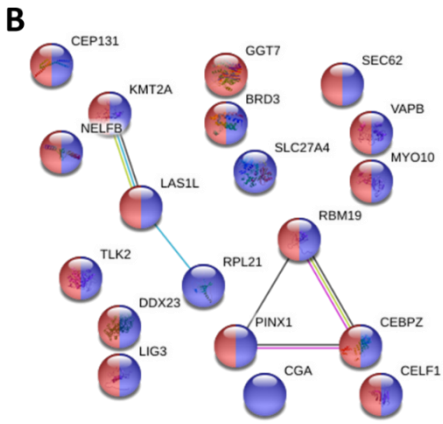

GO term/ pathway	description	count in gene set	FDR
GO:0008152	metabolic process	24 of 9569	3.10E-03
GO:0010467	gene expression	14 of 3733	1.08E-02
GO:0000398	mRNA splicing, via spliceosome	4 of 284	3.20E-02
GO:0005838	proteasome regulatory particle	2 of 21	5.50E-03
GO:0030141	secretory granule	5 of 828	3.30E-02

GO term/ pathway	description	count in gene set	FDR
KW-0597	Phosphoprotein	16 of 8066	1.53E-02
GO:0043231	intracellular membrane-bounded organelle	18 of 10365	1.42E-02

Figure 4.7 STRING analysis of secreted proteins that were altered in abundance in the secretomse from DENV-2 infected HEK293T cells, compared to mock infected cells.

The STRING database was searched to analyse secreted proteins that significantly (P-value < 0.05) increased **(A)** and decreased **(B)** ≥ 1.5 fold in response to DENV-2 infection. **(A)** Nodes representing proteins associated with the significantly enriched GO terms "metabolic process", "gene expression", "mRNA splicing, via spliceosome", "proteasome regulatory particle" and "secretory granule", are shaded in blue, red, yellow, pink and green, respectively. (**B**) Nodes representing proteins associated with the significantly enriched GO terms "intracellular membrane-bounded organelle" and the UP keyword "phosphoprotein" are shaded in blue and red, respectively. The number of coloured nodes/ total proteins involved for each term and the FDR of each GO term are listed in the table.

4.5 Bioinformatic analysis of cellular and secreted proteins that were commonly altered in abundance in both DENV-2 infected HEK293T and REP cells

4.5.1 Bioinformatic analysis of cellular proteins that commonly altered in abundance in both DENV-2 infected HEK293T and REP cells.

To identify cellular host proteins dysregulated by replication of the DENV genome, proteins that were commonly altered in DENV-2 infected HEK293T and REP cells compared to mock infected cells were analysed. There were 297 proteins that were significantly altered ≥ 1.3 fold, so a more stringent cut-off (≥ 1.5 fold) was applied for bioinformatics analysis to increase specificity. Thus, 71 and 20 common host proteins that significantly increased and decreased ≥ 1.5 fold, respectively, in DENV-2 infected cells and REP cells compared to mock infected cells were subjected to gene enrichment and network analysis using the DAVID and STRING analysis programs (Figures 4.8-4.9 and supplementary Table S4.3).

DAVID analysis showed that three clusters of proteins were significantly enriched in the proteins commonly increased in abundance. The clusters were associated with the GOCC terms "mitochondrion" (GO:0005739), "integral component of membrane" (GO:0016021), the UP keyword "Signal/signal peptide" (Figure 4.8) and the KEGG pathway "Metabolic pathways" (hsa01100: P-value= 3.10E-03). STRING analysis revealed a significant enrichment of proteins associated with the GOCC term "mitochondrial part" and the KEGG pathway "metabolic pathways", similar to the DAVID analysis. Moreover, STRING analysis also revealed enriched proteins associated with the GOBP terms "mitochondrion organization", "aerobic respiration" and "ATP metabolic process" (Figure 4.9A).

DAVID analysis of the proteins that significantly decreased in both DENV-2 infected HEK293T and REP cells compared to mock infected cells revealed no significantly enriched proteins. STRING analysis revealed that this group of proteins was only significantly enriched for proteins associated with the UP keyword "phosphoprotein" (Figure 4.9B).

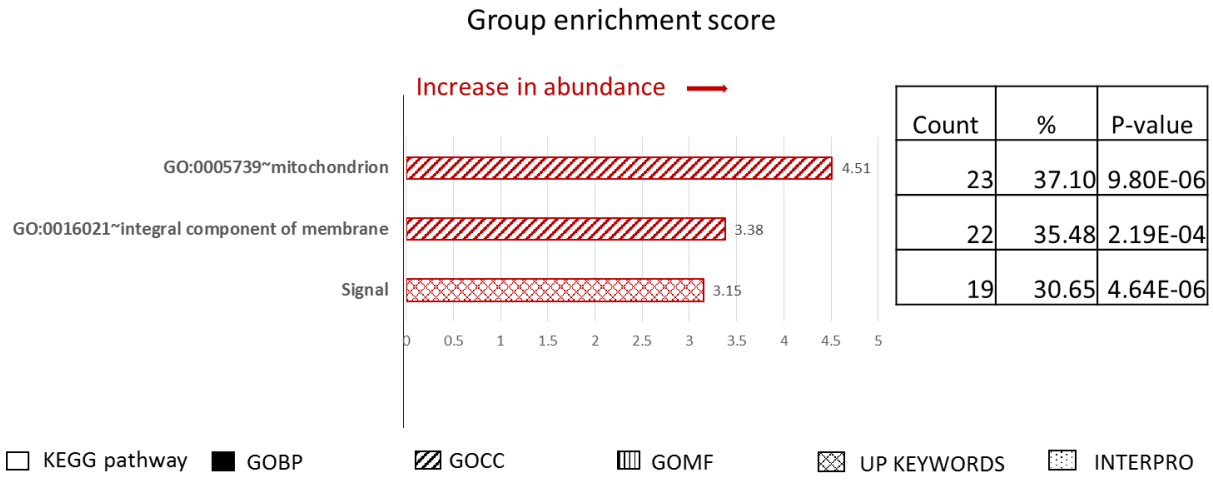

Count	%	P-value
23	37.10	9.80E-06
22	35.48	2.19E-04
19	30.65	4.64E-06

Figure 4.8 DAVID analysis of cellular proteins that were altered in abundance in both DENV-2 infected HEK293T and REP cells.

Proteins that were significantly (P-value < 0.05) altered in amount by ≥ 1.5 fold in both DENV-2 infected HEK293T and REP cells compared to mock infected cells were analysed using the DAVID database. The GO accession numbers/terms that were significantly enriched and the properties of the corresponding protein clusters are shown. The GES of significantly enriched GO terms are plotted as bar graphs (red) with the corresponding GES score shown. The shading shows the type of GO term (GOBP, GOCC or GOMF), UP keywords, Interpro term or KEGG pathway. The number of proteins in each cluster (count), number of proteins associated with each GO term/total number of proteins in the dataset (%) and P-value for each of the annotation terms are listed in the table.

A

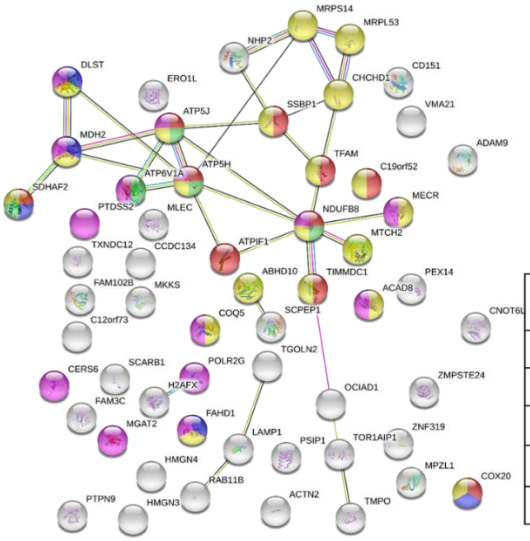

GO term/ pathway	description	count in gene set	FDR
GO:0007005	mitochondrion organization	10 of 424	6.70E-04
GO:0009060	aerobic respiration	5 of 71	1.50E-03
GO:0046034	ATP metabolic process	5 of 190	3.06E-02
GO:0044429	mitochondrial part	20 of 1015	1.38E-09
hsa01100	Metabolic pathways	14 of 1250	7.20E-04

B

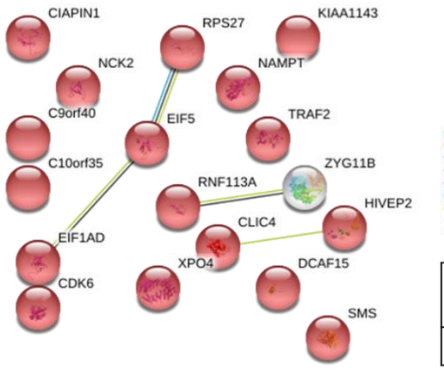

GO term/ pathway	description	count in gene set	FDR
KW-0597	Phosphoprotein	17 of 8066	2.40E-04

Figure 4.9 STRING analysis of cellular proteins that were altered in abundance in both DENV-2 infected HEK293T and REP cells, compared to uninfected cells.

The STRING database was searched to analyse cellular proteins that significantly (P-value < 0.05) increased **(A)** and decreased **(B)** ≥ 1.5 fold in both DENV-2 infected HEK293T and REP cells compared to mock infected cells. **(A)** Nodes representing proteins associated with the significantly enriched GO terms "mitochondrion organization", "aerobic respiration", "ATP metabolic process" and "mitochondrial part" as well as KEGG pathway "Metabolic pathways" are shaded in red, blue, green, yellow, and pink respectively. (**B**) Nodes representing proteins associated with the significantly enriched UP keyword "phosphoprotein" are shaded in red. The number of coloured nodes/ total proteins involved for each term and the FDR of each GO term are listed in the table.

4.5.2 Bioinformatic analysis of proteins commonly altered in abundance in the secretomes from both DENV-2 infected HEK293T and REP cells compared to mock infected cells.

Using a cut-off value of ≥ 1.5 fold, there were only 13 and 3 proteins that commonly significantly increased and decreased in secretomes from both DENV-2 infected HEK293T and REP cells compared with mock infected cells. Thus, a lower cut-off ≥ 1.3 fold was applied. The 33 and 13 secreted proteins (listed in Table 4.8) that commonly significantly increased and decreased, respectively, in secretomes from both DENV-2 infected HEK293T and REP cells were analysed using DAVID and STRING. There was no significant enriched cluster of proteins by DAVID analysis.

STRING analysis showed that almost all of the secreted proteins that significantly increased in abundance in the secretomes from both DENV infected and REP cells compared to mock infected cells were associated with the GOCC and GOBP terms "membrane-bounded organelle" (GO:0043227) and "cellular metabolic process" (GO:0044237) respectively (Figure 4.10A). Protein associated with the GOBP term "mRNA splicing, via spliceosome" (GO:0000398) and the GOCC term "spliceosomal complex" (GO:0005681) were also significantly enriched. Moreover, proteins associated with the GOBP term "mRNA export from nucleus" were significantly enriched among this group of proteins. The proteins that commonly decreased in the secretomes of DENV-2 infected HEK293T and REP cells showed an enrichment of proteins associated with the GOBP terms "positive regulation of viral process" and "positive regulation of viral genome replication" (Figure 4.10B).

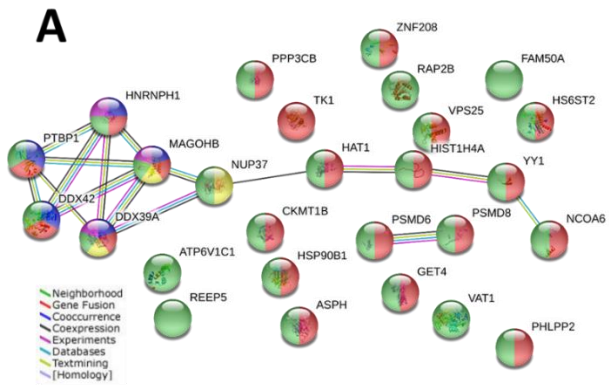

GO term/ pathway	description	count in gene set	FDR
GO:0044237	cellular metabolic process	21 of 8797	3.89E-02
GO:0000398	mRNA splicing, via spliceosome	5 of 284	2.97E-02
GO:0006406	mRNA export from nucleus	3 of 107	3.89E-02
GO:0043227	membrane-bounded organelle	26 of 11244	1.90E-04
GO:0005681	spliceosomal complex	3 of 187	2.35E-02

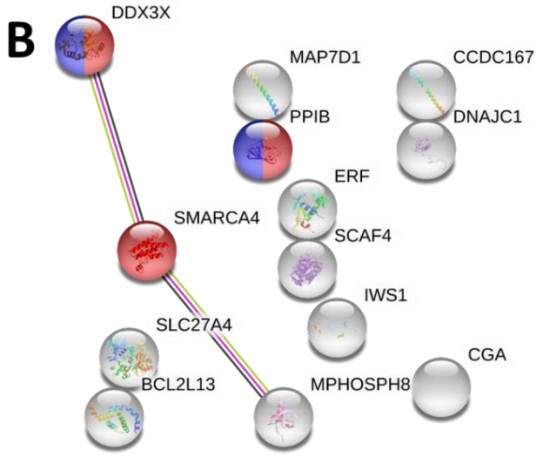

GO term/ pathway	description	count in gene set	FDR
GO:0048524	positive regulation of viral process	3 of 85	1.31E-02
GO:0045070	positive regulation of viral genome replication	2 of 35	4.03E-02

Figure 4.10 STRING analysis of secreted proteins that were altered in abundance in both secretomes from DENV-2 infected HEK293T and REP cells, compared in mock infected cells.

The STRING database was searched to analyse secreted proteins that significantly (P-value < 0.05) increased **(A)** and decreased **(B)** ≥ 1.3 fold in abundance in both the secretomes from DENV-2 infected HEK293T and REP cells compared to mock infected cells. **(A)** Nodes representing proteins associated with the significantly enriched GOBP "cellular metabolic process", "mRNA splicing, via spliceosome" and "mRNA export from nucleus" as well as GOCC of "membrane-bounded organelle" and "spliceosomal complex" are shaded in red, blue, yellow, green, and pink, respectively. (**B**) Nodes representing proteins associated with the significantly enriched GOBP "positive regulation of viral process" and "positive regulation of viral genome replication" are shaded in red and blue, respectively. The number of coloured nodes/total proteins involved for each term and the FDR of each GO term are listed in the table.

4.6 Analysis of proteins that significantly altered in abundance in the proteome and secretomes of DENV-2 infected HEK293T cells (≥1.3 fold) but not in REP cells (< 1.3 fold or not significant)

To determine the effect of the DENV structural proteins and virus assembly and secretion processes on the host proteome and secretome, proteins that significantly increased or decreased (≥1.3 fold) in DENV-2 infected HEK293T cells but not in REP cells (< 1.3 fold or not significant) compared to mock infected cells were analysed.

4.6.1 Bioinformatic analysis of cellular proteins that were significantly altered in only DENV-2 infected HEK293T cells but not in REP cells

The 208 and 28 proteins that significantly increased and decreased (≥1.3 fold), respectively, only in DENV-2 infected HEK293T cells but not in REP cells were analysed using the DAVID and STRING programs. DAVID analysis showed that the cellular proteins that increased in abundance only during DENV infection included 11 clusters of significantly enriched proteins (Figure 4.11 and Supplementary Table S4.4). The top three clusters were associated with the GO terms "integral component of membrane", "endoplasmic reticulum" and the keyword "signal/signal peptide" (Figure 4.11). The top two significant KEGG pathways were "protein processing in endoplasmic reticulum" (hsa04141: P-value= 3.75E-08) and "phagosome" (hsa04145: P-value= 7.95E-05) (Supplementary Table S 4.3). STRING analysis revealed a similar trend to the DAVID analysis, with an enrichment of proteins associated with the GOBP terms "cell redox homeostasis" and "response to unfolded protein" as well as the KEGG pathway terms "protein processing in endoplasmic reticulum" and "phagosome" (Figure 4.12A). Furthermore, there was a significant enrichment of proteins associated with GO terms related to processes known to be modified by DENV infection, including "ubiquitin-dependent" and "lipid metabolic process".

The proteins that significantly decreased (≥1.3 fold) in DENV infected HEK293T cells but not in REP cells were not significantly enriched in any cluster of proteins by DAVID analysis. However, STRING analysis revealed that this group of proteins was

significantly enriched in proteins associated with the UP keyword “phosphoprotein” and the KEGG pathway “Fanconi anemia” (hsa03460) (Figure 4.12B).

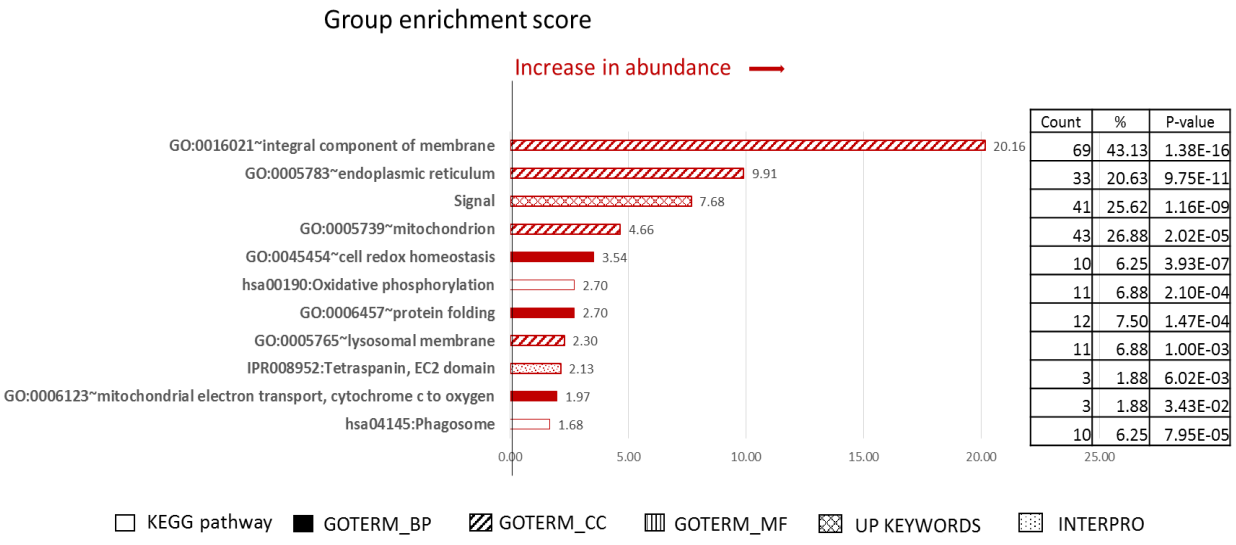

Count	%	P-value
69	43.13	1.38E-16
33	20.63	9.75E-11
41	25.62	1.16E-09
43	26.88	2.02E-05
10	6.25	3.93E-07
11	6.88	2.10E-04
12	7.50	1.47E-04
11	6.88	1.00E-03
3	1.88	6.02E-03
3	1.88	3.43E-02
10	6.25	7.95E-05

Figure 4.11 DAVID analysis of cellular proteins that were altered in only DENV-2 infected HEK293T cells but not in REP cells.

Proteins that were significantly (P-value < 0.05) altered in amount by ≥ 1.3 fold in DENV-2 infected HEK293T cells but not in REP cells (< 1.3 fold or not significant) compared to mock infected cells were analysed using the DAVID database. The GO accession numbers/terms that were significantly enriched and the properties of the corresponding protein clusters are shown. The GES of significantly enriched GO terms are plotted as bar graphs (red) with the corresponding GES score shown. The shading shows the type of GO term (GOBP, GOCC or GOMF), UP keywords, Interpro term or KEGG pathway. The number of proteins in each cluster (count), number of proteins associated with each GO term/total number of proteins in the dataset (%) and P-value for each of the annotation terms are listed in the table.

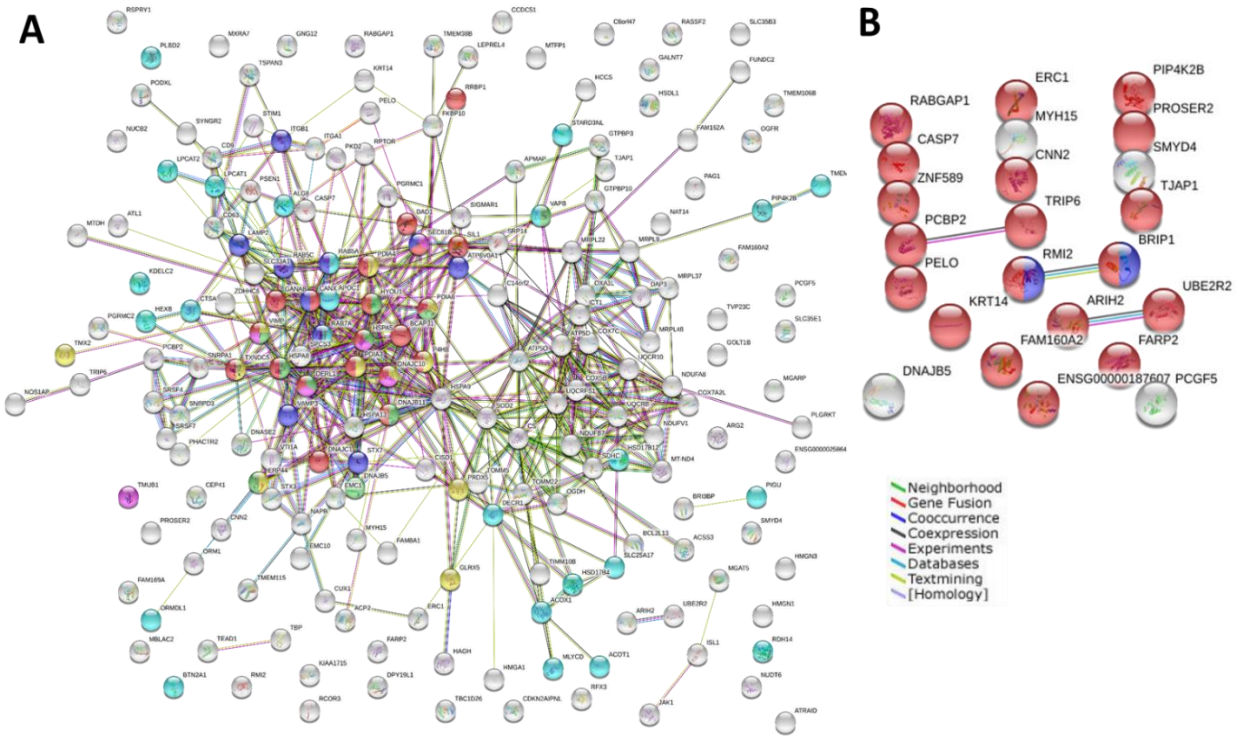

GOterm/ pathway	description	count in gene set	FDR
GO:0045454	cell redox homeostasis	11 of 68	1.38E-07
GO:0030433	ubiquitin-dependent	6 of 65	2.70E-03
GO:0006986	response to unfolded protein	10 of 153	3.10E-04
GO:0006629	lipid metabolic process	25 of 1192	1.22E-02
hsa04141	Protein processing in endoplasmic reticulum	20 of 161	2.20E-14
hsa04145	Phagosome	10 of 145	5.61e-05

GO term/ pathway	description	count in gene set	FDR
KW-0597	Phosphoprotein	19 of 8066	4.60E-02
hsa03460	Fanconi anemia pathway	2 of 51	4.21E-02

Figure 4.12 STRING analysis of cellular proteins that were altered in abundance in only DENV-2 infected HEK293T cells but not in REP cells.

The STRING database was searched to analyse cellular proteins that significantly (P-value < 0.05) increased (A) and decreased (B) ≥ 1.3 fold in in only DENV-2 infected cells but changed < 1.3 fold or not significantly changed in REP cells. (**A**) Nodes representing proteins associated with the significantly enriched GO terms "cell redox homeostasis", "ubiquitin-dependent" "response to unfolded protein" and "lipid metabolic process" as well as KEGG pathway "protein processing in endoplasmic reticulum" and "phagosome" are shaded in yellow, purple, green, light blue, red and blue, respectively. (**B**) Nodes representing proteins associated with the significantly enriched UP keyword "phosphoprotein" and KEGG pathway of "Fanconi anemia pathway" are shaded in red and blue, respectively. The number of coloured nodes/ total proteins involved for each term and the FDR of each GO term are listed in the table.

4.6.2 Bioinformatic analysis of proteins that were significantly altered (≥1.3 fold) in the secretome from DENV-2 infected HEK293T cells but not in those of REP cells

The 46 and 32 secreted proteins that significantly increased and decreased ≥ 1.3 fold, respectively, only in the secretome from DENV-2 infected HEK293T cells were subjected to functional analysis by DAVID and STRING. There were neither significantly enriched clusters of proteins nor KEGG pathways by DAVID analysis.

STRING analysis showed that the 46 proteins that significantly increased only in the secretomes from DENV infected cells were associated with the the KEGG pathway "non-homologous end-joining", GOBP term "cellular hyperosmotic salinity response" and GOMF term "RNA binding" (Figure 4.13A). By contrast, the majority of the 32 secreted proteins that significantly decreased in only the secretome of DENV-2 infected cells were associated with the GOCC and GOBP terms "intracellular membrane-bounded organelle" and "nucleic acid metabolic process", respectively (Figure 4.13B).

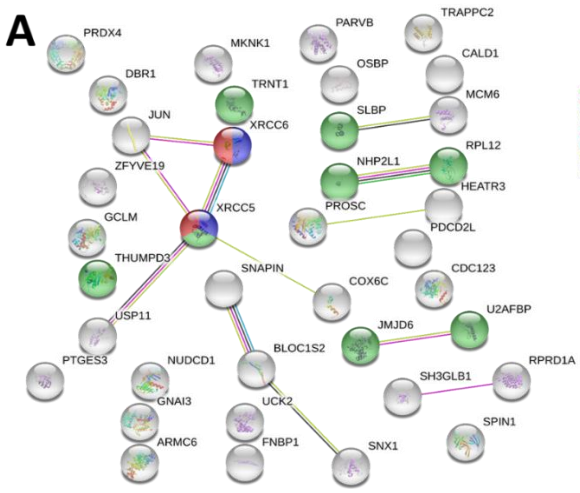

GO term/ pathway	description	count in gene set	FDR
hsa03450	Non-homologous end-joining	2 of 13	3.74E-02
GO:0071475	cellular hyperosmotic salinity response	2 of 3	4.52E-02
GO:0003723	RNA binding	8 of 850	2.47E-02

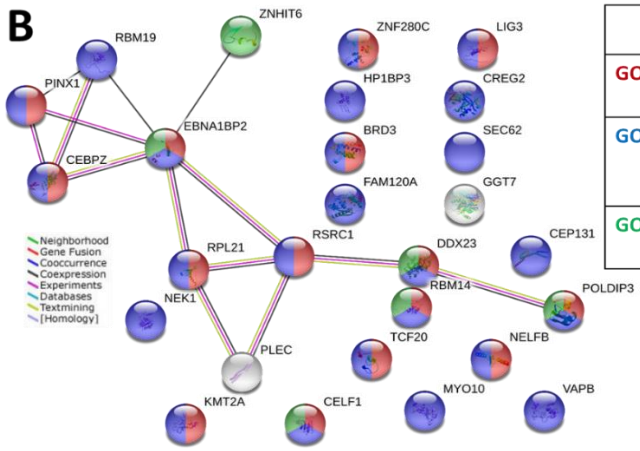

GOterm/ pathway	description	count in gene set	FDR
GO:0090304	nucleic acid metabolic process	15 of 3941	4.15E-02
GO:0043231	intracellular membrane-bounded organelle	24 of 10365	1.30E-02
GO:1990904	ribonucleoprotein complex	6 of 770	1.67E-02

Figure 4.13 STRING analysis of secreted proteins that were altered in abundance in only secretomes from DENV-2 infected HEK293T cells but not in those of REP cells.

The STRING database was searched to analyse secreted proteins that significantly (P-value < 0.05) increased (A) and decreased (B) ≥ 1.3 fold in only secretomes from DENV-2 infected cells but changed < 1.3 fold or did not significantly change in REP cells. (A) Nodes representing proteins associated with the significantly enriched KEGG pathway "non-homologous end-joining" and the GO terms "cellular hyperosmotic salinity response" and "RNA binding" are shaded in red, blue, and green, respectively. (B) Nodes representing proteins associated with the significantly enriched GO terms "nucleic acid metabolic process", "intracellular membrane-bounded organelle" and "ribonucleoprotein complex" are shaded in red, blue, and green, respectively. The number of coloured nodes/ total proteins involved for each term and the FDR of each GO term are listed in the table.

4.7 Validation of the LC-MS/MS analysis

4.7.1 Viral proteins

The DENV-2 NS1 protein, a 45 kDa glycoprotein, is well known as a secreted viral protein which plays an important role in DEN pathogenesis. As expected, LC-MS/MS analysis detected the NS1 protein in both the proteomes and secretomes of DENV-2 infected HEK293T and REP cells. The detection of the NS1 protein was successfully validated using both cell lysates and supernatants from DENV-2 infected HEK293T and REP cells (Figures 4.14A and B).

DENV-2 NS4B, an integral membrane protein, was also selected for validation. As expected, Western blotting analysis successfully validated the presence of NS4B in cell lysates of both DENV-2 infected HEK293T and REP cells (Figure 4.14A).

As GAPDH was found not to change in amount in DENV-2 infected HEK293T and REP cells compared to mock infected cells it was used as a loading control. However, GAPDH was not detected in the secretomes of DENV-2 infected HEK293T and REP cells.

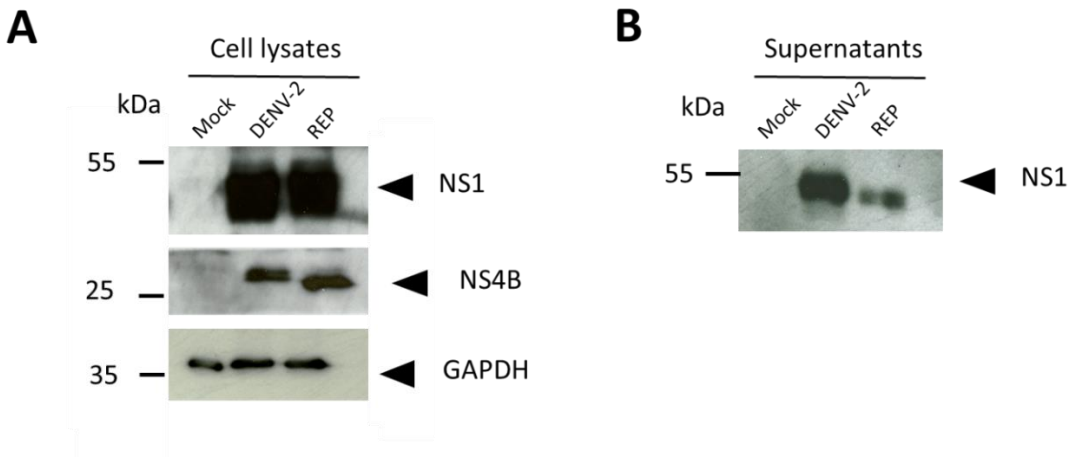

Figure 4.14 Detection of viral proteins in cell lysates and cell culture supernatants of DENV-2 infected HEK293T and REP cells.

HEK293T cells were infected with DENV-2 at a MOI of 5 or mock infected were harvested at 48 hpi and collected as total cell lysates and concentrated supernatants (by TCA precipitation). REP cells were also prepared in the same manner as mock infected cells. Equal amounts of protein from cell lysates (10 µg) and equal volumes of the concentrated culture supernatants (5 µl) were loaded in each lane and the proteins separated by SDS-PAGE prior to Western blotting. Antibodies raised against the NS1, NS4B and GAPDH proteins were used to detect the respective proteins (expected positions arrowed). GAPDH was used as a loading control for cell lysates. Relevant molecular mass markers are shown in kDa.

4.7.2 Host proteins

The bioinformatic analysis revealed that proteins that significantly changed in the proteome of DENV-2 infected HEK293T cells were enriched in proteins located in the ER or associated with ER processes such as the UPR. Thus, key ER proteins (ER markers) were selected for validation.

4.7.2.1 4.7.2.1 Endoplasmic reticulum chaperone BiP (HSPA5)

HSPA5 is a 78 kDa molecular chaperone located in the ER lumen which plays an important role in the UPR pathway. HSPA5 was increased 1.3 fold in DENV infected HEK293T cells and did not change in amount in REP cells compared to mock infected cells. Although HSPA5 was detected in the secretome by LC-MS/MS analysis, its level did not change in either DENV infected HEK293T or REP cells.

Western blotting analysis resulted in the detection of a faint HSPA5 band in cell lysates from DENV infected but not mock infected cells (Figure 14.5). Quantitation of the band intensity confirmed the increase in HSPA5 detected by proteomic analysis.

4.7.2.2 4.7.2.2 Calreticulin (CALR)

CALR is also an ER chaperone. The increase in CALR in both DENV infected HEK293T and REP cells compared with mock infected cells was confirmed by Western blotting (Figure 14.5). Although molecular the weight of CALR is approximately 48 kDa, the observed bands were around 55-60 kDa in size as reported by the antibody supplier.

4.7.2.3 4.7.2.3 ELKS/RAB6-interacting/CAST family member 1 (ERC1)

The ERC1 protein has previously been reported to decrease in DENV infection (Amemiya *et al*., 2019; Chiu *et al*., 2014). Although ERC1 may be involved in ER – Golgi trafficking, it was also selected for validation as a comparator to previous studies.

The significant decrease in ERC1 amounts in DENV infected HEK293T cells detected by LC-MS/MS analysis was also confirmed by Western blotting (Figure 4.15). However, ERC1 was not detected in the secretome of any cells by LC-MS/MS analysis.

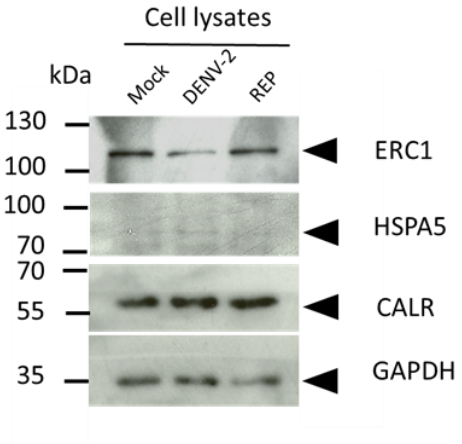

The measurement of the band intensity using ImageJ

Protein	Cells	Target protein value	GAPDH value	Target protein/GAPDH (Normalisation)	DENV-2 or REP/M (Normalisation)
ERC1	M	15405.52	33460.40	0.46	
	DENV-2	6440.46	45762.13	0.14	0.31
	REP	13051.96	44112.55	0.30	0.64
HSPA5	M	30183.39	34168.00	0.88	
	DENV-2	33373.99	25187.09	1.33	1.50
	REP	33186.23	23974.87	1.38	1.57
CALR	M	25634.40	34168.00	0.75	
	DENV-2	28930.69	25187.09	1.15	1.53
	REP	32282.47	23974.87	1.35	1.79

Figure 4.15 Detection of CALR, HSPA5 and ERC1 in DENV-2 infected HEK293T and REP cell lysates.

HEK293T cells were infected with DENV-2 at a MOI of 5 or mock infected, harvested at 48 hpi and used to make total cell lysates. REP cells were also prepared in the same manner as mock infected cells. Twenty µg of cell lysate was loaded in each lane and the proteins separated by SDS-PAGE prior to Western blotting. Antibodies raised against the CALR, HSPA5, ERC1 and GAPDH proteins were used to detect the respective proteins (expected positions arrowed). GAPDH was used as a loading control. Relevant molecular mass markers are shown in kDa. The densiometric intensity of the bands was measured using ImageJ and normalized to the intensity of the GAPDH bands in the mock samples in each experiment.

List of Supplementary Tables

Table S4.1 List of proteins that were significantly altered ≥ 1.5 fold in amount in the proteome or secretome of REP cells compared to mock infected cells.

Table S4.2 DAVID analysis of the cellular proteins that were altered in abundance in both DENV-2 infected HEK293T and REP cells compared to mock cells.

Table S4.3 DAVID analysis of cellular proteins that were altered in DENV-2 infected HEK293T cells but not in REP cells.

Table S4.4 DAVID analysis of cellular proteins that were altered in abundance in REP cells.

Table S4.5 DAVID analysis of secreted proteins that were altered in abundance in the secretome of REP cells.

4.8 Discussion

In this study, proteomic analyses of the cellular proteomes and secretomes of DENV-2 infected HEK293T cells and HEK293T cells stably expressing a DENV-2 replicon were performed and compared for the first time. Comparison of the effects of DENV/replicon replication on the proteomes and secretomes of HEK293T cells has identified several cellular processes dysregulated in these cells which can be compared to proteomic studies on other DENV infected cells to identify common and distinctly regulated cellular pathways. Furthermore, comparison of replicon expressing and DENV infected HEK293T cells allows the identification of cellular proteins and pathways that are dysregulated in response to genome replication, and viral assembly and release, respectively. The comparison also highlights pathways for which replicons may not be good models for DENV replication.

To interpret and generalise the results of the presented study, the properties of the cell line used should be considered. The HEK293 cell line is a transformed cell line created by integrating DNA of human adenovirus 5 to human embryonic kidney cells from an aborted foetus. However, the authentic cell type, tissue of origin, phenotype and karyotype

of this cell line are still debated (Stepanenko and Dmitrenko, 2015). Previous transcriptomic analysis has revealed no evidence of either a tissue-specific gene expression signature or expression associated with differentiated kidney structures (Stepanenko and Dmitrenko, 2015). Thus, the use of HEK293 cells as a model for studying kidney function is limited. However, in a study of the host cell immune responses to DENV infection, HEK293 cells were found to be susceptible to DENV infection and the most appropriate cell line, of a number screened, to study the production and secretion of chemokines (Medin *et al*., 2005). Overall, the HEK293 cell line and its derivatives have been useful as *in vitro* models to study specific aspects of the host cell response to DENV infection and mammalian cell function in general.

Cell lines stably expressing DENV replicons have been successfully established for a number of cell lines including HeLa, BHK, Huh-7 and HEK293 cells and used for DENV replication studies (Hafirassou *et al*, 2017; Medin *et al.*, 2005; Masse *et al.*, 2010). HEK293A cells expressing a DENV-2 replicon were used to study the induction of IL-8 (Medin *et al*., 2005) and HEK293FT cells expressing a DENV replicon were used to study the effect of an oligosaccharyltransferase (OST) inhibitor on DENV replication (Puschnik *et al*., 2017). Therefore, it was of interest to determine whether HEK293T cells stably expressing a DENV-2 replicon were comparable to DENV-2 infected HEK293T cells, in terms of protein dysregulation, both intracellularly and in the associated secretome.

Overall, compared to mock infected cells, there was a higher number of significantly altered proteins in the proteome and secretome of REP cells than DENV infected cells. Although the reason for this is unknown, it is hypothesised that the longer duration of viral protein production and stable RC complex formation in REP cells may lead to a greater dysregulation of host proteins. Whilst REP cells continually express viral proteins, in DENV infected cells after an initial lag phase there is a relatively short burst of viral protein synthesis. The difference in duration of viral protein expression may result in a smaller effect on host protein amounts.

This study resulted in the identification of a total of 3,867 proteins in the secretome of HEK293T cells. This value is much higher than the 428 proteins identified in a previous secretomic analysis of HEK293T cells, using cells that either overexpressed or were

depleted of signal peptide peptidase-like 3 (SPPL3) (Kuhn *et al*., 2015; mentioned in detail in Chapter 3). Approximately 62% (264 proteins) of the proteins detected in the secretome of HEK293T cells in the study of Kuhn *et al.* (Kuhn *et al*., 2015) were also detected in this study, providing confidence in our analysis.

Correlation of the changes that occurred in the proteome and secretome of DENV-2 infected and replicon containing HEK293T cells compared to mock infected cells.

Overall, 41.35% (2984 of 7217 proteins, Figure 4.3A) of the HEK293T cellular proteins identified were also secreted. However, there were only a small number of secreted proteins that were significantly changed in amount in response to DENV infection and only five that were commonly dysregulated in both the proteome and secretome. Thus, conclusions regarding correlations between the cellular and secreted proteins dysregulated in response to infection are problematic. By contrast, the larger amount of cellular and secreted proteins that were identified to be dysregulated in REP cells compared to mock infected cells mostly correlated in the direction of abundance change (Figure 4.3C), implying that the dysregulation of cellular proteins may impact directly on the levels of secreted proteins.

It is worth mentioning the changes in the levels of NUP37 and Cytochrome c oxidase subunit VIc (COX6C), as these two proteins were significantly increased in both the proteomes and secretomes of HEK293T cells in response to infection. Nucleoporins (NUPs) form the nuclear pore complex (NPC) which serves as a nucleocytoplasmic transport channel and RNA viruses are known to subvert the NPC to enhance viral replication (Nofrini *et al.,* 2016). Many NUPs have previously been reported to be associated with DENV infection. NUP50 was found to interact with DENV NS2B and NS5 by yeast two hybrid analysis (Khadka *et al.,* 2011). Furthermore, interactions between multiple NUPs and NS1, including NUP93, NUP205 and NUP210, were identified using a replicon expressing tagged-NS1 (Hafirassou *et al,* 2017). In addition, proteomic analysis of patient plasma using iTRAQ combined with LC-MS/MS, revealed a decrease in NUP210 in DENV infected patients with severe leakage compared to patients with warning signs (Nhi *et al.,* 2016). It is assumed that in data presented in this thesis the increase in the cellular level of NUP37 in both DENV infected and REP cells compared to mock infected

cells, resulted in increased NUP37 secretion. The reason NUP37 is secreted is unknown but this study suggests it is upregulated in response to DENV-2 genome replication.

COX6C is a member of the cytochrome c oxidase (COX) family of proteins which are involved in oxidative phosphorylation. The increase in COX6C in the HEK293T proteome and secretome in response to infection (but not in REP cells) correlated with the significant enrichment of the KEGG pathway term "oxidative phosphorylation" associated with proteins that were significantly dysregulated only in DENV infected cells. The results relating to other COX proteins are discussed in the next section. However, a previous study reported an interaction between COX proteins and the DENV-2 NS3 protein (Silva *et al*., 2019).

Comparison with previous studies

The results of previous proteomic studies investigating DENV infection differ depending on the cell type and proteomic technique used for analysis (reviewed in Table 1.2, Chapter 1). Previously, no analysis of the cellular proteome of HEK293T cells after DENV infection had been conducted and only a few studies have focused on changes in selected proteins in HEK293 cells by Western blotting (Chiu *et al*., 2014; Tongluan *et al*., 2017). Therefore, the results presented in this chapter were compared with both non-proteomic studies conducted in HEK293T cells, as well as proteomic studies conducted in different cells lines.

Similar alterations in the amounts of ERC1, CTSL1, MNF1 and HYOU1 were detected in this study and a previous study analysing DENV-2 infected HEK293 cells at 48 hpi by Western blotting (Chiu *et al*., 2014). The proteins PRAF2 and UBE2S, which were found to markedly decrease in Chiu's study were not identified to change in response to infection in this study.

Fatty acid synthase (FASN), a key protein of lipogenesis, was found to significantly decrease in the proteomes but not the secretomes of both DENV infected HEK293T and REP cells. In a previous study analysing DENV-2 and -4 infected HEK293T/17 cells, the mRNA levels of FASN were reported to initially increase early in infection, before markedly decreasing, whilst the protein level was slightly (but significantly) decreased

throughout infection (Tongluan *et al.*, 2017). However, FASN activity was reported to increase without major changes in the level of protein in DENV infected HeLa cells (Heaton *et al.*, 2010). In contrast, FASN was significantly decreased in DENV-2 infected Huh-7 cells compared with mock infected cells (Chiu HC, 2014). These results may reflect a cell type specific response of FASN to DENV infection.

In line with changes in FASN, we reported two additional proteins involved in lipid metabolism that changed in response to DENV infection. Interesting, neither of these proteins have previously been reported in DENV studies: long-chain fatty acid transport protein 4 (SLC27A4) and NPC intracellular cholesterol transporter 2 (NPC2). Both proteins significantly decreased in the secretomes from both DENV infected and REP cells. The dysregulation of cellular and secreted proteins involved in lipid metabolism in both DENV infected and REP cells may be a result of the modulation of host lipid metabolism that is known to occur during DENV RC formation or in response to production of the NS proteins. The results of this study suggest there may be cell type specific differences in the effects of DENV infection on lipid metabolism. Thus, the changes in proteins involved in lipid metabolism in response to DENV replication warrants further investigation.

A comparison of the results of proteomic studies investigating the effect of DENV infection on different cell types, shows that few proteins have been commonly identified as dysregulated across the different studies. HSPA5 was up regulated in DENV infected cells in this study similarly to a previous analysis of DENV infected Huh-7 cells and K652 cells (Pando-Robles *et a*l., 2014; Chiu, 2014; Wati *et al.*, 2009). HSP90 which decreased in DENV infected EA.hy926 and Huh-7 cells (Pattanakitsakul *et al*., 2010; Pando-Robles *et al.*, 2014) was also found to be significantly decreased in REP cells (but not changed in DENV infected HEK293T cells). The significant increases in heterogeneous nuclear ribonucleoprotein H1 (HNRNPH1) detected in the secretomes of both DENV infected and REP cells in this study were similar to the results reported in a study investigating DENV infected EA.hy926 cells (Kanlaya *et al*., 2009). In contrast, HNRNPH1 was reported to be decreased in DENV infected Huh-7 cells (Pando-Robles *et al*., 2014) (The details of studies mentioned in this section are summarised in Table 1.2.).

The results of the secretome analysis conducted in this thesis were also compared with a previous study which analysed the secretome of DENV-2 infected HepG2 cells (Higa *et al*., 2008). X-ray repair cross-complementing protein 5 (XRCC5) which was identified to significantly increase ≥ 1.5 fold in the secretomes of DENV infected HEK293T cells in data presented in this thesis, was also identified in the secretome of DENV infected HepG2 cells (Higa *et al*., 2008). However, the authors did not report whether XRCC5 abundance increased or decreased (Higa *et al*., 2008). XRCC5 (also known as nuclear factor IV, Ku80 and ATP-dependent DNA helicase II 80 kDa subunit) is a regulatory subunit of the DNA-dependent protein kinase. Furthermore, increased activity of all subunits of DNA-dependent protein kinase, including XRCC5, was identified in DENV-2 infected Huh-7 cells. Depletion of XRCC5 by siRNA knockdown resulted in a decrease in the IFN-β response (Vetter *et al*, 2012). Thus, the role of secretory XRCC5 in the viral immune response requires further investigation.

It is interesting to note that given then number of detected and identified proteins that altered in response to DENV infection in our analyses, few proteins overlapped with previously published proteomic studies. Literature of the top ten proteins that increased and decreased in amounts in DENV infected HEK293T cells compared with mock (listed in Table 4.4) revealed that 18/20 proteins had not previously been reported to associate with DENV infection. The only two proteins could be linked with the previous DENV studies were ERC1 and tyrosine-protein phosphatase protein. A decrease of ERC1 was previously reported in DENV (discussed in the next section). An increase of tyrosine-protein phosphatase protein in the proteome of HEK293T cell in response to DENV in this study was in line with an antiviral effect of tyrosine phosphatase inhibitors previously reported to inhibit DENV production in HepG2 cells (Limjindaporn *et al*, 2017).

A likely explanation for the discrepancy between these results is the different cell types and proteomic techniques used for analysis between these studies. Using different transformed cell line models will present snap shots of cell type specific responses to DENV infection and cannot reflect the whole *in vivo* pathogenesis of DEN. Thus, the *in vitro* results presented in this chapter should be compared with the *in vivo* results from

DEN patients to determine the processes for which HEK293T could be a good cellular model of studying pathogenesis of DEN.

Common host responses in DENV infection and replicon containing cells

The dysregulated proteins and biological processes commonly found in DENV infection and REP cells could pertain to downstream effects of viral replication or a direct consequence of the interaction of viral and host proteins, or a combination of the two.

The cellular proteins that were commonly dysregulated in DENV infected HEK293T and REP cells were enriched in proteins participating in metabolic pathways, especially mitochondrial proteins involved in cellular respiration for the production of ATP (Figure 4.9A). Mitochondrial markers including HSP60 and voltage-dependent anion channel 1 (VDAC1) were non-significantly increased in DENV-2 infected HEK293T cells but significantly increased in REP cells. As mentioned earlier, the COX family of proteins comprise enzymes that act in the last step of the mitochondrial electron transport chain. Multiple COX proteins were significantly increased in either DENV infected or REP cells; however, only COXC6 and COX20 were significantly increased in the proteome of both DENV-2 infected HEK293T and REP cells. Both functional and structural alterations in mitochondria were previously identified in DENV infected liver cells (El-Bacha *et al*., 2007; Barbier *et al*, 2017). The functional mitochondrial bioenergetic changes observed in response to DENV-2 infection of HepG2 cells included increases in cellular respiration and oxygen consumption and a decrease in ATP production (El-Bacha *et al.*, 2007). These changes led to a decrease in mitochondrial membrane electrochemical potential which is a hallmark of pro-apoptotic viruses (El-Bacha *et al.*, 2007). The study of Barbier *et al*., (Barbier *et al*, 2017) reported elongation of mitochondria together with an increase in mitochondrial respiration in DENV infected Huh-7 cells (Barbier *et al*, 2017). Co-localization of the mitochondria with the DENV RC was identified (Sripada *et al*, 2009), which suggests that dysregulation of mitochondria structures and functions results from DENV replication.

CALR, a multifunctional protein, plays important roles in protein folding, calcium homeostasis and regulation of gene expression. CALR regulates mitochondrial calcium and potassium homeostasis (Arnaudeau *et al.*, 2002; Shigaeva *et al*, 2014). In the ER,

CALR acts as an ER chaperone and works together with calnexin (CNX) to regulate oligosaccharide degradation in the calreticulin/calnexin cycle. Previously, an *in silico* computational drug repositioning approach was used to perform an integrated multi-omics analysis, resulting in the identification of five proteins/genes commonly altered in DENV infection: ACTG1, CALR, ERC1, HSPA5, SYNE2 (Amemiya *et al*., 2019). CALR was proposed as a potential therapeutic target (Amemiya *et al*., 2019). Thus, the common increase in CALR amounts in both DENV infected HEK293T and REP cells was selected for validation by Western blot analysis, which confirmed the proteomic results (Figure 4.15). CALR has been reported to interact with both the DENV E protein (Limjindaporn *et al*., 2009) and NS5 (Khadka *et al*., 2011) and knockdown of CALR resulted in a reduction of DENV replication in both DENV infected (Limjindaporn *et al.,* 2009) and replicon expressing cells (Khadka *et al*., 2011). Furthermore, colocalization of CALR with cytoplasmic NS5, NS3 and dsRNA was detected in DENV infected Huh-7 cells (Khadka *et al*., 2011). These findings suggest a vital role for CALR in early viral replication. The increase in CALR levels identified in this study, both in DENV infected HEK293T and REP cells, may occur in response to DENV modulation, in order to facilitate viral replication.

Interestingly, a group of DEAD-Box helicase (DDX) proteins were significantly altered in the secretomes of both DENV infected HEK293T and REP cells: DDX42 and DDX39A increased whilst DDX3X decreased. Furthermore, eukaryotic initiation factor 4A-III (also known as EIF4A3 and DDX2) was significantly increased in only the REP cell secretome. DDX proteins are multifunctional ATP-dependent RNA helicases involved in metabolic processes and host immunity. DDX42 induces IFN-β production and plays an important role in antiviral responses. A previous study proposed that an interaction between the JEV NS4A protein and DDX42 may antagonise the IFN response (Lin *et al.,* 2008). Decreases in DDX3X in DENV-2 infected Huh-7 and A549 cells at 48 hpi have been previously reported (Kumar *et al*, 2017). Moreover, the antiviral properties of DDX3X were demonstrated by knock down of DDX3X which resulted in an increase in viral titre, whilst overexpression caused a decreased infection rate and viral titre (Kumar *et al*, 2017). Interactions between DDX3X and the DENV C (Kumar *et al*, 2017) and NS5 proteins (Khadka *et al*., 2011) have been identified. As secretomes contain host immune

components which act in cell-cell signal transduction, the alteration of this group of proteins in response to DENV replication may play and important role in the antiviral immune response.

Selected biological processes that were only dysregulated by DENV infection.

A unique advantage of this study is that it facilitates a direct comparison of the proteomes and secretomes of DENV infected and replicon containing HEK293T cells. A focused analysis on the proteins and cellular processes which were only dysregulated in DENV infection was done to better understand the effect of specific viral processes on the host cell. Furthermore, this analysis could highlight any limitations in the use of replicon containing cells as models for DENV infection, apart from the obvious differences in viral assembly and release.

ER processing the UPR and UPS.

Bioinformatic analysis of the data showed that proteins associated with the GO terms "response to unfolded protein" and "ubiquitin-dependent ERAD pathway" and the KEGG pathway term "protein processing in endoplasmic reticulum" were enriched in DENV infected HEK293T cells but not in REP cells (Figure 4.13A). The increase in UPR stress is well documented as a general response to DENV infection and has been reported to occur in various cell lines including Huh-7 and A549 cells (Lee *et al.*, 2018) as well as the HEK293T cells used in this study.

Crosstalk between the UPR, UPS and autophagic processes are known to occur, including in DENV infection (Blazquez *et al*., 2014; Lee *et al.*, 2018), whilst crosstalk between ER processes and phagocytosis has also been reported. Several ER proteins including CALR, HSPA5 and protein transport protein Sec61 (SEC61) play a role in phagocytosis process *via* "ER-mediated phagocytotic" processes; for example, HSPA5 also acts as a phagocytosis receptor (Desjardins *et a*l., 2003).

DAVID analysis of the data presented in this chapter demonstrated enrichments in UPR and UPS terms in response to DENV infection. The ER markers, HSPA5 and SEC61B, were significantly increased in DENV infected HEK293T cells only. By contrast, proteins associated with autophagy related GO terms were not found to be enriched and

proteins that are key markers of autophagy such as autophagy related 5 (ATG5) and microtubule-associated proteins 1A/1B light chain 3B (MAP1LC3B2 or LC3) did not change in amount in response to infection. Although there was a significant enrichment of proteins associated with the GOBP term "lipid metabolic process" (Figure 4.13A) this may be due to the involvement of lipid metabolic processes apart from autophagy, such as lipogenesis (*via* FASN).

DENV replication occurs on ER membranes and structural changes to these membranes have been observed in DENV replicon containing cells by electron microscopy (Hafirassou *et al.,* 2014). It is of interest that the results of this study revealed that replicon replication has a 'weaker' effect on ER responses than DENV replication. This suggests that virion maturation, assembly and budding may cause ER stress and directly activate the UPR. Alternatively, cell lines that successfully stably express replicons may have been self-selected that maintain a balance with the ER stress response to avoid cytopathic effects.

The UPR is triggered by the binding of misfolded proteins to HSPA5, an important ER chaperone. HSPA5 has many alternative names including 78 kDa glucose-regulated protein (GRP78) or binding-immunoglobulin protein (BiP) and heat shock protein 70 family protein. HSPA5 contributes to DENV infection in many ways, it was identified as a DENV receptor in HepG2 cells (Jindadamrongwech *et al.*, 2004) and is involved in viral protein production/secretion (Wati *et al*., 2009; Songprakhon *et a*l., 2018); although the effect of HSPA5 on virion secretion is controversial. HSPA5 knockdown did not affect transiently expressed DENV replicon replication (viral genome production) but caused a decrease in both intracellular NS1 and sNS1 levels (Songprakhon *et al.,* 2018). Decreasing HSPA5 by siRNA knockdown resulted in a decrease in viral titre (Limjindaporn *et al*., 2009) whilst inhibiting HSPA5 expression by cleavage with a toxin did not (Wati *et al*., 2009). In addition, protein-protein interactions between HSPA5 and the DENV E (Limjindaporn *et al.,* 2009) and NS1 proteins (Songprakhon *et al*., 2018) have been reported by yeast two-hybrid and co-IP analyses, respectively. The observed increase in HSPA5 in response to DENV infection in data presented here may represent an overwhelming of the ER stress response by DENV infection. In contrast, the absence of

this effect in replicon containing cells suggests that this viral replication alone does not induce the same level of ER stress.

Phagosome

There were significant increases in key phagosomal proteins (Huynh *et al*, 2007; Garin *et al*, 2001) including V-type proton ATPase A, lysosome-associated membrane proteins 1 and 2 (LAMP-1 and LAMP-2) as well as CD63 antigen (an endocytosis marker) in DENV-2 infected cells but not in REP cells, compared to mock infected. However, other important phagosomal proteins such as HSP60, cathepsins and Ras-related proteins (Rabs) did not change in amount in response to infection. We can hypothesise that the significant enrichment of proteins involved in phagosomal and lysosomal activity in DENV infected cells but not in REP cells could be explained by a potential lack of the cellular response to pathogen invasion in REP cells. An increase in proteins involved in FcɤR-mediated phagocytosis with a corresponding decrease in proteins involved in lysosomal processes was detected in a proteomic analysis of THP cells infected with DENV (under conditions of ADE) compared with mock infected cells, by iTRAQ and LC-MS/MS (Ong *et al.*, 2017). The increase in Fc-ɤ receptor-mediated phagocytosis, in combination with a reduction in the acidification of the phagosome was proposed to facilitate DENV escape from lysosomal degradation (Ong *et al.*, 2017).

ERC1 was one of five proteins commonly identified to play a role in DENV infection by an integrated analysis of ‘omics data, as described above (Amemiya *et al*., 2019). Similar to the proteomic study of Chiu *et al.* (Chiu, 2014), a decrease in ERC1 was identified to occur in DENV-2 infected HEK293T cells but not in REP cells. The specific role of ERC1 in DENV infection remains unknown. However, an interaction between ERC1 and DENV NS5 was reported by yeast two-hybrid analysis (Khadka *et al*., 2011). The interaction between ERC1 and NS5 was further defined as serotype 2 specific, by co-IP analysis (Chiu, 2014). Cellular depletion of ERC1 by siRNA knockdown resulted in a significant decrease in the replication of a DENV replicon (Khadka *et al.*, 2011) and DENV infection efficiency (Chiu, 2014).

In conclusion, high throughput proteomic analyses of the proteomes and secretomes of DENV-2 infected HEK293T cells and replicon containing cells were

performed. Although HEK293T is a transformed cell line with unidentified tissue phenotype, results obtained from these cells still provided general host cell responses to DENV such as ER processes and UPR. The results from DENV infected HEK293T cell model will be compared with *in vivo* results from clinical specimens of DEN patient in Chapter 6 to determine the usefulness of this cell model in studying the pathogenesis of DENV. Overall, there was a good correlation between the proteomic results obtained using DENV infected HEK293T and REP cells, suggesting utility of the replicon system for this sort of analysis. Unfortunately, the limited number of proteins that changed in secretomes suggests that HEK293T cells may not represent the ideal cell model for analysing the effects of DENV infection on the cellular secretome. Nevertheless, proteins that might potentially play roles in host-virus immune responses such as DDX proteins and XRCC5 were significantly increased in the secretome in response to DENV infection.

CHAPTER 5. HIGH-THROUGHPUT PROTEOMIC ANALYSIS OF DENV INFECTED HUH-7 CELLS AND SECRETOMES.

5.1 Introduction

Hepatocytes, the major liver cell type, synthesize the majority of plasma proteins including carrier proteins, lipoproteins, complements, coagulation factors, acute phase response proteins and hormones (Kuscuoglu *et al*., 2018). The other functions of hepatocytes include detoxification, drug metabolism and bile production. The liver is one of the major target organs in DENV infection. Most symptomatic DEN patients have hepatomegaly (enlarged liver) and abnormal liver function tests (Dissanayake *et al*., 2017). Liver involvement in DEN patients can vary from mild abnormal liver function tests to liver failure, the latter resulting in high mortality from coagulopathy and uncontrolled bleeding. Previous studies using autopsy specimens from fatal DEN cases have provided evidence of DENV antigen and DENV replication in hepatocytes, Kupffer cells and liver endothelial cells (Póvoa *et al*, 2014). Due to the difficulties in examining DENV replication in the liver of infected individuals, liver hepatocyte cell lines such as Huh-7 and HepG2 provide useful *in vitro* models to study DEN pathogenesis and test potential therapeutics (Senevirantne *et al*., 2006). Importantly, previous studies have demonstrated that results obtained from the use of liver cell models can correlate well with results obtained from clinical studies. For example, increased levels of alpha-enolase (ENO1) in the plasma of DEN patients paralleled a large increase in the amounts of ENO1 in the secretome of DENV-2 infected HepG2 cells (Higa *et al*., 2014). Moreover, an increase in macrophage migration inhibitory factor (MIF) in the secretomes of DENV-2 infected cells was correlated with disease severity in patients (Salazar *et al*, 2014). Nevertheless, the involvement of the liver in DEN pathogenesis is still understudied and not well understood.

As the liver is the major producer of plasma proteins, proteomic analysis of DENV infected liver cells and/or the associated secretomes has the potential to increase our understanding of the role of the liver in DEN pathogenesis. This is especially true in relation to alterations in the levels of plasma proteins, produced by hepatocytes, that occur during DENV infection. As described above, a limited number of previous studies have analysed either the proteome of DENV infected liver cells or the associated secretome, but a simultaneous combined study of both has not been undertaken. Moreover, the results from previous proteomic studies on liver cell lines/secretomes in response to DENV infection were inconsistent and did not lead to an improved understanding of the effect of DENV infection on important biological hepatic processes. These include alterations in complement and coagulation cascades, platelet activation/degradation and lipid metabolism, as well as the acute phase response (Will *et al*., 2012; Nascimento *et al*., 2014; Fragnoud *et al.,* 2015). Proteomic analysis of DENV-2 infected HepG2 cells revealed changes in 17 proteins which were primarily involved in transcription and translational processes (Pattanakitsakul *et al*., 2008). By contrast, proteomic analysis of DENV-2 infected Huh-7 cells using high-throughput label-free LC-MS/MS, identified 155 differentially expressed proteins compared to mock infected cells (Pando-Robles *et al*., 2014). The differentially expressed proteins were involved in mitochondrial function including energy metabolism, RNA processing and negative regulation of apoptosis.

All secretome studies were conducted on samples derived from DENV-2 infected HepG2 cells with an initial study identifying secreted proteins found in serum protein databases (Higa *et al*., 2008). A follow-up study focused on a single protein, alpha-enolase (ENO1), and reported an increase in secretome but no changes in the intracellular production of this protein of DENV infected HepG2 cells (Higa *et al.,* 2014). More recently, a study was done that focused on secreted proteins that had been subject to proteolysis, rather than a general analysis of secreted proteins (Caruso *et al*., 2017). A simultaneous analysis of the alterations of the secretion that occur in both the proteome and secretome of liver cells in response to DENV infection could provide more systematic information on the dynamic changes that occur in the amounts of proteins that are secreted from liver cells.

Therefore, in this study simultaneous proteomic analysis of cell lysates and culture supernatants prepared from DENV-2 infected Huh-7 liver cells was done. The results identified relationships between cellular and secreted proteins and important biological pathways that are altered in Huh-7 liver cells in response to DENV infection. To determine if Huh-7 cells are a relevant model to study DEN pathogenesis, the results of the Huh-7 analysis were analysed together with the results of the serum proteomic analysis of clinical specimens presented in chapter 6.

Results

5.2 Proteomic analysis of the proteomes and secretomes from DENV-2, inactivated DENV-2 and mock infected Huh-7 cells.

To analyse the effects of DENV-2 infection on the total cell proteome and secretome of Huh-7 cells, these cells were infected with DENV-2, heat-inactivated DENV-2 (iDENV-2) or mock infected. An MOI of 5 was used to ensure all cells were infected; infections with iDENV-2 was conducted to control for the effects of viral particle uptake on the cells or for media effects. Additionally, the DENV-2 (and iDENV-2 derivative) stock was prepared from the supernatant of C6/36 cells infected with DENV-2 and may have contained stimulatory components from insect cells. Prior to infection, the cells were grown in complete media. After infection the cells were washed extensively with PBS and then grown in SFM for 30 h, at which time the culture supernatants and cells were harvested. The cell culture supernatants were then concentrated and cell lysates prepared using RIPA buffer (Figure 5.1). The infection rate was estimated to be 95%-100% at 30 hpi by IFA (Figure 5.2). The experiments were performed independently in triplicate. The amount of protein in the concentrated supernatants and cell lysates was estimated by BCA assay. Equal amounts of each sample were then used for TMT labelling and LC-MS/MS analysis by the Faculty Proteomics facility (done by Dr Kate Heesom and co-workers).

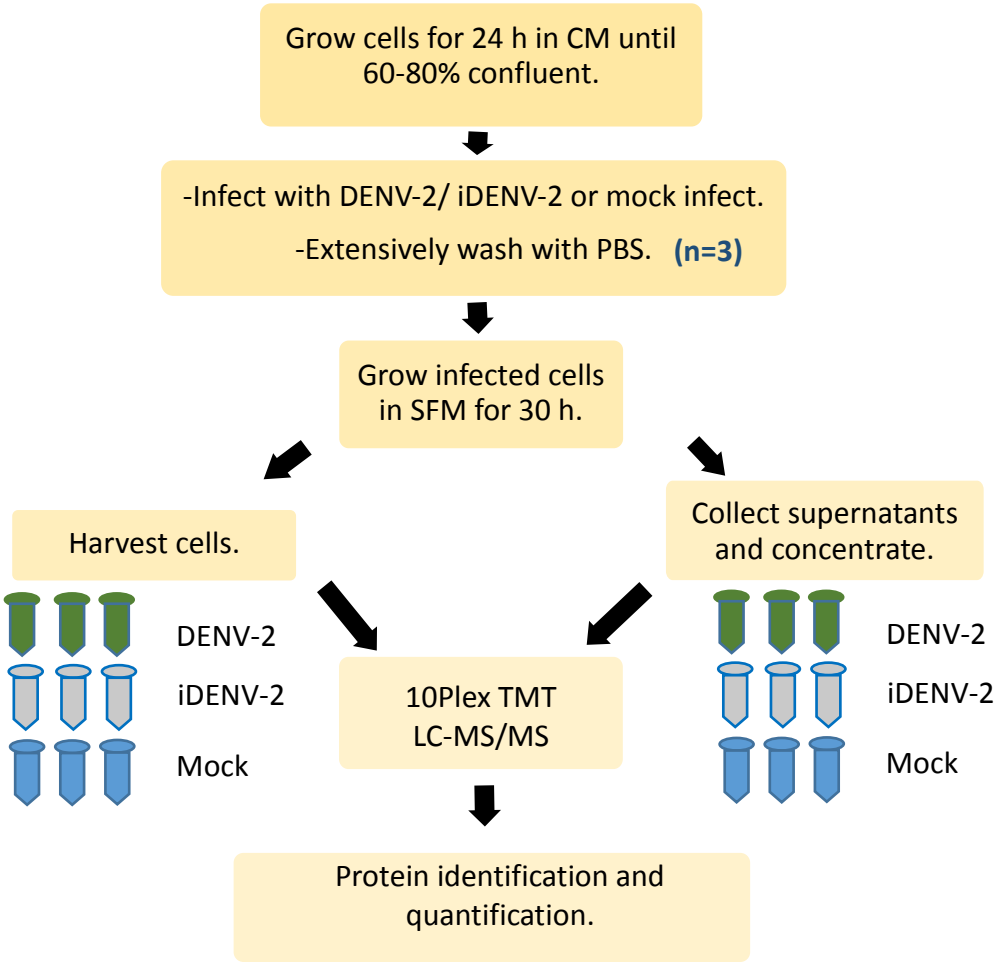

Figure 5.1 Study flow of the high-throughput proteomic analysis of the cellular proteomes and secretomes of DENV-2 infected Huh-7 cells.

In brief, Huh-7 cells were grown in CM for 24 h, divided into 3 groups and infected with DENV-2 and iDENV-2 at a MOI of 5 or mock infected. After infection, the cells were extensively washed with PBS and further grown in SFM for 30 h. At 30 hpi, the cells were harvested and cell cultured supernatants were concentrated. Experiments were done in triplicate. Proteins in the cell lysates and concentrated supernatants were TMT labelled and analysed by LC-MS/MS.

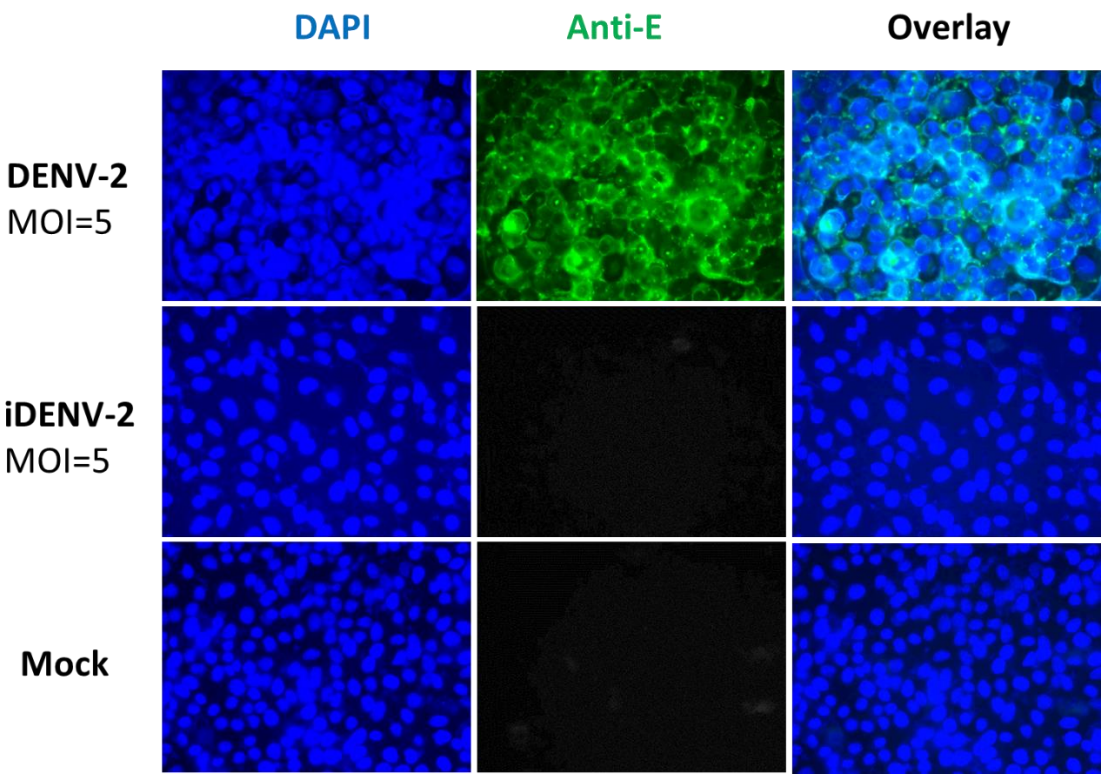

Figure 5.2 IFA analysis of Huh-7 cells infected with DENV-2, iDENV-2 or mock infected.

Huh-7 cells were infected with DENV-2 and iDENV-2 at MOI=5 or mock infected. After 30 h of incubation in SFM, the cells were fixed with ice cold methanol and immunostained with an antibody against the DENV-2 E protein (Anti-E, green), nuclear DNA was visualised with DAPI (blue). Images were taken using a Leica widefield microscope with 40X magnification.

5.3 Quantitative LC-MS/MS analysis

The spectral files from the LC-MS/MS analyses were analysed using Proteome Discoverer and statistical analysis and downstream processing was done using Perseus as described in section 2.8. A total of 7010 proteins were identified in the cell lysates, of which 6367 were reliably identified and quantified using ≥ 2 peptides (hereafter termed the proteome). Of these, 5706 host proteins that were quantified in at least 2 of 3 experiments were analysed further. The abundance of host proteins in the proteomes of DENV-2 and iDENV-2 infected cells were compared with their abundance in mock infected cells. The total number of proteins and proteins that significantly changed (P-value < 0.05) in amount (with fold cut-off values of ≥ 2, ≥ 1.5 and ≥ 1.3) between DENV and iDENV-2 and mock infected cells are summarised in Table 5.1.

A total of 3421 proteins were identified in the cell culture supernatants of which 2818 were reliably identified and quantified using ≥ 2 peptides (hereafter termed the secretome). Of these, 1811 host proteins that were quantified in at least 2 of 3 experiments were analysed further. The abundance of host proteins in the DENV-2 and iDENV-2 infected cells were compared with their abundance in mock infected cells. The total number of proteins and proteins that significantly changed ($p < 0.05$) in amount (with fold cut-off values of ≥ 2, ≥ 1.5 and ≥ 1.3) between DENV and iDENV-2 and mock infected cells are summarised in Table 5.2.

Table 5.1 Summary of the number of host proteins that changed in abundance in the proteomes of DENV-2 and iDENV-2 infected Huh-7 cells compared with mock infected cells.

	Number of proteins changed in abundance		Number of proteins significantly changed in abundance ($p < 0.05$)		
	DENV-2 /Mock	iDENV-2 /Mock	DENV-2 /Mock	iDENV-2 /Mock	Common proteins
Increased ≥ 2 fold	74	9	49	1	1
Increased ≥ 1.5 fold	225	64	121	6	3
Increased ≥ 1.3 fold	479	179	217	16	4
Decreased ≥ 2 fold	71	2	58	0	0
Decreased ≥ 1.5 fold	195	10	147	2	0
Decreased ≥ 1.3 fold	389	42	246	5	1

Table 5.2 Summary of the number of proteins that changed in abundance in the secretomes of DENV-2 and iDENV-2 infected Huh-7 cells compared with mock infected cells.

	Number of proteins changed in abundance		Number of proteins significantly changed in abundance ($p < 0.05$)		
	DENV-2 /Mock	iDENV-2 /Mock	DENV-2 /Mock	iDENV-2 /Mock	Common proteins
Increased ≥ 2 fold	23	5	9	1	1
Increased ≥ 1.5 fold	90	45	27	3	2
Increased ≥ 1.3 fold	207	147	48	11	4
Decreased ≥ 2 fold	43	2	21	0	0
Decreased ≥ 1.5 fold	182	20	75	0	0
Decreased ≥ 1.3 fold	308	71	95	0	0

Almost all DENV-2 structural and NS proteins, except NS2A and NS2B were detected in the proteome of DENV-2 infected Huh-7 cells, whilst all structural proteins, NS1 and NS4B were detected in the associated secretomes by LC-MS/MS analysis. The % coverage, number of peptides, unique peptides and PSMs of the DENV-2 proteins detected in the proteome/secretome of DENV-2 infected Huh-7 cells are summarised in Table 5.3.

Table 5.3 DENV-2 proteins detected in proteome and secretome of DENV-2 infected Huh-7 cells.

Description	MW (kDa)	Proteome				Secretome			
		% coverage	Peptides	Unique Peptides	PSMs	% coverage	Peptides	Unique Peptides	PSMs
C	13.2	29.82	5	5	18	39.47	5	5	21
E	54.3	20.61	3	3	27	36.57	18	18	86
pr	18.7	41.62	25	25	180	26.67	4	4	12
NS1	39.9	53.13	25	2	140	51.99	23	2	166
NS2A	23.7	ND	ND	ND	ND	ND	ND	ND	ND
NS2B	14	ND	ND	ND	ND	ND	ND	ND	ND
NS3	69.3	75.89	59	59	286	ND	ND	ND	ND
NS4A	14	29.13	3	3	10	ND	ND	ND	ND
NS4B	26.8	26.21	5	1	20	3.23	1	1	1
NS5	103.1	62.22	63	63	314	ND	ND	ND	ND

ND = not detected

Overall, the proteins that changed in abundance in the proteome and secretome of DENV-2 infected Huh-7 cells compared with mock infected cells decreased rather than increased. Proteins that significantly changed in the proteome and secretome of DENV-2 but not iDENV-2 infected cells were selected for further study and validation. Proteins that significantly changed in abundance, with a cut-off of a ≥ 1.5 fold change, in the proteome and secretome of DENV-2 infected cells compared to mock infected cells (listed in Tables 5.4 and 5.5 respectively) were selected for further downstream bioinformatic analysis.

Table 5.4 Proteins that were significantly changed ≥ 1.5 fold in amount, in proteome of DENV-2 infected Huh-7 cells compared to mock infected cells.

Accession	Description	Gene	Fold change DENV-2 /Mock	P-value
Increased in the proteome of DENV-2 infected cells compared to mock infected cells.				
Q8NEH6	Meiosis-specific nuclear structural protein 1	*MNS1*	32.71	1.77E-03
B4DDR3	Apoptosis inhibitor 5	*API5*	9.55	2.84E-04
S4R322	Centrosomal protein of 290 kDa	*CEP290*	8.70	3.79E-05
A8K171	Nuclear receptor interacting protein 1	*NRIP1*	6.90	2.21E-03
B4DHW9	Pantothenate kinase 4	*PANK4*	6.78	1.91E-04
Q9BXT8	RING finger protein 17	*RNF17*	6.74	2.62E-02
P51587	Breast cancer type 2 susceptibility protein	*BRCA2*	4.71	6.85E-03
Q15773	Myeloid leukemia factor 2	*MLF2*	4.55	2.86E-03
P0C7P0	CDGSH iron-sulfur domain-containing protein 3	*CISD3*	4.52	2.40E-04
Q13049	E3 ubiquitin-protein ligase TRIM32	*TRIM32*	4.48	8.23E-05
B4DZC6	Bardet-Biedl syndrome 5 protein	N/A	4.22	1.00E-02
Q8IXZ2	Zinc finger CCCH domain-containing protein 3	*ZC3H3*	4.16	8.16E-03
P35080	Profilin-2	*PFN2*	4.04	5.05E-03
Q14687	Genetic suppressor element 1	*GSE1*	3.50	1.66E-02
E7ETM0	Casein kinase I isoform alpha	*CSNK1A1*	3.05	2.24E-04
Q59GV6	Zinedin variant (Fragment)	*STRN4*	3.02	3.40E-02
Q8N9N7	Leucine-rich repeat-containing protein 57	*LRRC57*	2.93	6.71E-04
B9EH95	Armadillo repeat gene deletes in velocardiofacial syndrome	*ARVCF*	2.84	1.99E-02
Q6NSJ0	Uncharacterized family 31 glucosidase KIAA1161	*KIAA1161*	2.83	2.87E-03
B4DGG2	Sorting nexin-13	*SNX13*	2.82	7.65E-03
Q15697	Zinc finger protein 174	*ZNF174*	2.81	4.07E-02
Q63ZY3	KN motif and ankyrin repeat domain-containing protein 2	*KANK2*	2.74	4.03E-02
B2RBJ5	Alanine-glyoxylate aminotransferase 2 (AGXT2), nuclear gene encoding mitochondrial protein,	*AGXT2*	2.72	1.32E-02
Q6EMK4	Vasorin	*VASN*	2.64	5.60E-03
Q8NEB9	Phosphatidylinositol 3-kinase catalytic subunit type 3	*PIK3C3*	2.54	3.17E-03
Q9BZE9	Tether containing UBX domain for GLUT4	*ASPSCR1*	2.48	4.82E-03
A4UCS8	Enolase 1 (Fragment)	*ENO1*	2.47	4.68E-02

Q9BX84	Transient receptor potential cation channel subfamily M member 6	*TRPM6*	2.46	4.92E-02
Q96LX8	Zinc finger protein 597	*ZNF597*	2.46	1.02E-02
J9JIC5	Protein Njmu-R1 OS=Homo sapiens	*C17orf75*	2.39	2.68E-02
Q86X83	COMM domain-containing protein 2	*COMMD2*	2.33	7.37E-03
Q502W7	Coiled-coil domain-containing protein 38	*CCDC38*	2.31	3.71E-02
Q13627	Dual specificity tyrosine-phosphorylation-regulated kinase 1A	*DYRK1A*	2.30	4.40E-02
B4DTB1	cDNA FLJ52936, weakly similar to Tropomyosin alpha-4 chain	*TPM4*	2.29	4.59E-02
Q96SL4	Glutathione peroxidase 7	*GPX7*	2.27	2.07E-03
Q9H1A3	Methyltransferase-like protein 9	*METTL9*	2.26	1.88E-05
X5D907	Fragile X mental retardation 1 isoform C (Fragment)	*FMR1*	2.23	2.32E-02
E9PNJ4	Stromal interaction molecule 1	*STIM1*	2.21	3.31E-02
B4E0C5	Mitochondrial carrier homolog 1	*MTCH1*	2.11	2.96E-02
A0A0A0MTQ8	Coiled-coil domain-containing protein 175	*CCDC175*	2.09	8.95E-04
Q06787	Fragile X mental retardation protein 1	*FMR1*	2.09	7.70E-04
Q00577	Transcriptional activator protein Pur-alpha	*PURA*	2.08	3.83E-03
Q9UQL5	DEAD-box protein p72	*DDX17*	2.07	2.42E-02
B2R623	RNA guanylyltransferase and 5'-phosphatase (RNGTT), mRNA	*RNGTT*	2.07	5.67E-03
B3KQT6	Tetraspanin-13	*TSPAN13*	2.04	7.16E-03
C9JIF9	Acylamino-acid-releasing enzyme	*APEH*	2.03	3.01E-03
Q2Q1W2	E3 ubiquitin-protein ligase TRIM71	*TRIM71*	2.01	1.10E-03
Q9H008	Phospholysine phosphohistidine inorganic pyrophosphate phosphatase	*LHPP*	2.00	2.26E-02
P58107	Epiplakin	*EPPK1*	2.00	1.20E-02
Q15645	Pachytene checkpoint protein 2 homolog	*TRIP13*	1.99	6.56E-03
P16383	GC-rich sequence DNA-binding factor 2	*GCFC2*	1.98	4.60E-02
H0Y449	Nuclease-sensitive element-binding protein 1 (Fragment)	*YBX1*	1.98	3.10E-03
Q09428	ATP-binding cassette sub-family C member 8	*ABCC8*	1.97	3.62E-02
O00425	Insulin-like growth factor 2 mRNA-binding protein 3	*IGF2BP3*	1.94	4.07E-04
H7BYT1	Casein kinase I isoform delta	*CSNK1D*	1.93	5.41E-03
B7Z565	Alpha-actinin-1	*ACTN1*	1.93	1.31E-02
B4DY32	Asparagine synthetase (glutamine-hydrolyzing)	*ASNS*	1.91	1.28E-02
Q9NZI8	Insulin-like growth factor 2 mRNA-binding protein 1	*IGF2BP1*	1.91	1.49E-04
B0FTY2	NudC-like protein	*NUDCD3*	1.91	8.64E-03

Q9NZE8	39S ribosomal protein L35, mitochondrial	*MRPL35*	1.89	4.87E-04
B3KM36	BAG family molecular chaperone regulator 2	*BAG2*	1.87	3.47E-03
Q96L93	Kinesin-like protein KIF16B	*KIF16B*	1.86	4.89E-02
Q01991	Dihydrolipoamide S-acetyltransferase (Fragment)	*DLAT*	1.83	2.75E-02
E5KMK5	Mitochondrial DNA topoisomerase I	*TOP1MT*	1.83	5.13E-03
Q9P2P6	StAR-related lipid transfer protein 9	*STARD9*	1.83	3.39E-02
Q6PJG6	BRCA1-associated ATM activator 1	*BRAT1*	1.82	7.93E-03
A8K6I6	Golgi associated, gamma adaptin ear containing, ARF binding protein 3 (GGA3)	*GGA3*	1.81	2.38E-03
A1L3A7	Nuclear fragile X mental retardation protein interacting protein 2	*NUFIP2*	1.80	9.68E-04
Q92539	Phosphatidate phosphatase LPIN2	*LPIN2*	1.79	3.52E-02
Q96K19	E3 ubiquitin-protein ligase RNF170	*RNF170*	1.78	1.36E-03
P16989	Y-box-binding protein 3	*CSDA;YBX 3*	1.78	2.11E-03
Q14117	Dihydropyrimidinase	*DPYS*	1.78	3.16E-02
Q96A46	Mitoferrin-2	*SLC25A28*	1.77	4.42E-02
Q96QR8	Transcriptional activator protein Pur-beta	*PURB*	1.77	5.27E-03
Q9UN79	Transcription factor SOX-13	*SOX13*	1.77	9.00E-03
A0A0F7KYT8	Fragile X mental retardation autosomal homolog variant p2K	*FXR1*	1.76	3.12E-05
P51116	Fragile X mental retardation syndrome-related protein 2	*FXR2*	1.76	5.84E-04
Q9HAB8	Phosphopantothenate--cysteine ligase	*PPCS*	1.73	2.89E-02
A0A024R5Y1	Spastic paraplegia 21 (Autosomal recessive, Mast syndrome), isoform	*SPG21*	1.70	1.04E-03
Q69YJ7	Putative uncharacterized protein DKFZp667H197 (Fragment)	*RBM12*	1.69	1.13E-02
O15090	Zinc finger protein 536	*ZNF536*	1.69	3.45E-02
D3DTX6	Neurabin-2	*PPP1R9B*	1.68	6.11E-03
Q53G85	Elongation factor 1-alpha	*EEF1A1*	1.68	3.65E-02
Q9UKD1	Glucocorticoid modulatory element-binding protein 2	*GMEB2*	1.67	1.93E-02
Q59GL1	Synaptotagmin binding, cytoplasmic RNA interacting protein variant (Fragment)	*SYNCRIP*	1.67	3.37E-03
O15466	Alpha-2,8-sialyltransferase 8E	*ST8SIA5*	1.66	7.77E-03
H0YJ17	Neuroguidin (Fragment)	*NGDN*	1.66	1.28E-02
A0A024R6Q6	ATP-binding cassette, sub-family C (CFTR/MRP), member 11	*ABCC11*	1.65	3.21E-02
E7ERK9	Translation initiation factor eIF-2B subunit delta	*EIF2B4*	1.65	4.69E-02
V9HW43	Epididymis secretory protein Li 102	*HSPB1*	1.65	2.09E-02

Q96F86	Enhancer of mRNA-decapping protein 3	*EDC3*	1.65	7.20E-04
P26196	Probable ATP-dependent RNA helicase DDX6	*DDX6*	1.65	1.90E-03
B2R8X4	GA binding protein transcription factor, alpha subunit 60kDa (GABPA), mRNA	*GABPA*	1.64	2.48E-03
B3KQK5	Mitochondrial proteins import receptor	*TOMM70A ; TOMM70*	1.63	7.06E-03
A8IK34	Ankyrin repeat domain 40	*ANKRD40*	1.63	1.27E-02
Q9BUN8	Derlin-1 OS=Homo sapiens	*DERL1*	1.61	1.64E-02
Q9H5Z1	Probable ATP-dependent RNA helicase DHX35	*DHX35*	1.61	2.84E-02
P54652	Heat shock-related 70 kDa protein 2	*HSPA2*	1.61	1.06E-02
A8K613	HCG37164, isoform	*LYSMD3*	1.60	1.83E-02
Q8TE73	Dynein heavy chain 5, axonemal	*DNAH5*	1.60	4.20E-02
B4DL78	alpha-1,2-Mannosidase	*EDEM2*	1.59	1.92E-02
Q9NRY4	Rho GTPase-activating protein 35	*ARHGAP35*	1.59	2.07E-03
A0A0S2Z5L8	Methyltransferase like 17 isoform 4 (Fragment)	*METTL17*	1.59	1.06E-02
A0A024R1C2	DNA topoisomerase	*TOP3B*	1.59	2.02E-02
A4D1L5	Ubiquitin-conjugating enzyme E2H	*UBE2H*	1.58	7.70E-04
F8W930	Insulin-like growth factor 2 mRNA-binding protein 2	*IGF2BP2*	1.58	2.86E-03
Q9HC52	Chromobox protein homolog 8	*CBX8*	1.58	1.77E-03
Q8WUD1	Ras-related protein Rab-2B	*RAB2B*	1.57	1.82E-02
A0A024RDT4	Lymphocyte cytosolic protein 1 (L-plastin), isoform	*LCP1*	1.57	1.48E-02
Q53XS4	Tyrosine-protein phosphatase non-receptor type	*PTPN6*	1.57	1.02E-02
Q9ULM3	YEATS domain-containing protein 2	*YEATS2*	1.57	3.85E-02
H0UI97	Zinc finger, CCCH-type with G patch domain, isoform	*ZGPAT*	1.56	4.78E-02
Q6Y7W6	PERQ amino acid-rich with GYF domain-containing protein 2	*GIGYF2*	1.54	7.87E-05
A0A024RDB2	Ras-GTPase activating protein SH3 domain-binding protein 2	*G3BP2*	1.54	6.38E-03
C9JEJ2	Choline-phosphate cytidylyltransferase A	*PCYT1A*	1.54	1.83E-03
P13533	Myosin-6	*MYH6*	1.53	9.44E-03
Q96DH6	RNA-binding protein Musashi homolog 2	*MSI2*	1.52	1.58E-02
Q9BQF6	Sentrin-specific protease 7	*SENP7*	1.52	4.85E-02
Q8WWM7	Ataxin-2-like protein	*ATXN2L*	1.52	5.63E-03
Q8IY17	Neuropathy target esterase	*PNPLA6*	1.51	2.82E-02

Q9NZB2	Constitutive coactivator of PPAR-gamma-like protein 1	*FAM120A*	1.51	1.34E-03
Decreased in the <u>proteome</u> of DENV-2 infected cells compared to mock infected cells.				
H3BSS0	Metallothionein	*MT1G*	0.08	9.71E-04
P13640	Metallothionein-1G	*MT1G*	0.17	2.68E-03
B7ZL91	Metalloendopeptidase	*MEP1A*	0.18	6.49E-04
Q59EP2	Angiotensinogen variant (Fragment)	*AGT*	0.20	5.64E-04
A0A024R466	Integral membrane protein 2C, isoform	*ITM2C*	0.22	2.07E-02
Q68CJ9	Cyclic AMP-responsive element-binding protein 3-like protein 3	*CREB3L3*	0.23	4.81E-04
Q59GX7	Stearoyl-CoA desaturase variant (Fragment)	*SCD*	0.24	3.18E-03
A0A0K0K1J1	Cystatin	*CST3*	0.25	1.76E-04
Q7Z528	E3-16	*ITM2B*	0.28	3.84E-05
A8K6C9	Insulin-like growth factor 2 (somatomedin A)	*INS-IGF2*	0.29	1.71E-03
P00995	Serine protease inhibitor Kazal-type 1	*SPINK1*	0.30	3.40E-04
Q9UHP3	Ubiquitin carboxyl-terminal hydrolase 25	*USP25*	0.32	2.07E-04
E1U340	ZNF511/PRAP1 fusion protein	*ZNF511-PRAP1*	0.33	7.19E-03
P02760	Protein AMBP	*AMBP*	0.34	7.46E-04
P02771	Alpha-fetoprotein	*AFP*	0.34	7.22E-04
E9KL23	alpha-1-antitrypsin	*SERPINA1*	0.34	6.85E-04
O60487	Myelin protein zero-like protein 2	*MPZL2*	0.35	6.04E-03
M1V487	Tyrosine-protein kinase receptor	*LRIG3*	0.35	1.33E-03
X6R8F3	Neutrophil gelatinase-associated lipocalin	*LCN2*	0.36	3.98E-02
P02671	Fibrinogen alpha chain	*FGA*	0.36	1.28E-03
Q2M3R2	Protocadherin beta 3	*PCDHB3*	0.36	2.72E-03
P02763	Alpha-1-acid glycoprotein 1	*ORM1*	0.36	1.05E-03
P02795	Metallothionein-2	*MT2A*	0.36	1.39E-02
P80297	Metallothionein-1X	*MT1X*	0.37	1.11E-02
P04732	Metallothionein-1E	*MT1E*	0.38	1.52E-02
A0A024R6T4	Metallothionein	*MT1M*	0.38	2.91E-02
P02647	Apolipoprotein A-I	*APOA1*	0.39	9.29E-03
E9PGN7	Plasma protease C1 inhibitor	*SERPING1*	0.40	9.56E-03
Q8NBJ4	Golgi membrane protein 1	*GOLM1*	0.40	1.17E-03
V9HWA9	Complement C3	*C3*	0.40	2.77E-05
Q86WW8	Cytochrome c oxidase assembly factor 5	*COA5*	0.41	5.17E-03
V9HVY1	Fibrinogen beta chain	*FGB*	0.43	1.01E-03
V9GYM3	Apolipoprotein A-II	*APOA2*	0.44	8.43E-04

A8K7A2	cell division cycle associated 8	*CDCA8*	0.44	4.08E-03
K7ER74	Apolipoprotein C-II	*APOC2*	0.44	4.34E-04
P02753	Retinol-binding protein 4	*RBP4*	0.44	5.58E-04
P02679	Fibrinogen gamma chain	*FGG*	0.44	1.18E-03
B2R7U4	Heme oxygenase (decycling) 1 (HMOX1), mRNA	*HMOX1*	0.45	7.61E-03
B2R778	Cadherin 17, LI cadherin (liver-intestine) (CDH17), mRNA	*CDH17*	0.46	2.48E-03
O95445	Apolipoprotein M	*APOM*	0.46	2.99E-02
Q53H26	Transferrin variant (Fragment)	*TF*	0.46	2.03E-03
A0A024R462	Fibronectin 1, isoform	*FN1*	0.47	5.21E-03
Q06481	Amyloid-like protein 2	*APLP2*	0.47	2.25E-03
A8K7Q1	nucleobindin 1 (NUCB1), mRNA	*NUCB1*	0.47	8.30E-04
X5D2G8	Fibroblast growth factor receptor 3 isoform A	*FGFR3*	0.47	1.24E-03
Q59F30	Fibroblast growth factor receptor 4 variant	*FGFR4*	0.48	9.83E-04
P49715	CCAAT/enhancer-binding protein alpha	*CEBPA*	0.48	6.22E-03
Q567V2	Mpv17-like protein 2	*MPV17L2*	0.48	4.00E-02
Q9NQZ5	StAR-related lipid transfer protein 7, mitochondrial	*STARD7*	0.48	3.08E-02
Q01581	Hydroxymethylglutaryl-CoA synthase, cytoplasmic	*HMGCS1*	0.48	3.51E-04
Q6NT76	Homeobox-containing protein 1	*HMBOX1*	0.49	7.59E-04
Q08830	Fibrinogen-like protein 1	*FGL1*	0.49	1.94E-02
P07307	Asialoglycoprotein receptor 2	*ASGR2*	0.49	4.78E-03
O43405	Cochlin	*COCH*	0.49	2.30E-02
A8K5A4	Ceruloplasmin (ferroxidase) (CP), mRNA	*CP*	0.49	3.90E-04
P00738	Haptoglobin	*HP*	0.49	2.46E-02
P04733	Metallothionein-1F	*MT1F*	0.50	1.75E-02
A0A024R9D9	Transcription and mRNA export factor ENY2	*ENY2*	0.50	9.73E-04
D0PNI2	Lysyl oxidase	*LOX*	0.50	8.83E-03
P80294	Metallothionein-1H	*MT1H*	0.51	7.43E-03
A0A087WY68	Proprotein convertase subtilisin/kexin type 6	*PCSK6*	0.51	3.79E-02
Q9BXS6	Nucleolar and spindle-associated protein 1	*NUSAP1*	0.52	1.15E-02
P78556	C-C motif chemokine 20	*CCL20*	0.52	3.59E-02
P34741	Syndecan-2	*SDC2*	0.52	9.55E-03
Q5S3G3	MHC class I antigen	*HLA-A*	0.52	4.79E-03
P18827	Syndecan-1	*SDC1*	0.52	1.50E-02
B2RCP7	connective tissue growth factor (CTGF), mRNA	*CTGF*	0.52	3.59E-02

A0A0G2JIF2	HLA class I histocompatibility antigen, A-3 alpha chain	*HLA-A*	0.53	3.23E-03
Q16626	Male-enhanced antigen 1	*MEA1*	0.53	2.68E-04
P42830	C-X-C motif chemokine 5	*CXCL5*	0.53	6.11E-03
B4DRF2	Complement factor I	*CFI*	0.54	1.99E-03
P05997	Collagen alpha-2(V) chain	*COL5A2*	0.54	9.92E-03
O95864	Fatty acid desaturase 2	*FADS2*	0.54	1.67E-02
Q8NG11	Tetraspanin-14	*TSPAN14*	0.54	3.73E-02
Q9BRK5	45 kDa calcium-binding protein	*SDF4*	0.54	1.24E-03
P01031	Complement C5	*C5*	0.54	7.61E-03
B1AHL2	Fibulin-1	*FBLN1*	0.55	4.01E-03
E5RIM7	Copper transport protein ATOX1	*ATOX1*	0.55	3.19E-02
Q8IZ52	Chondroitin sulfate synthase 2	*CHPF*	0.55	5.02E-02
P05067	Amyloid beta A4 protein	*APP*	0.55	2.18E-03
O00762	Ubiquitin-conjugating enzyme E2 C	*UBE2C*	0.55	4.81E-04
Q12772	Sterol regulatory element-binding protein 2	*SREBF2*	0.56	8.15E-03
P10909	Clusterin	*CLU*	0.56	2.95E-02
A0A024RB84	Receptor protein-tyrosine kinase	*ERBB3*	0.56	2.98E-03
P84101	Small EDRK-rich factor 2	*SERF2*	0.56	2.82E-03
Q8NC54	Keratinocyte-associated transmembrane protein 2	*C5orf15*	0.56	2.29E-03
Q9NXH8	Torsin-4A	*TOR4A*	0.57	2.24E-02
B4E1Z4	Complement factor B	*N/A*	0.58	1.84E-02
A0A024R9G2	Ankyrin repeat domain 46, isoform	*ANKRD46*	0.58	8.74E-03
B3KM21	Family with sequence similarity 36, member A, isoform	*COX20*	0.58	1.66E-03
A0A024RE02	Phosphoglycerate dehydrogenase like 1, isoform	*UBAC2*	0.59	1.34E-02
D3DRR6	Inter-alpha (Globulin) inhibitor H2, isoform	*ITIH2*	0.59	2.23E-02
A0A024QYT5	Serpin peptidase inhibitor, clade E (Nexin, plasminogen activator inhibitor type 1), member 1, isoform	*SERPINE1*	0.60	4.81E-02
Q13530	Serine incorporator 3	*SERINC3*	0.60	9.30E-03
Q9BTY2	Plasma alpha-L-fucosidase	*FUCA2*	0.60	3.53E-03
A0A024R944	Antithrombin III	*SERPINC1*	0.61	3.82E-02
F1D8T1	Hepatocyte nuclear factor 4	*HNF4A*	0.61	1.98E-02
Q4ZIN3	Membralin	*C19orf6 TMEM259*	0.61	1.34E-02
Q8NET6	Carbohydrate sulfotransferase 13	*CHST13*	0.61	1.17E-02
A0A087X2H1	E3 ubiquitin-protein ligase HECTD1	*HECTD1*	0.61	4.80E-03

A0A024R7B0	Ubiquitin-like 5, isoform	*UBL5*	0.61	1.66E-02
P20290	Transcription factor BTF3	*BTF3*	0.61	4.13E-02
F1CME6	Hepatitis A virus cellular receptor 1a	*HAVCR1*	0.61	3.20E-02
E9PGC5	Receptor-type tyrosine-protein phosphatase kappa		0.61	1.19E-02
Q9NR09	Baculoviral IAP repeat-containing protein 6	*BIRC6*	0.61	9.35E-03
Q8NFH9	MLL/SEPTIN6 fusion protein (Fragment)	*N/A*	0.62	2.13E-02
Q8IWK6	Adhesion G protein-coupled receptor A3	*GPR125; ADGRA3*	0.62	2.22E-02
P33908	Mannosyl-oligosaccharide 1,2-alpha-mannosidase IA	*MAN1A1*	0.62	1.16E-02
Q8TCT8	Signal peptide peptidase-like 2A	*SPPL2A*	0.62	3.04E-02
A0A024R3H2	Sortilin-related receptor, L(DLR class) A repeats-containing	*SORL1*	0.62	1.02E-02
P00734	Prothrombin	*F2*	0.62	3.72E-02
P48740	Mannan-binding lectin serine protease 1	*MASP1*	0.62	3.68E-03
P14543	Nidogen-1	*NID1*	0.62	7.47E-03
B3KUE5	Phospholipid transfer protein, isoform	*PLTP*	0.62	2.86E-02
B2R8Y9	Tissue factor pathway inhibitor(lipoprotein-associated coagulation inhibitor) (TFPI), mRNA	*TFPI*	0.63	1.61E-02
Q9H0X4	Protein FAM234A	*ITFG3 FAM234A*	0.63	1.16E-02
Q6IAX1	FDFT1 protein	*FDFT1*	0.63	2.18E-02
A0A024QYX3	RNA binding motif (RNP1, RRM) protein 3, isoform	*RBM3*	0.63	1.04E-02
Q53YP0	PreS1 binding protein	*GLTSCR2; NOP53*	0.63	3.62E-02
Q96EH3	Mitochondrial assembly of ribosomal large subunit protein 1	*MALSU1*	0.63	2.62E-02
A0A024R9N5	Solute carrier family 35, member D2, isoform	*SLC35D2*	0.64	3.51E-02
A0A024R9G0	Polymerase (RNA) II (DNA directed) polypeptide K, 7.0kDa, isoform	*POLR2K*	0.64	3.79E-02
Q658Y4	Protein FAM91A1	*FAM91A1*	0.64	1.86E-02
B3KMC8	WW domain-binding protein 4	*WBP4*	0.64	2.45E-02
A0A024R0T8	Apolipoprotein C-I, isoform	*APOC1*	0.64	3.61E-03
Q9ULW0	Targeting protein for Xklp2	*TPX2*	0.64	8.24E-03
A0A024RD39	Phospholipase A2, group VII (Platelet-activating factor acetylhydrolase, plasma), isoform	*PLA2G7*	0.65	1.70E-03
Q59ER8	Leucine-rich repeat-containing G protein-coupled receptor 4 variant (Fragment)	*LGR4*	0.65	1.24E-02

G3XAN8	Mitochondrial import inner membrane translocase subunit Tim8 B	*TIMM8B*	0.65	2.44E-02
H7C3C4	Anion exchange protein (Fragment)	*SLC4A7*	0.65	8.14E-03
Q15904	V-type proton ATPase subunit S1	*ATP6AP1*	0.65	2.78E-02
A6NMH8	Tetraspanin	*CD81*	0.65	1.05E-02
Q96KR6	Protein FAM210B	*FAM210B*	0.65	3.39E-03
Q59FM9	TYRO3 protein tyrosine kinase variant (Fragment)	*TYRO3*	0.65	6.65E-03
Q9HAT2	Sialate O-acetylesterase	*SIAE*	0.65	1.84E-03
A0A024R6U8	Matrix metallopeptidase 15 (Membrane-inserted), isoform	*MMP15*	0.65	2.83E-02
O75506	Heat shock factor-binding protein 1	*HSBP1*	0.66	4.42E-03
A0A024R3K2	RNA pseudouridylate synthase domain containing 4, isoform	*RPUSD4*	0.66	4.96E-02
Q8NC42	E3 ubiquitin-protein ligase RNF149	*RNF149*	0.66	8.93E-03
A0A0C4DFL7	Lanosterol 14-alpha demethylase	*CYP51A1*	0.66	2.87E-02
A0A0S2Z3Y2	Interferon gamma receptor 1 isoform 1 (Fragment)	*IFNGR1*	0.66	1.24E-03
Q07954	Prolow-density lipoprotein receptor-related protein 1	*LRP1*	0.66	1.46E-03
Q5SRD1	Putative mitochondrial import inner membrane translocase subunit Tim23B	*TIMM23B; LINC00843; LOC100652748*	0.66	1.19E-02
A8KAF0	CCR6 chemokine receptor (CMKBR6) gene	*CCR6*	0.67	4.35E-03
A0A0A0MR51	Fatty acid desaturase 1	*FADS1*	0.67	6.40E-03
Q9BU23	Lipase maturation factor 2	*LMF2*	0.67	5.79E-03
P08236	Beta-glucuronidase	*GUSB*	0.67	4.39E-03

Table 5.5 Proteins that were significantly changed ≥ 1.5 fold in amount, in the secretome of DENV-2 infected Huh-7 cells compared to mock infected cells.

Accession	Description	Gene	Fold change DENV-2 /Mock	P-value
Increased in the secretome of DENV-2 infected cells compared to mock infected cells.				
Q13724	Mannosyl-oligosaccharide glucosidase	*MOGS*	7.01	1.03E-02
Q5SRE5	Nucleoporin NUP188 homolog	*NUP188*	3.00	1.19E-02
Q9UKL6	Phosphatidylcholine transfer protein	*PCTP*	2.80	3.50E-02
Q8WWI1	LIM domain only protein 7	*LMO7*	2.77	2.45E-02
Q5T5H1	Alpha-endosulfine	*ENSA*	2.54	1.36E-04
P05204	Non-histone chromosomal protein HMG-17	*HMGN2*	2.23	2.79E-02
Q9H2M9	Rab3 GTPase-activating protein non-catalytic subunit	*RAB3GAP 2*	2.13	8.06E-03
B2RA03	Keratin 18 (KRT18), mRNA	*KRT18*	2.13	1.24E-02
P05787	Keratin, type II cytoskeletal 8	*KRT8*	2.07	9.34E-03
P58166	Inhibin beta E chain	*INHBE*	1.93	2.43E-02
O00469	Procollagen-lysine,2-oxoglutarate 5-dioxygenase 2	*PLOD2*	1.86	1.95E-03
B7Z809	C-1-tetrahydrofolate synthase, cytoplasmic	*MTHFD1*	1.75	9.84E-03
Q01970	1-phosphatidylinositol 4,5-bisphosphate phosphodiesterase beta-3	*PLCB3*	1.73	3.09E-02
B2RA34	BCL2-associated athanogene 4 (BAG4), mRNA	*BAG4*	1.69	4.69E-02
Q13740	CD166 antigen	*ALCAM*	1.69	5.10E-03
A8K8X0	Nap1 P120	*NAA25*	1.68	1.70E-02
Q92484	Acid sphingomyelinase-like phosphodiesterase 3a	*SMPDL3A*	1.67	2.36E-02
Q59GW6	Acetyl-CoA acetyltransferase, cytosolic variant (Fragment)	*ACAT2*	1.67	2.26E-02

Q8N1G4	Leucine-rich repeat-containing protein 47	*LRRC47*	1.64	4.18E-02
Q9H4F8	SPARC-related modular calcium-binding protein 1	*SMOC1*	1.63	2.74E-03
Q9NP79	Vacuolar protein sorting-associated protein VTA1 homolog	*VTA1*	1.63	2.20E-02
Q92896	Golgi apparatus protein 1	*GLG1*	1.60	3.26E-02
A0A024RAF7	Endothelin converting enzyme 1, isoform	*ECE1*	1.58	4.43E-02
P35222	Catenin beta-1	*CTNNB1*	1.57	4.86E-02
E7EPT4	NADH dehydrogenase [ubiquinone] flavoprotein 2, mitochondrial	*NDUFV2*	1.56	2.26E-02
P30048	Thioredoxin-dependent peroxide reductase	*PRDX3*	1.51	3.61E-02
A0A0A1TTQ0	Lutheran blood group glycoprotein	*BCAM*	1.50	1.77E-02
Decrease in the <u>secretome</u> of DENV-2 infected cells compared to mock infected cells.				
P19652	Alpha-1-acid glycoprotein 2	*ORM2*	0.67	1.624E-02
P16870	Carboxypeptidase E	*CPE*	0.67	1.527E-02
P08697	Alpha-2-antiplasmin	*SERPINF2*	0.67	3.539E-02
B2R5S1	Angiotensinogen	*AGT*	0.67	2.941E-02
Q11201	CMP-N-acetylneuraminate-beta-galactosamide-alpha-2,3-sialyltransferase 1	*ST3GAL1*	0.67	4.361E-03
E9KL23	Alpha-1-antitrypsin	*SERPINA1*	0.66	5.140E-03
P02768	Serum albumin	*ALB*	0.65	2.584E-03
Q9NZL9	Methionine adenosyltransferase 2 subunit beta	*MAT2B*	0.65	3.979E-02
A0A0R7FJH5	Coagulation factor XII	*F12*	0.65	9.296E-03
A0A024R5F9	UDP-GlcNAc:betaGal beta-1,3-N-acetylglucosaminyltransferase 6	*B3GNT1; B4GAT1*	0.65	7.891E-03
E7ETH0	Complement factor I	*CFI*	0.65	4.296E-02
B2R888	Monocyte differentiation antigen CD14	*CD14*	0.65	9.747E-03

A8K8T3	N-deacetylase/N-sulfotransferase (heparan glucosaminyl) 1	*NDST1*	0.64	1.801E-02
D9ZGG2	Vitronectin	*VTN*	0.64	2.278E-02
A0A0K0K1J1	Cystatin	*CST3*	0.64	1.318E-02
A0A024R6I9	Serpin peptidase inhibitor, clade A (Alpha-1 antiproteinase, antitrypsin), member 4, isoform	*SERPINA4*	0.64	8.577E-03
Q9BTY2	Plasma alpha-L-fucosidase	*FUCA2*	0.63	2.949E-02
Q9UHG3	Prenylcysteine oxidase 1	*PCYOX1*	0.63	6.875E-03
A0A0S2Z4L3	Protein S isoform 2 (Fragment)	*PROS1*	0.63	4.254E-02
B2R9F2	Proteinase inhibitor, clade A (alpha-1 antiproteinase, antitrypsin), member 6	*SERPINA6*	0.63	6.231E-04
B3KME2	Cartilage-associated protein	*CRTAP*	0.62	2.342E-02
P05160	Coagulation factor XIII B chain	*F13B*	0.62	1.876E-02
Q8WXD2	Secretogranin-3	*SCG3*	0.62	1.078E-02
P05546	Heparin cofactor 2	*SERPIND1*	0.62	7.537E-03
C0JYY2	Apolipoprotein B	*APOB*	0.61	3.347E-02
Q8NE71	ATP-binding cassette sub-family F member 1	*ABCF1*	0.61	9.291E-03
P22352	Glutathione peroxidase 3	*GPX3*	0.60	4.154E-03
Q8NBP7	Proprotein convertase subtilisin/kexin type 9	*PCSK9*	0.60	4.762E-03
P34096	Ribonuclease 4	*RNASE4*	0.60	9.785E-03
P10909	Clusterin	*CLU*	0.60	2.182E-02
O94985	Calsyntenin-1	*CLSTN1*	0.59	2.240E-02
B3KUE5	Phospholipid transfer protein, isoform	*PLTP*	0.59	1.184E-03
D0PNI2	Lysyl oxidase	*LOX*	0.59	3.187E-02
Q8IWW6	Rho GTPase-activating protein 12	*ARHGAP12*	0.59	4.523E-02
A4D2D2	Procollagen C-endopeptidase enhancer	*PCOLCE*	0.58	1.211E-02
Q9BRP8	Partner of Y14 and mago OS=Homo sapiens	*PYM1*	0.57	3.818E-02

P02771	Alpha-fetoprotein	*AFP*	0.57	8.815E-04
P23142	Fibulin-1	*FBLN1*	0.57	1.386E-02
P00742	Coagulation factor X	*F10*	0.57	1.335E-02
P15169	Carboxypeptidase N catalytic chain	*CPN1*	0.56	9.341E-05
E9PLM6	Midkine	*MDK*	0.56	1.908E-02
P03950	Angiogenin	*ANG*	0.56	1.124E-02
B4DM05	Nidogen-1	*NID1*	0.56	2.183E-02
O95445	Apolipoprotein M	*APOM*	0.56	6.453E-03
A0A024RD39	Phospholipase A2, group VII (Platelet-activating factor acetylhydrolase, plasma), isoform	*PLA2G7*	0.56	5.919E-04
B7Z4R3	T-complex protein 1 subunit beta	*CCT2*	0.55	2.933E-02
O00264	Membrane-associated progesterone receptor component 1	*PGRMC1*	0.55	3.648E-02
P35443	Thrombospondin-4	*THBS4*	0.55	3.386E-02
O75787	Renin receptor	*ATP6AP2*	0.54	4.417E-02
B4DUV1	Fibulin-1	*FBLN1*	0.54	2.460E-02
A0A024R943	Torsin family 3, member A, isoform	*TOR3A*	0.54	4.635E-04
B7ZL91	Metalloendopeptidase	*MEP1A*	0.54	1.163E-02
P09668	Pro-cathepsin H	*CTSH*	0.52	1.670E-02
B3KM35	Beta-1,4-galactosyltransferase 4	*B4GALT4*	0.52	4.009E-02
Q15904	V-type proton ATPase subunit S1	*ATP6AP1*	0.52	2.149E-02
P55001	Microfibrillar-associated protein 2	*MFAP2*	0.51	6.122E-03
A8K5T0	Complement factor H (CFH), mRNA	*CFH*	0.51	1.813E-02
Q08830	Fibrinogen-like protein 1	*FGL1*	0.50	8.244E-03
P07307	Asialoglycoprotein receptor 2	*ASGR2*	0.50	7.190E-03
P22792	Carboxypeptidase N	*CPN2*	0.46	6.812E-03
P02679	Fibrinogen gamma chain	*FGG*	0.45	1.017E-02
Q13443	Disintegrin and metalloproteinase domain-containing protein 9	*ADAM9*	0.45	4.531E-02
V9HVY1	Epididymis secretory sperm binding protein Li 78p	*FGB*	0.44	2.673E-03
B3KQT8	Procollagen C-endopeptidase enhancer 2	*PCOLCE2*	0.44	7.505E-03

P02671	Fibrinogen alpha chain	*FGA*	0.44	1.894E-02
O95025	Semaphorin-3D	*SEMA3D*	0.43	4.898E-02
B4DN31	Chitinase domain-containing protein 1	*CHID1*	0.43	2.612E-02
F5H8G6	Probable 28S rRNA (cytosine(4447)-C(5))-methyltransferase	*NOP2*	0.43	4.641E-02
Q86UD1	Out at first protein homolog	*OAF*	0.41	3.596E-03
P02647	Apolipoprotein A-I	*APOA1*	0.40	7.162E-04
D3DP16	Fibrinogen gamma chain, isoform	*FGG*	0.40	2.487E-02
V9GYM3	Apolipoprotein A-II	*APOA2*	0.39	3.569E-04
E1U340	ZNF511/PRAP1 fusion protein	*ZNF511-PRAP1*	0.38	4.794E-06
K7ER74	Apolipoprotein C-II	*APOC2*	0.36	8.661E-03
Q13444	Disintegrin and metalloproteinase domain-containing protein 15	*ADAM15*	0.35	2.843E-02
Q5U676	B3GAT3 protein (Fragment)	*B3GAT3*	0.33	3.872E-02
B0YIW2	Apolipoprotein C-III	*APOC3*	0.11	3.394E-02
A0A087WW81	Rootletin (Fragment)	*CROCC*	0.09	6.940E-04

In addition to the individual analysis of the proteins that changed in abundance in either the proteome or secretome of DENV-2 infected cells compared to mock infected cells, an integrated analysis of the proteins that significantly changed in both was done to determine the relationship of intracellular and secreted proteins. There were 1469 host proteins that were commonly identified in both proteome and secretome (Figure 5.3). A lower cut-off of 1.3 fold was used to analyse the combined data set, to ensure all proteins that changed in abundance in the same direction were identified. There were 30 proteins that were found to be significantly altered (≥1.3 fold) in both the proteome and secretome of DENV2 infected cells compared to mock infected cells (Figure 5.4 and Table 5.6). As for the individual datasets, it was found that the majority of the commonly modulated proteins were decreased in abundance upon infection. There were 1 and 27 host proteins that significantly increased and decreased in both the proteome and secretome, respectively. Whereas, 2 proteins, mannosyl-oligosaccharide glucosidase (MOGS) and cadherin 17 (CDH17), were identified to significantly decrease in the proteome but increase in the secretome after infection. Among the 27 proteins that significantly decreased in both the proteome and secretome, 20 proteins that decreased ≥ 1.5 fold were subjected to further bioinformatic analysis. A higher cut-off was applied for this analysis to identify a more stringent set of related biological processes.

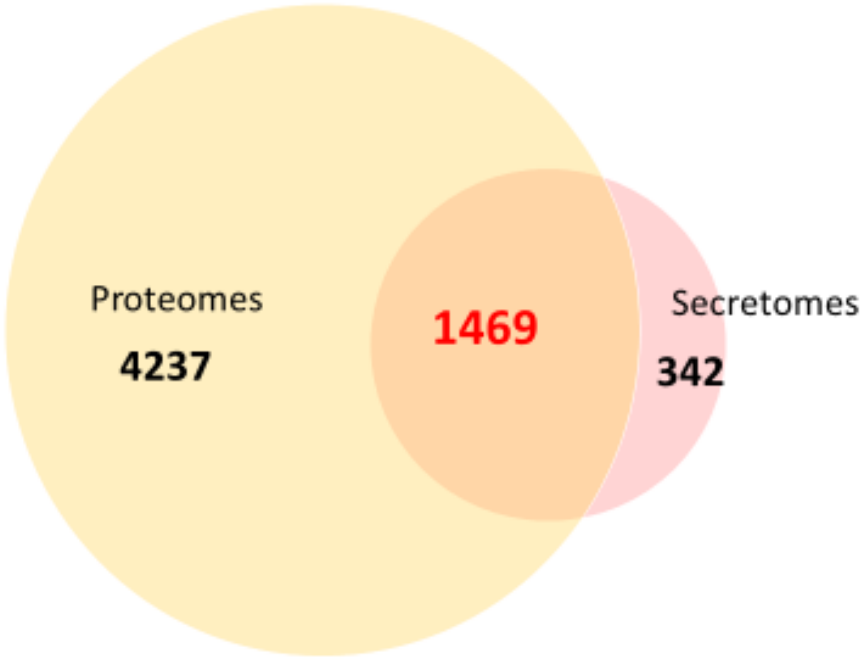

Figure 5.3 Overlap between the cellular and secreted proteins detected.

Venn diagram shows the number of proteins that were detected in the proteome and secretome of DENV-2 infected Huh-7 cells.

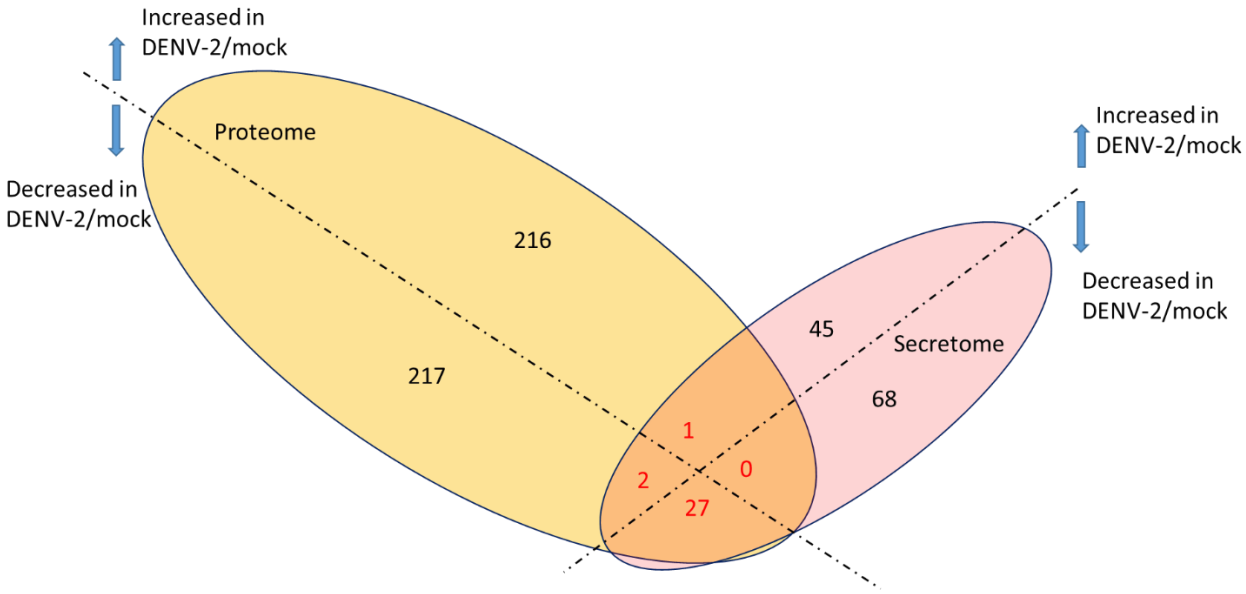

Figure 5.4 Overlap between cellular and secreted proteins significantly altered (≥ 1.3 fold) in DENV-2 infection.

Venn diagram shows the number of proteins that significantly (P-value < 0.05) increased and decreased (≥1.3 fold) in the proteome and secretome of DENV-2 infected Huh-7 cells compared to mock infected cells.

Table 5.6 Proteins that were commonly significantly changed ≥ 1.3 fold in amount in both proteome and secretome of DENV-2 infected Huh-7 cells compared to mock infected cells.

Accession	Description	Gene name	Cell lysates		Secretomes	
			Fold change DENV-2/Mock	P-value	Fold change DENV-2/Mock	P-value
Increased in both the proteome and secretome of DENV-2 infected Huh-7 cells						
P25685	DnaJ homolog subfamily B member 1	*DNAJB1*	1.34	1.64E-02	1.42	3.11E-02
Increased in the proteome but decreased in the secretome of DENV-2 infected Huh-7 cells						
None						
Decreased in the proteome but increased in the secretome of DENV-2 infected Huh-7 cells						
Q13724	Mannosyl-oligosaccharide glucosidase	*MOGS*	0.67	8.12E-03	7.01	1.03E-02
B2R778	Cadherin 17, LI cadherin	*CDH17*	0.46	2.48E-03	1.39	1.43E-02
Decreased in both the proteome and secretome of DENV-2 infected Huh-7 cells						
B3KQT8	Procollagen C-endopeptidase enhancer 2	*PCOLCE2*	0.69	9.31E-03	0.44	7.50E-03
Q15904	V-type proton ATPase subunit S1	*ATP6AP1*	0.65	2.78E-02	0.52	2.15E-02
A0A024RD39	Phospholipase A2, group VII (Platelet-activating factor acetylhydrolase, plasma)	*PLA2G7*	0.65	1.70E-03	0.56	5.92E-04
B3KUE5	Phospholipid transfer protein, isoform	*PLTP*	0.62	2.86E-02	0.59	1.18E-03
P00734	Prothrombin	*F2*	0.62	3.72E-02	0.72	3.47E-02
P33908	Mannosyl-oligosaccharide 1,2-alpha-mannosidase IA	*MAN1A1*	0.62	1.16E-02	0.69	1.54E-02
Q9BTY2	Plasma alpha-L-fucosidase	*FUCA2*	0.60	3.53E-03	0.63	2.95E-02
P10909	Clusterin	*CLU*	0.56	2.95E-02	0.60	2.18E-02
D0PNI2	Lysyl oxidase	*LOX*	0.50	8.83E-03	0.59	3.19E-02

P07307	Asialoglycoprotein receptor 2	*ASGR2*	0.49	4.78E-03	0.50	7.19E-03
Q08830	Fibrinogen-like protein 1	*FGL1*	0.49	1.94E-02	0.50	8.24E-03
Q53H26	Transferrin variant	*TF*	0.46	2.03E-03	0.71	3.51E-02
O95445	Apolipoprotein M	*APOM*	0.46	2.99E-02	0.56	6.45E-03
P02679	Fibrinogen gamma chain	*FGG*	0.44	1.18E-03	0.45	1.02E-02
P02753	Retinol-binding protein 4	*RBP4*	0.44	5.58E-04	0.69	1.57E-02
K7ER74	Apolipoprotein C-II	*APOC2*	0.44	4.34E-04	0.36	8.66E-03
V9GYM3	Apolipoprotein A-II	*APOA2*	0.44	8.43E-04	0.39	3.57E-04
V9HVY1	Fibrinogen beta chain	*FGB*	0.43	1.01E-03	0.44	2.67E-03
P02647	Apolipoprotein A-I	*APOA1*	0.39	9.29E-03	0.40	7.16E-04
P02763	Alpha-1-acid glycoprotein 1	*ORM1*	0.36	1.05E-03	0.71	7.53E-03
P02671	Fibrinogen alpha chain	*FGA*	0.36	1.28E-03	0.44	1.89E-02
E9KL23	Alpha -1-Antitrypsin	*SERPINA1*	0.34	6.85E-04	0.66	5.14E-03
P02771	Alpha-fetoprotein	*AFP*	0.34	7.22E-04	0.57	8.82E-04
P02760	Protein AMBP	*AMBP*	0.34	7.46E-04	0.68	1.05E-02
E1U340	ZNF511/PRAP1 fusion protein	*ZNF511-PRAP1*	0.33	7.19E-03	0.38	4.79E-06
A0A0K0K1J1	Cystatin	*CST3*	0.25	1.76E-04	0.64	1.32E-02
B7ZL91	Metalloendopeptidase	*MEP1A*	0.18	6.49E-04	0.54	1.16E-02
	Fibulin-1	FBLN1	0.55	4.01E-03	0.54	2.46E-02

*The proteins that significantly (P-value <0.05) decreased ≥1.5 fold in both proteome and secretome of DENV-2 infected Huh-7 cells are coloured in red.

5.4 Bioinformatic analysis of cellular and secreted proteins altered in abundance in response to DENV-2 infection

5.4.1 Bioinformatic analysis of cellular proteins altered in abundance in response to DENV-2 infection.

The 121 and 147 proteins that significantly increased and decreased ≥ 1.5 fold, respectively, in the proteome of DENV-2 cells compared to mock infected cells were subjected to gene enrichment and network analysis using the DAVID and STRING analysis programs (Figures 5.5 and 5.6 and Supplementary Table S 5.1).

DAVID analysis of the proteins that significantly increased in response to DENV-2 infection identified three functional annotation clusters associated with significantly enriched GO terms (Figure 5.5). The GOBP term "negative regulation of translation" (GO:0017148) was the most enriched, followed by the terms "CRD-mediated mRNA stabilization" (GO:0070934) and "negative regulation of transcription from RNA polymerase II promoter" (GO:0000122). The biological processes related to DEN pathogenesis identified by the STRING analysis included "negative regulation of gene expression" (GO:0010629), "negative regulation of translation" (GO:0017148) and "cytoplasmic stress granule" (GO:0010494) (Figure 5.6A). None of the proteins were associated with significantly enriched KEGG pathway terms.

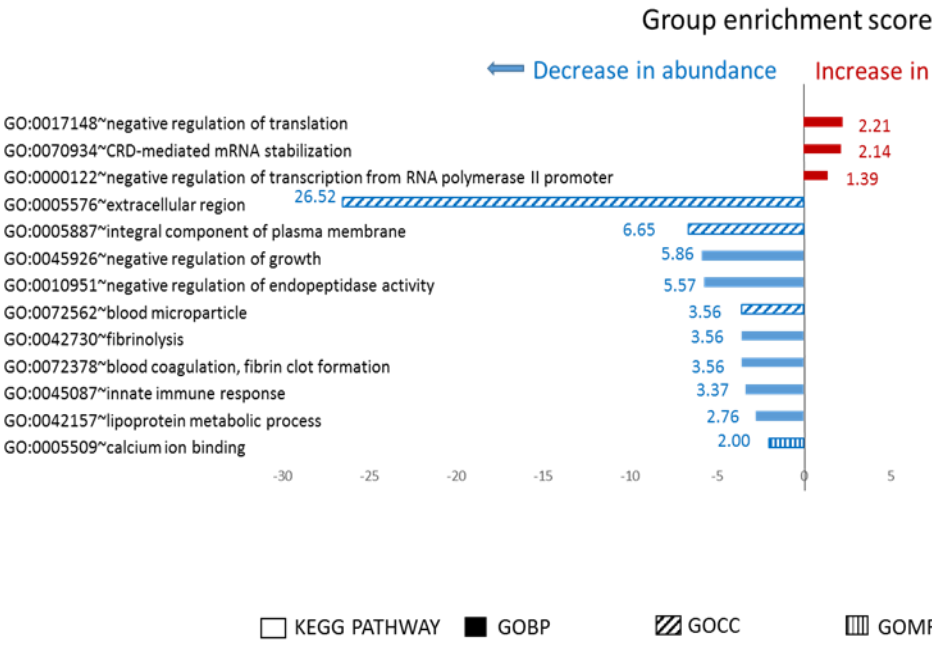

Count	%	P-Value
10	8.55	1.11E-08
3	2.56	3.99E-03
12	10.26	3.32E-03
35	24.65	7.26E-22
19	13.38	3.89E-07
7	4.93	8.97E-08
11	7.75	8.70E-10
15	10.56	3.75E-12
6	4.23	3.68E-06
4	2.82	5.99E-05
9	6.34	3.11E-04
6	4.23	2.20E-05
11	7.75	2.40E-03

Figure 5.5 DAVID analysis of cellular proteins that were altered in abundance in DENV-2 infected Huh-7 cells.

Proteins that were significantly (P-value < 0.05) altered in amount by ≥ 1.5 fold in DENV-2 infected Huh-7 cells compared to mock infected cells were analysed using the DAVID database. The GO accession numbers/terms that were significantly enriched and the properties of the corresponding protein clusters are shown. The GES of protein clusters associated with GO terms that significantly increased and decreased in response to infection are shown in red and blue, respectively. The shading shows the type of GO term (GOBP, GOCC or GOMF), UP keywords, Interpro term or KEGG pathway. The number of proteins in each cluster (count), number of proteins associated with each GO term/total number of proteins in the dataset (%) and P-value for each of the annotation terms are listed in the table.

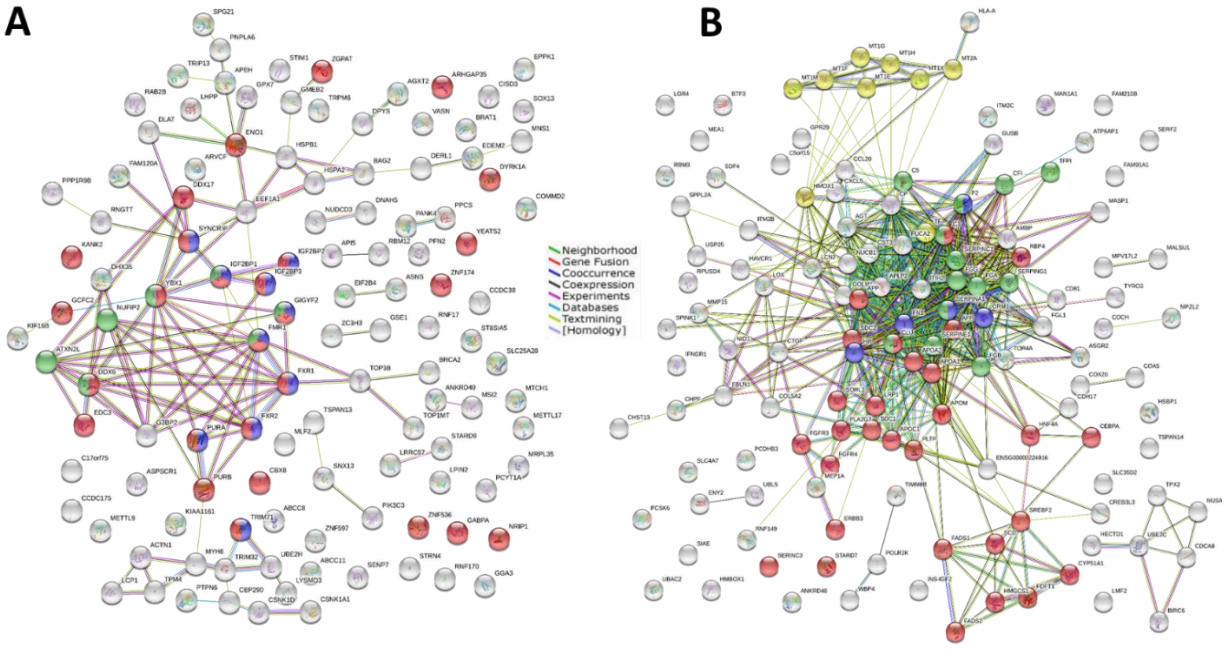

GO term/ pathway	Description	Count in gene set	FDR
GO:0010629	negative regulation of gene expression	27 of 1670	2.90E-04
GO:0017148	negative regulation of translation	8 of 117	1.40E-04
GO:0010494	cytoplasmic stress granule	6 of 51	3.75E-05

GO term/ pathway	Description	Count in gene set	FDR
GO:0006629	lipid metabolic process	29 of 1192	3.36e-07
GO:0006953	acute-phase response	5 of 45	0.00041
hsa04610	Complement and coagulation cascades	13 of 78	6.31e-12
hsa04978	Mineral absorption	9 of 51	1.83e-08

Figure 5.6 STRING analysis of cellular proteins that were altered in abundance in DENV-2 infected Huh-7 cells.

The STRING database was searched to analyse cellular proteins that significantly (P-value < 0.05) increased **(A)** and decreased **(B)** ≥ 1.5 fold in response to DENV-2 infection. **(A)** Nodes representing proteins associated with the significantly enriched GO terms "negative regulation of gene expression", "negative regulation of translation" and "cytoplasmic stress granule" are shaded in red, blue and green, respectively. (**B**) Nodes representing proteins associated with the significantly enriched GO terms "lipid metabolic process", "acute-phase response", "complement and coagulation cascades" and "mineral absorption" are shaded in red, blue, green and yellow respectively. The number of coloured nodes/total proteins involved for each term and the FDR of each GO term are listed in the table.

By contrast, DAVID analysis of the proteins that significantly decreased in DENV-2 infected Huh-7 cells compared to mock infected cells identified 19 functional annotation clusters that were associated with significantly enriched GO terms (the top ten clusters are shown in Figure 5.5). The most significantly enriched GO terms were the GOCC terms "extracellular region" (GO: 0005576; with keywords "signal peptide"), followed by "integral component of plasma membrane" (GO:0005887) and the GOBP terms, "negative regulation of growth" (GO:0045926; with keywords "metal-binding/metallothionein"), "negative regulation of endopeptidase activity" (GO:0010951), "blood coagulation" (GO0072378) and "innate immune response" (GO0045087) (Figure 5.5; Supplement table S 5.2).

STRING analysis revealed that cellular proteins that decreased in response to DENV-2 infection included clusters of proteins associated with the significantly enriched GOBP terms, "acute-phase response" (GO:0006953) and "lipid metabolic process" (GO:0006629) (Figure 5.6B). Protein clusters were also associated with the enriched KEGG pathways "complement and coagulation cascades" (hsa04610) followed by "mineral absorption" (hsa04978).

5.4.2 Bioinformatic analysis of the secretome from DENV-2 infected Huh-7 cells

The 27 and 75 host proteins that significantly increased and decreased ≥ 1.5 fold, respectively, in the secretome of DENV-2 infected Huh-7 cells compared to mock were subjected to gene enrichment and network analysis using the DAVID and STRING analysis programs (Figures 5.7 and 5.8). The analysis revealed the same trends as for the cellular proteome analysis. DAVID analysis showed that the proteins that were increased in amount after DENV-2 infection were not associated with a significant enrichment of any GO term. Whereas STRING analysis identified only one cluster of proteins, associated with the GOMF term "protein C-terminus binding" (GO:0008022) (Figure 5.8A).

By contrast, DAVID analysis of the proteins significantly decreased in abundance in the secretome from DENV-2 infected cells identified 6 functional annotation clusters that were associated with significantly enriched GO terms (Figure 5.7, Supplementary Table S5.2). The top three significantly enriched clusters were the keywords "signal

peptide/secreted", followed by the GOCC "blood microparticle" (GO:0072562) and GOBP "lipoprotein metabolic process" (GO:0042157). Furthermore, the GOBP term "innate immune response" (GO:0045087) was also significantly enriched. The most enriched KEGG pathway was "complement and coagulation cascades" (hsa04610: 11 proteins count (15.23%), P-value =1.94 E-07) followed by "PPAR signaling pathway" (hsa03320: 4 proteins count (5.55%), P-value = 4.20 E-03) (Supplementary Table S 5.2). In addition, STRING analysis revealed protein clusters significantly enriched in the complementary GOBP terms, "post-translational protein modification" and "regulation of acute inflammatory response" as well as the KEGG pathway terms "complement and coagulation cascades" (hsa04610) and "cholesterol metabolism" (hsa04978) (Figure 5.8B).

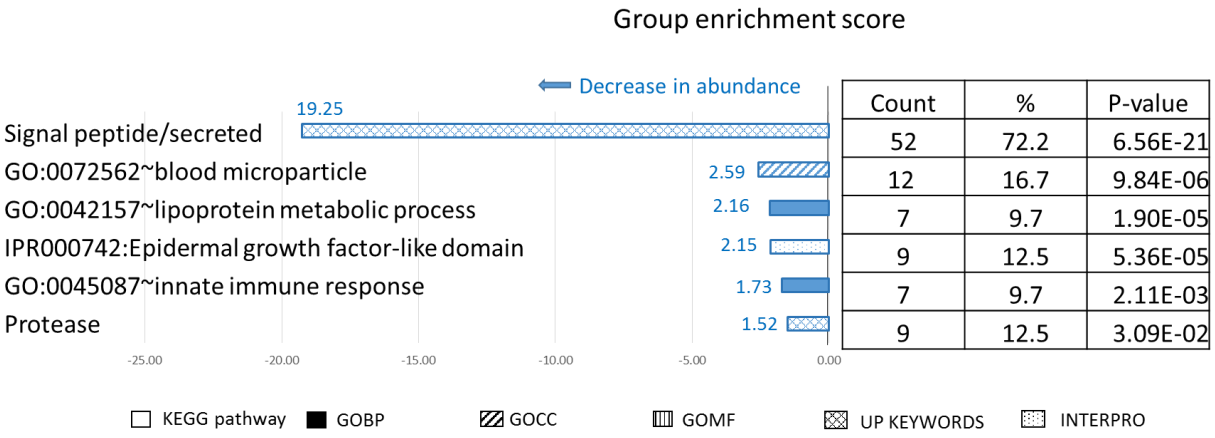

Count	%	P-value
52	72.2	6.56E-21
12	16.7	9.84E-06
7	9.7	1.90E-05
9	12.5	5.36E-05
7	9.7	2.11E-03
9	12.5	3.09E-02

Figure 5.7 DAVID analysis of proteins that were altered in abundance in the secretomes of DENV-2 infected cells.

Proteins that were significantly (P-value < 0.05) altered in amount by ≥ 1.5 fold in the secretomes of DENV-2 infected Huh-7 compared to mock infected cells were analysed using the DAVID database. The GO accession numbers/terms that were significantly enriched and the properties of the corresponding protein clusters are shown. The GES of protein clusters associated with significantly enriched GO terms are plotted as bar graphs (blue) with the corresponding GES score shown. The shading shows the type of GO term (GOBP, GOCC or GOMF), UP keywords, Interpro term or KEGG pathway. The number of proteins in each cluster (count), number of proteins associated with each GO term/total number of proteins in the dataset (%) and P-value for each of the annotation terms are listed in the table.

A

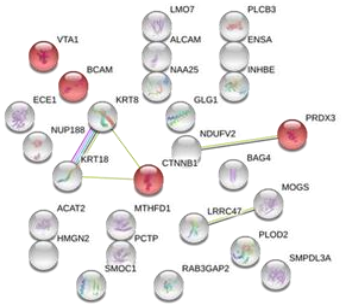

GO term/ pathway	Description	Count in gene set	FDR
GO:0008022	protein C-terminus binding	4 of 194	3.3E-02

B

GO term/ pathway	description	Count in gene set	false discovery rate
GO:0043687	post-translational protein modification	13 of 365	6.09E-08
GO:0002673	regulation of acute inflammatory response	8 of 92	1.74E-07
hsa04610	Complement and coagulation cascades	13 of 78	3.45E-16
hsa04978	Cholesterol metabolism	6 of 48	1.01E-06

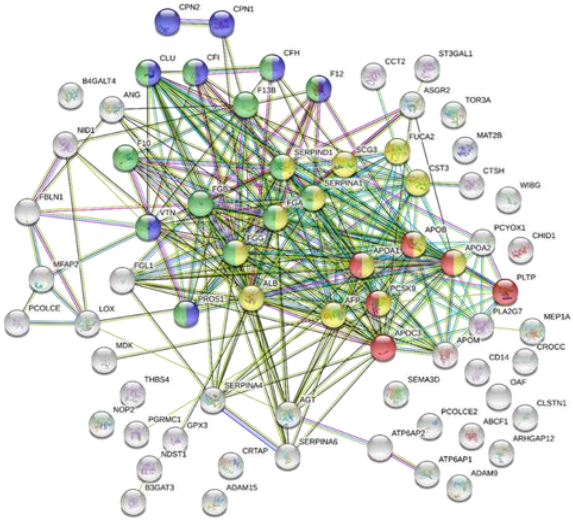

Figure 5.8 STRING analysis of proteins that were altered in abundance in the secretome of DENV-2 infected cells.

The STRING database was searched to analyse secreted proteins that significantly ($p < 0.05$) increased **(A)** and decreased **(B)** ≥ 1.5 fold in response to DENV-2 infection. **(A)** Nodes representing proteins associated with the significantly enriched GO terms "protein C-terminus binding" are coloured in red. (**B**) Nodes representing proteins associated with the significantly enriched GO terms "post-translational protein modification", "regulation of acute inflammatory response", "complement and coagulation cascades" and "Cholesterol metabolism" are coloured in yellow, blue, green and red, respectively. The number of coloured nodes/total proteins involved for each term and the FDR of each GO term are listed in the table.

5.4.3 Focused analysis on proteins that decreased in both proteome and secretome in response to DENV infection

Further GO term enrichment analysis was also done for the 20 proteins (shaded in red in Table 5.6) that significantly decreased ≥ 1.5 fold in both the proteome and secretome of DENV infected Huh-7 cells compared with mock. DAVID analysis identified 5 functional annotation clusters that were associated with significantly enriched GO terms (Figure 5.9). The most significantly enriched GO terms were the keywords "signal peptides/secreted", followed by the GOCC term "extracellular space" (GO:0005615) and the GOBP terms "platelet degranulation" (GO:0002576), "lipid transport" (GO:0006869) and "cellular protein metabolic process" (GO:0044267) (Figure 5.9, Supplement table S 5.3).

STRING analysis identified protein clusters associated with the significantly enriched GO terms "cholesterol metabolism", "PPAR signaling pathway" and "platelet activation" and the enriched KEGG pathway "complement and coagulation cascades" (Figure 5.10). Of note, some proteins are multifunctional and involved in many pathways. For instance, fibrinogen peptides (including fibrinogen α chain (FGA), fibrinogen β chain (FGB) and fibrinogen ɤ chain (FGG)) were associated with the KEGG pathway terms "complement and coagulation cascades" and "platelet activation". Similarly, apolipoprotein A1 and A2 and phospholipid transfer protein (PLTP) were associated with the KEGG pathway terms "cholesterol metabolism" and "PPAR signaling".

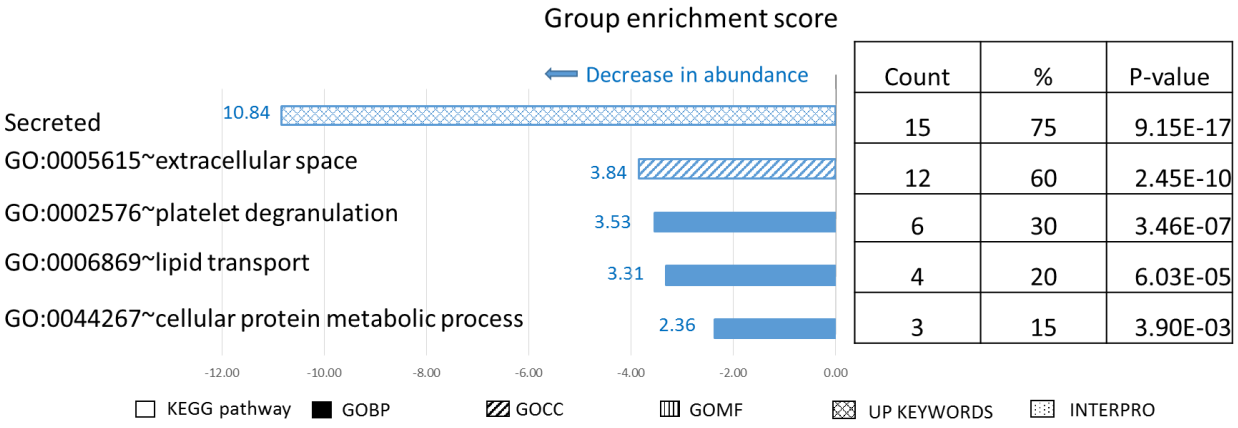

Count	%	P-value
15	75	9.15E-17
12	60	2.45E-10
6	30	3.46E-07
4	20	6.03E-05
3	15	3.90E-03

Figure 5.9 DAVID analysis of proteins that decreased in abundance in the proteome and secretome of DENV-2 infected Huh-7 cells.

Proteins that were significantly (P-value < 0.05) altered in amount by ≥ 1.5 fold in both the proteome and secretome of DENV-2 infected Huh-7 cells compared to mock infected cells were analysed using the DAVID database. The GO accession numbers/terms that were significantly enriched and the properties of the corresponding protein clusters are shown. The GES of protein clusters associated with significantly enriched GO terms are plotted as bar graphs (blue) with the corresponding GES score shown. The shading shows the type of GO term (GOBP, GOCC or GOMF), UP keywords, Interpro term or KEGG pathway. The number of proteins in each cluster (count), number of proteins associated with each GO term/total number of proteins in the dataset (%) and P-value for each of the annotation terms are listed in the table.

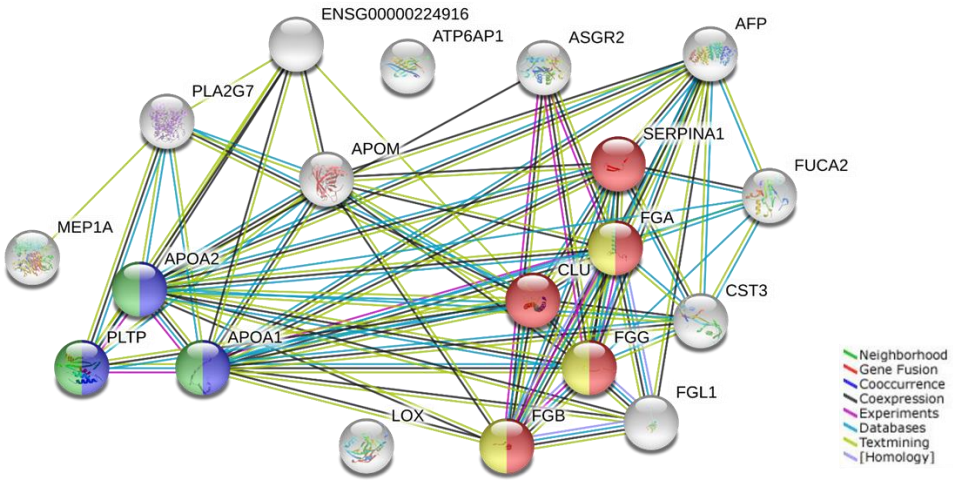

GO term/ pathway	Description	Count in gene set	FDR
hsa04610	Complement and coagulation cascades	5 of 78	3.09E-07
hsa04979	Cholesterol metabolism	3 of 48	1.80E-04
hsa03320	PPAR signaling pathway	3 of 72	3.80E-04
hsa04611	Platelet activation	3 of 123	1.30E-03

Figure 5.10 STRING analysis of proteins that decreased in abundance in both the proteome and secretome of DENV-2 infected cell

The STRING database was searched to analyse proteins that significantly ($p < 0.05$) decreased ≥ 1.5 fold in both the proteome and secretome in response to DENV-2 infection. Nodes representing proteins associated with the significantly enriched KEGG pathway terms "Complement and coagulation cascades", "Cholesterol metabolism", "PPAR signaling pathway" and "Platelet activation" are shaded in red, blue, green and yellow, respectively. The number of coloured nodes/ total proteins involved for each term and the FDR of each GO term are listed in the table.

5.5 Validation of the LC-MS/MS analysis

In order to validate the results of the proteomic analyses, a selection of viral and cellular proteins that were detected to change in abundance were analysed by Western blotting. The rationale for the selection of the proteins and the results of the validation are described below.

5.5.1 Viral proteins

Similar to the results presented in Chapter 4, DENV NS1 and NS4B were selected for validation in the cell lysates by Western blotting. As expected, the DENV-2 NS1 and NS4B proteins were detected in cell lysates from DENV-2 but not iDENV-2 nor mock infected Huh-7 cells (Figure 5.11). For the supernatants, DENV NS1 was also selected for validation. The results showed the presence of NS1 only in the supernatant from DENV-2 infected Huh-7 cells (Figure 5.11).

5.5.2 Host proteins

Based on the results of the bioinformatic analysis and a review of the literature, selected host proteins, that were associated with the KEGG pathway terms "complement and coagulation cascades" and "cholesterol metabolism", were selected for validation by Western blotting. All of the proteins significantly decreased ≥1.5 fold in DENV-2 infected Huh-7 cells and/or secretomes compared to mock infected cells. The rationale for selecting the specific proteins is as follows.

Proteins involved in complement and coagulation cascades

Proteins associated with "complement and coagulation" pathways were found to be the major group of proteins that were commonly dysregulated intracellularly and in the secretome from DENV infected Huh-7 cells. Mapping of the identified proteins on the KEGG "complement and coagulation" pathways showed that they were involved in a number of diverse processes in both the coagulation and complement cascades (Figure 5.12). Proteins associated with the complement and coagulation pathways have previously been found to play a role in DEN pathogenesis *in vivo* (Van Gorp *et al*, 2002; Chen, 2004;

Well *et al*, 2012; Conde *et al*, 2017). Therefore, it was decided to focus on this group of proteins to validate the proteomic analysis as follows.

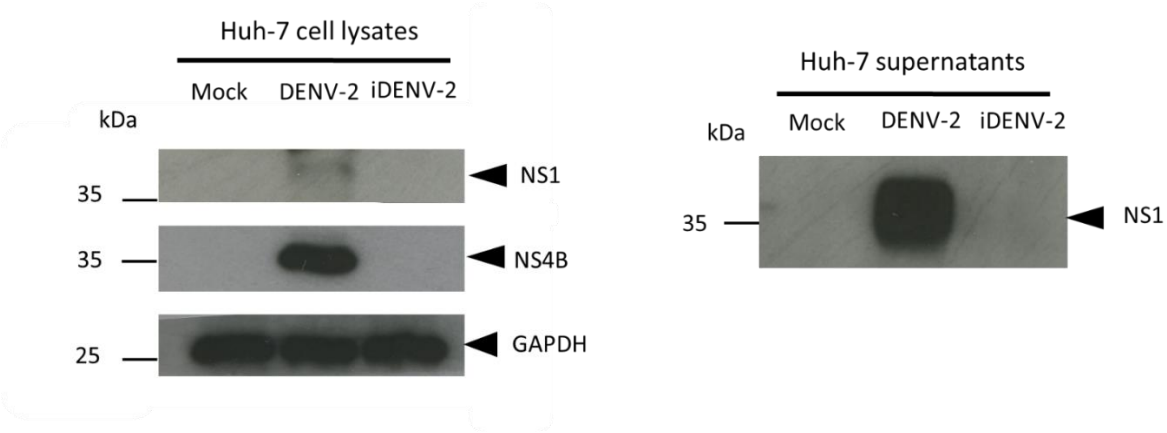

Figure 5.11 Detection of viral proteins in cell lysates and cell culture supernatants of DENV-2 infected Huh-7 cells.

Huh-7 cells were infected with DENV-2 or iDENV-2 at a MOI of 5 or mock infected, harvested at 30 hpi and collected as a total cell lysate and concentrated supernatants. Equal amounts of protein from cell lysates (10 µg) and equal volumes of the concentrated culture supernatants (5 µl) were loaded in each lane and the proteins separated by SDS-PAGE prior to Western blotting. Antibodies raised against the NS1, NS4B and GAPDH proteins were used to detect the respective proteins (expected positions arrowed). GAPDH was used as a loading control for cell lysates. Relevant molecular mass markers are shown in kDa.

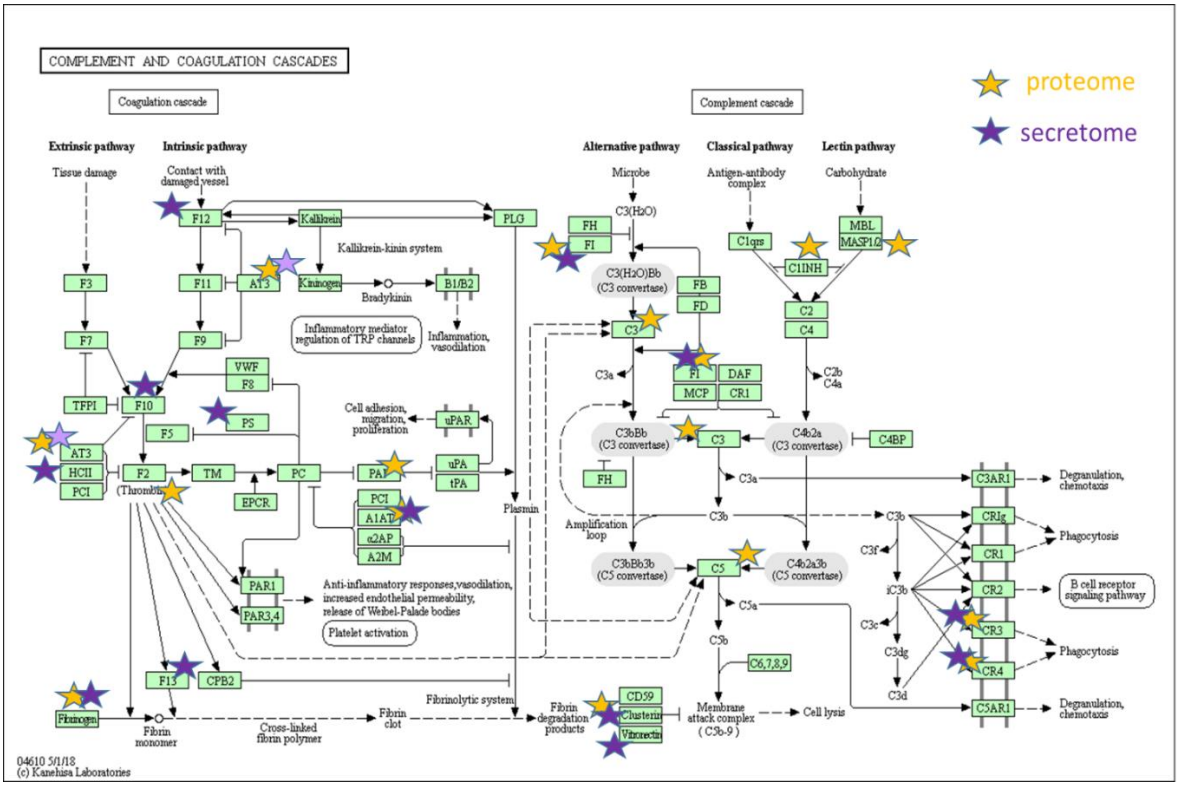

CD46 molecule(CD46), CD55 molecule (Cromer blood group)(CD55), CD59 molecule(CD59), alpha-2-macroglobulin(A2M), bradykinin receptor B1(BDKRB1), bradykinin receptor B2(BDKRB2), carboxypeptidase B2(CPB2), coagulation factor II, thrombin receptor(F2R), coagulation factor II, thrombin(F2), coagulation factor III, tissue factor(F3) ,coagulation factor IX(F9), coagulation factor V(F5), coagulation factor VII(F7), coagulation factor VIII(F8), coagulation factor X(F10), coagulation factor XI(F11), coagulation factor XII(F12), coagulation factor XIII A chain(F13A1), coagulation factor XIII B chain(F13B), complement C1q A chain(C1QA), complement C1q B chain(C1QB), complement C1q C chain(C1QC), complement C1r(C1R), complement C1s(C1S), complement C2(C2), complement C3(C3), complement C3a receptor 1(C3AR1), complement C3b/C4b receptor 1 (Knops blood group)(CR1), complement C3d receptor 2(CR2), complement C4A (Rodgers blood group)(C4A), complement C4B (Chido blood group)(C4B), complement C5(C5), complement C5a,receptor 1(C5AR1), complement C6(C6), complement C7(C7), complement C8 alpha chain(C8A), complement C8 beta chain(C8B), complement C8 gamma chain(C8G), complement C9(C9), complement component 4 binding protein alpha(C4BPA), complement component 4 binding protein beta(C4BPB), complement factor B(CFB), complement factor D(CFD), complement factor H(CFH), complement factor I(CFI), fibrinogen alpha chain(FGA), fibrinogen beta chain(FGB), fibrinogen gamma chain(FGG), kallikrein B1(KLKB1), kininogen 1(KNG1), mannan binding lectin serine peptidase 1(MASP1), mannan binding lectin serine peptidase 2(MASP2), mannose binding lectin 2(MBL2), plasminogen activator, tissue type(PLAT), plasminogen activator, urokinase receptor(PLAUR), plasminogen activator, urokinase(PLAU), plasminogen(PLG), protein C, inactivator of coagulation factors Va and VIIIa(PROC), protein S (alpha)(PROS1), serpin family A member 1(SERPINA1), serpin family A member 5(SERPINA5), serpin family C member 1(SERPINC1),serpin family D member 1(SERPIND1), serpin family E member 1(SERPINE1), serpin family F member 2(SERPINF2), serpin family G member 1(SERPING1), thrombomodulin(THBD), tissue factor pathway inhibitor(TFPI), von Willebrand factor(VWF)

Figure 5.12 Complement and coagulation cascade pathways.

Proteins that significantly decreased (≥1.5 fold) in DENV-2 infected Huh-7 cells and secretomes compared with mock infected cells are identified on the KEGG pathway "complement and coagulation cascades" (KEGG pathway term hsa04610). The yellow and purple stars indicate proteins that significantly decreased in cells and secretomes, respectively, in response to DENV-2 infection. Anti-thrombin III (SERPINC1), a protein which decreased, but not significantly, in DENV-2 infected cells, is indicated in faint purple (decreased 1.73 fold, P-value = 0.059).

5.5.2.1 5.6.2.1 Fibrinogen (FBG)

Fibrinogen (FBG) or coagulation factor I is the most important protein in the coagulation process. Furthermore, it also plays an important role as a liver acute phase protein and in platelet activation. The fibrinogen protein is composed of three fibrinopeptides: FGA, FGB and FGG. All fibrinopeptides were found to be significantly decreased (≥2 fold) in both DENV-2 infected Huh-7 cells and the associated secretomes compared with mock infected cells and did not change in amount in iDENV-2 infected cells. These results were validated by Western blotting analysis. For all fibrinopeptides there was a decrease in the band intensity in lysates from DENV-2 infected cells compared with mock infected cells (Figure 5.13). For the secretome samples, equal volumes of concentrated supernatants were analysed as there was no standard loading control. The results clearly showed a decrease in all fibrinopeptides in the secretomes of DENV-2 infected cells compared with mock infected cells.

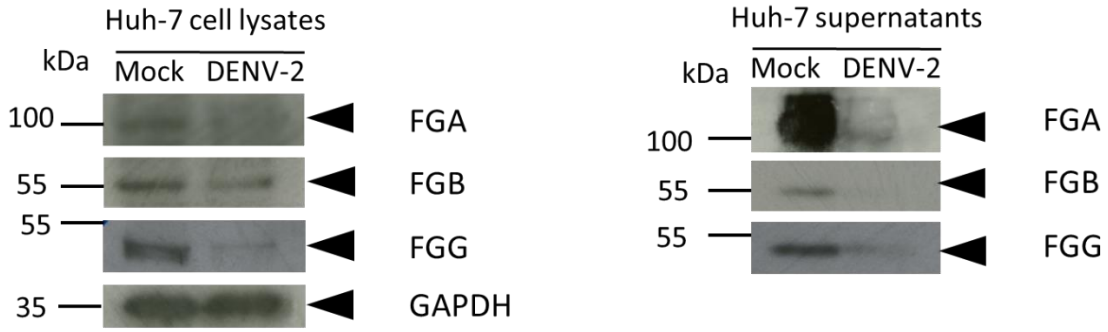

Figure 5.13 Analysis of fibrinopeptides in cell lysates and secretomes of DENV-2 infected Huh-7 cells.

Huh-7 cells were infected with DENV-2 at a MOI of 5 or mock infected, harvested at 30 hpi and collected as total lysates and concentrated supernatants. Twenty µg of protein from each cell lysate and 10 µl of the concentrated supernatants were loaded in each lane and the proteins separated by SDS-PAGE prior to Western blotting. Antibodies against FGA, FGB, FGG and GAPDH were used to detect the relevant proteins. GAPDH was used as loading control for cell lysates and the positions of relevant molecular mass markers are shown in kDa.

5.5.2.2 5.6.2.2 Alpha-1-antitrypsin (SERPINA1)

Alpha-1-antitrypsin (SERPINA1), encoded by the *SERPINA1* gene, is a multifunctional protein in the serpin family. SERPINA1, a highly abundant glycoprotein in plasma is synthesized mainly by the liver but also by cells in the lung (Kalsheker *et al*, 2002). It plays an important role in coagulation and like FBG, is one of the liver acute phase response proteins. In this study, SERPINA1 significantly decreased ≥2 fold and ≥ 1.5 fold in DENV-2 infected Huh-7 cells and secretomes respectively, compared with mock infected cells. These changes were confirmed by Western blotting (Figure 5.14A).

5.5.2.3 5.6.2.3 Antithrombin III (SERPINC1)

Antithrombin III (SERPINC1), encoded by the *SERPINC1* gene, is a glycopeptide in the serpin (serine protease inhibitor) superfamily. SERPINC1 significantly decreased > 1.5 fold in DENV-2 infected Huh-7 cells. Although the results from the LC-MS/MS analysis identified a non-significant decrease (1.73 fold decrease, P-value = 0.059) in amount in the secretomes of DENV-2 cells compared with mock infected cells, this protein was selected because it plays important roles in multiple steps in the coagulation pathways (as shown in Figure 5.12). SERPINC1 is also a liver acute phase response protein similar to FBG and SERPINA1. The results of the Western blotting analysis showed a clear decrease in the amount of the protein in cell lysates and secretomes from DENV-2 infected cells compared to mock infected cells (Figure 5.14B).

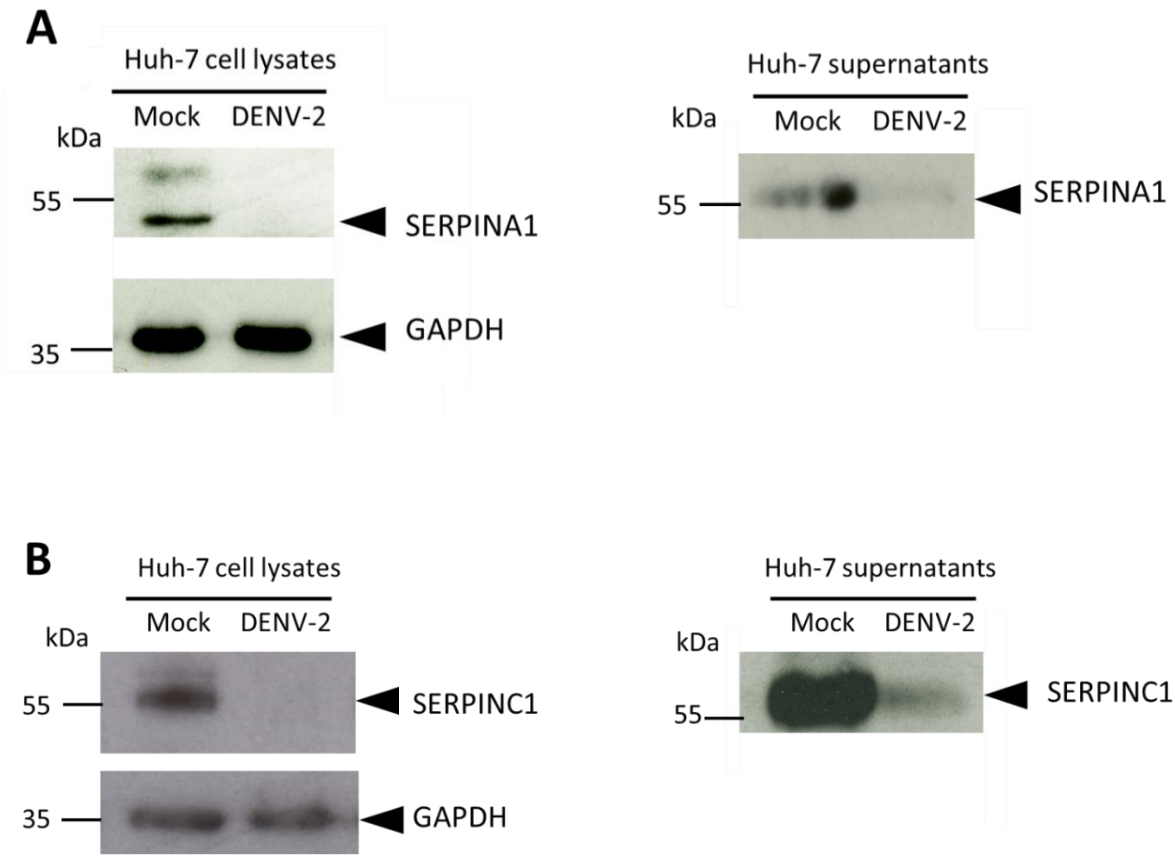

Figure 5.14 Analysis of SERPINA1 and SERPINC1 in cell lysates and secretomes of DENV-2 infected Huh-7 cells.

Huh-7 cells were infected with DENV-2 at a MOI of 5 or mock infected, harvested at 30 hpi and collected as total lysates and concentrated supernatants for Western blotting analysis for SERPINA1 **(A)** and SERPINC1 **(B)**. Equal amounts of protein in cell lysates (30 µg for SERPINA1 and 20 µg for SERPINC1) and 10 µl of concentrated supernatants were loaded in each lane and the proteins separated by SDS-PAGE prior to Western blotting. Antibodies against SERPINA1, SERPINC1 and GAPDH were used to detect the relevant proteins. GAPDH was used as loading control for cell lysates and the positions of relevant molecular mass markers are shown in kDa.

5.5.2.4 5.6.2.4 Clusterin (CLU)

Clusterin (CLU) or apolipoprotein J has many isoforms with different molecular weights. The mature form is composed of two subunits, the α- and β-chains, around 40 kDa in size. In the complement pathway this protein inhibits terminal complement complex formation. In this study, CLU was found to be significantly decreased (≥1.5 fold) in DENV-2 infected Huh-7 cells and secretomes compared with mock infected cells. However, Western blotting analysis only demonstrated a decrease in the CLU 40 kDa bands in cell lysates of DENV-2 infected Huh-7 cells (Figure 5.15A). CLU could not be detected in the corresponding secretome samples from either mock or DENV-2 infected cells (data not shown).

5.5.2.5 5.6.2.5 Vitronectin (VTN)

Vitronectin (VTN) is a multifunctional glycoprotein. Similar to CLU, VTN blocks membrane attack complex formation (MAC) at the end of the complement cascade to prevent cell lysis (Figure 5.12). In this study, VTN was not changed in abundance in cells in response to DENV-2 infection but significantly decreased in abundance (≥1.5 fold) in the secretome of DENV-2 infected Huh-7 cells compared with mock infected cells. Western blotting analysis demonstrated a decrease in VTN amount in the supernatants of DENV-2 cells compared with mock infected cells (Figure 5.15B).

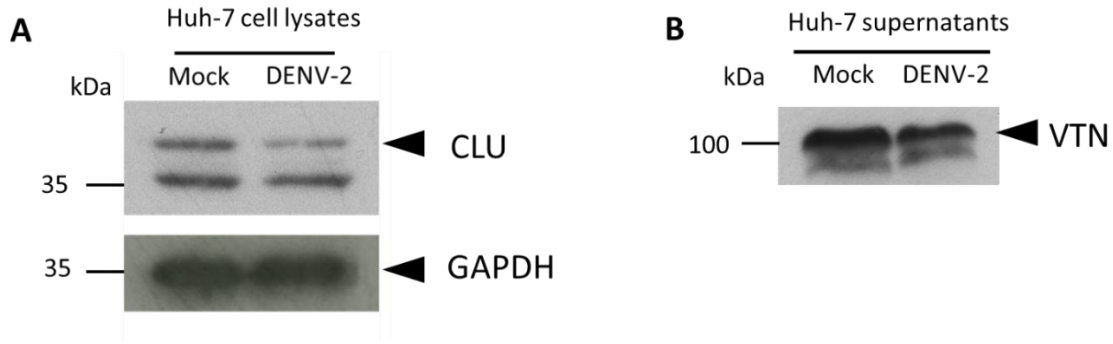

Figure 5.15 Analysis of CLU and VTN by Western blotting.

Huh-7 cells were infected with DENV-2 at a MOI of 5 or mock infected, harvested at 30 hpi and collected as total lysates and concentrated supernatants for Western blotting analysis for CLU **(A)** and VTN **(B)**. Equal amounts of protein in either cell lysates (20 µg for CLU) and 10 µl of concentrated supernatants (for VTN) were loaded in each lane and the proteins separated by SDS-PAGE prior to Western blotting. Antibodies against CLU, VTN and GAPDH were used to detect the relevant proteins. GAPDH was used as a loading control for cell lysates and the positions of relevant molecular mass markers are shown in kDa.

Analysis of proteins involved in cholesterol metabolism

Apolipoproteins and proteins involved in "cholesterol metabolism" were significantly altered in Huh-7 cells and the associated secretomes in response to DENV-2 infection. Mapping of the identified proteins on the KEGG "cholesterol metabolism" pathways showed that they were particularly involved in lipoprotein production/formation (Figure 5.16). Additionally, DENV infection is well known to modulate host lipid metabolism (Fischl and Bartenschlager, 2011). Thus, a selection of proteins that were identified to be altered in response to DENV-2 infection and involved in "cholesterol metabolism" were selected for validation.

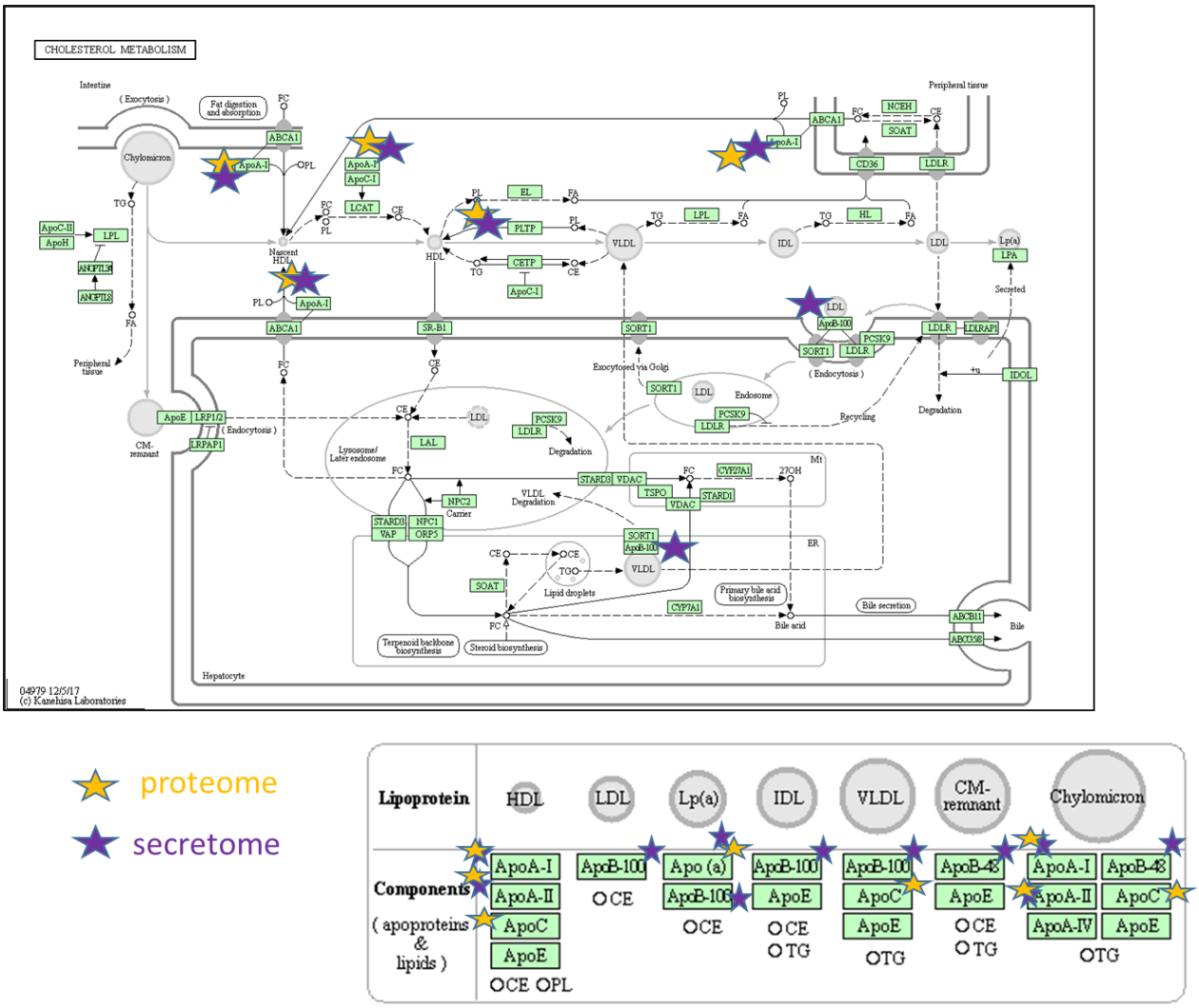

Figure 5.16 Cholesterol metabolism pathways

Proteins that significantly decreased (≥1.5 fold) in DENV-2 infected Huh-7 cells and secretomes compared with mock infected cells are identified on the KEGG pathways "cholesterol metabolism" (KEGG pathway term hsa04979). The yellow and purple stars indicate proteins that significantly decreased in cells and secretomes, respectively in response to DENV-2 infection.

5.6.2.6 Apolipoprotein AI (APOA1)

Apolipoprotein AI (APOA1), encoded by the *APOA1* gene, is an important component of the high-density lipoprotein complex in plasma. Thus, it plays an important role in lipid metabolism and was proposed as a biomarker for many diseases including DEN (Manchala *et al,* 2017).

APOA1 was identified to be significantly decreased (≥2 fold) in both DENV-2 infected Huh-7 cells and secretomes compared to mock infected cells by LC-MS/MS analysis. Although Western blotting analysis successfully detected a recombinant APOA1 down to a level of 50 ng, APOAI was not detectable in cell lysates from mock or DENV-2 infected cells (Figure 5.17A). Whereas a decrease in APOA1 abundance in the supernatants from Huh-7 infected cells compared to mock infected cells was detected by Western blotting analysis (Figure 5.17B).

In addition to APOA1, validation of the amounts of the APOC2 protein was attempted. However, the protein was not detectable in either cell lysates or the corresponding secretomes (data not shown). As for some of the proteins analysed this may reflect the sensitivity of LC-MS/MS in comparison to the Western blotting /antibodies used to detect these proteins.

List of Supplementary Tables

Table S5.1 DAVID analysis of the cellular proteins that were altered in abundance in DENV-2 infected Huh-7 cells compared to mock infected cells.

Table S5.2 DAVID analysis of the proteins that were altered in abundance in secretome of DENV-2 infected Huh-7 cells compared to mock infected cells.

Table S5.3 DAVID analysis of proteins that significantly decreased ≥ 1.5 fold in both the proteome and secretome of DENV-2 infected cells compared with mock infected cells.

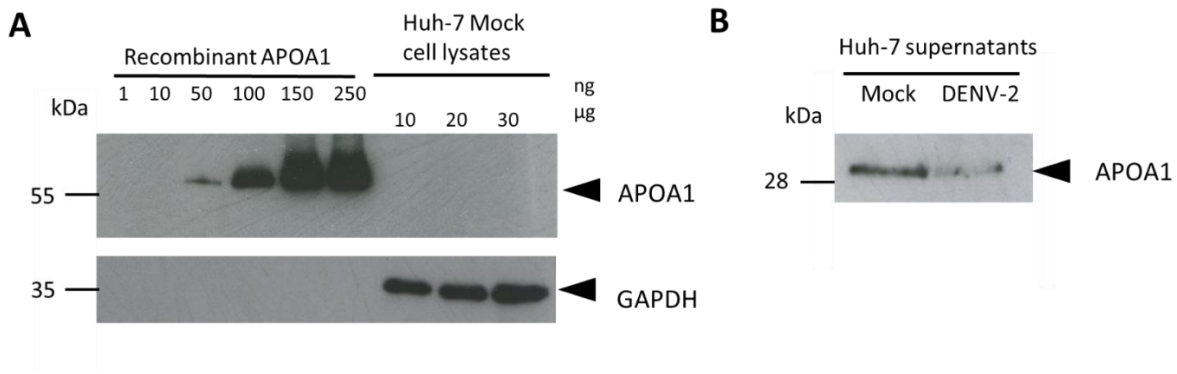

Figure 5.17 Analysis of APOA1 in cell lysates and secretomes of DENV-2 infected Huh-7 cells.

Huh-7 cells were infected with DENV-2 at a MOI of 5 or mock infected, harvested at 30 hpi and collected as total lysates and concentrated supernatants. **(A)** Recombinant APOA1 protein ranging from 1-250 ng and mock infected Huh-7 cell lysate containing 10 - 30 µg of protein was analysed by Western blotting. **(B)** Ten µl of concentrated supernatants from DENV-2 and mock infected cells was used for Western blotting. Antibodies against APOA1 and GAPDH were used to detect the relevant proteins. GAPDH was used as loading control for cell lysates and the positions of relevant molecular mass markers are shown in kDa.

5.6 **Discussion**

This study reports for the first time an integrated analysis of the Huh-7 cellular proteome and secretome in response to DENV-2 infection. A total of 268 (121 up- and /147 down-regulated) cellular proteins and 102 (27 up- and 75 down-regulated) secreted host proteins were significantly dysregulated (≥1.5 fold in amount) in DENV-2 infected Huh-7 cells compared with mock infected cells, respectively. Bioinformatic analysis of proteins that increased in the cellular proteome during infection, revealed an enrichment of proteins associated with the GO terms "negative regulation of gene expression" and "negative regulation of translation", whilst for proteins that decreased during infection, proteins associated with the terms "lipid metabolic process", "complement and coagulation cascades", "innate immunity/acute phase response" and "mineral absorption" were enriched. By contrast, during infection, the secretome was enriched in proteins that decreased in amount and were associated with the GO terms "lipid metabolic process", "complement and coagulation cascades", "innate immunity" and "post-translational protein modification". As the major change in both the proteome and secretome was the proteins that decreased in response to infection and many of these proteins participated in biological pathways that appeared relevant to DEN pathogenesis, they are the focus of this discussion.

Correlation of protein alterations in the cellular proteome and secretome.

Although liver cell models are widely used for DENV studies, an integrated analysis of the changes that occur in the proteome and secretome of any liver cell line in response to DENV infection has never been done. One fourth of cellular proteins (1469 of 5706) were detected in secretome, presumably as they were secreted (Figure 5.3). This reflects the role of hepatocytes in secretory and plasma protein production (Kuscuoglu *et al*., 2018).

Proteins that were commonly dysregulated in the proteome and secretome changed in abundance in the same direction implying that dysregulation of these proteins in the cellular proteome affected their abundance in the secretome. The proteins highlighted in this study that were decreased in both the proteome and secretome of Huh-7 cells in response to DENV infection are involved in the pathways of "complement and coagulation

cascade" and "cholesterol metabolism", both of which are important in DEN pathogenesis. The results suggest that DENV infection leads to a decrease in cellular complement and coagulation proteins as well as lipoproteins, which in turn decreases the amounts of these proteins secreted from hepatocytes.

However, the changes revealed in the proteome cannot explain all changes detected in the secretome. Amongst the 104 proteins that were significantly altered (≥1.5 fold) in the secretome of DENV-2 infected cells compared with mock infected cells, 67 were also found in cell lysates. Of these, only 21 proteins were significantly changed in amount, both intracellularly and in the secretomes, whilst the alterations in the amounts of the majority of the proteins (46) in the secretome cannot be explained by the change in the cellular protein level. These proteins may be mainly found as secreted proteins and are not stored or function intracellularly. Further studies on the effect of DENV infection on protein secretory pathways are required to fully answer this question.

Comparison with previous studies.

The proteins that were significantly altered in the cellular proteome in this study were compared with previous proteomic studies (listed in section 1.6.1 and also in the introduction of this chapter) that analysed DENV-2 infected liver cell lines (both Huh-7 and HepG2) using a systematic search by gene name (Figure 5.18 and Table 5.7). The comparison also included two unpublished studies done in the laboratory in which the cellular proteomes of DENV-2 (at the high MOI) and mock infected Huh-7 cells were analysed by SILAC and TMT labelling and LC-MS/MS by Dr. Han-Chen Chiu and Dr. Amjad Yousuf, respectively (Chiu, 2014; Yousuf, 2016). The only previous secretome analysis of DENV infected liver cells described only the presence or absence of the secreted proteins in the secretome and did not perform statistical analysis (Higa *et al.*, 2008). Thus, this comparison was described in the text.

Commonalities between the proteins identified to alter in response to DENV infection between the studies described above are summarised and compared in Figure 5.18 and Table 5.7. Overall, the results of this study were more comparable with the studies done in the laboratory (Chiu, 2014; Yousuf, 2016). The difference in the results across studies might be due to the use of different cell lines (Huh-7 or HepG2), virus strains,

infection conditions, infection rate and proteomic analysis techniques used for the studies. The results from Pattanakitsakul and coworkers identified only two proteins in common with other studies, this may be due to the analysis of DENV-2 infected HepG2 cells (while other studies used Huh-7 cells) or more likely the limitations of 2D SDS-PAGE based proteomic approach used for the study (Pattanakitsakul *et al*., 2007). There were three cellular proteins that were identified to increase in response to infection in the study of Pando-Robles *et. al*. (Pando-Robles *et al*., 2014), but decreased in this study; heme oxygenase (decycling) 1 (HMOX1), fibronectin 1 (FN1) and RNA binding motif protein 3 (RBM3) (Table 5.7). HMOX1 was also identified to decrease significantly in the proteome of DENV infected Huh-7 cells compared to mock infected cells in the study of Dr. Chiu and FN1 was significantly decreased in both previous proteomic studies in the laboratory (Chiu, 2014; Yousuf, 2016), whereas RBM3 was only identified to significantly decreased in this study. Although the study from Pando-Robles *et al*., also used a DENV-2 infected Huh-7 cell model, the low infection rate (13.96%) and shorter time of infection (24 hpi) might explain the difference in results (Pando-Robles *et al*., 2014). Interestingly, among the 146 proteins identified to significantly decrease (≥1.5 fold) in proteome of DENV infected cells in this study, 43 proteins were also reported to decrease in previous studies. This set of proteins included proteins involved in complement and coagulations including; FGA, FGB, FGG, CLU, SERPINA1, SERPINE1 and C3 as well as other proteins of interest including APOA2, CD81, HMOX1 and FN1.

A number of acute phase proteins (APPs), including FBG, SERPINA1, and transferrin (TS), were identified to decrease in the proteome of DENV infected liver cells in this study and previous studies (Table 5.7). Furthermore, this study also identified decreases in the cellular levels of SERPINC1, haptoglobin (HP) and ceruloplasmin (CP) and a decrease in both the cellular and secreted levels of prothrombin (F2) in response to DENV infection. APPs can be divided into positive and negative APPs which increase and decrease, respectively, in the blood in response to infection/inflammation, APPs are reviewed in detail in section 7.1. The decrease in the negative APPs SERPINC1 and TF was predictable. However, the decrease in positive APP (FBG, SERPINA1, F2, HP, and CP) levels, both in the cellular proteome and secretome, was an interesting finding, as these proteins are typically produced in greater amounts by the liver, in response to various

infections. Further studies surrounding the mechanism by which DENV infection modulates this important host response is required to determine if the effect may have an impact on pathogenesis.

This study: decreased	(147)									
This study: increased	(121)	0								
Yousuf 2016: decreased	(176)	**27**	0							
Yousuf 2016: increased	(52)	0	1	0						
Chiu 2014: increased	(448)	0	**16**	2	2					
Chiu 2014: decreased	(176)	**24**	3	**16**	0	0				
Pattanasakul 2007: increased	(10)	0	1	0	0	1	0			
Pattanasakul 2007: decreased	(7)	0	0	0	0	0	0	0		
Pando-Robles 2014: increased	(64)	3	1	1	0	**9**	**9**	0	0	
Pando-Robles 2014: decreased	(91)	0	2	0	0	**19**	2	0	0	0
		This study: decreased	This study: increased	Yousuf 2016: decreased	Yousuf 2016: increased	Chiu 2014: increased	Chiu 2014: decreased	Pattanasakul 2007: increased	Pattanasakul 2007: decreased	Pando-Robles 2014: increased
		(147)	(121)	(176)	(52)	(448)	(176)	(10)	(7)	(91)

Figure 5.18 A comparison of the liver cell proteins identified to alter in amount in response to DENV-2 infection in this study and previous proteome studies.

The proteins that significantly (P-value < 0.05) increased and decreased (≥1.5 fold) in cell lysates from this study were searched using the gene names against the corresponding gene names of proteins identified to change in previous proteomic studies of DENV-2 infected liver cells. The numbers of proteins that were commonly detected between these studies are shown and the total number of differentially expressed proteins that were reported to be significantly altered in each study are listed in brackets.

Table 5.7 A list of the liver cell proteins identified to alter in amount in response to DENV-2 infection in this study and previous proteomic studies.

Increased in this study		Decreased in this study	
Protein	Description	Protein	Description
Increased in Pando-Robles *et al*., 2014			
EEF1A1	Elongation factor 1-alpha	HMOX1	Heme oxygenase
		FN1	Fibronectin 1, isoform
		RBM3	RNA binding motif protein 3
Decreased in Pando-Robles *et al*., 2014			
YBX1	Nuclease-sensitive element-binding protein 1	None	
HSPB1	Heat shock protein beta 1		
Increased in Yousuf, 2016			
ASNS	Asparagine synthetase (glutamine-hydrolyzing)	None	
Decreased in Yousuf, 2016			
None		MEP1A	Metalloendopeptidase
		AGT	Angiotensinogen variant
		SCD	Stearoyl-CoA desaturase variant
		CST3	Cystatin
		AMBP	Protein AMBP
		AFP	Alpha-fetoprotein
		SERPINA1	alpha-1-antitrypsin
		FGA	Fibrinogen alpha chain
		GOLM1	Golgi membrane protein 1
		C3	Complement C3
		FGB	Fibrinogen beta chain
		TF	Transferrin variant
		FN1	Fibronectin 1
		FGFR3	Fibroblast growth factor receptor 3 isoform A
		FGFR4	Fibroblast growth factor receptor 4 variant
		ASGR2	Asialoglycoprotein receptor 2
		NUSAP1	Nucleolar and spindle-associated protein 1
		SDC2	Syndecan-2
		SDC1	Syndecan-1
		COL5A2	Collagen alpha-2(V) chain
		APP	Amyloid beta A4 protein
		SERF2	Small EDRK-rich factor 2
		TOR4A	Torsin-4A
		FUCA2	Plasma alpha-L-fucosidase
		HECTD1	E3 ubiquitin-protein ligase HECTD1

		MAN1A1	Mannosyl-oligosaccharide 1,2-alpha-mannosidase IA
		NID1	Nidogen-1
Increased in Chiu, 2014			
TRIM32	E3 ubiquitin-protein ligase TRIM32	None	
PFN2	Profilin-2		
ENO1	Enolase 1		
TRIP13	Pachytene checkpoint protein 2 homolog		
ACTN1	Alpha-actinin-1		
ASNS	Asparagine synthetase		
IGF2BP1	Insulin-like growth factor 2 mRNA-binding protein 3		
BRAT1	BRCA1-associated ATM activator 1		
PPCS	Phosphopantothenate--cysteine ligase		
EEF1A1	Elongation factor 1-alpha		
EIF2B4	Translation initiation factor eIF-2B subunit delta		
EDC3	Enhancer of mRNA-decapping protein 3		
DDX6	Probable ATP-dependent RNA helicase DDX6		
IGF2BP2	Insulin-like growth factor 2 mRNA-binding protein 3		
GIGYF2	PERQ amino acid-rich with GYF domain-containing protein 2		
ATXN2L	Ataxin-2-like protein		
Decreased in Chiu, 2014			
METTL9	Methyltransferase-like protein 9	AGT	Angiotensinogen variant (Fragment)
TSPAN13	Tetraspanin-13	ITM2C	Integral membrane protein 2C, isoform
EPPK1	Epiplakin	SCD	Stearoyl-CoA desaturase variant
		ITM2B	Integral membrane protein 2B
		AFP	Asialoglycoprotein receptor 2
		FGA	Fibrinogen alpha chain
		GOLM1	Golgi membrane protein 1
		FGB	Fibrinogen beta chain
		APOA2	Apolipoprotein A-II
		FGG	Fibrinogen gamma chain
		HMOX1	Heme oxygenase (decycling) 1
		CDH17	Cadherin 17, LI cadherin
		FN1	Fibronectin 1, isoform
		APLP2	Amyloid-like protein 2
		NUCB1	Nucleobindin 1 (NUCB1)
		APP	Amyloid beta A4 protein

		CLU	Clusterin
		TOR4A	Torsin-4A
		SERPINE1	Plasminogen activator inhibitor type 1
		HNF4A	Hepatocyte nuclear factor 4
		GLTSCR2	PreS1 binding protein
		CD81	Tetraspanin
		RNF149	E3 ubiquitin-protein ligase RNF149
		LRP1	Prolow-density lipoprotein receptor-related protein 1
Increased in Pattanasakul *et al*., 2007			
DDX17	DEAD-box protein p72	None	
Decreased in Pattanasakul *et al*., 2007			
None		None	

The results of the secretome analysis were compared with a study analyzing the secretome of DENV-2 infected HepG2 cells, which identified 65 (of a total of 107) proteins previously reported (Higa *et al*., 2008). However, amongst the 65 proteins, only 5 proteins were significantly altered (≥1.5 fold) in this study; only nucleophosmin (NPM1) was increased while the four proteins; proprotein convertase subtilisin/kexin type 9 (PCSK9), calsyntenin-1 (CLSTN1), fibulin-1 (FBLN1) and ALB were decreased.

ENO1 was previously identified to increase in the secretome of DENV-2 infected HepG2 cells without either a change in cellular protein or mRNA levels (Higa *et al.,* 2014). ENO1 was also found to increase in the plasma of DEN patients compared to healthy patients (Higa *et al*., 2014). By contrast, in this study and the study of Chiu (Chiu, 2014) a significant increase (≥ 1.5 fold) in the cellular level of ENO1 was identified, in response to DENV infection of Huh-7 cells, but the level in the secretome remained unchanged. This difference may be due to a cell type specific response or the difference in the study protocol, as discussed in detail in Chapter 3.

FBLN1, a protein believed to play a role in thrombosis (Argraves *et al*., 2009) was also found to be significantly decreased in both the proteome and secretome of DENV infected cells compared with mock infected cells. FBLN1 was previously detected in the secretome of both DENV and mock infected HepG2 cells, although the relative levels were not quantitated (Higa *et al.*, 2008). FBLN1 can bind with fibronectin and FBG and play a role in extracellular matrix (ECM) formation and clot formation respectively (Argraves *et al*., 2009). Furthermore, binding of FBLN1 with fibrinogen can facilitate platelet adhesion (Godyna *et al*., 1996).

Tissue factor pathway inhibitor (TFPI), a major anti-coagulant, was identified only in the secretome of DENV infected HepG2 cells but not in those of mock cells in a previous study (Caruso *et al*., 2016). Although this protein significantly decreased (≥1.5 fold) in the cellular proteome, it was non-significantly decreased >1.3 fold in the secretome of DENV infected Huh-7 cells in this study. The change in the cellular concentration may not have been sufficient to cause a significant decrease in TFPI in the secretome. The difference in the methods used for secretome preparation may also explain this result, as the study of Caruso *et. al*., focussed on secreted proteins that had been subject to proteolysis.

The results of this study were also compared with other proteomic studies using various DENV infected cell lines. The similarities and differences in cellular proteins commonly identified and a major focus of previous proteomic studies are highlighted below.

HSPA5 has commonly been identified to increase in response to DENV infection in many studies and was also identified to increase >1.3 fold in DENV-2 infected Huh-7 cells but not in the associated secretome in this study. The alteration in HSPA5 amounts was similar to the results found after proteomic analysis of DENV-2 infected HEK293T cells, as described in Chapter 4. The details of HSPA5 and DENV infection were reviewed and discussed in Chapter 4.

A number of translation elongation factors have been reported to be dysregulated in DENV infection in many studies using various cell lines. Elongation factor 1-alpha (EEF1A1) is a protein chaperone and translation factor and has been shown to be recruited as a cofactor for RNA virus replication, including DENV (Li *et al*, 2013). EEF1A1 was found to significantly increased in the cellular proteome, in response to DENV infection, in this study and two previous studies (Pando-Robles *et al.*, 2014; Chiu, 2014). However, EEF1A1 was reported to decrease in DENV infected endothelial cells (Kanlaya *et al*., 2010) which might be due to a cell-specific response to infection. Apart from EEF1A1, significant increases in translation initiation factor eIF-2B subunit delta (EIF2B4) and eukaryotic translation initiation factor 4E nuclear import factor 1(EIF4ENIF1) ($\geq$ 1.5 and $\geq$ 1.3 fold, respectively) were also detected in the proteome of DENV infected Huh-7 cells. Proteomic studies have identified an increase in elongation factor tu (EF-tu) in DENV infected HepG2 cells (Pattanakitsakul *et al.*, 2007) and a decrease in elongation factor 2 (EF2) in DENV infected endothelial cells (Kanlaya *et al*., 2009; Kanlaya *et al*., 2010). Both EF-tu and EF2 were detected in this study but did not change in amount in response to infection. A recent study also reported changes (both increased and decreased) in a number of additional proteins involved in translation elongation (including EIF3E, EIF3J, EIF4A2, EIF5, EIF4EBP2, EEF1B2, EEF2K and TSFM) in DENV infected K562 cells (Miao *et al.*, 2019); however, none of these proteins were detected in this study. The role of translation elongation factors in DENV replication requires further investigation.

Other host proteins that were only identified to be dysregulated in response to DENV infection in this study and worthy of mention include, alpha-fetoprotein (AFP) and cadherin 17 or LI cadherin (CDH17). AFP was significantly decreased in both the proteome and secretome of DENV infected cells, whilst CDH17 was decreased in the proteome but increased in the secretome in response to DENV-2 infection (Table 5.6). Both AFP and CDH17 were extensively studied in other disease conditions but have never been linked with DEN. Both proteins are used clinically as tumor markers for hepatocellular carcinoma and gastric cancer, respectively. AFP was also proposed as a marker of acute liver injury (Schiodt *et al*., 2006). Increased levels of AFP, related to hepatic regeneration have been associated with a favorable outcome in patients with acute liver failure (Schiodt *et al.*, 2006). However, as Huh-7 cells are a cancer derived cell line, the results obtained with these two tumor markers should be used with caution.

Interestingly, alpha subunit of metalloendopeptidase meprin A (MEP1A) significantly decreased ≥1.5 fold in both the proteome and secretome in response to DENV-2 infection. Moreover, a number of proteins associated with the GO term "metal-binding/metallothionein" were significantly decreased in the proteome, including many forms of metallothionein (MT1G, MT1F, MT1X, MT1M, MT1E, MT2A) and HMOX1 (Table 5.4, Figure 5.5 and 5.6B). However, only MEP1A was found to be decreased in the secretome. Compared with previous proteomic studies using DENV infected liver cells, changes in level of metallothionein proteins has never been reported and there is inconsistency in reports describing the cellular level of HMOX1; an increase was identified in the study of Pando-Robles *et al*. (Pando-Robles *et al*., 2014), whilst HMOX1 was reported to decreased in the study of Chiu (Chiu, 2014) and this study (Table 5.7). A decrease in cellular MEP1A was also identified in the study of Yousuf (Yousuf, 2016). In contrast, the mRNA transcript levels of HMOX1 and multiple proteins in metallothionein group (MT1A, MT2A, MT1E, MT1F, MT1G, MT1H and MT1X) but not MEP1A were reported to be increased as a component of the anti-oxidant response to DENV-2 infection in dendritic cells (Olagnier *et al*, 2014). Moreover, overexpression of HMOX1 was found to inhibit DENV replication in Huh-7 cells (Tseng *et al*, 2016). Secreted merpins are important extracellular proteolytic enzymes that regulate the levels of inflammatory cytokines and ECM remodeling, MEP1A is responsible for cleavage of IL-6, IL-6 receptor

(IL6R) and thymosin-β4 as well as collagen proteins type 1 (Arnold *et al*, 2017). Dysregulation of MEP1A secretion may therefore affect host immune responses. So far, MEP1A has never be linked with DENV or any other viral infection. Thus, validation and further studies regarding the role of MEP1A in DENV pathogenesis are required.

Pathway of complement and coagulation cascades

Dysregulation of the coagulation system, both in the levels of coagulation factors (pro-clot formation effect) and proteins inhibiting coagulation (anti-clot formation effect/fibrinolysis), has been described as playing a key role in DEN pathogenesis (Mairuhu *et al.,* 2003). Activation of the complement system has been widely studied as a major contributing factor to the pathogenesis of plasma leakage and shock (reviewed in Conde *et al*., 2017). Furthermore, both complements and coagulation proteins (eg. thrombin, plasmin, C1q, C3, C4 and C5) can regulate platelet function (Peerschke *et al*, 2009). The liver is the key organ for protein synthesis, including complement and coagulation proteins and the alteration of these proteins in the sera of DEN patients has been previously reported (discussed in detail in Chapter 6). Thus, the dysregulation of these proteins in the cellular proteomes and secretomes of DENV-2 infected hepatocytes was expected. However, so far, previous DENV proteomic studies using liver cell models (summarised in Table 1.2) have not focused on investigating any alterations in the levels of proteins involved in complement and coagulation cascades. The complement and coagulation proteins that decreased in both proteome and secretome and/or were previously reported to be dysregulated in clinical specimens from DENV patient were therefore selected for validation and further study. The selected complement and coagulation proteins included FBG, SERPINA1, SERPINC1, CLU and VTN.

Decreased levels of FBG in the plasma of DENV infected patients has been previously documented in clinical studies and found to be associated with disease severity (Will *et al*., 2002). The significant decrease in the cellular level of FBGs identified in this study, are consistent with previous proteomic studies of DENV infected Huh-7 cells, which identified either decreases in all FBGs (Chiu, 2014) or decreases in FGA and FGG (Yousuf, 2016). Decreased levels of FBG in the secretome of DENV infected cells has never been

reported. Apart from its major role in clot formation, FBG is also involved in wound healing and platelet degranulation.

Similar to FGB, SERPINA1 and SERPINC1 were selected for validation as they play important roles in the coagulation system and are liver APPs that are regulated by acute inflammation/infection. SERPINA1, a protease inhibitor, inhibits plasmin, thrombin and plasminogen activator. In the coagulation system, there are three main anticoagulant pathways; the protein C system, antithrombin (SERPINC1) and TFPI (de Azeredo *et al.,* 2015). SERPINC1 is important in regulating the balance of coagulation. There is limited *in vitro* information about changes that may occur in the levels of these two proteins in DENV infection. However a yeast two-hybrid study has identified an interaction between SERPINC1 and DENV NS3 (Silva *et al*., 2019). Similarly, an interaction between SERPINA1 and the DENV-2 E protein was identified using affinity purification followed by MS analysis (Huerta *et al*., 2016).

Both CLU and VTN inhibit membrane attack complex (MAC), resulting in the prevention of cell lysis in the final stage of the complement pathway. Decreases in both CLU and VTN in the secretome of DENV infected cells in this study might result in cell lysis due to stimulation of the complement system. CLU was found to interact with both the DENV-2 C and prM proteins in an *in vitro* yeast two-hybrid experiment (Folly *et al*., 2011). Furthermore, an interaction between DENV NS1 and CLU in the plasma of DEN patients was also detected by co-IP followed by MS (Kurosu *et al*., 2007). Kurosu *et al*. proposed that the clearance of NS1-CLU complexes from plasma by the host immune response may cause a decrease in CLU levels in DENV patients (Kurosu *et al*., 2007); however, decreased amounts of CLU in clinical specimens have never been reported before. The decrease in CLU in both the proteome and secretome of DENV-2 infected Huh-7 cells identified in this study implies that a decrease in cellular levels results in a decrease in CLU secretion from hepatocytes which may affect levels in plasma. Furthermore, a significant decrease in CLU in the proteome of DENV-2 infected Huh-7 cells was also detected in another study (Chiu, 2014). VTN was proposed as biomarker for diagnosis and to predict DEN disease severity of DEN in a previous serum proteomic study that used label free MS/MS (Poole-Smith *et al*., 2014). There was an increase in VTN in

all forms of DEN compared with healthy controls and VTN levels decreased in more severe DEN cases compared with DF (Poole-Smith *et al*., 2014). An interaction between VTN and NS1 was previously detected using a yeast two-hybrid system and a NS1–VTN complex was also identified in plasma from DEN patients (Conde *et al*., 2016). To date a change in the cellular/secretome level of VTN has never been reported and the cellular mechanisms involved in the dysregulation of VTN in DEN patienst is still unknown.

Pathway of cholesterol metabolism

Flaviviruses, including DENV, modulate host cell lipid metabolism to facilitate viral entry, replication complex formation, viral assembly, virion secretion and control of the IFN response (Osuna-Ramos *et al*., 2018). The liver is the key organ for apolipoprotein and lipoprotein production (Feingold KR and Grunfeld, 2000); thus, the alterations in proteins involved in cholesterol/lipid metabolism in DENV infected Huh-7 cells identified in this study were expected.

APOA1, synthesised by the liver and intestine, functions in lipid metabolism as a lipid transporter and the major protein component of HDL. Moreover, it has anti-inflammatory effects (Vuilleumier *et al*., 2013). So far, no study has identified a change in apolipoprotein amounts in DENV infected cells. The decrease in both cellular and secreted APOA1 in response to DENV infection identified in this study implies that the decrease in secreted APOA1 is due to a decrease at the cellular level. The decrease in APOA1 could not be validated, although a recombinant APOA1 protein could be detected down to a level of 50 ng. Therefore it appeared that the detection of APOAI by LC-MS/MS analysis was more sensitive than the Western blot detection system used in this study. As APOA1 is a secretory protein mainly synthesised and secreted from hepatocytes, it may be present at a very low level in liver cells whilst being enriched in the secretome. A previous study using HepG2 cells found that replication of hepatitis virus B (HBV) resulted in a decrease in both the protein and mRNA levels of APOA1 (Wang *et al.*, 2016). High-throughput yeast two-hybrid assay analysis revealed an interaction between APOA1 and the DENV NS2A protein (Khadka *et al*., 2011). Moreover, pre-incubating U937 cells with supernatants derived from HEK293 cells transfected with an APOA1 expression plasmid resulted in an increase in DENV production, in a dose dependent manner, suggesting that APOA1 could

promote DENV infection in cell experiments (Li *et al*., 2013). The decrease in the cellular levels and secretion of APOA1 found in this study may be a host cell response to suppress DENV replication.

In conclusion, this study identified novel alterations in the proteome and secretome of Huh-7 cells in response to DENV infection, as well as changes in the levels of proteins that have previously been reported. An integrated analysis of the proteome and secretome datasets was done, which revealed dysregulation of specific proteins involved in "complement and coagulation cascade" and "cholesterol metabolism" at the cellular level leading to alterations in the amounts of these proteins in the secretome. The proteomic data was validated for representative proteins associated with these biological pathways, which have relevance to DEN pathogenesis.

CHAPTER 6. HIGH-THROUGHPUT PROTEOMIC ANALYSIS OF SERUM FROM DENV INFECTED INDIVIDUALS

6.1 Introduction

A major challenge in the diagnosis of DEN is the lack of diagnostic markers in the late phase of the disease (when there is no antigenemia or viremia) which coincides with the onset of severe disease and the lack of biomarkers to predict whether a patient will progress to severe disease. Serum/plasma proteomic analysis has been widely used to identify potential biomarkers for many infectious diseases, including DEN (Ray *et al*., 2014). The workflow of serum/plasma proteomic analysis starts with clinical specimen selection, followed by sample processing and storage, then downstream proteomic analysis (Ray *et al*., 2014). A discovery proteomic approach is typically used to first identify a panel of potential biomarkers of interest. These potential biomarkers are then validated on a larger population size using immunoassays and/or targeted proteomics to measure the amounts of specific proteins in clinical specimens, to produce a refined set of biomarkers (Ray *et al*., 2014). A challenge with plasma/serum proteomic analysis is that human blood contains a wide dynamic range of proteins, varying by up to 10^{10} fold, whilst the detection range of LC-MS/MS is only 10^{3}-10^{6} fold (Jacobs *et al*., 2005). Unfortunately, many potential biomarkers are only present at a low concentration in blood; for example, the basal level of IL-6 is only 5 pg/ml whilst the level of ALB is 50 mg/ml (Geyer *et al*., 2017). To enhance the detection of these low concentration "secreted proteins" which have typically been transiently secreted from cells in response to different disease conditions, protein depletion strategies are often applied to decrease the level of highly abundant proteins "classic proteins" in blood, such as ALB, IgG, and serum amyloid A (Jacobs *et al*., 2005).

Among previous proteomic studies that analysed the differential expression of serum/plasma proteins in response to DENV infection, there were seven studies that used healthy persons as the control group to compare with DENV infected patients (Jadhav *et*

al., 2017; Huy *et al.* 2013; Ray *et al*. 2013; Kumar *et al*., 2012; Albuquerque *et al.*, 2009; Thayan *et al*., 2009a; Thayan *et al*., 2009b) whilst other studies compared only patients with different DEN disease severities (Brasier *et al*., 2012; Fragnoud *et al.*, 2105, Nhi *et al*.,2016). A comparison of the seven studies is summarized in Table 6.1. Of note, in two of these studies either, peripheral blood mononuclear cells (PBMC) or circulating immune complexes (CIC) were isolated from plasma and used for proteomic analysis rather than analysing whole serum/plasma (Thayan *et al*., 2009a; Huy *et a*l., 2013). Overall, there were more proteins that were significantly up-regulated than down-regulated in DEN patients compared to healthy controls. The total numbers of proteins identified, and the number which were shown to be significantly differentially expressed in DEN patients, varied between studies. Variations in the populations analysed (in terms of race, age, infecting DENV serotype and study time after infection), serum/plasma preparation techniques, as well as proteomic analysis techniques are all factors that potentially contribute to the variation in the results in these studies. Almost all of the previous studies included only DF and DHF patients (only the study of Huy *et al*. included a SD group) which were compared with heathy controls. All studies except that of Albuquerque *et al*. (Albuquerque *et al.*, 2009), enrolled DEN patients infected with all DENV serotypes. Four of the studies used 2D-DIGE followed by LC-MS/MS for proteomic analysis, which is relatively low-throughput and led to the identification of a limited number of differentially expressed proteins. The other three studies used isobaric labelling in combination with LC-MS/MS which led to the quantitation and identification of a much larger number of proteins but using a small number of patient samples for analysis. Kumar *et al*., used pooled patient serum for analysis, which increased the number of samples analysed, but may have masked patient-to-patient variability (Kumar *et al*., 2012).

Table 6.1 Summary of proteomic studies using clinical specimens from DENV infected patients compared with healthy persons.

Study	Participants	Type of specimens	Time of specimens collection	Proteomic technique	Total detected protein	No. and important differential expression proteins (DENV/healthy)			Validation	Functional classification /IPA
						Cut-off	Important* increased proteins	Important* decreased proteins		
Thayan *et al*., 2009a	9 DF, 9 DHF, 8 Healthy, Malaysian	PBMC, non-pool	day 5-7 of illness	2D-DIGE followed by MS/MS	N/A	≥ 2 fold	8; Aldolase, alpha tubulin, TSA1p, FBG	None	None	None
Thayan *et al*., 2009b	10 DF, 10 DHF, 8 Healthy, Malaysian	serum, non-pool	at diagnosis	2D-DIGE followed by MS/MS	N/A	N/A	2; SERPINA1, NS1	None	Western blotting-NS1	None
Albuquerque *et a*l., 2009	13 SD (all DENV-3), 13 healthy, Indian	non-pool, plasma	at diagnosis	2D-DIGE followed by MS/MS	N/A	≥ 2 fold	7; C1 inhibitor, SERPINA3, FGG, CLU, C3c	7; A2M, F2, APOA4, C3b, TTR	None	None
Ray *et al*., 2012	6 DF, 8 malaria, 8 healthy, Indian	serum, non-pool	at diagnosis	2D-DIGE followed by MS/MS	N/A	≥ 1.2 fold	11; C4, SERPINA1, CLU, CFB, CFH, APCS	7; HPX, APOA4, HP, C3	Western blotting: CLU, HPX, HPX	KEGG pathway: complement and coagulation cascades
Kumar *et al*., 2012	44 DF, 18 DHF, 50 healthy, Singaporean	pooled serum	3 time-points: febrile, defervescence and recovery	iTRAQ	90	> 1.5 fold	30; SAA, LRG, HBA1, actin, HP, SERPINA1, SERPINC1, CLU, APOA1, SERPINA3	5; APOC1, APOC2, PBP	None	Functional group of proteins: APP 38%, Serpin 18%, lipid transport 12%, Serpin 18%
Huy *et al*., 2013	5 DF, 5 DHF, 5 DSS, 5 healthy, Vietnamese	CIC, non-pool,	at diagnosis	LC-MS/MS	111	N/A	N/A	N/A	None	None
Jadhav *et al*., 2017	12 DF, 24 DHF, 16 healthy, Indian	serum, non-pool	at diagnosis	iTRAQ	128	> 1.2 fold	SERPINA1, A2M, APOA1, CP, HCII, AGT		Western blotting: AGT	DAVID: renin angiotensin system, PPARs signaling, complement and coagulation cascades

*Proteins that were further investigated and/or discussed in the studies

Comparisons between cellular and/or secreted proteins that are dysregulated in response to DENV infection in cell-based experiments and in clinical specimens are very limited and have often focussed on specific proteins. For example, an increase in serum ENO1 during DEN has been correlated with increased amounts of ENO1 in the secretome of DENV-2 infected HepG2 cells (Higa *et al*., 2014). A review article by Salazar and coworkers (Salazar *et al*., 2014) linked the detection of macrophage migration inhibitory factor (MIF) in the secretome of DENV infected HepG2 cells (Higa *et al*., 2008) with increased MIF in patient serum, as a predictor of DEN disease severity (Chen *et al*., 2006). A systematic study to compare the results of cell-based experiments and clinical studies is required to determine which cell-based systems are relevant models for the study of DEN pathogenesis and can serve as a relevant tool for translational medicine studies.

Therefore, in this chapter, a high-throughput proteomic analysis of sera from patients with different DEN disease severities was undertaken, to identify proteins dysregulated in response to DENV infection and which may correlate with disease severity. An integrated comparative analysis of the results of the proteomic analyses of both DENV infected HEK293T and Huh-7 cells and the associated secretomes, with the results of the serum proteomic analysis was then done. By undertaking an integrated analysis it was aimed to determine whether DENV replication in cultured cells results in changes in the levels of cellular and secreted proteins that are also modulated in clinical samples.

Results

6.2 Study setting and clinical characteristics of the study population

The Philippines is a DEN endemic country in which the incidence of laboratory confirmed cases varies from 16-66 per 1,000 person years depending on the study (Agrupis *et al.,* 2019). Moreover, both the DEN incidence and mortality rate were estimated to increase by 24% and 29%, respectively, over the last three decades (Agrupis *et al*., 2019).

The sera used in this study (and associated clinical and DENV diagnostic data) were collected from a multicentre cohort in Metropolitan Manila, from August 2014 to November 2015. Among the 119 cases in cohort, there were 66 cases of DEN. Specimens were selected (jointly with Dr. Davidson), based on confirmed DENV infection (by RT-

PCR and NS1 postivity) and an early sampling time (day after fever onset). The ages and genders were balanced in each group as much as possible.

A total of 41 serum samples from DENV infected patients with varying disease severities were selected for proteomic analysis: 19 cases of DEN w/o WS, 13 cases of DEN w WS and nine cases of SD (Table 6.2 and Supplementary Table 6.1). The cohort included both adult and paediatric patients. The age and sex distribution in each group of DENV infected patients were not obviously different. However, the sera of nine healthy persons were collected from only adult volunteers. It should be noted that, the time of specimen collection (days after onset of fever) was longer in the SD group compared with the other groups. The diagnosis and confirmatory tests for DENV infection were performed in the Philippines at the time of enrolment. A DENV specific RT-PCR test was performed for all cases whilst DENV NS1 and specific IgM (using rapid tests) were performed in some cases. The DENV serotype was identified in ~ 57% of RT-PCR positive cases.

Table 6.2 Basic characteristics of DENV infected patients and healthy controls

	DEN (N=41)			Healthy (N=9)
	DEN w/o WS (N=19)	DEN w WS (N=13)	SD (N=9)	
Age (years), Median (range)	14 (3-39)*1	14 (8-40)	13 (2-40)	25 (19-27)*1
Male:Female	9:10	7:6	4:5	4:4*1
Specimen collection (days after onset of fever), Median (range)	4 (2-7)	5 (3-6)	6.5 (5-7)*2	NA
NS1 Ag (no. of positive/available data)	7/8	3/5	1/7	NA
Dengue IgM (no. of positive/available data)	7/19	7/10	7/7	NA
Positive Dengue RT-PCR (no. of positive/available data)	18/19	13/13	4/9	NA
Serotype, 1:2:3:4	3:3:6:1	3:1:1:0	2:0:0:0	NA

*Number of patients with missing data was indicated after the asterisk.

6.3 Quantitative LC-MS/MS analysis of serum proteomic

The sera were depleted of ALB and IgG (performed by Dr. Davidson) as described in Chapter 2 (section 2.6.2). The amount of protein in each specimen was determined by BCA assay (performed by Dr. Davidson). TMT labelling was performed by Dr. Davidson and Dr. Kate Heesom and co-workers at the Proteomic Facility. A total of six sets of 10-plex TMT labelled samples were analysed by LC-MS/MS were performed. A "mastermix" reference (described in section 2.6.2) was included in all runs to compare the results across different runs.

The spectral files from the LC-MS/MS analysis of all clinical specimens were combined, and protein identification and quantitation performed using Proteome Discoverer 2.1. The spectra were searched against the human proteome retrieved from Uniprot as well as the individual protein, and complete polyprotein, amino acid sequences encoded by 20 DENV reference strains covering all serotypes. Further refined quantification of the proteins was then done using the software BayesProt, a mixed-effects model (Freeman *et al*., 2016), recently extended to support TMT (https://github.com/biospi/bayesprot); (done by Professor Andrew Dowsey (University of Bristol) and PhD student Alex Philips (University of Liverpool)). There were a total of 1818 proteins that were reliably quantified using at least 1 unique peptide in the clinical samples.

Students t-tests, assuming unequal variance, were performed for each pair of conditions to calculate P-values, and these were FDR-adjusted using the Benjamini-Hochberg method by Dr Philip Lewis. Statistical significance was determined by an FDR-adjusted P-value (FDR) of less than 0.05 (Benjamini and Hochberg, 1995).

6.3.1 Proteomic analysis of serum protein altered in response to DENV infection

To identify proteins changed during disease processes, the healthy group was used as a control group. Proteins that changed by a statistically significant amount were defined by global FDR of < 0.05 and a cut-off of a ≥ 1.2 fold increase or decrease. A significant increase/decrease in at least one comparison (DEN w/o WS/healthy, DEN w WS/healthy or SD/healthy) was defined as a significant alteration (Supplementary Table S6.2). There

were 216 proteins that significantly altered in amount (both increased and decreased) in DENV infected patients compared with healthy persons, listed in Table 6.3. This set of proteins was subjected to further downstream bioinformatics analysis in section 6.4.

Table 6.3 A list of proteins significantly (FDR < 0.05) altered (≥ 1.2 fold) in abundance in the serum of DENV infected patients compared with healthy persons.

Accession	Description	Gene	Serum proteome (Compared with healthy)					
			DEN wo WS/healthy		DEN w WS/healthy		SD/healthy	
			Fold change	FDR	Fold change	FDR	Fold change	FDR
A8K3K1	Actin, cytoplasmic 1	*ACTC*	2.97	5.28E-05	3.14	1.15E-04	4.52	3.20E-03
Q76LX8	A disintegrin and metalloproteinase with thrombospondin motifs 13	*ADAMTS13*	0.84	8.69E-02	0.80	3.27E-02	0.73	7.59E-03
P43652	Afamin	*AFM*	0.63	4.26E-03	0.53	5.08E-03	0.72	2.46E-01
P00352	Retinal dehydrogenase 1	*ALDH1A1*	2.21	2.31E-02	1.90	9.66E-02	1.35	6.46E-01
J3KPS3	Fructose-bisphosphate aldolase A	*ALDOA*	1.65	5.82E-04	1.57	5.89E-03	1.80	3.43E-02
B7Z8Q2	Alpha-2-HS-glycoprotein	*AHSG*	0.73	9.22E-04	0.75	7.22E-03	0.77	4.02E-02
P02760	Protein AMBP	*AMBP*	0.69	4.92E-03	0.72	1.12E-02	0.74	4.82E-02
P02647	Apolipoprotein A-I	*APOA1*	0.73	4.69E-03	0.60	1.18E-03	0.55	1.17E-02
P06727	APOA4 protein	*APOA4*	0.47	3.61E-05	0.46	4.04E-03	0.65	4.47E-02
C0JYY2	Mutant Apo B 100	*APOB*	0.64	4.92E-03	0.65	4.90E-03	0.66	1.52E-01
A0A024R0T8	Apolipoprotein C-I	*APOC1*	0.43	1.69E-06	0.38	1.15E-04	0.48	6.60E-02
B0YIW2	Apolipoprotein C-III	*APOC3*	0.43	6.13E-05	0.52	2.85E-03	0.77	4.16E-01
P55056	Apolipoprotein C-IV	*APOC4*	0.35	5.97E-04	0.37	1.34E-03	0.38	1.51E-02
K7ER74	Apolipoprotein C-II	*APOC2*	0.36	2.06E-04	0.44	2.17E-03	0.90	8.30E-01
C9JF17	Apolipoprotein D	*APOD*	0.79	6.61E-02	0.71	2.07E-02	0.70	1.17E-02
Q13790	Apolipoprotein F	*APOF*	0.86	4.80E-01	0.71	4.07E-02	0.66	2.38E-02
P02749	Beta-2-glycoprotein 1	*APOH*	0.38	1.27E-05	0.33	3.09E-05	0.42	5.54E-03
P61204	ADP-ribosylation factor 3	*ARF3*	3.27	3.43E-02	3.32	5.58E-02	3.41	4.78E-02

O75882	Attractin	*ATRN*	0.81	4.58E-03	0.78	2.61E-03	0.75	2.95E-02
P25311	Zinc-alpha-2-glycoprotein	*AZGP1*	0.55	1.87E-04	0.52	1.64E-04	0.61	1.94E-02
P80723	Brain acid soluble protein 1	*BASP1*	2.72	5.17E-04	1.77	8.58E-03	2.20	8.16E-02
D3DNN4	Carboxylic ester hydrolase	*BCHE*	0.78	3.27E-02	0.81	5.55E-02	0.81	1.18E-01
B4E0X1	Beta-2-microglobulin	*B2M*	1.90	5.97E-04	1.77	1.97E-03	1.90	3.96E-03
P02745	Complement C1q subcomponent subunit A	*C1QA*	0.59	1.05E-05	0.59	2.22E-03	0.54	8.14E-02
P02746	Complement C1q subcomponent subunit B	*C1QB*	0.73	3.05E-03	0.70	1.06E-02	0.75	3.10E-01
P02747	Complement C1q subcomponent subunit C	*C1QC*	0.69	1.67E-03	0.65	9.55E-03	0.67	1.91E-01
Q9NZP8	Complement C1r subcomponent-like protein	*C1RL*	1.17	1.94E-01	1.32	1.05E-02	1.16	5.73E-01
P09871	Complement C1s subcomponent	*C1S*	0.81	2.20E-02	0.91	5.04E-01	0.93	8.65E-01
Q53HP3	Complement component 2 variant	*C2*	1.16	1.67E-01	1.27	2.35E-02	1.22	2.69E-01
P01031	Complement C5	*C5*	0.74	3.22E-02	0.72	2.61E-02	0.68	3.92E-02
P13671	Complement component C6	*C6*	0.84	1.33E-01	0.80	1.14E-01	0.72	1.67E-02
P07357	C8A protein	*C8A*	0.84	4.57E-02	0.79	1.60E-02	0.74	4.11E-03
P07358	Complement component C8 beta chain	*C8B*	0.87	2.42E-01	0.76	9.16E-02	0.60	5.94E-03
A0A024R035	Complement component 9, isoform	*C9*	1.32	2.49E-02	1.27	5.58E-02	1.26	3.38E-01
E7EMB3	Calmodulin 2	*CALM2*	2.16	4.49E-03	2.22	1.06E-02	3.84	2.18E-02
B2R888	Monocyte differentiation antigen CD14	*CD14*	1.66	2.27E-07	1.78	4.23E-06	1.46	1.72E-01
Q86VB7	Scavenger receptor cysteine-rich type 1 protein M130	*CD163*	1.39	1.92E-02	1.30	1.52E-01	1.67	3.20E-03
A8K6C1	Cholesteryl ester transfer protein	*CETP*	0.55	3.04E-03	0.55	4.77E-03	0.61	2.12E-01
A6XNE2	Complement factor D	*CFD*	0.84	4.87E-01	0.74	2.36E-01	0.61	3.42E-02
P08603	Complement factor H	*CFH*	0.62	4.39E-02	0.68	1.06E-01	0.57	8.99E-03
B2RA39	Complement factor H-related 5 (CFHL5)	*CFHL5*	0.46	9.41E-04	0.44	1.34E-03	0.36	3.77E-03
Q03591	Complement factor H-related protein 1	*CFHR1*	0.65	9.04E-02	0.65	6.76E-02	0.60	2.24E-02
P36980	Complement factor H-related protein 2	*CFHR2*	0.54	4.59E-02	0.58	8.77E-02	0.72	4.49E-01
B4DRF2	Complement factor I	*CFI*	0.80	3.23E-02	0.76	9.15E-03	0.77	2.60E-02
E9PK25	Cofilin-1	*CFL1*	1.94	1.79E-02	1.77	9.74E-03	2.60	4.11E-02
A0A0S2Z4I5	Complement factor properdin isoform 1	*CFP*	0.59	3.37E-04	0.50	1.17E-03	0.41	3.20E-03

Q05315	Galectin-10	*CLC*	2.98	2.77E-02	1.94	3.55E-01	4.23	1.94E-01
Q2KHT3	Protein CLEC16A	*CLEC16A*	0.60	7.87E-01	0.11	2.80E-01	0.09	3.34E-02
P12109	Collagen alpha-1(VI) chain	*COL6A1*	1.74	2.93E-04	1.87	1.64E-04	2.21	2.27E-02
A0A024R9J3	Collectin sub-family member 10	*COLEC10*	0.73	5.76E-03	0.79	1.85E-01	0.94	8.37E-01
A0A024R611	Coronin	*CORO1A*	1.72	8.59E-02	1.70	1.30E-01	2.79	1.03E-02
Q96IY4	Carboxypeptidase B2	*CPB2*	0.41	3.04E-08	0.41	2.33E-06	0.45	3.64E-04
P02741	C-reactive protein	*CRP*	7.63	7.81E-05	4.42	5.54E-03	1.53	5.27E-01
Q9NQ79	Cartilage acidic protein 1	*CRTAC1*	0.75	4.63E-02	0.64	4.85E-03	0.67	1.81E-02
B2RBF5	Di-N-acetylchitobiase	*CTBS*	0.76	4.49E-03	0.87	2.48E-01	0.97	9.44E-01
J3KQ18	D-dopachrome decarboxylase	*DDT*	2.23	3.83E-03	2.67	1.62E-03	1.82	3.41E-01
Q6MZL2	Putative uncharacterized protein	*DKFZp686M0562*	0.69	1.43E-03	0.66	2.59E-04	0.81	2.72E-01
B4DID6	Dickkopf-related protein 3G	*DKK3*	4.27	3.27E-02	2.92	1.45E-01	2.97	4.49E-01
Q16610	Truncated extracellular matrix protein 1	*ECM1*	0.65	7.13E-04	0.65	4.77E-03	0.58	1.57E-03
P13639	Elongation factor 2	*EEF2*	3.07	7.67E-02	5.06	1.32E-02	3.79	6.08E-02
P08246	Neutrophil elastase	*ELANE*	2.95	4.53E-02	1.93	3.11E-01	0.97	9.84E-01
A0A024R6D3	Ectonucleoside triphosphate diphosphohydrolase 5	*ENTPD5*	2.25	4.29E-02	2.01	6.44E-02	1.48	4.16E-01
Q9NZ08	Endoplasmic reticulum aminopeptidase 1	*ERAP1*	1.71	3.81E-02	1.78	3.03E-02	1.29	5.42E-01
P00742	Coagulation factor X	*F10*	0.71	5.96E-03	0.75	1.61E-02	0.80	2.63E-01
P03951	Coagulation factor XI	*F11*	0.61	3.84E-04	0.56	4.04E-03	0.44	4.74E-04
B2R6V9	Coagulation factor XIII, A1 polypeptide	*F13A1*	0.40	1.30E-05	0.58	3.15E-02	0.48	5.92E-02
P05160	Coagulation factor XIII B	*F13B*	0.58	7.37E-05	0.60	1.75E-04	0.72	7.71E-02
P00734	Prothrombin	*F2*	0.71	1.84E-03	0.73	4.50E-03	0.67	6.20E-03
F2RM37	Coagulation factor IX	*F9*	0.57	3.61E-05	0.60	2.04E-04	0.60	3.20E-03
Q15485	Ficolin-2	*FCN2*	0.67	6.97E-02	0.63	2.07E-02	0.52	9.94E-02
P02671	Fibrinogen alpha chain	*FGA*	0.32	4.19E-04	0.46	1.33E-01	0.22	7.10E-02
C9JEU5	Fibrinogen gamma chain	*FGG*	0.30	9.73E-04	0.48	1.53E-01	0.22	7.63E-02
D3DP16	Fibrinogen gamma chain	*FGG*	0.23	5.69E-04	0.49	2.06E-01	0.21	9.19E-02
Q08830	Fibrinogen-like protein 1	*FGL1*	2.83	3.12E-05	2.76	1.66E-03	1.40	6.46E-01

Q14314	Fibroleukin	*FGL2*	2.01	2.28E-02	1.90	3.37E-02	1.91	1.03E-01
A0A024R462	Fibronectin	*FN1*	0.55	6.57E-03	0.63	9.66E-02	0.66	1.94E-01
B4DTH2	Fibronectin splice variant E	*FN1*	0.63	3.97E-02	0.74	2.98E-01	0.86	6.51E-01
Q12841	Follistatin-related protein 1	*FSTL1*	1.43	4.88E-04	1.25	3.03E-02	1.41	1.04E-01
P04066	Tissue alpha-L-fucosidase	*FUCA1*	1.56	1.21E-02	1.62	2.27E-02	1.08	9.39E-01
Q9BTY2	Plasma alpha-L-fucosidase	*FUCA2*	1.34	8.81E-02	1.48	2.65E-02	1.72	6.89E-02
P04406	Glyceraldehyde-3-phosphate dehydrogenase	*GAPDH*	2.19	3.22E-04	2.25	2.45E-04	2.19	4.27E-02
A8K335	Gamma-glutamyl hydrolase	*GGH*	1.22	3.83E-02	1.37	5.56E-03	1.72	6.31E-03
P09681	Gastric inhibitory polypeptide	*GIP*	0.07	4.42E-02	0.19	NA	0.38	NA
A0A024R056	Guanine nucleotide-binding protein subunit beta-4	*GNB1*	2.78	2.32E-03	2.42	1.33E-02	3.13	1.33E-02
Q8NBJ4	Golgi membrane protein 1	*GOLM1*	3.77	1.30E-05	3.12	1.15E-04	2.38	1.67E-02
P40197	Platelet glycoprotein V	*GP5*	2.14	3.22E-02	0.84	7.25E-01	2.41	8.27E-02
A0A0A0MTS2	Glucose-6-phosphate isomerase	*GPI*	1.84	1.10E-04	1.97	1.95E-04	1.83	3.43E-02
P80108	Phosphatidylinositol-glycan-specific phospholipase D	*GPLD1*	0.65	4.38E-03	0.56	4.50E-03	0.52	5.81E-03
P06396	Gelsolin	*GSN*	0.50	6.57E-03	0.44	1.46E-03	0.39	3.20E-03
V9H1C1	Gelsolin exon 4	*GSN*	0.56	1.47E-03	0.58	4.85E-03	0.51	3.20E-03
B2R983	Glutathione S-transferase omega-1	*GSTO1*	1.80	5.99E-04	2.00	2.54E-04	2.08	1.54E-02
R4GMU1	GDH/6PGL endoplasmic bifunctional protein	*H6PD*	1.40	3.17E-02	1.30	1.29E-01	1.33	2.63E-01
Q6LAM1	Complement factor I	*CFI*	0.79	5.20E-02	0.75	1.68E-02	0.75	3.13E-02
V9HWK2	Vinculin	*VCL*	1.55	1.39E-04	1.54	1.64E-04	2.32	2.88E-02
V9HWC7	Peroxiredoxin-6	*PRDX6*	1.54	4.56E-02	1.90	1.87E-02	1.42	5.47E-01
A0A0K0K1L8	Proteasome activator complex subunit 1	*PSME1*	3.26	1.03E-02	3.12	8.74E-03	4.54	2.71E-02
V9HWI3	Cathepsin D	*CTSD*	2.61	1.66E-07	2.08	3.74E-04	1.87	4.82E-02
A0A0K0K1K4	Proteasome subunit alpha type	*PSMA7*	1.91	1.10E-01	1.96	1.20E-01	3.37	3.30E-02
V9HWC9	Superoxide dismutase	*SOD1*	1.52	3.27E-02	1.72	1.33E-02	1.44	5.04E-01
V9HWA9	Complement C3	*C3*	0.84	1.58E-01	0.76	6.50E-02	0.77	2.98E-02
V9HW22	Heat shock cognate 71 kDa protein	*HSPA8*	2.33	1.33E-04	2.52	3.23E-04	2.88	4.65E-03

V9HVY1	Fibrinogen beta chain	*FGB*	0.29	5.97E-04	0.48	1.65E-01	0.24	6.79E-02
V9HWB4	Endoplasmic reticulum chaperone BiP	*HSPA5*	0.73	4.49E-03	0.87	3.97E-01	1.11	5.80E-01
V9HW88	Calreticulin	*CALR*	1.35	4.63E-05	1.50	2.04E-04	1.80	3.30E-02
B2R4R0	Histone H4	*HIST1H4H*	2.96	1.52E-02	3.55	5.89E-03	3.52	1.37E-02
P07900	Heat shock protein HSP 90-alpha	*HSP90AA1*	3.76	1.18E-04	4.32	1.72E-04	4.16	8.22E-03
P14625	Endoplasmin	*HSP90B1*	1.56	9.41E-04	1.75	1.18E-03	1.77	1.52E-02
A0A0G2JIW1	Heat shock 70 kDa protein 1	*HSPA1B*	2.40	7.59E-03	2.51	5.89E-03	2.52	2.20E-02
P05362	Intercellular adhesion molecule 1	*ICAM1*	1.34	8.47E-04	1.34	9.90E-03	1.39	6.80E-03
B2R5M8	Isocitrate dehydrogenase, cytoplasmic	*IDH*	2.07	3.27E-02	2.04	3.62E-02	1.86	1.88E-01
P05019	Insulin-like growth factor 1	*IGF1*	0.56	2.21E-01	0.67	4.19E-01	0.42	4.82E-02
P17936	Insulin-like growth factor binding protein 3	*IGFBP3*	0.58	5.17E-04	0.54	5.89E-03	0.47	1.51E-02
P24592	Insulin-like growth factor-binding protein 6	*IGFBP6*	0.77	2.58E-02	0.74	9.15E-03	0.70	6.56E-02
S6BGF5	IgG H chain	*IgGHchain*	7.81	1.99E-02	3.48	2.84E-01	3.78	3.72E-01
A0A087WWF0	Protein IGHV3-64	*IGHV3-64*	0.64	2.54E-01	0.62	2.66E-02	0.36	3.31E-02
P01703	Ig lambda chain V-I	*IGLV1-40*	1.93	3.67E-01	2.27	2.02E-01	5.15	1.67E-02
G3V1C5	Interleukin-18-binding protein	*IL18BP*	3.01	2.32E-03	2.59	6.51E-03	2.15	1.62E-01
B7Z8B6	Inter-alpha-trypsin inhibitor heavy chain H1	*ITIH1*	0.68	2.76E-03	0.62	9.93E-04	0.62	3.20E-03
D3DRR6	Inter-alpha-trypsin inhibitor heavy chain H2	*ITIH2*	0.64	1.67E-03	0.63	1.83E-03	0.69	2.91E-02
H0YAC1	Kallikrein B	*KLKB1*	0.61	5.93E-04	0.59	1.34E-03	0.54	3.20E-03
G3XAI2	Laminin subunit beta-1	*LAMB1*	1.12	3.15E-01	1.27	8.28E-03	1.18	3.63E-01
P18428	Lipopolysaccharide-binding protein	*LBP*	1.98	2.28E-06	1.68	2.17E-03	0.95	9.35E-01
P04180	Phosphatidylcholine-sterol acyltransferase	*LCAT*	0.72	1.84E-03	0.71	1.92E-03	0.75	2.89E-02
A0A024RDT4	Lymphocyte cytosolic protein 1	*LCP1*	1.94	1.09E-04	2.10	1.25E-03	2.79	1.51E-02
P00338	L-lactate dehydrogenase A chain	*LDHA*	1.61	1.52E-03	1.62	4.72E-03	1.84	1.11E-02
Q5U077	L-lactate dehydrogenase B chain	*LDHB*	1.41	8.10E-03	1.41	2.63E-02	1.85	2.24E-02
A0A0S2Z3Y1	Galectin-3-binding protein	*LGALS3BP*	2.22	4.19E-04	2.43	2.61E-03	2.10	9.94E-02

H2B4M4	Leukocyte immunoglobulin-like receptor A	*LILRA3*	2.58	1.29E-01	4.07	1.61E-02	3.31	9.63E-02
Q6NXN2	Hypothetical LOC441242	*LOC441242*	0.31	1.01E-01	0.21	4.56E-02	0.19	1.22E-01
Q07954	Prolow-density lipoprotein receptor-related protein 1	*LRP1*	1.15	3.38E-01	1.28	5.58E-02	1.58	3.36E-02
P33908	Mannosyl-oligosaccharide 1,2-alpha-mannosidase IA	*MAN1A1*	1.18	7.69E-02	1.31	1.29E-02	1.50	3.58E-02
Q16706	Alpha-mannosidase 2	*MAN2A1*	1.44	1.67E-03	1.42	2.77E-03	1.42	8.12E-02
P29966	Myristoylated alanine-rich C-kinase substrate	*MARCKS*	2.26	4.81E-03	2.38	5.47E-03	3.61	8.79E-03
P48740	Mannan-binding lectin serine protease 1	*MASP1*	0.77	2.77E-02	0.82	1.26E-01	0.92	8.09E-01
B2R7D2	Multiple inositol polyphosphate histidine phosphatase 1	*MINPP1*	0.76	9.96E-02	0.82	2.89E-01	0.66	3.42E-02
A0A024R6R4	Matrix metallopeptidase 2	*MMP2*	0.76	2.58E-02	0.84	3.76E-01	0.95	8.81E-01
P05164	Myeloperoxidase	*MPO*	1.72	2.20E-02	1.41	1.47E-01	1.38	2.51E-01
B9EJA8	Macrophage mannose receptor 1	*MRC1L1*	1.23	7.95E-02	1.34	3.80E-02	1.29	2.22E-01
P26038	Moesin	*MSN*	2.74	5.56E-06	2.64	3.26E-05	3.11	3.10E-03
G3XAK1	Macrophage stimulating 1 (Hepatocyte growth factor-like)	*MST1*	0.80	1.14E-02	0.78	2.09E-02	0.87	2.49E-01
B7Z809	Methylenetetrahydrofolate dehydrogenase (NADP+ dependent) 1	*MTHFD1*	1.33	5.74E-01	2.33	3.88E-02	1.86	5.81E-01
A8K8T3	Bifunctional heparan sulfate N-deacetylase/N-sulfotransferase 1	*NDST1*	0.53	5.60E-02	0.46	1.41E-02	0.37	4.53E-02
P14543	Nidogen-1	*NID1*	1.95	2.90E-06	2.04	2.26E-05	2.52	3.20E-03
J3KNK3	NTPase KAP family P-loop domain-containing protein 1	*NKPD1*	0.60	2.35E-01	0.57	3.84E-02	0.45	4.02E-02
A8K7Q1	Nucleobindin 1	*NUCB1*	3.40	1.69E-06	4.05	1.15E-04	3.08	9.49E-02
Q86UD1	Out at first protein homolog	*OAF*	1.58	2.95E-04	1.72	1.92E-03	1.52	2.15E-01
B4DI63	Osteoglycin OG	*OGN*	1.62	4.53E-01	2.94	3.03E-02	1.85	3.24E-01
B2R7N9	Osteomodulin	*OMD*	2.22	8.10E-03	3.19	6.30E-03	4.09	3.13E-02
P02763	Alpha-1-acid glycoprotein 1	*ORM1*	1.69	5.47E-04	1.78	3.23E-04	1.52	7.65E-02
P19652	Alpha-1-acid glycoprotein 2	*ORM2*	1.32	6.74E-02	1.49	9.86E-03	1.27	3.85E-01
Q99497	Protein deglycase DJ-1	*PARK7*	2.06	2.07E-03	2.12	1.83E-03	2.00	3.27E-02
Q8NBP7	Proprotein convertase subtilisin/kexin type 9	*PCSK9*	1.59	1.37E-05	1.62	2.97E-03	1.54	6.07E-02
Q9UHG3	Prenylcysteine oxidase	*PCYOX1*	0.58	7.14E-05	0.62	4.31E-03	0.60	2.97E-02

P02776	Platelet factor 4	*PF4*	3.05	2.12E-04	2.90	1.97E-03	5.72	3.20E-03
P17858	ATP-dependent 6-phosphofructokinase	*PFKL*	3.91	1.31E-01	5.44	6.24E-02	7.92	3.27E-02
P07737	Profilin-1	*PFN1*	3.63	1.74E-05	3.20	6.68E-05	5.40	1.11E-02
Q6FHK8	Phosphoglycerate mutase 1	*PGAM1*	2.88	4.86E-02	4.09	1.28E-02	3.91	7.81E-02
Q96PD5	N-acetylmuramoyl-L-alanine amidase	*PGLYRP2*	0.62	2.57E-05	0.60	2.01E-04	0.71	1.33E-02
P00747	Plasminogen	*PLG*	0.70	1.15E-03	0.73	4.77E-03	0.76	2.88E-02
B3KUE5	Phospholipid transfer protein	*PLTP*	0.81	1.92E-01	0.77	3.94E-02	0.78	4.93E-01
P27169	Serum paraoxonase/arylesterase 1	*PON1*	0.78	4.59E-02	0.70	9.90E-03	0.61	3.10E-03
A8K486	Peptidyl-prolyl cis-trans isomerase	*PPIA*	1.87	2.78E-03	1.86	1.17E-03	2.47	2.74E-02
B2R4P2	Peroxiredoxin-1	*PRDX1*	1.89	1.07E-02	2.02	5.54E-03	1.62	3.72E-01
A0A024QZL1	Proteoglycan 1	*PRG1*	1.81	8.20E-02	1.32	5.55E-01	2.53	3.30E-02
B4DPQ3	Protein C	*PROC*	0.63	6.57E-03	0.64	9.90E-03	0.68	8.27E-02
A0A0S2Z4L3	Protein S	*PROS1*	0.78	1.41E-02	0.77	1.71E-02	0.71	1.14E-02
Q59EN5	Prosaposin	*PSAP*	1.94	1.69E-06	1.65	8.48E-04	1.44	8.22E-03
P25786	Proteasome subunit alpha type-1	*PSMA1*	2.18	9.99E-03	2.76	1.18E-02	3.98	1.51E-02
P25788	Proteasome subunit alpha type-3	*PSMA3*	1.67	2.27E-02	1.96	2.61E-03	2.46	2.18E-02
P25789	Proteasome subunit alpha type-4	*PSMA4*	1.74	2.64E-02	2.13	8.14E-03	3.21	3.49E-02
G3V5Z7	Proteasome subunit alpha type-6	*PSMA6*	1.81	8.95E-02	2.18	2.72E-02	3.46	3.30E-02
P20618	Proteasome subunit beta type-1	*PSMB1*	2.39	2.77E-02	3.12	5.00E-03	4.06	3.67E-02
O00391	Sulfhydryl oxidase 1	*QSOX1*	0.78	4.81E-03	0.66	4.31E-03	0.74	2.20E-02
A0A024RB87	Ras-related protein Rap-1b	*RAP1B*	3.49	1.97E-02	1.95	2.92E-01	2.93	5.25E-02
P02753	Retinol binding protein 4	*RBP4*	0.50	1.20E-03	0.57	6.51E-03	0.66	8.85E-02
A8K9C4	Elongation factor 1-alpha 2	*EEF1A2*	3.43	2.24E-02	3.39	5.58E-02	6.65	1.01E-01
B4DUP2	UTP--glucose-1-phosphate uridylyltransferase	*UGP2*	2.53	4.07E-02	3.31	1.18E-02	3.57	5.77E-02
Q59ER5	WD repeat domain 1	*WDR1*	2.17	8.46E-02	2.19	6.45E-02	3.47	3.42E-02
B4E3S9	Leiomodin-1	*LMOD1*	1.63	3.77E-01	1.80	2.90E-01	4.26	3.30E-02
B1N7B6	Cryocrystalglobulin CC1 heavy chain variable region	*N/A*	0.74	4.53E-02	0.74	1.52E-01	0.61	5.26E-02

B7Z539	Inter-alpha-trypsin inhibitor heavy chain H1	*ITIH1*	0.64	6.27E-04	0.62	5.67E-04	0.60	2.96E-03
Q6ZVX0	Protein Tro alpha1 H,myeloma	*N/A*	0.54	1.01E-01	0.66	1.82E-01	0.42	2.07E-02
B2R582	C-type lectin domain family 3, member B	*CLEC3B*	0.46	4.02E-02	0.72	3.76E-01	0.59	4.77E-02
A0A125QYY7	IBM-B1 heavy chain variable region	*N/A*	0.45	6.57E-01	0.34	5.04E-01	0.20	4.77E-02
A0A068LKQ8	Ig heavy chain variable region	*N/A*	0.26	2.58E-02	0.35	8.22E-02	0.27	1.42E-01
Q8TE92	cDNA FLJ23782 fis, clone HEP20947	*N/A*	0.20	3.25E-04	0.51	2.35E-01	0.26	8.12E-02
P06702	Protein S100-A9	*S100A9*	2.52	1.59E-01	3.59	3.03E-02	2.26	4.16E-01
Q6UWP8	Suprabasin	*SBSN*	1.63	3.25E-02	1.55	2.21E-02	1.28	5.47E-01
P18827	Syndecan 1	*SDC1*	19.65	3.79E-02	24.53	2.50E-01	38.99	5.27E-01
Q13228	Selenium-binding protein 1	*SELENBP1*	1.44	4.44E-02	1.67	5.89E-03	1.34	4.97E-01
P49908	Selenoprotein P	*SELENOP*	0.54	1.25E-05	0.51	3.94E-05	0.52	3.20E-03
A0A024R8Z0	L-selectin	*SELL*	1.30	2.41E-03	1.27	1.06E-02	1.24	1.70E-01
Q86U17	Serpin A11	*SERPINA11*	1.25	7.69E-02	1.42	4.77E-03	1.27	2.03E-01
B3KS79	Alpha-1-antichymotrypsin	*SERPINA3*	1.57	1.18E-04	1.53	2.50E-04	1.42	1.09E-01
A0A024R6I9	Alpha-1 antiproteinase	*SERPINA4*	0.56	3.96E-05	0.55	1.64E-04	0.61	3.76E-03
A0A024R6N9	Plasma serine protease inhibitor	*SERPINA5*	0.30	1.66E-07	0.34	1.58E-04	0.34	4.21E-05
A0A024R944	Antithrombin III	*SERPINC1*	0.72	2.87E-03	0.87	4.59E-01	0.88	6.38E-01
P36955	Pigment epithelium-derived factor	*SERPINF1*	0.74	2.08E-02	0.68	7.98E-03	0.63	3.20E-03
P05155	Plasma protease C1 inhibitor	*SERPING1*	1.21	1.68E-01	1.36	2.61E-02	1.38	2.63E-01
D3DPK5	SH3 domain binding glutamic acid-rich protein like 3	*SH3BGRL3*	3.18	6.74E-02	2.47	1.47E-01	4.31	2.27E-02
A0A024RDE2	Secreted phosphoprotein 1	*SPP1*	3.67	6.56E-02	5.45	3.08E-02	3.02	3.85E-01
Q13103	Secreted phosphoprotein 24	*SPP2*	0.59	1.92E-03	0.96	8.96E-01	1.21	5.64E-01
P37802	Transgelin-2	*TAGLN2*	2.39	1.84E-03	1.79	1.17E-03	4.10	3.30E-02
P37837	Transaldolase	*TALDO1*	2.17	1.09E-04	2.37	3.15E-04	3.20	3.20E-03
P29401	Transketolase	*TKT*	2.77	2.29E-05	3.02	3.09E-05	3.45	6.20E-03
J3QSU6	Tenascin C	*TNC*	1.55	4.62E-05	1.41	1.40E-03	1.51	1.11E-02

P60174	Triosephosphate isomerase	*TPI1*	1.97	8.25E-03	2.05	6.69E-03	1.96	1.42E-01
P67936	Tropomyosin alpha-4 chain	*TPM4*	1.98	2.28E-02	1.57	2.35E-02	3.00	1.14E-01
H9ZYJ2	Thioredoxin	*TXN*	1.67	1.62E-01	1.93	3.84E-02	1.91	1.60E-01
P19320	Vascular cell adhesion protein 1	*VCAM1*	2.03	2.27E-07	2.24	1.72E-04	2.53	1.51E-02
P23381	Tryptophan--tRNA ligase	*WARS*	3.89	2.79E-05	5.08	1.64E-04	5.50	3.76E-03
P62258	14-3-3 protein epsilon	*YWHAE*	2.56	7.41E-02	3.70	1.22E-02	3.63	9.62E-02
P61981	14-3-3 protein gamma	*YWHAG*	3.64	1.92E-02	4.55	7.57E-03	9.58	3.10E-03
P63104	14-3-3 protein zeta/delta	*YWHAZ*	2.19	5.69E-04	2.05	9.12E-04	2.85	3.13E-02

6.3.2 Analysis of the serum proteome of DEN patients with different grades of disease severity

To identify potential protein markers to predict DEN disease severity, the DEN w/o WS group was used as control to compare with DEN w WS and SD. In addition, the SD and DEN w WS groups were compared. From this analysis, there were no proteins that were significantly differentially regulated between SD and either DEN w WS or DEN w WS compared with DEN w/o WS. While, there were two proteins that were significantly (FDR < 0.05) altered (≥ 1.2 fold) in SD compared with DEN w/o WS: C-reactive protein (CRP) and APOC2 (Table 6.4). Interestingly, these two proteins were also significantly altered in DENV infected patients compared with healthy controls (Table 6.3).

Table 6.4 Proteins significantly (FDR < 0.05) altered (≥ 1.2 fold) in abundance in the serum of DEN patients with SD compared to DEN patients with lesser disease severity.

Description	Gene	Compared with healthy						Compared for severity					
		DEN w/o WS/healthy		DEN w WS/healthy		SD/healthy		DEN w WS/ DEN wo WS		SD/ DEN w/o WS		SD/ DEN wo WS	
		Fold change	FDR	Fold change	FDR	Fold change	FDR	Fold change	FDR	Fold change	FDR	Fold change	FDR
Apolipoprotein C-II	*APOC2*	0.36	2.06E-04	0.44	2.17E-03	0.90	8.30E-01	1.21	9.39E-01	2.50	4.94E-02	2.06	4.78E-01
C-reactive protein	*CRP*	7.63	7.81E-05	4.42	5.54E-03	1.53	5.27E-01	0.58	9.39E-01	0.20	4.94E-02	0.35	8.24E-01

6.4 Bioinformatic analysis of proteins that were significantly altered in the serum of DEN patients compared to controls.

Because of the low number of significantly altered proteins in patients with SD compared to DEN w/o WS, further bioinformatics analysis and discussion were focused on the serum proteins that significantly changed in DENV infected patients compared with healthy persons.

The 216 proteins that significantly increased/decreased ≥ 1.2 fold in DENV infected patients compared to healthy controls were subjected to gene enrichment and network analysis using the DAVID and STRING analysis programs (Figures 6.1-6.2 and Supplementary Table S6.3).

DAVID analysis showed that the proteins that were significantly altered in the serum of DEN patients compared to controls were enriched in eight clusters of proteins (Figure 6.1). The top three clusters were associated with the GOCC term "extracellular region/secreted" (GO:0005576), the GOMF term "serine-type endopeptidase activity" (GO:0004252) and the GOBP term "fibrinolysis" (GO:0042730), respectively. Other protein clusters associated with GO terms related to DENV infection included; "lipoprotein metabolic process" (GO:0042157) and "ubiquitin protein ligase binding" (GO:0031625) as well as the KEGG pathway "Complement and coagulation cascades" (hsa04610).

STRING analysis revealed that serum proteins that were significantly altered in the serum of DEN patients compared to controls were associated with multiple significantly enriched GO terms. Those related to DEN pathogenesis included "immune response" (GO:0006955), "platelet degranulation" (GO:0002576), lipid transport (GO:0006869) and "acute-phase response" (GO:0006953) (Figure 6.2). Protein clusters were also associated with the enriched KEGG pathways "complement and coagulation cascades" (hsa04610) and "Cholesterol metabolism" (hsa04979).

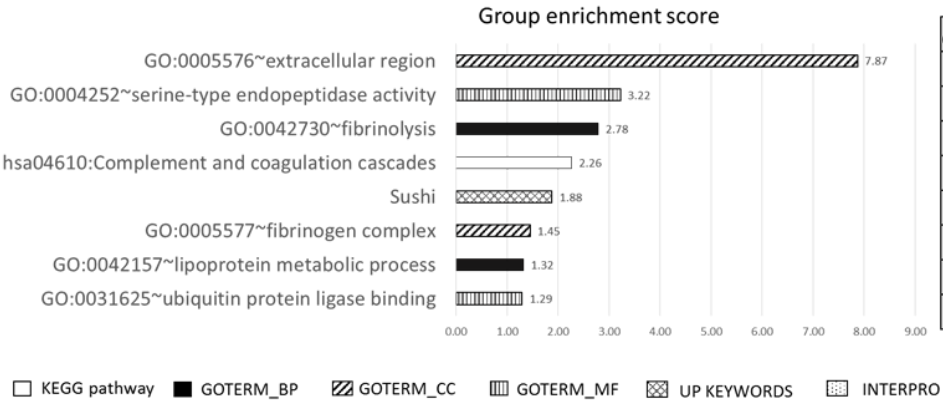

Count	%	P-value
93	46.5	3.89E-13
23	11.5	1.65E-02
9	4.5	5.83E-04
29	14.5	1.25E-09
10	5	6.40E-03
6	3	5.10E-03
9	4.5	1.67E-03
10	5	4.33E-03

Figure 6.1 DAVID analysis of proteins that were significantly altered in the serum of DEN patients compared to controls.

Proteins that were significantly (FDR < 0.05) altered in amount by ≥ 1.2 fold in the serum of DEN patients compared to controls were analysed using the DAVID database. The GO accession numbers/terms that were significantly enriched and the properties of the corresponding protein clusters are shown. The GES of significantly enriched GO terms are plotted as bar graphs with the corresponding GES score shown. The shading shows the type of GO term (GOBP, GOCC or GOMF), UP keywords, Interpro term or KEGG pathway. The number of proteins in each cluster (count), number of proteins associated with each GO term/total number of proteins in the dataset (%) and P-value for each of the annotation terms are listed in the table.

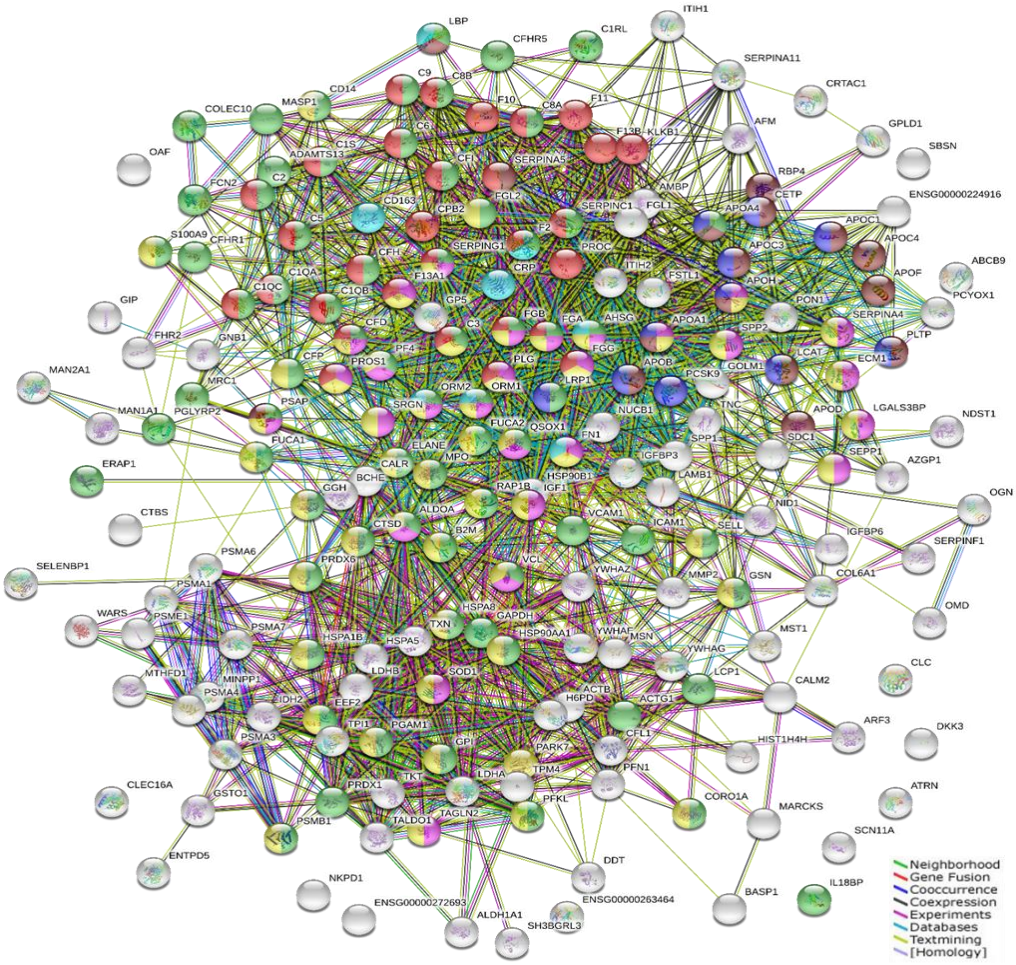

GO term/ pathway	Description	Count in gene set	FDR
GO:0006955	immune response	71 of 1560	1.10E-25
GO:0002576	platelet degranulation	28 of 129	8.18E-25
GO:0032940	secretion by cell	54 of 959	7.31E-23
GO:0006869	lipid transport	16 of 272	6.76E-07
GO:0006953	acute-phase response	8 of 45	1.06E-06
hsa04610	Complement and coagulation cascades	30 of 78	2.73E-33
hsa04979	Cholesterol metabolism	11 of 48	5.99E-10

Figure 6.2 STRING analysis of proteins that were significantly altered in the serum of DEN patients compared to controls.

The STRING database was searched to analyse serum proteins that significantly (FDR < 0.05) increased or decreased ≥ 1.2 fold in response to DENV-2 infection. Nodes representing proteins associated with the significantly enriched GO terms "immune response", "platelet degranulation", "secretion by cell", "lipid transport" and "acute-phase response" as well as the KEGG pathway "complement and coagulation cascades" and "cholesterol metabolism" are shaded in green, purple, yellow, brown, light blue, red and blue, respectively. The number of coloured nodes/ total proteins involved for each term and the FDR of each GO term are listed in the table.

6.5 Comparative analysis proteins that were commonly found in proteomes and secretomes of DENV-2 infected HEK293T cells and clinical specimen from DEN patients.

6.5.1 Proteins that were commonly detected in the proteomes and secretomes of DENV-2 infected HEK293T cells and clinical specimens from DEN patients.

To determine whether HEK293T cells may be a useful model for examining DENV infection *in vitro*, the results of the proteome and secretome analysis of DENV-2 infected HEK293T cells (described in Chapter 4) were compared with the proteomic analysis of serum samples from DENV infected patients compared to healthy persons. Overall, 407 and 441 proteins that were detected in the proteome and secretome of HEK293T cells, respectively, were also detected in the serum proteomic analysis (Figure 6.3). Among these, 293 serum proteins were detected in both the proteome and secretomes of HEK293T cells.

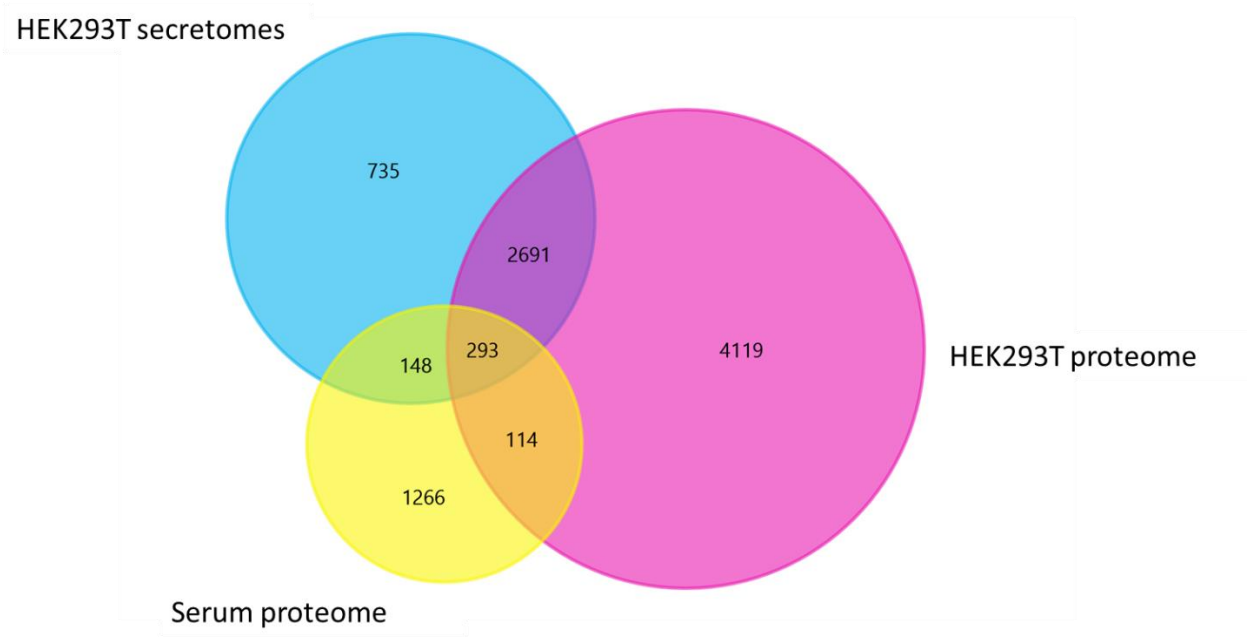

Figure 6.3 Overlap between proteins identified in the proteome and secretome of DENV-2 infected HEK293T cells and the serum proteome of DENV infected patients.

Venn diagram shows the number of proteins that were detected in DENV-2 infected HEK293T cells or secretomes or serum of DEN patients.

Proteins which altered significantly (P-value < 0.05 and ≥ 1.3 fold) in abundance across both the proteomes and secretomes of DENV-2 infected HEK293T cells compared with mock cells,were compared with the proteins that significantly altered (FDR < 0.05 and ≥ 1.2 fold) in the serum of DENV infected patients patients compared to healthy persons (Figure 6.4, Table 6.5). Four proteins which fit both of these criteria were HSPA5, CALR, Peptidyl-prolyl cis-trans isomerase (PPIC) and Folate gamma-glutamyl hydrolase (carboxypeptidase G). Of these proteins, CALR and HSPA5 were significantly increased > 1.5 fold and > 1.3 fold, respectively, in DENV-2 HEK293T cells validated by Western blotting (described in Chapter 4).

Histone H4 (HIST1H4L) was the only secreted protein that significantly increased > 2 fold in both the secretomes from DENV-2 infected cell HEK293T cells and the serum of DENV infected patients (Figure 6.4 and Table 6.5). Unfortunately, there were no proteins that were significantly altered in all data sets (proteome, secretome and serum proteome) in response to DENV infection.

6.5.2 Bioinformatic analysis of proteins that were significantly altered in both HEK293T cells and serum in response to infection

As there were only four proteins that were significantly altered in both HEK293T cells and patient serum in response to infection, DAVID analysis was not possible. Interestingly, STRING analysis revealed that this set of proteins was associated with the significantly enriched GOBP term “ATF6-mediated unfolded protein response” (GO:0036500) and the KEGG pathway term “Protein processing in endoplasmic reticulum” (hsa04141) (Figure 6.4B).

Table 6.5 A list of proteins commonly significantly altered in the proteomes and secretomes of DENV-2 infected HEK293T cells and clinical specimen from DEN patients.

			Proteome		Secretome		Serum proteome (Compared with healthy)					
							DEN wo WS/healthy		DEN w WS/healthy		SD/healthy	
Accession	Description	Gene	DENV-2/mock ratio	P-value	DENV-2 /mock ratio	P-value	Fold change	FDR	Fold change	FDR	Fold change	FDR
A8K486	Peptidyl-prolyl cis-trans isomerase	PPIA	0.72	5.04E-03	NSC	NSC	1.87	2.78E-03	1.86	1.17E-03	2.47	2.74E-02
A8K335	Folate gamma-glutamyl hydrolase	N/A	1.46	4.31E-02	NSC	NSC	1.37	3.83E-02	1.72	5.56E-03	1.12	6.31E-03
V9HW88	Calreticulin	CARL	1.58	2.29E-02	NSC	NSC	1.35	4.63E-05	1.50	2.04E-04	1.80	3.30E-02
V9HWB4	Endoplasmic reticulum chaperone BiP	HSPA5	1.43	4.08E-02	NSC	NSC	0.73	4.49E-03	0.87	3.97E-01	1.11	5.80E-01
B2R4R0	Histone H4	HIST1H4H	NSC	NSC	2.971	1.87E-02	2.96	1.52E-02	3.55	5.89E-03	3.52	1.37E-02

NSC= non-significant change

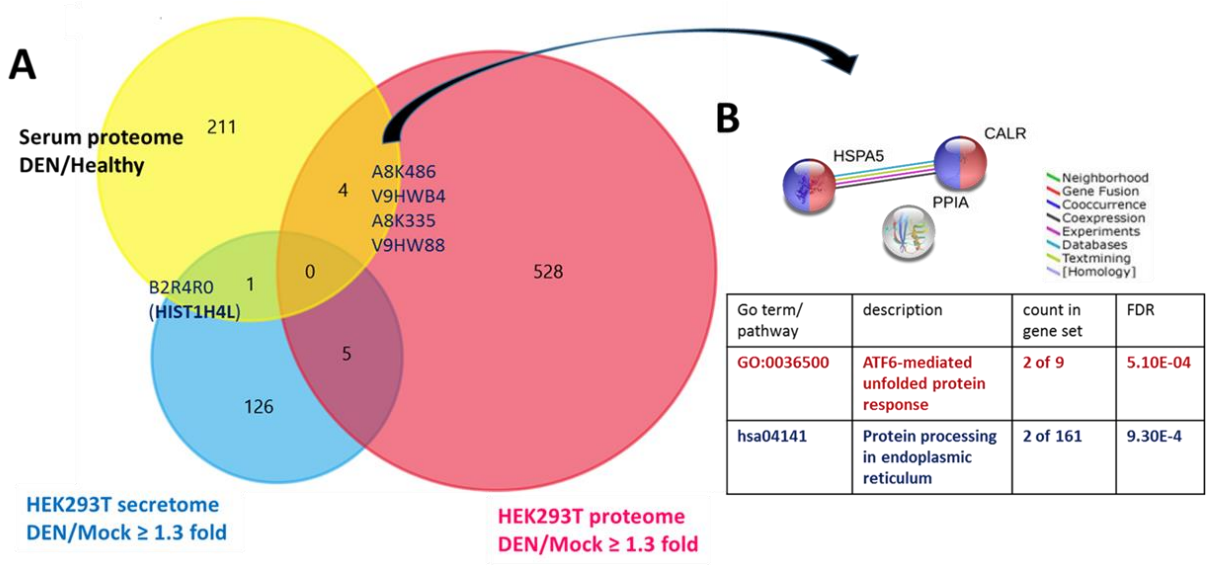

Go term/ pathway	description	count in gene set	FDR
GO:0036500	ATF6-mediated unfolded protein response	2 of 9	5.10E-04
hsa04141	Protein processing in endoplasmic reticulum	2 of 161	9.30E-4

Figure 6.4 Proteins that were commonly significantly altered in the proteomes and secretomes of DENV-2 infected HEK293T cells and clinical specimen from DEN patients.

(A) Venn diagram shows the number of proteins that were significantly (P-value <0.05) altered ≥1.3 fold in DENV-2 infected HEK293T cells or the associated secretomes compared with mock cells or significantly (FDR <0.05) altered ≥1.2 in the serum of DENV infected patients compared with healthy controls. **(B)** STRING analysis of proteins that were significantly altered in abundance in both DENV-2 infected HEK293T cells and serum of DENV infected patients. The STRING database was searched to analyse proteins that significantly altered in abundance in both DENV-2 infected HEK293T cells and the serum of DENV infected patients. Nodes representing proteins associated with the significantly enriched GOBP "ATF6-mediated unfolded protein response" and the KEGG pathway "Protein processing in endoplasmic reticulum" are shaded in red and blue, respectively. The number of coloured nodes/ total proteins involved for each term and the FDR of each GO term are listed in the table.

6.6 Comparative analysis of proteins that were commonly found in both the proteomes and secretomes of DENV-2 infected Huh-7 cells and clinical specimens from DEN patients.

6.6.1 Proteins that were commonly detected in the proteomes and secretomes of DENV-2 infected Huh-7 cells and clinical specimen from DEN patients.

To determine whether Huh-7 cells may be a useful model for examining DENV infection *in vitro*, the results of the proteome and secretome analysis of DENV-2 infected Huh-7 cells (described in Chapter 5) were compared with the proteomic analysis of serum samples from DENV infected patients compared to healthy persons. Overall, 533 and 489 proteins that were detected in the proteomes and secretomes of Huh-7 cells, respectively, were also detected in the serum proteome (Figure 6.5). Among these, 379 proteins were detected in both the proteome and secretomes of Huh-7 cells and serum proteome of DEN patients.

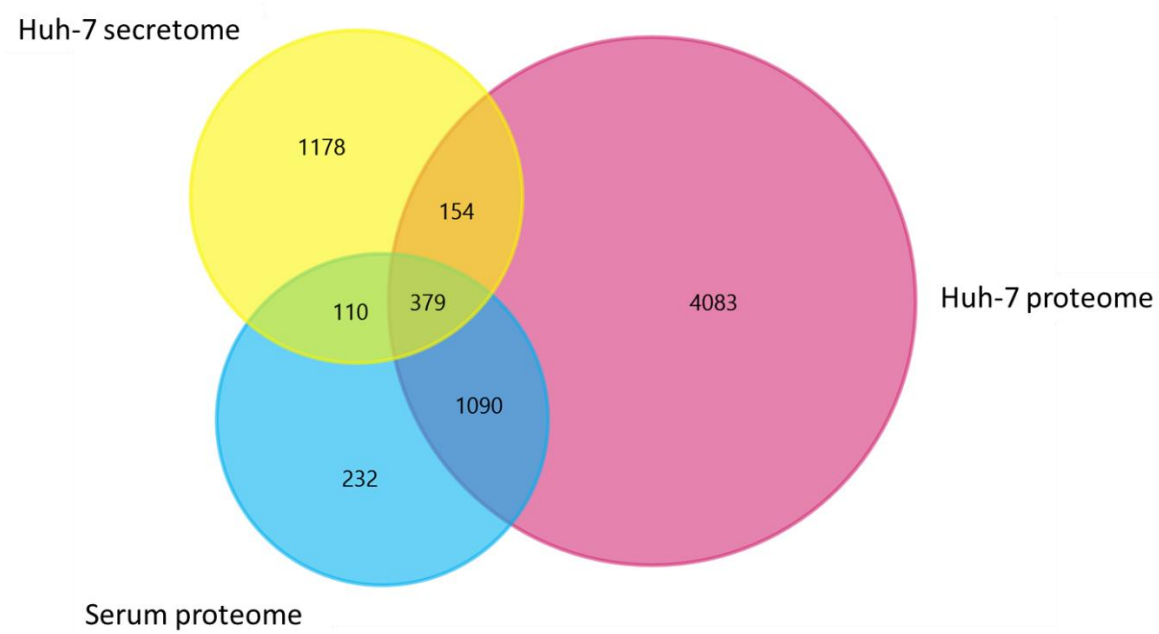

Figure 6.5 Proteins identified in the proteome and secretome of DENV-2 infected Huh-7 cells and the serum proteome of DENV infected patients.

Venn diagram shows the number of proteins that were detected in the proteome and secretome of DENV-2 infected Huh-7 cells and the serum of DENV infected patients.

Of the proteins found in both proteomics datasets, there were 50 proteins that were significantly (P-value < 0.05 and ≥ 1.3 fold) changed in the proteomes and/or secretomes from DENV-2 infected Huh-7 cellscompared with mock infected cells and significantly (FDR < 0.05 and ≥ 1.2 fold) altered in abundance in the serum of DENV infected patients compared to healthy persons (Figure 6.6 and Table 6.6). There were 18 proteins that were significantly altered only in Huh-7 cells and patient serum in response to DENV infection and 16 proteins that were significantly altered only in the secretome from Huh-7 cells and patient serum in response to DENV infection. Interestingly, there were 16 proteins that were significantly altered in response to DENV infection in all data sets (Huh-7 cells and associated secretomes and the serum of DEN patients).

Twelve of 16 proteins that were significantly altered in all three data sets in response to DENV infection were significantly decreased in response to DENV infection in cells, secretomes and serum (Table 6.6). These 12 proteins were FGA, FGB, FGG, F2, CFH, CFI, APOA1, APOC2, phospholipid transfer protein (PLTP), protein AMBP (AMBP), retinol binding protein 4 (RBP4) and nidogen-1(NID1). Interestingly, most of them were proteins involved in coagulation and lipid metabolism. In contrast, Fibrinogen-like protein 1 (FGL1), plasma alpha-L-fucosidase (FUCA2), mannosyl-oligosaccharide 1,2-alpha-mannosidase IA (MAN1A1) and alpha-1-acid glycoprotein 1 (ORM1) were significantly decreased in both DENV-2 infected Huh-7 cells and the associated secretome but increased in the serum of DEN patients.

Table 6.6 A list of proteins commonly significantly altered in the proteomes and secretomes of DENV-2 infected Huh-7 cells and clinical specimen from DEN patients.

Description	Gene	Proteome DENV-2/mock		Secretome DENV-2/mock		Serum proteome (Compared with healthy)					
						DEN wo WS/healthy		DEN w WS/healthy		SD/healthy	
		Fold change	P-value	Fold change	P-value	Fold change	FDR	Fold change	FDR	Fold change	FDR
Cellular proteome, secretome and serum proteome											
Apolipoprotein C-II	*APOC2*	0.44	4.34E-04	0.36	8.66E-03	0.36	2.06E-04	0.44	2.17E-03	0.90	8.30E-01
Apolipoprotein A-I	*APOA1*	0.39	9.29E-03	0.40	7.16E-04	0.73	4.69E-03	0.60	1.18E-03	0.55	1.17E-02
Fibrinogen alpha chain	*FGA*	0.36	1.28E-03	0.44	1.89E-02	0.32	4.19E-04	0.46	1.33E-01	0.22	7.10E-02
Fibrinogen beta chain	*FGB*	0.43	1.01E-03	0.44	2.67E-03	0.29	5.97E-04	0.48	1.65E-01	0.24	6.79E-02
Fibrinogen-like protein 1	*FGL1*	0.49	1.94E-02	0.50	8.24E-03	2.83	3.12E-05	2.76	1.66E-03	1.40	6.46E-01
Phospholipid transfer protein	*PLTP*	0.62	2.86E-02	0.59	1.18E-03	0.81	1.92E-01	0.77	3.94E-02	0.78	4.93E-01
Plasma alpha-L-fucosidase	*FUCA2*	0.60	3.53E-03	0.63	2.95E-02	1.34	8.81E-02	1.48	2.65E-02	1.72	6.89E-02
Protein AMBP	*AMBP*	0.34	7.46E-04	0.68	1.05E-02	0.69	4.92E-03	0.72	1.12E-02	0.74	4.82E-02
Retinol-binding protein 4	*RBP4*	0.44	5.58E-04	0.69	1.57E-02	0.50	1.20E-03	0.57	6.51E-03	0.66	8.85E-02
Mannosyl-oligosaccharide 1,2-alpha-mannosidase IA	*MAN1A1*	0.62	1.16E-02	0.69	1.54E-02	1.18	7.69E-02	1.31	1.29E-02	1.50	3.58E-02
Alpha-1-acid glycoprotein 1	*ORM1*	0.36	1.05E-03	0.71	7.53E-03	1.69	5.47E-04	1.78	3.23E-04	1.52	7.65E-02
Prothrombin O	*F2*	0.62	3.72E-02	0.72	3.47E-02	0.71	1.84E-03	0.73	4.50E-03	0.67	6.20E-03
Fibrinogen gamma chain	*FGG*	0.44	1.18E-03	0.40	2.49E-02	0.23	5.69E-04	0.49	2.06E-01	0.21	9.19E-02
Complement factor I	*CFI*	0.54	1.99E-03	0.65	4.30E-02	0.80	3.23E-02	0.76	9.15E-03	0.77	2.60E-02
Nidogen-1	*NID1*	0.62	7.47E-03	0.56	2.18E-02	1.95	2.90E-06	2.04	2.26E-05	2.52	3.20E-03
Complement factor H	*CFH*	0.68	3.51E-03	0.51	1.81E-02	0.62	4.39E-02	0.68	1.06E-01	0.57	8.99E-03
Cellular proteome and serum proteome											
Golgi membrane protein 1	*GOLM1*	0.40	1.17E-03	NSC	NSC	3.77	1.30E-05	3.12	1.15E-04	2.38	1.67E-02
Complement C3	*C3*	0.40	2.77E-05	NSC	NSC	0.84	1.58E-01	0.76	6.50E-02	0.77	2.98E-02
Fibronectin 1	*FN1*	0.47	5.21E-03	NSC	NSC	0.55	6.57E-03	0.63	9.66E-02	0.66	1.94E-01
Nucleobindin 1	*NUCB1*	0.47	8.30E-04	NSC	NSC	3.40	1.69E-06	4.05	1.15E-04	3.08	9.49E-02
Syndecan-1	*SDC1*	0.52	1.50E-02	NSC	NSC	19.65	3.79E-02	24.53	2.50E-01	38.99	5.27E-01
Complement C5	*C5*	0.54	7.61E-03	NSC	NSC	0.74	3.22E-02	0.72	2.61E-02	0.68	3.92E-02
Inter-alpha (Globulin) inhibitor H2	*ITIH2*	0.59	2.23E-02	NSC	NSC	0.64	1.67E-03	0.63	1.83E-03	0.69	2.91E-02
Antithrombin III	*SERPINC1*	0.61	3.82E-02	NSC	NSC	0.72	2.87E-03	0.87	4.59E-01	0.88	6.38E-01

Mannan-binding lectin serine protease 1	*MASP1*	0.62	3.68E-03	NSC	NSC	0.77	2.77E-02	0.82	1.26E-01	0.92	8.09E-01
Apolipoprotein C-I	*APOC1*	0.64	3.61E-03	NSC	NSC	0.43	1.69E-06	0.38	1.15E-04	0.48	6.60E-02
Prolow-density lipoprotein receptor-related protein 1	*LRP1*	0.66	1.46E-03	NSC	NSC	1.15	3.38E-01	1.28	5.58E-02	1.58	3.36E-02
Beta-2-glycoprotein 1	*APOH*	0.69	1.58E-02	NSC	NSC	0.38	1.27E-05	0.33	3.09E-05	0.42	5.54E-03
Selenoprotein P	*SEPP1*	0.74	6.43E-03	NSC	NSC	0.54	1.25E-05	0.51	3.94E-05	0.52	3.20E-03
Lymphocyte cytosolic protein 1	*LCP1*	1.57	1.48E-02	NSC	NSC	1.94	1.09E-04	2.10	1.25E-03	2.79	1.51E-02
Heat shock cognate 71 kDa protein	*HSPA8*	1.44	2.96E-03	NSC	NSC	2.33	1.33E-04	2.52	3.23E-04	2.88	4.65E-03
Endoplasmic reticulum chaperone BiP	*HSPA5*	1.38	1.03E-02	NSC	NSC	0.73	4.49E-03	0.87	3.97E-01	1.11	5.80E-01
Plasma protease C1 inhibitor	*SERPING1*	0.40	9.56E-03	NSC	NSC	1.21	1.68E-01	1.36	2.61E-02	1.38	2.63E-01
Tropomyosin alpha-4 chain	*TPM4*	2.29	4.59E-02	NSC	NSC	1.98	2.28E-02	1.57	2.35E-02	3.00	1.14E-01
Secretome and serum proteome											
Apolipoprotein B	*APOB*	NSC	NSC	0.61	3.35E-02	0.64	4.92E-03	0.65	4.90E-03	0.66	1.52E-01
Apolipoprotein C-III	*APOC3*	NSC	NSC	0.11	3.39E-02	0.43	6.13E-05	0.52	2.85E-03	0.77	4.16E-01
Monocyte differentiation antigen CD14	*CD14*	NSC	NSC	0.65	9.75E-03	1.66	2.27E-07	1.78	4.23E-06	1.46	1.72E-01
Carboxypeptidase B2	*CPB2*	NSC	NSC	0.68	2.50E-03	0.41	3.04E-08	0.41	2.33E-06	0.45	3.64E-04
Coagulation factor X	*F10*	NSC	NSC	0.57	1.34E-02	0.71	5.96E-03	0.75	1.61E-02	0.80	2.63E-01
Coagulation factor XIII B chain	*F13B*	NSC	NSC	0.62	1.88E-02	0.58	7.37E-05	0.60	1.75E-04	0.72	7.71E-02
C-1-tetrahydrofolate synthase, cytoplasmic	*MTHFD1*	NSC	NSC	1.75	9.84E-03	1.33	5.74E-01	2.33	3.88E-02	1.86	5.81E-01
N-deacetylase/N-sulfotransferase 1	*NDST1*	NSC	NSC	0.64	1.80E-02	0.53	5.60E-02	0.46	1.41E-02	0.37	4.53E-02
Out at first protein homolog	*OAF*	NSC	NSC	0.41	3.60E-03	1.58	2.95E-04	1.72	1.92E-03	1.52	2.15E-01
Alpha-1-acid glycoprotein 2	*ORM2*	NSC	NSC	0.67	1.62E-02	1.32	6.74E-02	1.49	9.86E-03	1.27	3.85E-01
Proprotein convertase subtilisin/kexin type 9	*PCSK9*	NSC	NSC	0.60	4.76E-03	1.59	1.37E-05	1.62	2.97E-03	1.54	6.07E-02
Prenylcysteine oxidase 1	*PCYOX1*	NSC	NSC	0.63	6.87E-03	0.58	7.14E-05	0.62	4.31E-03	0.60	2.97E-02
Serum paraoxonase/ arylesterase 1	*PON1*	NSC	NSC	0.72	1.21E-02	0.78	4.59E-02	0.70	9.90E-03	0.61	3.10E-03
Protein S isoform 2	*PROS1*	NSC	NSC	0.63	4.25E-02	0.78	1.41E-02	0.77	1.71E-02	0.71	1.14E-02
Alpha-1 antiproteinase	*SERPINA4*	NSC	NSC	0.64	8.58E-03	0.56	3.96E-05	0.55	1.64E-04	0.61	3.76E-03
Pigment epithelium-derived factor	*SERPINF1*	NSC	NSC	0.69	2.25E-02	0.74	2.08E-02	0.68	7.98E-03	0.63	3.20E-03

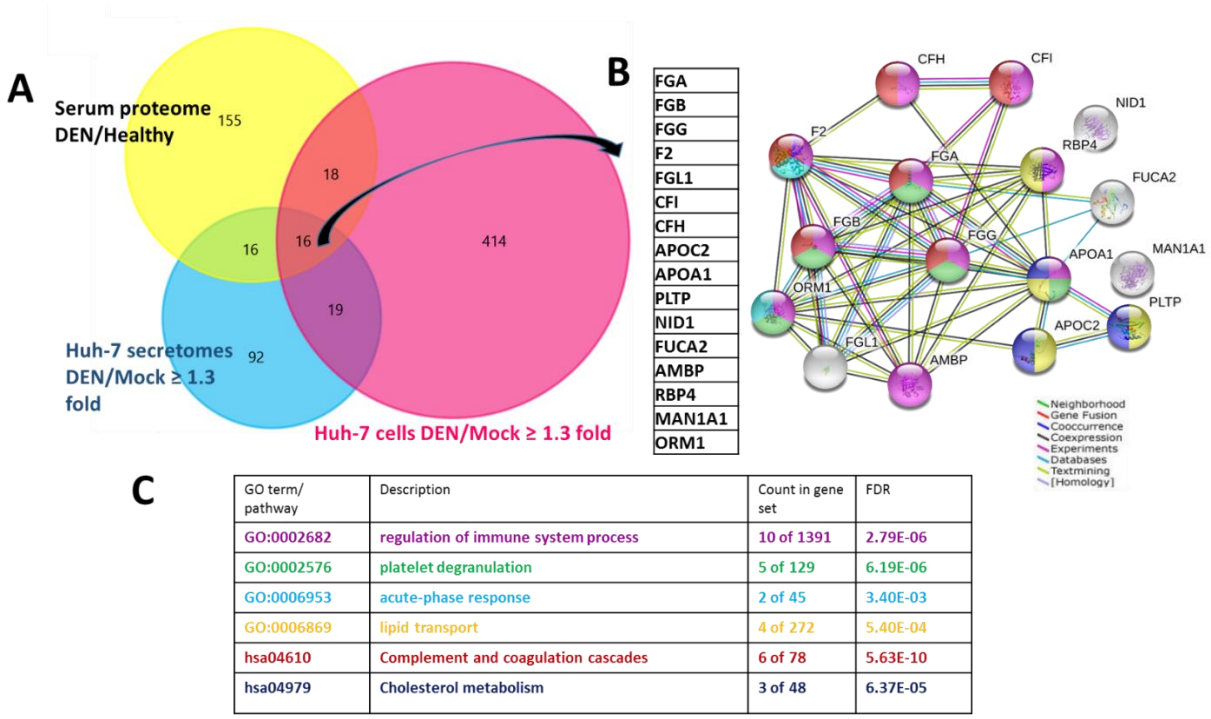

C

GO term/ pathway	Description	Count in gene set	FDR
GO:0002682	regulation of immune system process	10 of 1391	2.79E-06
GO:0002576	platelet degranulation	5 of 129	6.19E-06
GO:0006953	acute-phase response	2 of 45	3.40E-03
GO:0006869	lipid transport	4 of 272	5.40E-04
hsa04610	Complement and coagulation cascades	6 of 78	5.63E-10
hsa04979	Cholesterol metabolism	3 of 48	6.37E-05

Figure 6.6 Proteins that were significantly altered in the proteome and secretome from DENV-2 infected Huh-7 cells and the serum proteome of DENV infected patients.

(A) Venn diagram shows the number of proteins that were significantly (P-value <0.05) altered ≥1.3 fold in DENV-2 infected Huh-7 cells or associated secretomes compared with mock cells or significantly (FDR <0.05) altered ≥1.2 in serum of DENV infected patients compared with healthy controls **(B)** The table lists 16 intersect proteins that were significantly altered in abundance in response to infection in DENV-2 infected Huh-7 cells/secretomes and serum of DENV infected patients **(C)** STRING analysis of 16 intersect proteins that were significantly altered in abundance in response to infection in DENV-2 infected Huh-7 cells/secretomes and serum of DENV infected patients. The STRING database was searched to analyse proteins that were commonly significantly altered in abundance in the proteome and secretome of DENV-2 infected Huh-7 cells and the serum proteome of DEN patients compared to controls. Nodes representing proteins associated with the significantly enriched GOBP "regulation of immune system process", "platelet degranulation", acute-phase response and "lipid transport" as well as the KEGG pathway of "Complement and coagulation cascades" and "Cholesterol metabolism" are shaded in purple, green, light blue, yellow, red and blue, respectively. The number of coloured nodes/ total proteins involved for each term and the FDR of each GO term are listed in the table.

6.6.2 Bioinformatic analysis of proteins that were commonly significantly altered in the proteomes and secretomes of DENV-2 infected Huh-7 cells and serum samples from DEN patients.

To identify proteins and cellular processes that were commonly dysregulated in Huh-7 cells and patient serum in response to DENV infection, 50 proteins that were significantly altered in the serum of DEN patients and the proteome and/or secretomes of Huh-7 cells were subjected to downstream bioinformatics analysis.

DAVID analysis revealed that common proteins that were significantly altered in amount in Huh-7 cells and/or secretomes and in patient serum in response to infection were enriched in 12 clusters of proteins (Figure 6.7, Supplementary Table S6.4). The top three clusters were associated with the UP keywords "secreted/signal peptide", the GOCC term "extracellular region" (GO:0005576) and the GOBP term "negative regulation of endopeptidase activity" (GO:0010951), respectively. Moreover, the common dysregulated proteins were also significantly enriched in proteins associated with the GOCC term "blood microparticle" (GO:0072562) and the GOBP terms "innate immune response" (GO:0045087) and "lipoprotein metabolic process" (GO:0042157).

STRING analysis revealed that serum proteins that were altered in response to DENV-2 infection were associated with multiple significantly enriched GO terms. GOBP terms that were associated with DEN pathogenesis included "immune response" (GO:0006955), "platelet degranulation" (GO:0002576), "acute-phase response" (GO:0006953) and "post-translational protein modification" (GO:0043687) (Figure 6.8). Protein clusters were also associated with the enriched KEGG pathways "complement and coagulation cascades" (hsa04610) and "Cholesterol metabolism" (hsa04979).

In addition, 16 proteins that were significantly altered in all data sets (Huh-7 proteome and secretome and serum proteome) were also analyzed by STRING analysis. The results revealed that these 16 proteins were associated with significantly enriched GOBP terms that were also related to DENV infection including "regulation of immune system process" (GO:0002682), "platelet degranulation" (GO:0002576), "acute-phase response" (GO:0006953) and "lipid transport" (GO:0006869) as well as the KEGG

pathway terms “Complement and coagulation cascades” (hsa04610) and “Cholesterol metabolism” (hsa04979) (Figure 6.6).

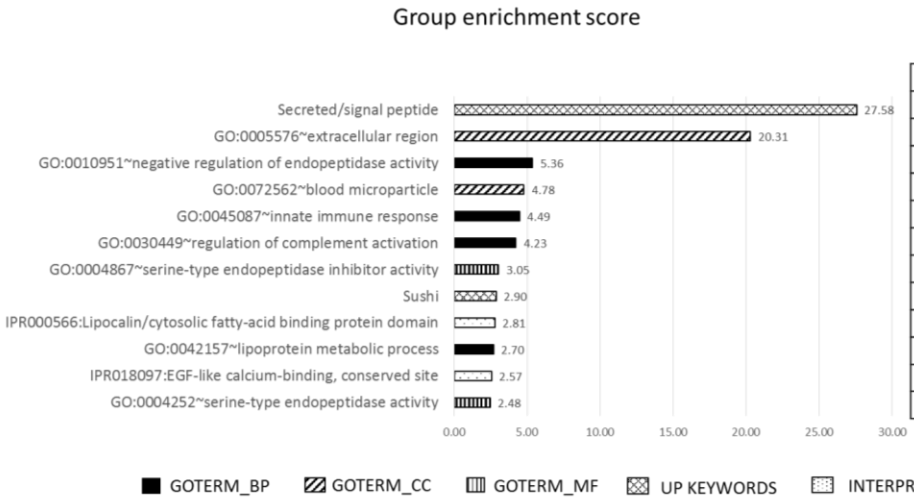

Count	%	P-value
29	59.18	1.05E-32
24	48.98	2.81E-25
8	16.33	1.02E-09
15	30.61	2.57E-20
4	8.16	1.53E-02
5	10.20	2.58E-06
5	10.20	1.15E-05
3	6.12	1.05E-03
3	6.12	1.11E-03
6	12.24	5.17E-08
4	8.16	1.63E-04
5	10.20	1.29E-04

Figure 6.7 DAVID analysis of proteins that were commonly altered in abundance in the cellular proteome and/or secretome of DENV-2 infected Huh-7 cells and the serum proteome.

Proteins that were significantly (FDR < 0.05) altered in amount by ≥ 1.2 fold in DENV-infected patient serum compared to healthy controls and significantly (P-value < 0.05) altered (≥ 1.3 fold) in the proteome and/or secretomes of DENV-2 infected Huh-7 cells were analysed using the DAVID database. The GO accession numbers/terms that were significantly enriched and the properties of the corresponding protein clusters are shown. The GES of significantly enriched GO terms are plotted as bar graphs with the corresponding GES score shown. The shading shows the type of GO term (GOBP, GOCC or GOMF), UP keywords, Interpro term or KEGG pathway. The number of proteins in each cluster (count), number of proteins associated with each GO term/total number of proteins in the dataset (%) and P-value for each of the annotation terms are listed in the table.

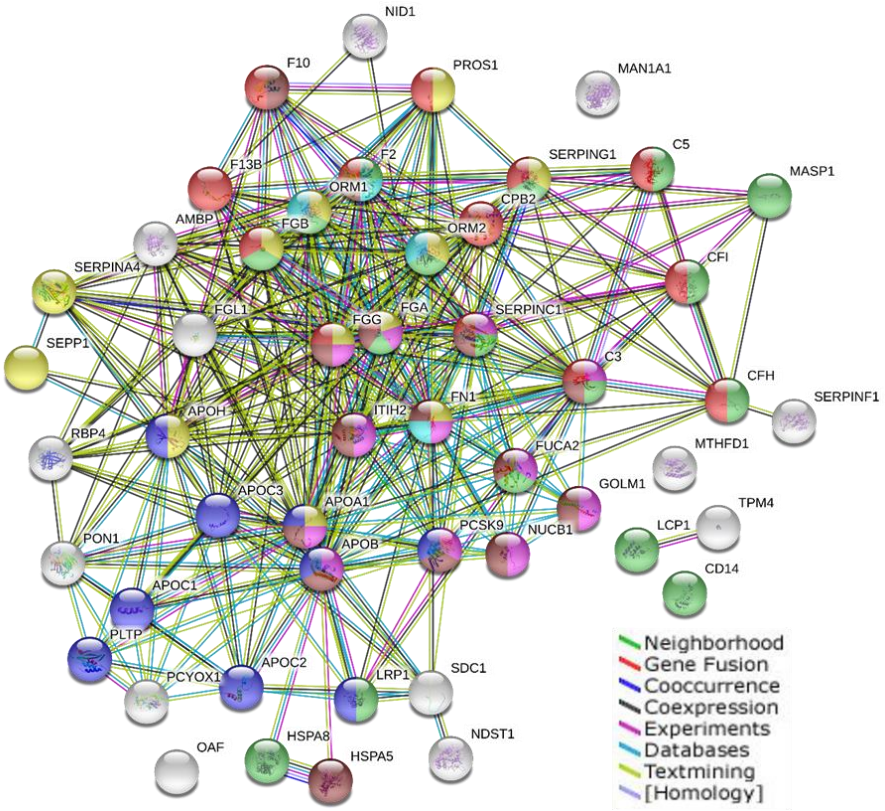

GO term/ pathway	Description	Count in gene set	FDR
GO:0002576	platelet degranulation	12 of 129	7.11E-13
GO:0006955	immune response	17 of 1560	2.71E-06
GO:0006953	acute-phase response	4 of 45	7.51E-05
GO:0043687	post-translational protein modification	12 of 365	6.64E-09
GO:0005788	endoplasmic reticulum lumen	15 of 299	4.33E-14
hsa04610	Complement and coagulation cascades	14 of 78	4.13E-20
hsa04979	Cholesterol metabolism	9 of 48	4.96E-13

Figure 6.8 STRING analysis of cellular proteins that were altered in abundance in the cellular proteome and/or secretome of DENV-2 infected Huh-7 cells and the serum proteome.

The STRING database was searched to analyse proteins that were significantly (FDR < 0.05) altered in amount by ≥ 1.2 fold in DENV-infected patient serum compared to healthy controls and significantly (P-value < 0.05) altered (≥ 1.3 fold) in the proteome and/or secretome of DENV-2 infected Huh-7 cells. Nodes representing proteins associated with the significantly enriched GOBP "platelet degranulation", "immune response", "acute-phase response", and "post-translational protein modification" as well as the KEGG pathway "Complement and coagulation cascades" and "Cholesterol metabolism" are shaded in yellow, green, purple, light blue, red and blue, respectively. The number of coloured nodes/ total proteins involved for each term and the FDR of each GO term are listed in the table.

6.7 Effect of DENV infection on *in vitro* and *in vivo* changes of the complement and coagulation cascades

The integrated analysis of the proteome and secretome data from DENV infected Huh-7 cells and the serum proteomic data from DENV infected patients, and the subsequent downstream bioinformatic analysis, identified proteins involved in "complement and coagulation cascades" to be commonly dysregulated in response to DENV infection. Thus, these proteins, highlighted in the KEGG pathway "complement and coagulation proteins" (Figure 6.9.) were a focus of further investigation.

In terms of the "coagulation cascade", there were common alterations in proteins involved in both the coagulation and fibrinolysis systems. The decrease in the cellular level of all FBG subunit proteins and F2 in response to DENV infection could explain their decrease in the cell secretome which also correlated with the decreased amounts detected in the serum from DEN patients compared with healthy individuals. Proteins involved in the anticoagulation system including SERPINC1, heparin cofactor II (HCII or SERPIND1) and protein C inhibitor (PCI or SERPINA5) were also altered in the Huh-7 cell model and/or in the serum proteome. In terms of proteins involved in the complement system, DENV infection effected proteins involved in all three pathways (classical, alternative and lectin) both *in vitro* and *in vivo*.

List of Supplementary Tables

Table S 6.1 Characteristics of DENV infected patients and healthy controls participating in the study

Table S 6.2 Results of serum proteomic analysis of DENV infected patients and healthy controls (all protein list)

Table S 6.3 DAVID analysis of proteins that were significantly altered in the serum of DEN patients compared to healthy controls.

Table S 6.4 DAVID analysis of proteins that were commonly altered in abundance in the cellular proteome and/or secretome of DENV-2 infected Huh-7 cells and the serum proteome.

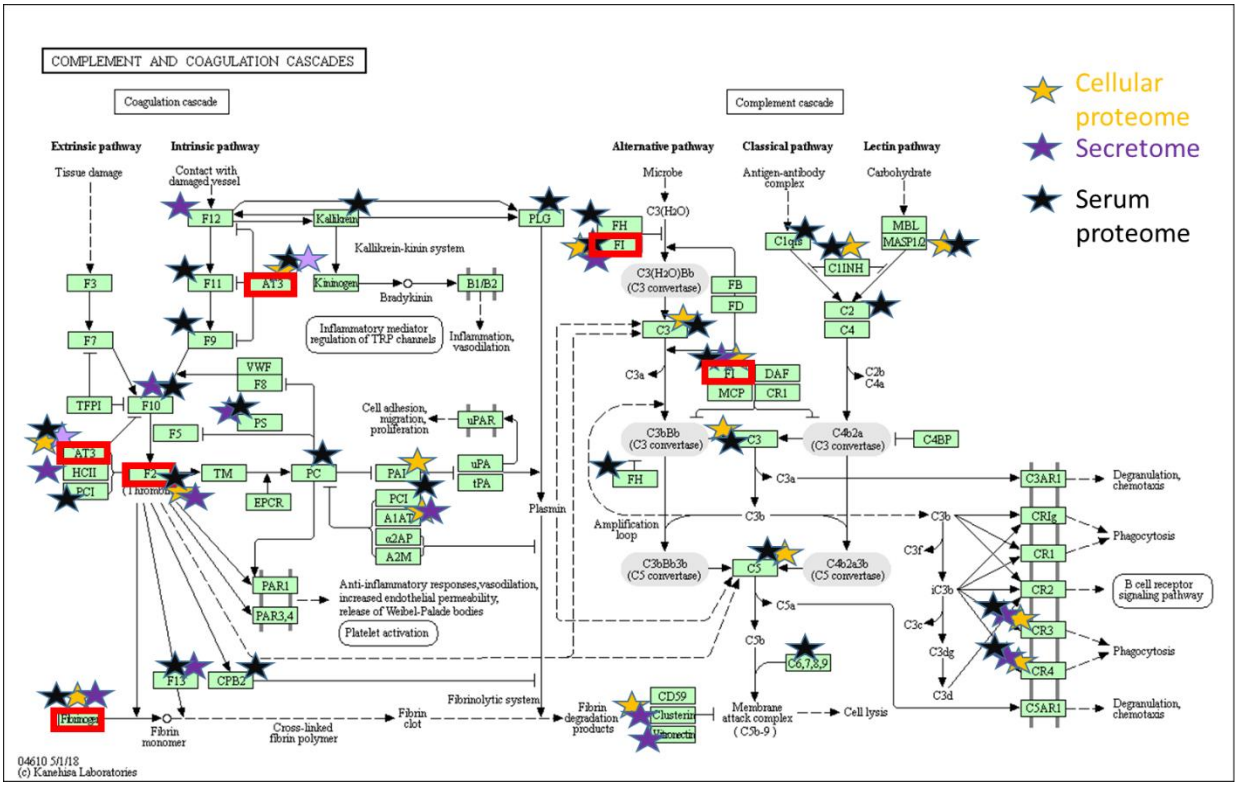

CD46 molecule(CD46), CD55 molecule (Cromer blood group)(CD55), CD59 molecule(CD59), alpha-2-macroglobulin(A2M), bradykinin receptor B1(BDKRB1), bradykinin receptor B2(BDKRB2), carboxypeptidase B2(CPB2), coagulation factor II, thrombin receptor(F2R), coagulation factor II, thrombin(F2), coagulation factor III, tissue factor(F3) ,coagulation factor IX(F9), coagulation factor V(F5), coagulation factor VII(F7), coagulation factor VIII(F8), coagulation factor X(F10), coagulation factor XI(F11), coagulation factor XII(F12), coagulation factor XIII A chain(F13A1), coagulation factor XIII B chain(F13B), complement C1q A chain(C1QA), complement C1q B chain(C1QB), complement C1q C chain(C1QC), complement C1r(C1R), complement C1s(C1S), complement C2(C2), complement C3(C3), complement C3a receptor 1(C3AR1), complement C3b/C4b receptor 1 (Knops blood group)(CR1), complement C3d receptor 2(CR2), complement C4A (Rodgers blood group)(C4A), complement C4B (Chido blood group)(C4B), complement C5(C5), complement C5a,receptor 1(C5AR1), complement C6(C6), complement C7(C7), complement C8 alpha chain(C8A), complement C8 beta chain(C8B), complement C8 gamma chain(C8G), complement C9(C9), complement component 4 binding protein alpha(C4BPA), complement component 4 binding protein beta(C4BPB), complement factor B(CFB), complement factor D(CFD), complement factor H(CFH), complement factor I(CFI), fibrinogen alpha chain(FGA), fibrinogen beta chain(FGB), fibrinogen gamma chain(FGG), kallikrein B1(KLKB1), kininogen 1(KNG1), mannan binding lectin serine peptidase 1(MASP1), mannan binding lectin serine peptidase 2(MASP2), mannose binding lectin 2(MBL2), plasminogen activator, tissue type(PLAT), plasminogen activator, urokinase receptor(PLAUR), plasminogen activator, urokinase(PLAU), plasminogen(PLG), protein C, inactivator of coagulation factors Va and VIIIa(PROC), protein S (alpha)(PROS1), serpin family A member 1(SERPINA1), serpin family A member 5(SERPINA5), serpin family C member 1(SERPINC1),serpin family D member 1(SERPIND1), serpin family E member 1(SERPINE1), serpin family F member 2(SERPINF2), serpin family G member 1(SERPING1), thrombomodulin(THBD), tissue factor pathway inhibitor(TFPI), von Willebrand factor(VWF)

Figure 6.9 Complement and coagulation cascade pathways.

Proteins that significantly (P-value < 0.05) altered (≥ 1.3 fold) in DENV-2 infected Huh-7 cells and associated secretomes compared to mock infected cells as well as serum proteins that were significantly (FDR < 0.05) altered (≥1.2 fold) in DENV infected patients compared to healthy controls are identified on the KEGG pathways "complement and coagulation cascades (KEGG pathway term hsa04610). The yellow, purple and black stars indicate proteins that significantly altered in proteomes, secretomes and serum proteome, respectively in response to DENV-2 infection. SERPINC1, a protein which decreased, but not significantly, in DENV-2 infected cells, is indicated in faint purple

6.8 Discussion

In this chapter, the proteomic analysis of serum from a cohort of DENV infected patients and healthy individuals was performed. In total, 216 serum proteins were significantly altered in abundance in response to DENV infection and two proteins (CRP and APOC2) were significantly altered which correlated with disease severity. The serum proteome was then compared with cellular proteomes and secretomes from HEK293T and Huh-7 cell models to identify common protein responses to DENV infection.

Analysis of serum and other samples from such a cohort can provide invaluable insight into the global protein changes in the blood in response to DENV infection. A significant strength of the human cohort analysed in this study is the large age range and disease severity coverage it achieved. However, owing to the logistics of sample collection and processing, analysis of this cohort does carry certain caveats which are presented below. The nature of retrospective studies using archived clinical specimens meant that some data, both clinical and relating to basic characteristics, were not available or not collected. Moreover, age matching was not complete between healthy and DENV infected individuals. Additionally, over half of the patients with SD (five of nine cases) were diagnosed using a positive IgM test result but had a negative DENV RT-PCR result. This was not unexpected as SD typically manifests after viremia or NS1 antigenemia subside.

Some aspects of the serum proteomic analysis are worth mentioning to clarify the interpretation of the results. First is the effect of ALB and IgG depletion, which is an essential part of serum/plasma proteomics sample preparation. ALB and IgG were depleted but due to varying starting concentrations and depletion efficiencies in different samples it is challenging to normalise the total amounts of protein in each sample. This step might also result in the loss of proteins that bind to ALB (Jacobs *et al*., 2005). Both endogenous and exogenous (drug and toxin) molecules/substances bind with ALB in serum, the endogenous molecules included hormones, ions (such as calcium and copper), fat-soluble vitamins, fatty acids and lipoproteins (Throop *et al*., 2004). Furthermore, the effect of DEN on ALB as a key volume regulator and negative APP cannot be interpreted because it was depleted to different extents in different samples.

Importantly, when measuring the levels of proteins involved in coagulation, blood samples are collected into tubes containing anticoagulants to prevent clot formation, then cells are removed by centrifugation to produce plasma. By contrast, in serum preparation, blood is left around 30–60 mins at RTemp for clot formation, before centrifugation, to remove the clot and cells. Therefore, coagulation factors are consumed during clot formation in the preparation of serum. Because coagulation factors such as FBG, SERPINA1 and alpha-2-macroglobulin (A2M) are present in high abundance in whole blood (Kuscuoglu *et al*., 2018), the coagulation proteins may still be present in serum after clot formation. Thus, when analysing serum using proteomics, results pertaining to coagulation proteins should be interpreted with caution. To help solve this problem, the results from the serum proteomic analysis in this study were compared with the results of available clinical studies primarily designed to study complement and coagulations proteins in DENV infected patients (discussed in the next section). On the other hand, the levels of complement proteins can be analysed in either serum or plasma samples however the 'normal range' of these proteins differs between the two sample types (Yang *et al*., 2015).

Finally, other factors including gender, genetics, nutritional status and co-morbidities as well as previous or current medications are likely to affect the serum proteomic profiles of all sampled individuals. However, due to lack of data about other mentioned factors, only age and gender could be used for interpretation. All these aspects (serum effects and available demographic data) were taken in account in the interpretation of the serum proteomic results presented here.

Proteomic analysis of serum samples from DENV infected patients

The major serum proteins dysregulated in response to DENV infection identified in this study are associated with processes relating to "complement and coagulation" proteins and "lipoproteins/lipid transport" proteins. The results presented in this thesis were compared with previous studies that analysed blood samples from DENV infected patients compared with healthy controls (summarised in Table 6.1). In terms of methodology, four of these studies conducted 2D-DIGE followed by MS/MS (Ray *et al*. 2013; Albuquerque *et al*., 2009; Thayan *et al*., 2009a; Thayan *et al*., 2009b) whilst two others conducted

iTRAQ based proteomic analysis (Jadhav *et al*., 2017; Kumar *et al*., 2012). In comparison to these previous serum/proteomic studies, the data presented in this thesis represents the biggest non-pooled serum study conducted to date. The disadvantage of pooling specimens is that outlier values can skew the results and information pertaining to with-in group variation is lost (Geyer *et al*., 2017). Moreover, our use of advanced TMT labelling LC-MS/MS enabled a substantially higher resolution proteomic analysis, enabling the detection of a greater number of DENV induced protein alterations than in previously published studies.

The overlap of proteins which were identified to be altered in abundance in response to DENV infection in different studies is shown in Figure 6.10 and listed in Table 6.7. The study of Huy *et al.,* (Huy *et al*., 2013) was excluded from this comparison as they reported only proteins detected in CIC for each group of patients but quantification data was not provided. Overall, proteins with an altered abundance in response to DENV infection that were commonly detected between our study and other studies are involved in complement coagulation cascades and lipid metabolism including; FGG, F2, C3, SERPINC1, alpha 1-antichymotrypsin (SERPINA3), C1 inhibitor (SERPING1), APOA1, APOA4 and APOB.

Overall the majority of the proteins commonly altered in the "complement and coagulation" pathways in this study and previous studies change in the same direction. A similar decrease in F2 was reported in this study and the study of Albuquerque *et al*. (Albuquerque *et al*., 2009). Similarly, SERPINA3 and SERPING1 were increased in DEN patients in this study and previous studies. C3 was decreased in this study and the study of Albuquerque *et al*. but increased in the study of Ray *et al*. (Ray *et al*., 2012). Similar increases in C9 were observed in this study and the study of Kumar *et al.*, (Kumar *et al., 2012*). Opposite results were reported for both FGG and SERPINC1, these two proteins were decreased in this study but increased in other previous studies. However, the results of this study, which were more similar to clinical studies primarily done to study these two proteins in DEN patients, may be more accurate (discussed later). However, SERPINA1, which was not significantly decreased in our data, was found to be significantly altered in DENV infected patients in four other studies (Ray *et al*. 2013; Thayan *et al*., 2009a; Jadhav *et al.,* 2017; Kumar *et al.,* 2012). Only Thayan's study reported a decreased in serum

SERPINA1 while the other three studies reported significant increases in SERPINA1 during DENV infection.

This study	(216)						
Kumar et al., 2012/35	(35)	17					
Ray et al., 2012	(18)	4	6				
Thayan et al., 2009a (PBMC)	(8)	3	1	0			
Thayan et al., 2009b (serum)	(1)	0	1	1	0		
Jadhav et al., 2017	(16)	6	5	3	0	1	
Albuquerque et al., 2009	(14)	7	6	3	1	0	6
		This study	Kumar	Ray	Thayan a	Thayan b	Jadhav
		(216)	(35)	(18)	(8)	(1)	(16)

Figure 6.10 Comparison of proteins altered in DENV infected patients compared to healthy controls from published studies and the data presented in this thesis.

The proteins that were significantly (FDR < 0.05) increased and decreased (≥1.2 fold) in the serum of DENV infected patients compared to healthy persons in this study were compared with reported changes in previous serum/plasma proteomic studies of DENV infected patients using the gene name. The numbers of proteins that were commonly detected between these studies are showed and the total number of differentiated proteins that were reported to be significantly altered in each study are listed in brackets.

Table 6.7 A list of serum proteins commonly altered in response to DENV infection in this study and other studies

Study	Kumar *et al.*, 2012	Albuquerque *et al.*, 2009	Jadhav *et al.*, 2017	Ray *et al.*, 2012	Thayan *et al.*, 2009a
no. of common altered proteins/total proteins altered in the study	17/35	7/14	6/16	4/18	3/8
Proteins	ACTB AHSG APOA1 APOC1 APOC3 APOC4 APOC2 C9 GPLD1 IGFBP3 ITIH2 ORM1 ORM2 PON1 SERPINA3 SERPINC1 SERPING1	APOA1 F2 FGG C3 ORM1 SERPINA3 SERPING1	APOA1 APOB AZGP1 CFH ITIH1 SERPING1	APOA4 CFH C3 SERPINA3	ACTB ALDOA FGG

The observed significant decreases in complement and coagulation proteins in serum from infected individuals compared to controls in our study is in line with data from other clinical studies previously done on DENV patients with standard protocols for blood collection to study complement and coagulation proteins (Wills *et al*., 2002, Bokischet *et al.*, 1973). The significant decreases in FBG, protein C (PROC), protein S (PROS1) and SERPINC1 in patients with DEN compared to healthy patients presented in this study is similar to previous findings. Specifically, Wills *et al*., prospectively studied the levels of coagulation proteins in plasma samples from children with DSS at the time of illness compared with one month after illness (used as a control) (Wills et al., 2002). Similarly, decreases in C1q, C3, C5 and C8 but increases in C9 were also observed in complement samples from children with DHF or DSS compared to healthy control children (Bokisch *et al.*, 1973). By contrast, Viktor *et al.*, (Viktor *et al*., 1973) observed a reduced abundance of C2 and C4 in DHF patients was not observed in this study. Moreover, decreases in plasma FBG levels but an increase in fibrinogen degradation product (FDP) were also demonstrated in DHF patients compared to healthy children in the study of Bokisch *et al*., (Bokisch et al., 1973).

Similar decreases in lipoproteins including APOA1, APOA4, APOB and APOC were observed in DENV infected patients compared with healthy individuals in this study and all previous studies. However, the interpretation of lipoproteins as potential biomarkers for DEN has some limitations. Firstly, certain types of lipid sub-classes such as cholesterol and triglycerides (TG) should be measured using samples collected from individuals in a fasting state ($\geq$ 9 h); however, collection of such samples from DENV infected patients during their first presentation is not possible. Importantly, comorbidities such as hyperlipidaemia and cardiovascular diseases directly affect baseline lipid profiles. The high APOB levels and a low APOA1 level were proposed to be a strong predictor of ischemic heart diseases and mortality (Walldius *et al*., 2001). Moreover, lipid lowering agents which are commonly used nowadays may modulate the results of lipid profiles. Finally, as this study was retrospective in nature, data describing comorbidities and medications as well as baseline lipid profiles were not available. As such the dysregulation of lipoproteins identified in this study cannot be reliably interpreted as a response from DENV infection.

The functional groups of proteins, biological processes and pathways changed in response to DENV infection identified in this study were also reported in previous studies. In the iTRAQ-based serum proteomic study of DEN patients compared with healthy, the most common functional group of proteins was the acute phase response, followed by serpin group proteins, lipid transporters and complement factors (Kumar *et al*., 2012). A study that analysed virus-enriched fractions from pooled plasma of DF and SD patients by LC-MS/MS identified the top enriched pathways as "acute phase response signalling" followed by, "LXR/RXR activation pathway", "complement system" and "coagulation system" (Fragnoud *et al.,* 2105). Moreover, proteins associated with the KEGG pathway "complement and coagulation cascades" were significantly enriched in patients infected with DENV compared with healthy controls in non-pooled serum proteomic studies (Ray *et al*., 2012, Jadhav *et al*., 2017).

Apart from clinical parameters such as Hct, Plt and WBC count and liver enzyme levels, CRP has been proposed as a potential protein biomarker to distinguish DEN from other OFI. CRP, a liver APP, is an inflammatory marker widely used in clinical practice; moreover, the RDTs for CRP is available. As a positive APP, CRP is elevated above the normal range in all infection including DEN. Many studies have compared clinical and laboratory findings to distinguish between disease caused by DEN and OFI and reported that the CRP level in DEN was significantly lower than infections of other origins including leptospirosis (Le Turnier *et al.,* 2019) and malaria (Kutsuna *et al.,* 2014). One prospective study in Thailand proposed CRP levels as an indicator of viral vs bacterial infection, with a greater reduction in CRP observed for the former compared with the latter (Wangrangsimakul *et al*., 2018). Whilst the normal level of serum CRP in healthy patients is < 3 mg/L, values of mean IQRs for CRP in DENV infected patients of 5.1 (IQR 2.7–9.3) and 12.5 (6.0–26.0) respectively have been reported (Kutsuna *et al.,* 2014; Wangrangsimakul *et al.,* 2018). This study also detected significant increases in CRP abundance in DENV infected patients when compared with healthy controls.

Serum proteins correlate with disease severity

As an inflammatory marker, CRP was also previously proposed as a predictive biomarkers of disease severity, and indeed a significant decrease in the abundance of CRP

in serum from patients with SD compared to other DEN patients was identified in this study. In contrast, analysis of CRP levels in adult DEN patients demonstrated a significantly higher level of CRP in severe compared with non-severe DEN in both the febrile and critical phases (Chen *et al.*, 2015). Another study, which compared clinical and laboratory findings to predict severity of DEN in children, reported no difference in CRP in different severities of the disease (Prabhavathi et al., 2017). The contradictory results may result from differences in the age range of sampled patients between these studies. This is supported by results of a study of clinical and laboratory findings which included both children and adult DEN patients and revealed significantly lower CRP in children compared to adults (Ho *et al*., 2013).

Decreases in APOC2 in response to DENV infection were found both *in vivo* and *in vitro* (Huh-7 cells and the associated secretome). There is only one *in vivo* study which previously reported changes in APOC2 in DENV. An analysis of sera from DF, DHF and healthy individuals by iTRAQ/LC-MS/MS also reported a significant decrease in APOC2 abundance in samples from DF patients compared to healthy controls in the acute phase of the disease (Kumar *et al*, 2012). However, APOC2 is a component of very low density lipoproteins (LDL) and chylomicrons; thus, fasting blood is required for reliable measurement. Further investigation of the role of APOC2 as a biomarker for DENV diagnosis and predicting disease severity are required.

<u>Comparative analysis of proteins dysregulated in both the proteome and secretome from HEK293T cells and serum in response to DENV infection.</u>

Whilst there were hundreds of proteins that were commonly detected in the proteome and secretome of HEK293T cells and serum samples, only four cellular and one secreted protein were significantly altered in response to DENV infection, both *in vitro* and *in vivo*. The cellular proteins that were significantly altered in both HEK293T cells and patient sera in response to infection were associated with the UPR.

As mentioned in Chapter 4, HSPA5 and CALR are ER chaperones that were commonly found to be increased in response to DENV infection in many cell-based proteomic studies (Pando-Robles *et al*., 2014; Chiu *et al*., 2014; Chiu, 2014) and an integrated ‘omic’ analysis (Amemiya *et al*., 2019). To date, dysregulation of both HSPA5

and CALR has not been reported in a clinical study. The data presented here therefore constitutes the first reported alteration of these two proteins in clinical specimens in response to DENV infection. The significant increase in the abundance of CALR in response to infection in DENV-2 infected HEK293T cells correlates with an increase in the abundance of CALR in the sera of DEN patients of all severities compared to the healthy controls. However, whilst HSPA5 was increased in various DENV-2 infected cell lines (Pando-Robles et al., 2014; Chiu *et al*., 2014) including those used in this study, it's abundance was significantly decreased in serum from patients with DEN w/o WS compared to healthy controls (and not significantly decreased in DEN w WS and SD compared to controls). The use of HSPA5 and CALR as biomarkers for diagnosis warrants further investigation as well as analysis of the mechanism driving the opposing changes in protein abundance between cellular and serum HSPA5 levels in response to DENV infection.

However, other proteins that were significantly enriched in serum in response to DENV infection and associated with GO terms such as "complement and coagulation cascades", "lipid metabolism" and "immune response" were either not detected or not significantly enriched in HEK293T cells infected with DENV compared to mock controls. This may be because HEK293T cells are not major contributors to haemostatic and lipid protein synthesis.

As a part of the histone complex, HIST1H4L, is a major protein component of chromatin and plays a role in gene regulation. HIST1H4L was significantly increased in response to DENV infection in both the secretome from HEK293T cells and sera. To date there is only a single study analyzing the interplay between histones and DENV infection. An interaction between the DENV C protein and all types of histones (analysed by tandem-affinity purification and Co-IP) and co-localization between DENV C protein and histones was demonstrated using DENV-2 infected Huh-7 cells (Colpitts *et al*., 2011). Moreover, the DENV C protein was proposed to act as a histone mimic, forming heterodimers with core histones and binding with DNA (Colpitts *et al*., 2011). This may explain the increase in the level of HIST1H4L in DENV infection.

Taken together, these results show that HEK293T cells may be used as a model for studying changes in general host cellular pathways such as the UPR or ER in response to DENV infection *in vivo.* In contrast, they have limited utility for studying processes such complement and coagulation pathways, lipid metabolism and immune response proteins *in vivo*. Unfortunately, the low number of significantly altered proteins in the secretomes of DENV-2 infected HEK293T cells detected in this study correlates poorly with the serum proteomic results. Thus, the relevance of the HEK293T cell secretomes study to DENV infection *in vivo* is inconclusive.

Comparative analysis of proteins that are dysregulated in the proteome and secretome from Huh-7 cells and serum in response to DENV infection.

Bioinformatic analysis revealed that the proteins that were significantly altered in response to DENV infection in both the serum from infected patients and the proteome and/or secretomes of Huh-7 cells were associated with the GO terms 'complement and coagulation", "lipid metabolism" as well as "immune response". This demonstrated the usefulness of DENV infected liver cell models for the study of pathogenesis and therapeutic intervention in these processes/pathways.

Among the 50 serum proteins (listed in Table 6.6) that were significantly altered in response to DENV infection in both the serum of patients and the proteome and/or secretome of liver cells, the majority (36 of 50 proteins) were changed in the same direction (decreased in cells and/or secretome and serum). Most of these proteins were involved in "complement and coagulation cascades" and "lipid metabolism". The effect of DENV on the liver cells, as the source of serum proteins (Kuscuoglu *et al.,* 2018), may explain in part the pathogenesis of DENV *in vivo* in relation to "complement and coagulation" and "lipid metabolism" processes.

There were 13 proteins that were significantly decreased in liver cells and/or the associated secretome but increased in serum in response to DENV infection. This may be due to these proteins being synthesized by other cell types; for example, ORM1 and ORM2. These proteins act as APPs and transport proteins; ORM is mainly synthesized in the liver but heart, stomach and lung cells can also synthesize and secrete these proteins in response

to inflammation (Taguchi *et al.*, 2013). Similar to the results obtained from HEK293T cells, HSPA5 was increased in the proteome but decreased in the serum proteome.

The main group of lipids that are dysregulated in response to DENV infection in both Huh-7 cells and clinical specimens are the apolipoproteins, APOA1, APOC and APOB. The liver and intestine are the main source of apolipoproteins. The apolipoproteins are the major component of lipoproteins and function as carrier molecules for lipids in blood and the lymphatic system (Dominiczak and Caslake, 2011). The concentration of apolipoproteins are regulated by production (eg in APOA2) or degradation (eg in APOB and APOA1) (Dominiczak and Caslake, 2011). Most clinical studies focused on using serum lipoproteins to predict disease severity. Only one study reported significant decreases in LDL and HDL but increased TG and VLDL in DEN patients compared with healthy controls (Marin-Palma *et al.*, 2019). The decreases in serum HDL and LDL reported in Marin-Palma's study correlates with decreases of APOA1, APOC and APOB in both clinical specimens and Huh-7 cells because APOA1 and APOC are the components of HDL while APOB is a component of LDL. However, the increase of VLDL in Marin-Palma's study (Marin-Palma *et al.*, 2019) does not correlate with the decreases in APOA4, APOC and APOB (which are components of VLDL) in the sera and/or Huh-7 cells in this study. Furthermore, the limitations mentioned earlier especially age and the race of subjects in the study should be considered in the interpretation and comparison of the results of this group of proteins.

The focus of this thesis on the role of coagulation cascades was informed by the following. Firstly, it was one of the more enriched biological processes among proteins that were dysregulated in response to infection in both *in vivo* and *in vitro* studies. FBG is the most important element in formation of the fibrin clot and plays an important role in PLT activation. Moreover, SERPINA1 is strongly bound within the fibrin clot (Talens *et al.*, 2013). F2 plays an important role in the activation of FBG to fibrin and coagulation factor XIII (F13) also stabilizes clot formation. On the other hand, the important anticoagulants that regulate the balance of clot formation are SERPINC1, PROC and PROS1. The results of this study demonstrate for the first time that decreases in the cellular abundance of coagulation proteins in DENV infected liver cells result in decreases in the

secretion of these proteins which correlates with the findings obtained analyzing serum from DEN patients. Secondly, dysregulation of coagulation cascades due to an imbalance between coagulation and fibrinolysis processes may play a key role in the pathogenesis of infectious diseases including DEN (Gorp *et al.*, 2002). A deficiency in coagulation factors and thrombocytopenia result in coagulopathy and bleeding, a characteristic feature of SD. Additionally, excessive clots in DIC (which are also found in DEN) consume the coagulation factors which can lead to aggravation of the coagulopathy. Finally, some of the coagulation proteins including FBG, F2, SERPINA1 and SERPINC1 are also liver APPs. The dysregulation of APPs in DENV infected cells was demonstrated in this study and previous proteomic studies, as discussed before.

Although a decrease in complement and coagulation proteins has been previously demonstrated as a key feature of DEN pathogenesis *in vivo*, it was believed to result from increases in its consumption and/or loss from leakage processes. The increase in consumption of coagulation factors was confirmed by an increase in DIC (Srichaikul *et al.*, 1977; Bokisch *et al.*, 1973). Apart from increased in consumption, Wills *et al*., studied plasma levels and urinary clearance of proteins including ALB, IgG and SERPINC1 in DSS and reported reductions in the plasma concentrations of all proteins with increased fractional clearance (Wills *et al.*, 2004). Thus, a decrease in the cellular levels of complement and coagulation proteins, with a concomitant decrease in their secretion from hepatocytes, may play a role in the pathogenesis of DEN and merits further analysis.

In summary, the use of an advanced serum proteomic approach employing 10plex-TMT labelling of non-pooled samples and LC-MS/MS for the analysis of a large DEN patient cohort, encompassing all disease severities, enabled detection of 216 serum proteins that were significantly altered in response to DENV infection. This group of proteins were associated with the biological processes “complement and coagulation cascades”, “cholesterol metabolism”, “immune response”, “acute-phase response” and UPS. Furthermore, CRP and APOC2 were identified as proteins that correlated with more severe disease forms. DENV infected Huh-7 cells represent a good model for studying complement and coagulation proteins, APPs as well as lipoproteins *in vivo*. The dysregulation of the FBG complex and APPs during DENV infection of the liver may

represent a key step in pathogenesis and was further investigated in the studies described in Chapter 7.

CHAPTER 7. FBG AND APPS IN DENV INFECTED LIVER CELLS

7.1 Introduction

The studies described in the previous chapters showed that the dysregulation of FBG and other APPs that occurred in Huh-7 cells in response to DENV infection correlated well with the changes that occurred in the levels of these proteins in the serum of DEN patients. Furthermore, the *in vitro* results agreed with other studies that reported an enrichment of APPs among dysregulated proteins in the blood of DEN patients (Kumar *et al*., 2012; Brasier *et al.*, 2015). Thus, the dysregulation of FBG and APPs that occurred in Huh-7 cells during DENV infection was further investigated to understand the mechanisms involved and provide a greater understanding of DEN pathogenesis.

7.1.1 Fibrinogen (FBG): structure, function and regulation.

FBG consists of two copies of three peptide chains Aα, Bβ, and ɤ encoded by the *FGA*, *FGB* and *FGG* genes respectively (Fish and Neerman-Arbez, 2012). The FBG subunits are synthesised in hepatocytes and secreted into the blood as a hexamer. FBG is an abundant plasma protein with a normal concentration of 1.5-3.5 g/L (almost equal to that of albumin) and a half-life of approximately four days (Kuscuoglu *et al*., 2018). In clot formation, thrombin (active form of F2) and F13 cleave FBG in to fibrin. Crosslinking of fibrin with PLT forms a clot to stop bleeding. In fibrinolysis, the clot is dissolved by plasmin into fibrin degradation products (FDPs). Apart from its role in haemostasis, FBG plays a major role in wound healing and inflammation, acting as an APP. As a pro-inflammatory mediator, FBG interacts with vascular endothelial cells to modulate permeability, PLT to promote PLT aggregation as well as monocytes and macrophages to induce the release of cytokines (Davalos and Akassoglou, 2012).

The regulation of FBG gene expression in the basal and acute phase response are summarized in Figure 7.1. In the basal state, hepatocyte nuclear factor 1 (HNF1) and CAAT/enhancer-binding protein (CEBP) bind to the *FGA*, *FGB* and *FGG* gene promotors and initiate mRNA transcription (Fish and Neerman-Arbez, 2012). Hepatocyte nuclear

factor 4α (HNF4A) regulates the transcription of hepatocyte genes including *HNF1*, apolipoproteins and coagulation factors. Apart from the FBG genes, HNF4A also regulates *SERPINA1, SERPINC1* and angiotensinogen (*AGT*) (Kalsheker *et al.*, 2002; Gonzalez *et al*.2008). Studies using mouse models have shown that HNF4A controls *F5, F9, F11, F12* and *F13B* transcription (Inoue *et al*., 2006). MicroRNAs (miRNA) are involved in the post-transcriptional regulation of the FBG genes; for instance, many miRNA including miR-29a, miR-218, miR-409-3p miR-let7e and miR-let7c down-regulate FBG while a smaller number including miR769-5 and miR-106a up-regulate FBG protein production (Fort *et al.*, 2010). Furthermore, miR-18a, miR-629 and miR-24 are involved in the regulation of *HNF4A* expression (Babeu and Boudreau, 2014).

In the acute phase response, cytokines modulate transcription of the FBG genes. The main regulator is interleukin (IL) 6. IL-6 activated signal transducer and activator of transcription 3 (STAT3) phosphorylation leads to increased transcription of the FBG genes (Fish and Neerman-Arbez, 2012). Whereas IL-1β down-regulates FBG gene transcription by prolonged STAT3 phosphorylation (*via* NFkB). Glucocorticoids (GC) up-regulate FBG transcription *via* both the glucocorticoid receptor (GR) and by indirectly reducing negative control of IL-6.

The synthesis of fibrinogen β chain takes longer than the other chains and is the rate limiting step of FBG production (Redman and Xia, 2001). After translation, all chains of FBG translocate to the ER lumen for assembly. ER chaperones including HSPA5 contribute to the folding and assembly of FGB (Redman and Xia, 2001). Any unassembled FBG chains are degraded. A study investigating FGB stability by radiolabeling HepG2 cells expressing single FBG chains found that the Aα-ɤ chains were degraded *via* proteasomal degradation while free FGG was degraded by the lysosome (Redman and Xia, 2001).

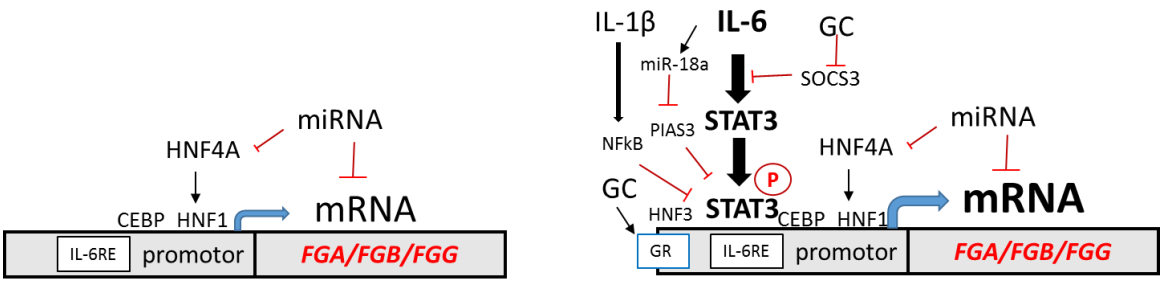

Figure 7.1 Regulation of FBG transcription in the basal state and acute phase response. Figure is adapted from Fish and Neerman-Arbez, 2012.

7.1.2 Hepatic APPs and IL-6

APPs are defined as plasma proteins that are altered in concentration by at least 25% in response to inflammatory disorders (Morley and Kushner, 1982). Hepatocytes are the main cells that produce APPs in response to stimuli (Gabay and Kushner, 1999). Hepatic APPs contain many categories of proteins including secreted pathogen recognition receptors (e.g. CRP, soluble CD14 and serum amyloid P), proteinase inhibitors (e.g. SERPINA1, A2M), complements, proteins involved in iron homeostasis (hepcidin and transferrin), transport proteins (ALB, HP and CP) and coagulation proteins (e.g. FBG, F2, plasminogen (PLG) and PROC) as well as other unclassified proteins (e.g. AGT and fibronectin) (Gabay and Kushner, 1999; Bodes *et al*., 2012). Under the stress from infection, inflammation, injury or during tumor growth, cytokines released from macrophages, monocytes and Kupffer cells (liver macrophages) modify the production of liver APPs. The main cytokines that regulate liver APPs are IL-6and IL-1β. Liver APPs can be classified into two subclasses (Bode *et al.*, 2012). Class I APPs are synergistically regulated by IL-1β and IL-6, and include CRP, HP and SAA. Whereas Class II APPs include FBG and A2M and are mainly regulated by IL-6. Furthermore, the regulation of APPs also depends on the nature of the inflammatory stimuli and other hormones, particularly glucocorticoids and insulin (Bode *et al.*, 2012).

APPs are also classified by their change in concentration in response to stress into positive (increased in level) and negative (decreased in level) APPs. Examples of positive APPs are CRP, FBG, F2, SERPINA1, HP, CP, serum amyloid A (SAA) and complements while negative APPs include ALB, SERPINC1, transferrin (Jain *et al*., 2011).

In *in vitro* experiments, IL-6 has been added to hepatocytes in various doses (ranging from 5-100 ng/ml final concentration) and treatment times (6-24 h) to study the APP response (Ray *et al*, 2000; Ait-Goughoulte *et a*l., 2009; Brock *et al*., 2011). However, limited studies have been done on the effect of IL-6 treatment on flavivirus infection. In a study on YFV, pre-incubating PH5CH8 hepatocytes with 5 ng/ml of IL-6 for five days before infection resulted in a decrease in viral titre (Woodson and Holbrook, 2011) and an increase in FBG level (Woodson *et al*., 2013) compared with untreated infected cells.

Unfortunately, the effect of IL-6 on DENV infection, either pre- or post-infection, and its effect on liver APP production during DENV infection are unknown.

7.1.3 FBG and APPs in DEN

A decrease in FBG amount in peripheral blood has been associated with DEN severity (Mairuhu *et al*., 2003) and suggested to arise as a result of increased consumption by DIC processes (Sricahiakul *et al*., 1977). Nevertheless, the overt process of DIC was not detected by clinical or laboratory studies in all patients with severe DEN (Wills *et al.,* 2002). Increases in IL-6 and IL-1β concentrations in the blood of DENV infected patients has been reported (Bozza *et al*., 2008; Priyadarshini *et al.,* 2010). Thus, increases in the production of FBG and other positive APPs from hepatocytes are expected. Surprisingly, all FBG chain were found to be decreased in liver cells in response to DENV infection in this study and previous proteomic studies investigating DENV infection of Huh-7 liver cells (Chiu, 2014; Yousuf, 2016). Dysregulation of liver production and secretion of FBG, an important multifunctional protein that potentially plays a key role in DEN pathogenesis, warrants further investigation. A better understanding of the mechanisms underlying these processes could potentially lead to an increased understanding of DEN pathogenesis and identify targets against which therapeutics could be designed.

Apart from FBG, changes in the amounts of other APPs including SERPINA1, SERPINC1, CRP and HP in the serum/plasma of DEN patients have been reported. However, there are some inconsistencies between studies. For example, both increases and decreases in the serum/plasma levels of CRP and SERPINA1 have been reported (as discussed in Chapter 6). SERPINC1 has been proposed as a biomarker for both diagnosis of DEN and predicting severe disease based on previous proteomic analyses of serum/plasma from patients with DEN, but with inconsistent results between studies. A decrease in SERPINC1 was found in the serum proteome of DEN patients compared with healthy controls in the investigation presented in Chapter 6, whereas increased levels were found in the previous serum proteomic studies comparing DEN patients to healthy controls (Kumar *et al.,* 2012). In an iTRAQ-based plasma proteomic study comparing children with SD to those with DEN with WS (Nhi *et al*., 2016), SERPINC1 was increased in patients with SD whereas the reverse was found in a plasma proteomic study examining

children with SD compared with DF (Fragnoud *et al.,* 2012). Although HP was not significantly changed in the sera of DENV infected patients compared with healthy patients in this study (as described in Chapter 6), HP was significantly increased in DENV infected patients compared with healthy controls in a previous serum proteomic analysis (Kumar's *et al*., 2012). Furthermore, changes in the levels of APPs have predominantly been reported *in vivo* studies and there is limited data about changes that occur in liver cells.
Therefore, this chapter focused on examining the dysregulation of liver APPs at the cellular level using cultured cell lines. The mechanisms underlying the changes were explored.

Results

According to the results presented in Chapter 5, the decreased amounts of FGA, FGB and FGG and other APPs in the secretome of DENV infected Huh-7 cells correlated with a decrease in intracellular levels. Therefore it was decided to study the mechanism/s underlying the dysregulation of these proteins by examining their intracellular levels rather than the level in the secretome, as the previous results showed that the proteins could be more robustly detected in cell lysates and the levels of RNA transcripts corresponding to the FGB /APP genes could be simultaneously analysed. Moreover, some APPs of interest, such as HP, were only altered in amount in the proteome of DENV-2 infected cells.

As IL-6 is a major regulator of FBG and APP gene transcription and increased levels of IL-6 have been reported during DENV infection, studying the effect of IL-6 on the cellular levels of FBG and APPs was vital. Therefore initially experiments were done to optimise the induction of the IL-6 regulated genes. The next step was then to explore the mechanism underlying the decreased in FGB/APP amounts by analysing mRNA levels and protein stability. Finally, interactions between selected viral and host proteins were examined.

7.2 Protocol optimization

7.2.1 Optimal dose and duration of IL-6 treatment

To study the effect of IL-6 on the FBG protein levels, firstly conditions for IL-6 treatment were optimised. The dosage and duration of IL-6 treatment of liver cell lines were varied, based on previous studies, ranging from 5-100 ng/ml (final concentration) in dose and 6-24 h of duration of treatment (Ray *et al*, 2000; Ait-Goughoulte *et al*., 2009; Brock *et al.,* 2011). The appropriate dose and duration of IL-6 treatment on FBG protein levels was identified by adding 20, 50 and 100 ng/ml of recombinant human IL-6 to Huh-7 cells for 6, 12 and 24 h before harvesting and preparing cell lysates. Then, the cell lysates were analysed by Western blotting (Figure 7.2). As expected, IL-6 treatment resulted in an increase in the level of all FBG protein subunits and this effect depended on the dose and duration of treatment. The optimal dose of IL-6 and duration of treatment were 50 ng/ml (final concentration) and 12-24 h duration respectively.

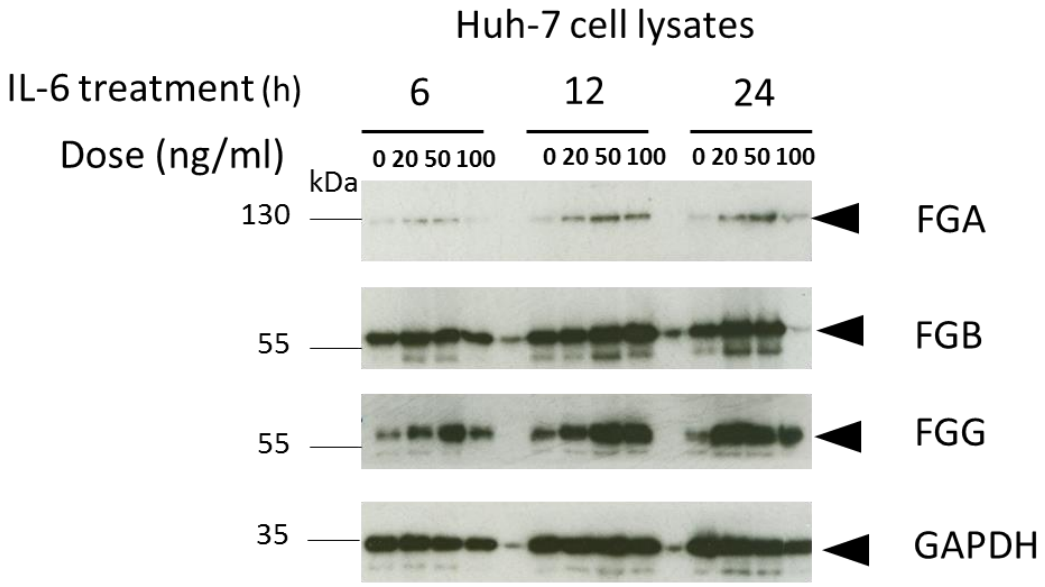

Figure 7.2 Effect of dose and duration of IL-6 treatment on the level of FGA, FGB and FGG proteins in Huh-7 cells.

To determine the appropriate dose and duration of IL-6 treatment, various doses of IL-6 (0 as a negative control, 20, 50, 100 ng/ml, (final concentration)) were added to Huh-7 cells for varying times (6, 12, 24 h before harvesting as cell lysates). Twenty µg of cell lysate was loaded in each lane and the proteins separated by SDS-PAGE prior to Western blotting. Antibodies against FGA, FGB, FGG and GAPDH were used to detect the amount of relevant proteins. GAPDH was used as loading control for cell lysates and the positions of relevant molecular mass markers are shown in kDa.

7.2.2 Effect of IL-6 on DENV infection

It is well known that some cytokines such as type I IFNs have anti-viral effects against DENV; however, the effect of IL-6 on DENV replication has not been studied. Thus, the effect of IL-6 treatment on DENV infection was tested to ensure that the effect of IL-6 on the proteins of interest was not due to an alteration in DENV infection. Previously, treatment with IFN-α and β either pre- or post-DENV infection resulted in a decreased infection rate in many cell types, including HepG2 cells, as determined by flow cytometry and plaque assay (Diamond *et al*., 2000). Thus, the effect of IL-6 on DENV infection, either pre- or post- infection, was tested by adding 50 ng/ml of IL-6 to Huh-7 cells 12 h before infection and 6 hpi (followed by a 24 h duration of IL-6 treatment which had the maximum effect on FBG protein levels from the previous experiment). Mock and DENV-2 infections were done as previously described. The cells were fixed at 30 hpi followed by IFA (Figure 7.3A). The supernatants were collected to measure virus titre and viral genome copies (Figure 7.3B and C). The experiments were done independently in duplicate. The infection rate determined by IFA was approximately 100% using a MOI of 5 when IL-6 was added either pre- or post-infection. The viral titres were not significantly different (P-value > 0.05) when comparing infection either with or without IL-6 treatment (pre- or post-infection).

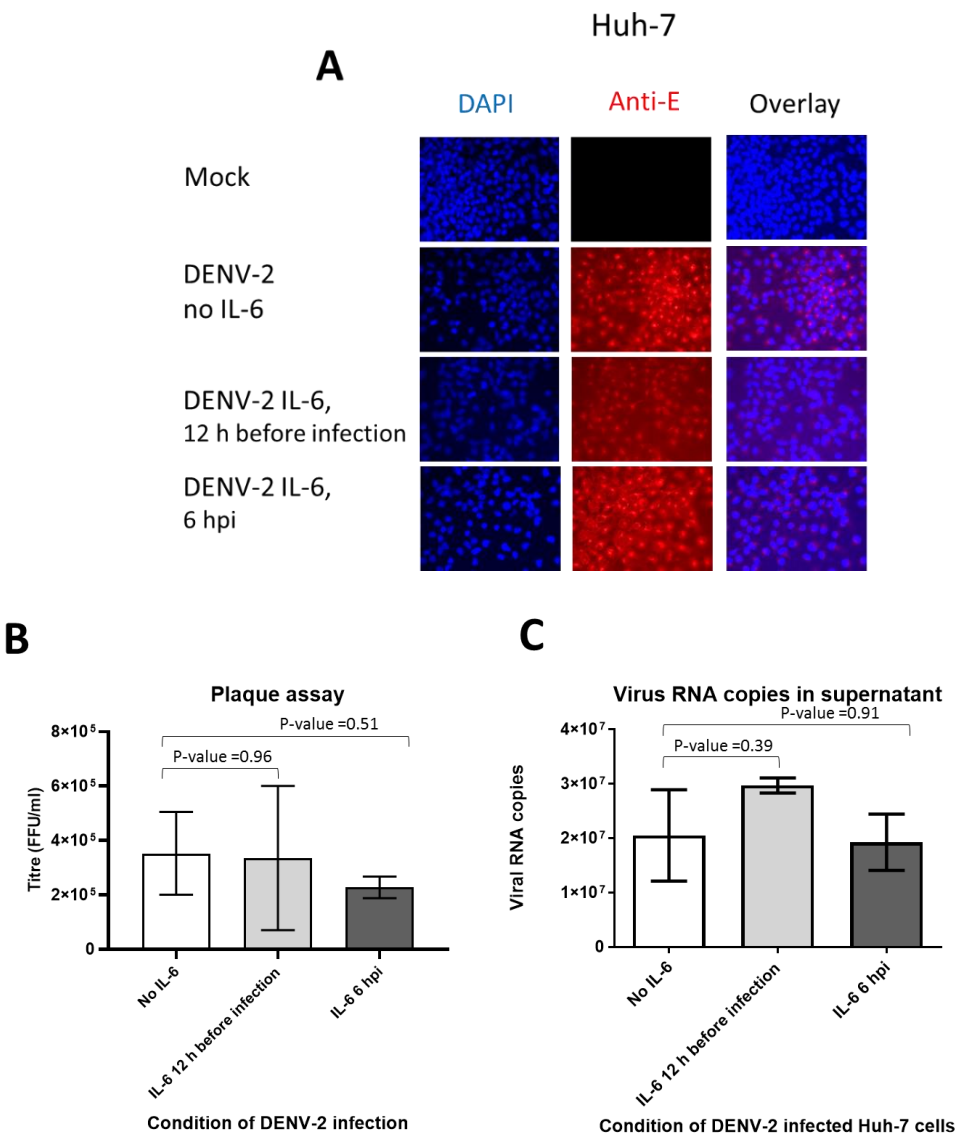

Figure 7.3 Analysis of the effect of IL-6 on the number of cells that DENV-2 infected, titre and genome levels.

Huh-7 cells were infected with DENV-2 at MOI=5 or mock infected. IL-6 (50 ng/ml) was added either 12 h before infection or 6 hpi. At 30 hpi, the cell culture supernatants were collected and the cells fixed and permeabilised with ice cold methanol. **(A)** IFA analysis was performed by immunostaining with an antibody against the DENV-2 E protein (Anti-E, red), nuclear DNA was visualised with DAPI (blue). Images were taken using a Leica widefield microscope with 40X magnification. The viral titre in culture supernatants were measured by IF **(B)** and viral RNA copies by qPCR **(C)**. The experiments were done independently in duplicate. Plaque assays were done in duplicate in each experiment and qRT-PCR was done in triplicate. Data are presented in terms of mean ± SEM. An independent Students *t-test* was performed to compare IL-6 treatment to the non-treatment group, all P-value >0.05.

7.2.3 Selecting proteins/genes for study

According to the previous results, the proteins involved in "complement and coagulation cascades" and "acute phase response" processes were significantly enriched in the cellular proteome and secretomes of DENV-2 infected Huh-7 cells. This data correlates with the results of the clinical proteomic study of DENV infected patients presented in Chapter 6, and with previous studies (Fragnoud *et al.*, 2105; Ray *et al*., 2012, Jadhav *et al*., 2017). Thus, this part of the investigation focussed on an examination of liver proteins that i) were significantly dysregulated in response to infection ii) involved in coagulation and iii) were APPs (FGA, FGB, FGG, SERPINA1, F2 and SERPINC1). HP, as a positive liver APP was also targeted. The levels of HNF4A and CEBPA, which are the modulators of FBG production were also significantly decreased in DENV-2 infected Huh-7 cells and included in the examination. Although IL-6 was not detectable in the proteomic analysis of Huh-7 infected cells, it was also examined as a protein/gene of interest. The alterations that occurred in the selected proteins in the proteome/secretome of DENV-2 infected Huh-7 cells compared with mock infected cells (Chapter 5) and the sera of DENV patients compared with healthy controls (Chapter 6) are summarised in Table 7.1. The successful validation of these selected proteins in DENV and mock infected Huh-7 cells by Western blotting was achieved for FGA, FGB, FGG, SERPINA1 and SERPINC1 in Chapter 5 as well as HP and HNF4A in this Chapter.

Table 7.1 Summary of coagulation proteins and APPs changed in the proteome/secretome of DENV-2 infected Huh-7 cells compared with mock cells and the sera of DENV patients compared with healthy patients.

			Huh-7 proteome		Huh-7 secretome		DEN w/o WS		DEN w WS		SD	
Protein	Gene	Uniport accession	Fold change DENV-2 /Mock	P-value	Fold change DENV-2 /Mock	P-value	Fold change	FDR	Fold change	FDR	Fold change	FDR
Fibrinogen alpha	*FGA*	P02671	0.36	1.28E-03	0.44	1.89E-02	-1.66	4.19E-04	-1.13	1.33E-01	-2.16	7.10E-02
Fibrinogen beta	*FGB*	V9HVY1	0.43	1.01E-03	0.44	2.67E-03	-1.78	5.97E-04	-1.05	1.65E-01	-2.08	6.79E-02
Fibrinogen gamma	*FGG*	P02679	0.44	1.18E-03	0.40	2.49E-02	ND	ND	ND	ND	ND	ND
Fibrinogen gamma	*FGG*	D3DP16	1.00	1.00E+00	1.00	1.00E+00	-2.12	5.69E-04	-1.02	2.06E-01	-2.23	9.19E-02
Fibrinogen gamma	*FGG*	C9JEU5	1.00	1.00E+00	1.00	1.00E+00	-1.72	9.73E-04	-1.05	1.53E-01	-2.21	7.63E-02
Hepatocyte neclear factor 4alpha	*HNF4A*	F1D8T1	0.61	1.98E-02	ND	ND	ND	ND	ND	ND	ND	ND
CCAAT/enhancer-binding protein alpha	*CEBPA*	P49715	0.48	6.22E-03	ND	ND	ND	ND	ND	ND	ND	ND
IL6	*IL6*	ND	ND	ND	ND	ND	ND	ND	ND	ND	ND	ND
Antithrombin III	*SERPINC1*	A0A024R944	0.61	3.82E-02	0.58	5.92E-02	-0.48	2.87E-03	-0.20	4.59E-01	-0.18	6.38E-01
Alpha-1-antitrypsin	*SERPINA1*	E9KL23	0.34	6.85E-04	0.66	5.14E-03	ND	ND	ND	ND	ND	ND
Alpha-1-antitrypsin	*SERPINA1*	A0A0B4J278	ND	ND	ND	ND	-0.28	8.76E-01	0.20	9.28E-01	-1.09	6.97E-01
Alpha-1-antitrypsin	*SERPINA1*	G3V2B9	ND	ND	ND	ND	1.01	2.02E-01	1.08	1.58E-01	1.69	1.42E-01
Coagulation factor XIII B chain	*F13B*	P05160	NA	NA	0.62	1.88E-02	-0.77	7.37E-05	-0.73	1.75E-04	-0.47	7.71E-02
Prothrombin	*F2*	P00734	0.62	3.72E-02	ND	ND	-0.49	1.84E-03	-0.46	4.50E-03	-0.57	6.20E-03
Prothrombin	*F2*	P00747	ND	ND	0.51	1.49E-01	ND	ND	ND	ND	ND	ND
Haptoglobin	*HP*	P00738	0.49	2.46E-02	0.96	9.11E-01	ND	ND	ND	ND	ND	ND
Haptoglobin	*HP*	H0Y300	ND	ND	ND	ND	0.35	7.22E-01	0.50	5.27E-01	-0.28	8.20E-01

7.2.4 Primer optimisation for qRT-PCR

Before analysis of the mRNA levels of the genes of interest (Table 7.1) by qRT-PCR, primer sets were selected for each gene transcript, purchased commercially (Table 2.6) and analysed for specificity and sensitivity. To determine if the mRNAs of interest were expressed at detectable levels in Huh-7 cells and determine the quality of primers, total RNA extracted from Huh-7 cells, both with and without IL-6 treatment, was amplified by RT-PCR and the products analysed by agarose gel electrophoresis (Figure 7.4). A cDNA reaction without RT was used as negative control. The results revealed no detectable RT-PCR product using the *IL-6* primer set and only faint bands for the *F13B* RT-PCR products, using RNA extracted from Huh-7 cells treated with and without IL-6. RT-PCR products were obtained for all the other gene transcripts isolated from Huh-7 cells with and without IL-6 stimulation. The primer sets that were suitable for RT-PCR detection were then tested for their qRT-PCR amplification efficiency.

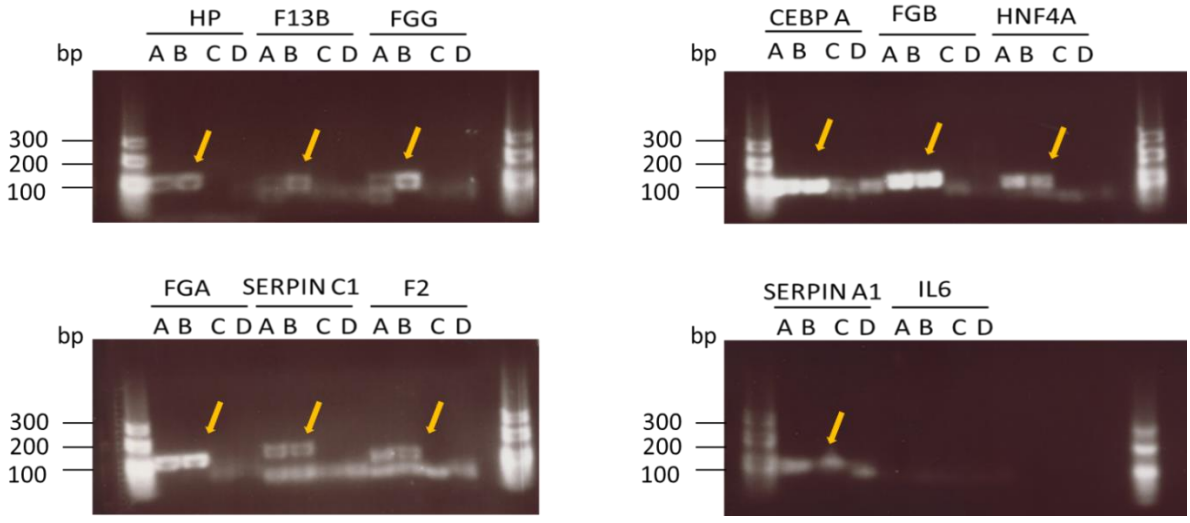

Figure 7.4 Detection of selected RT-PCR products using RNA from Huh-7 cells with and without IL-6 treatment.

Total RNA was extracted from Huh-7 cells without (A and C) and with IL-6 (B and D) treatment (50 ng/ml for 12 h). After cDNA synthesis using random primers, primer sets for *FGA*, *FGB*, *FGG*, *SERPINA1*, *SERPINC1*, *F2*, *F13B*, *HNF4A*, *CEBP*, *HP* and *IL-6* were used for PCR amplification. Equal amounts of DNA RT-PCR product were loaded into each lane and analysed using a 2% agarose gel. The no RT reactions (C and D) were used as negative controls. The positions of relevant nucleic acid markers are shown in bp. A= Huh-7 without IL-6 + RT, B= Huh-7 with IL-6 +RT, C= Huh-7 without IL-6, no RT, D= Huh-7 with IL-6, no RT.

After the primer sets were confirmed to be capable of amplifying detectable RT-PCR products they were further tested for their use in qRT-PCR. Standard curves were produced for the primer sets corresponding to the *FGA, FGB, FGG, SERPINA1, SERPINC1*, *F2, HNF4A, CEBP, HP* and *GAPDH* (used as control) transcripts as described in section 2.4. GAPDH was selected as a control for both Western blotting analysis and qRT-PCR as its' level did not change in the proteomic analysis of DENV-2 infected cells described in Chapter 5. Theoretically, the acceptable efficiency ranges from 90 to 110% (with a slope of the curve approximately of -3.3 (for an efficiency of 100%)). The appropriated R^2 of the curve should be > 0.99 for a good correlation. Moreover, standard curves for all of the selected genes should have a similar slope as the housekeeping gene − *GAPDH* in this study. The acceptable standard curves for the selected primer sets are shown in Figure 7.5.

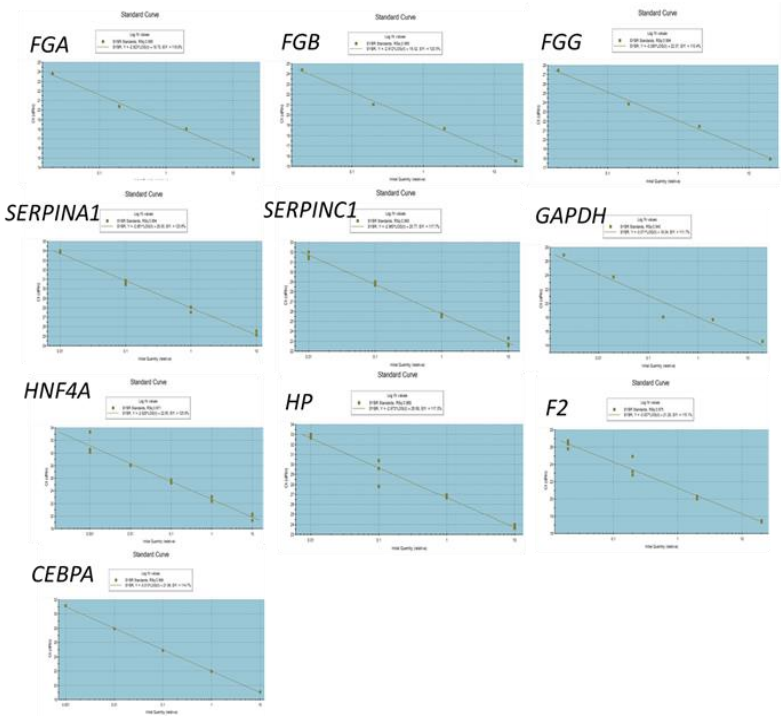

Gene	Efficiency (%)	Slope	R^2
GAPDH	111.7%	-3.071	0.943
FGA	119.8%	-2.923	0.995
FGB	120.5%	-2.995	0.995
FGG	110.4%	-3.095	0.994
HNF4A	125.9%	-2.826	0.971
SERPINA1	123.6%	-2.861	0.994
SERPINC1	117.7%	-2.960	0.993
HP	117.0%	-2.973	0.968
CEBPA	114.7%	-3.013	0.999
F2	115.1%	-3.007	0.975

Figure 7.5 Standard qRT-PCR amplification curves for the selected primers.

Total RNA was extracted from Huh-7 cells and used for cDNA synthesis. Ten ng of cDNA was used neat or subjected to 10-fold serial dilution and used for qRT-PCR amplification. Primer sets for *FGA, FGB, FGG, SERPINA1, SERPINC1, F2, HNF4A, CEBP, HP* and *GAPDH* (as a house keeping gene) were used for PCR amplification. The SoftMax Pro program was used to quantify CT values and calculate efficiency curves. The efficiency (%), slope of curve and R^2 value for each primer set are listed in the table.

Gene transcripts were selected for further study based on the change in protein amount in DENV-2 infected Huh-7 cells, the results of the validation with Western blotting, the results of the serum proteomic analysis of DENV infected patients described in Chapter 6, review of the literature and primer suitability. Finally, the six APPs selected for examination were FGA, FGB, FGG, SERPINA1, SERPINC1 and HP as well as HNF4A (as an important regulator of FBG and other APPs).

7.3 Effect of IL-6 on FBG and APPs in DENV infected liver cells

7.3.1 FBG proteins

To determine whether IL-6 could stimulate an increase in the levels of the FBG proteins and APPs during DENV infection, Huh-7 cells were either infected with DENV-2 at MOI=5 or mock infected. Immediately after infection, IL-6 (50 ng/ml) was added to media and at 6, 12 and 24 hpi, which corresponded to treatment durations of 30, 24, 12, and 6 h respectively, at the time of harvest. The cells were harvested at 30 hpi and used to prepare cell lysates that were analysed by Western blotting (Figure 7.6). The results revealed that an IL-6 treatment period of 24 h had an optimal stimulation on the amount of cellular FBG proteins in mock cells and DENV-2 infection blunted the IL-6 stimulated increase in FGA, FGB and FGG at all time points.

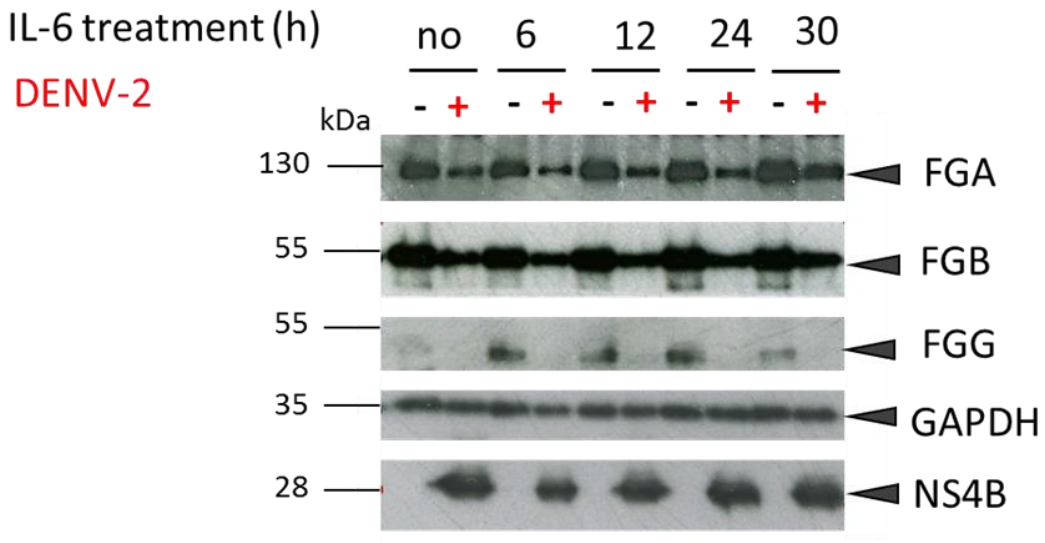

Figure 7.6 Analysis of FGB proteins in cell lysates from DENV-2 infected Huh-7 cells after IL-6 treatment.

Huh-7 cells were infected with DENV-2 at a MOI of 5 or mock infected. IL-6 treatment was performed by adding IL-6 (50 ng/ml) to the media immediately after infection or at 6, 12 and 24 hpi. The cells were harvested at 30 hpi and collected as total lysates. Twenty µg of cell lysate was loaded in each lane and the proteins separated by SDS-PAGE prior to Western blotting. Antibodies against FGA, FGB, FGG, NS4B and GAPDH were used to detect the amount of the relevant proteins. GAPDH and NS4B were used as a loading control and marker of infection, respectively. The positions of relevant molecular mass markers are shown in kDa.

7.3.2 HNF4A

The previous proteomic results (Table 5.4) demonstrated that HNF4A decreased in amount in DENV infected Huh-7 cells which might modulate the production of FBG. Although HNF4A is not an APP and theoretically regulates FBG production in the basal state, the effect of IL-6 stimulation on HNF4A was also studied by Western blotting. A single IL-6 treatment duration of 24 h was selected for the experiment based on the previous results examining FBG amounts. Either no IL-6 or 50 ng/ml of IL-6 was added to DENV and mock infected Huh-7 cells at 6 hpi (24 h treatment) and harvested at 30 hpi to prepare cell lysates for Western blotting (Figure 7.7A). The amount of HNF4A changed in a similar fashion as FBG in DENV-2 infected Huh-7 cells with or without IL-6 stimulation.

7.3.3 Other APPs: SERPINA1, SERPINC1 and HP

The effect of IL-6 treatment on the amounts of SERPINA1, SERPINC1 and HP in DENV-2 infected Huh-7 cells was studied in the same manner as described above for HNF4A (Figure 7.7B). For SERPINA1 and HP which are positive APPs, similar results as for FBG were observed. The proteins increased in amount in mock infected cells after IL-6 treatment but this effect was not found in DENV infected Huh-7 cells. In contrast, there was no increase in the amount of SERPINC1, which is a negative APP, with IL-6 treatment in either mock or DENV-2 infected Huh-7 cells. Similar to FBG, the effects of IL-6 treatment on positive APPs were not detected when the cells were infected with DENV.

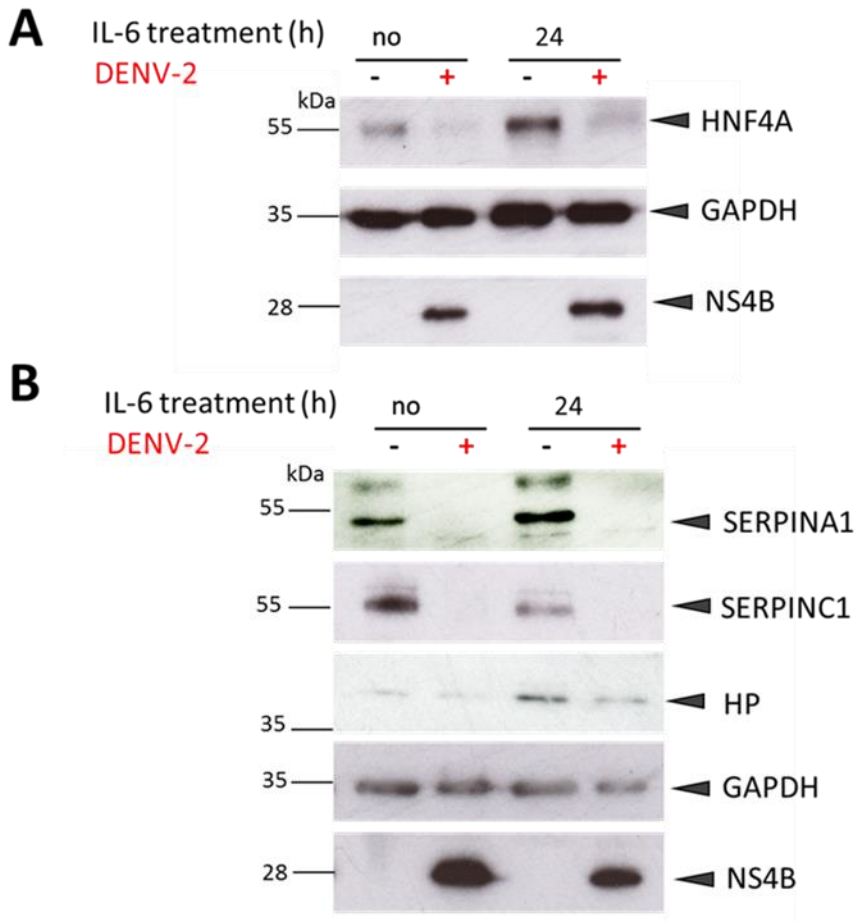

Figure 7.7 Analysis of HNF4A and APPs in cell lysates from DENV-2 infected Huh-7 cells after IL-6 treatment.

Huh-7 cells were infected with DENV-2 at a MOI of 5 or mock infected. IL-6 (50 ng/ml) was added or not to the media at 6 hpi. Cells were harvested at 30 hpi and collected as total lysates. The amount of HNF4A **(A)** and the APPs, SERPINA1, SERPINC1 and HP, **(B)** were analysed by Western blotting. Twenty µg of cell lysate (30 µg for SERPINA1) were loaded in each lane and the proteins separated by SDS-PAGE prior to Western blotting. Antibodies against HNF4A, SERPINA1, SERPINC1, HP, NS4B and GAPDH were used to detect the amounts of the relevant proteins. GAPDH and NS4B were used as a loading control and a marker of infection, respectively. The positions of relevant molecular mass markers are shown in kDa.

7.3.4 Effect of IL-6 treatment on HepG2 cells

To confirm that the effects of DENV infection on FBG and APP levels were not specific to Huh-7 cells, the same set of experiments were then performed with another liver cell line, HepG2 cells, in the same manner (Figures 7.8). At 24 h after seeding, HepG2 cells were infected with DENV-2 (at MOI of 5) or mock infected and IL-6 treatment was performed by either adding IL-6 (50 ng/ml final concentration) or media alone at 6 and 18 hpi (24 and 12 h treatment duration). At 30 hpi, the cells were fixed for IFA and/or harvested as cell lysates. The results showed approximately 95% infection rate either with or without IL-6 treatment (Figure 7.8A). An increase in the amounts of the FBG proteins was detected after IL-6 treatment of mock cells (the peak effect was after 24 h of treatment) but the increase was much less in DENV-2 infected HepG2 cells, which was similar to results obtained using Huh-7 cells (Figure 7.8B).

The effect of DENV infection and IL-6 treatment on HNF4A amounts was also studied. There was a decrease in the amount of HNF4A in DENV-2 infected HepG2 cells compared with mock infected cells which was similar to the result obtained using Huh-7 cells. In contrast, IL-6 stimulation did not affect the amount of HNF4A in HepG2 cells as was observed for Huh-7 cells (Figure 7.8C).

Unfortunately, SERPINA1 and HP could not be detected in lysates from HepG2 cells by Western blotting under any conditions. SERPINC1 was successfully detected and similar to the results obtained using Huh-7 cells, the amount of SERPINC1 decreased during DENV-2 infection compared with mock infected cells (Figure 7.8D). In contrast to Huh-7 cells, there was an increase in the amount of SERPINC1 after IL-6 treatment of mock infected cells. Interestingly, DENV infection also blunted the IL-6 stimulatory effect on SERPINC1 in HepG2 cells was as observed using Huh-7 cells.

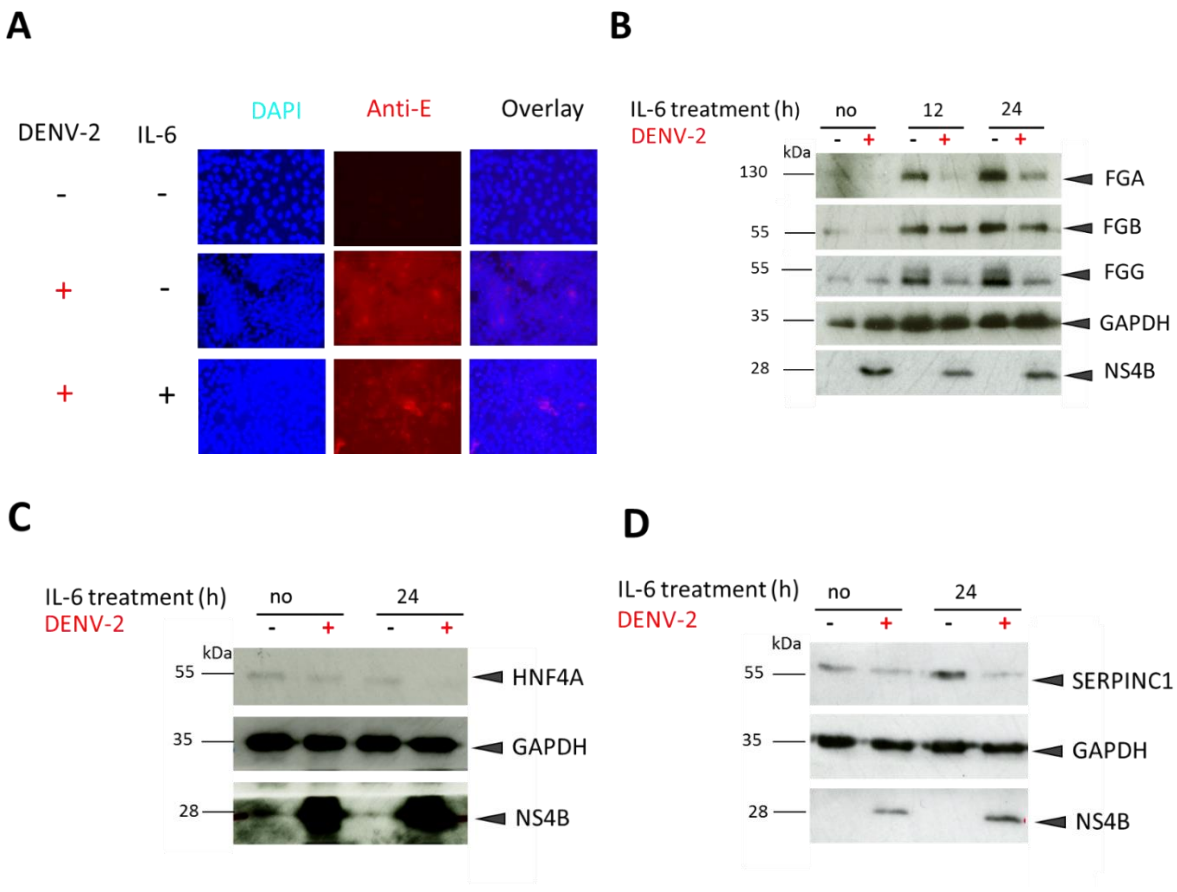

Figure 7.8 Analysis of the FBG proteins and APPs in cell lysates from DENV-2 infected HepG2 cells after IL-6 treatment.

HepG2 cells were infected with DENV-2 at a MOI of 5 or mock infected. IL-6 (50 ng/ml) was added or not to the media at 6 hpi (and 18 hpi for FBG). At 30 hpi, the cells were fixed for IFA and/or collected as total lysates. IFA analysis was performed **(A)** by immunostaining with an antibody against the DENV-2 E protein (Anti-E, red), nuclear DNA was visualised with DAPI (blue). Images were taken using a Leica widefield microscope with 40X magnification. The amounts of the FBG proteins (**A**), HNF4A **(B)** and SERPINC1 **(C)** were analysed by Western blotting. Twenty µg of cell lysate was loaded in each lane and the proteins separated by SDS-PAGE prior to Western blotting. Antibodies against FGA, FGB, FGG, HNF4A, SERPINC1, NS4B and GAPDH were used to detect the amounts of the relevant proteins. GAPDH and NS4B were used as a loading control and a marker of infection, respectively. The positions of relevant molecular mass markers are shown in kDa.

7.4 FBG and APP transcript levels in DENV infected liver cells

To study whether or not the alterations in FBG and the APPs in DENV infected cells were a result of altered mRNA transcript levels corresponding to those proteins, the mRNA transcript levels were quantified by qRT-PCR. Huh-7 and HepG2 cells were prepared in the same manner as described above for the Western blotting analysis. The cells were infected with DENV-2 and IL-6 added to a final concentration of 50 ng/ml at 6 hpi. The cells were harvested at 30 hpi and used for total RNA extraction. In these experiments the cells were only analysed at a single time point, after infection and IL-6 treatment. The time point selected was based on the Western blot analysis and previous gene expression analysis. Total RNA was used for qRT-PCR analysis of the levels of each gene transcript. The experiments were done in triplicate (Figure 7.9).

In DENV-2 infected Huh-7 cells not treated with IL-6, there was a significant decrease in the *FGA, FGB, HP* and *HNF4A* transcript levels compared with mock infected cells (Figure 7.9A). These results correlated with the decrease in protein levels. In contrast, there was no change in the *FGG* and *SERPINA1* transcript levels and the *SERPINC1* transcript showed a non-significant increase in response to DENV-2 infection.

Analysis of the mRNA transcript levels in mock infected cells in response to IL-6 treatment showed that the transcript levels of the positive APPs including *FGA, FGB* and *FGG* and *HP* increased in response to IL-6 treatment but the trend was only statistically significant for the *FGA* and *HP* transcripts. The *SERPINA1* and *SERPINC1* transcript levels significantly decreased after IL-6 stimulation. The *HNF4A* transcript level did not change after IL-6 treatment.

Analysis of the effects of both DENV infection and IL-6 treatment showed that the mRNA transcript levels for *FGA, FGB, FGG, HP* and *HNF4A* increased in DENV-2 infected Huh-7 cells in comparison to infected cells not treated with IL-6 but that the transcript levels were still lower than in mock infected cells treated with IL-6. In contrast to the Western blotting results there was a significant increase in *SERPINA1* and non-significant increase in *SERPINC1,* transcript levels in DENV-2 infected Huh-7 cells treated with IL-6 compared to mock infected cells with or without IL-6 treatment.

The same experiment was done using HepG2 cells. Overall, the changes observed in the mRNA transcript levels corresponding to FGA, FGB, FGG and the APPs in response to DENV-2 infection and IL-6 treatment corresponded to those that occurred in Huh-7 cells. This included a decrease in the *FGA, FGB, FGG and HP* transcript levels in response to DENV-2 infection with a positive response to IL-6 treatment, no significant differences in the *SERPINA1* transcript levels in response to DENV-2 infection or IL-6 treatment and an increase *SERPINC1* transcript levels in response to DENV-2 infection with negative response to IL-6 treatment (Figure 7.9B). However, the effects on the *HNF4A* transcripts in HepG2 cells showed some dissimilarity. There was no decrease *HNF4A* transcript levels in DENV-2 infected HepG2 cells as for Huh-7 cells but a significant decrease in the *HNF4A* transcript level in response to IL-6 treatment.

The dysregulation in mRNA transcript levels in response to DENV-2 infection both with and without IL-6 stimulation could not explain all of the changes in protein amounts observed in response to DENV infection. Multiple mechanisms might be involved in the dysregulation of the APPs. Therefore the role of post-translational protein stability especially the role of protein degradation by the proteasome was next investigated.

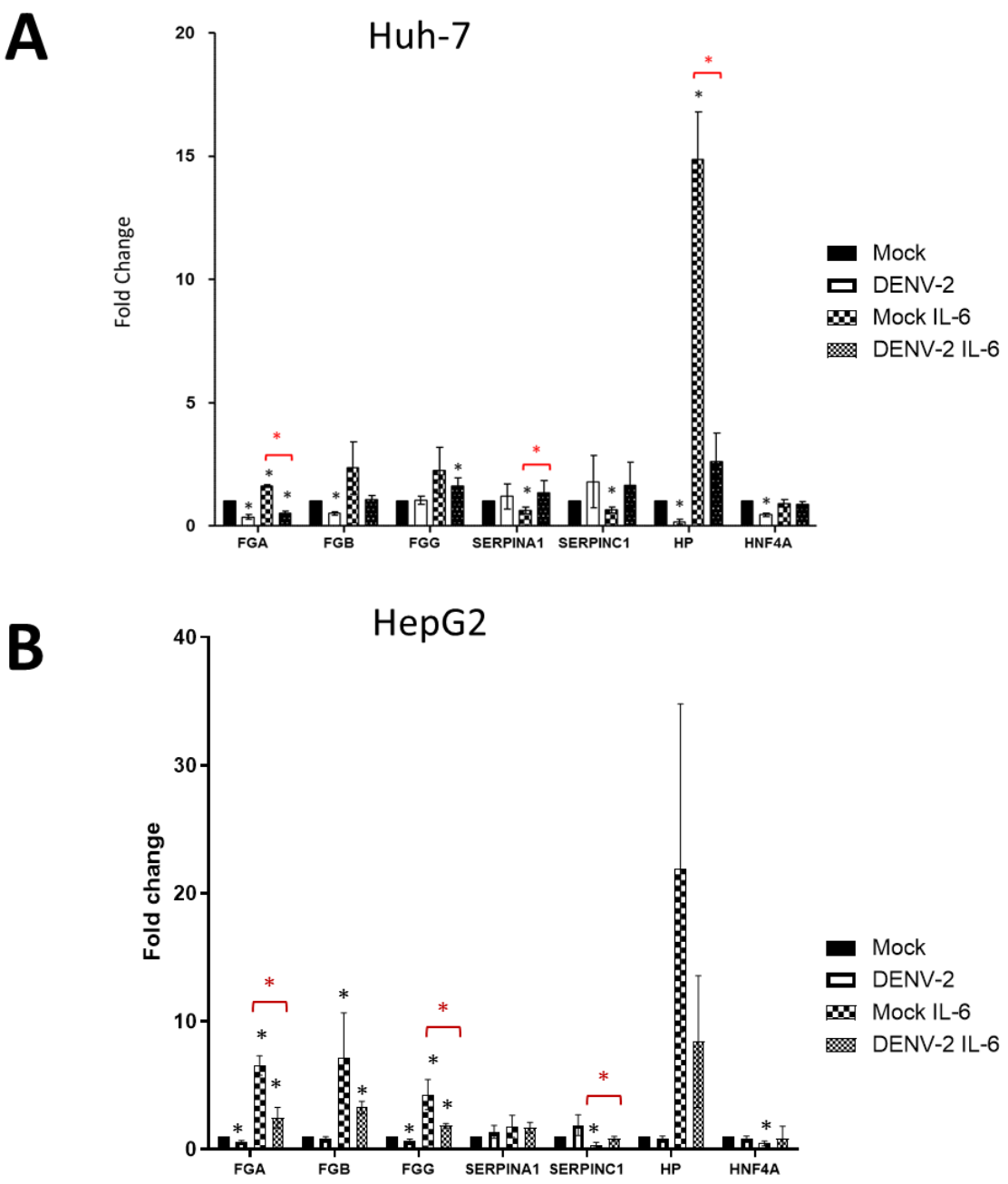

Figure 7.9 Analysis of the effect of IL-6 on FBG and APPs mRNA transcript levels by qRT-PCR.

Huh-7 **(A)** and HepG2 **(B)** cells were infected with DENV-2 at a MOI of 5 or mock infected. IL-6 (50 ng/ml) was added or not to the media at 6 hpi. Cells were harvested for analysis at 30 hpi. Relative quantitation of mRNA level was performed by qRT-PCR. The experiments were done in triplicate. Data was presented in term of mean ± SD. * = P-value ≤ 0.05.

7.5 Posttranslational protein degradation

Because the majority of proteins are degraded by the ubiquitin-proteasome system, MG132, which is a potent proteasome inhibitor was used to investigate whether the alteration in proteins level observed in response to DENV-2 infection were a result of proteasomal degradation. Firstly, the dose and duration of MG132 treatment were determined. The survival and general condition of Huh-7 cells incubated with MG132 at doses of 1-5 μM for up to 24 h was determined by microscopic examination (data not shown). Then the effect of MG132 on protein stability during DENV-2 infection was analysed by adding either a low (1 μM) or high dose (5 μM) of MG132 to both DENV-2 (at MOI of 5) and mock infected cells at 6 and 12 hpi (18 and 24 h of treatment, respectively). An equivalent volume of DMSO was used as control. There was no difference in the DENV-2 infection rate due to MG132 treatment as determined by IFA (Figure 7.10). The effect of MG132 treatment on the level of the proteins of interest during DENV-2 infection was then determined by Western blotting. STAT2 was selected as a positive control because it is known to be degraded by the proteasome during DENV infection (Ashour *et al*., 2008). The addition of MG132 was found to rescue the decrease in the FBG proteins, HNF4A and SERPINC1 observed in DENV infection (Figure 7.11). Moreover, the effect was dose dependent more than time dependent.

These findings reveal that the decrease the amounts of FBG and APPs in response to DENV infection is at least in part a result of proteasomal degradation.

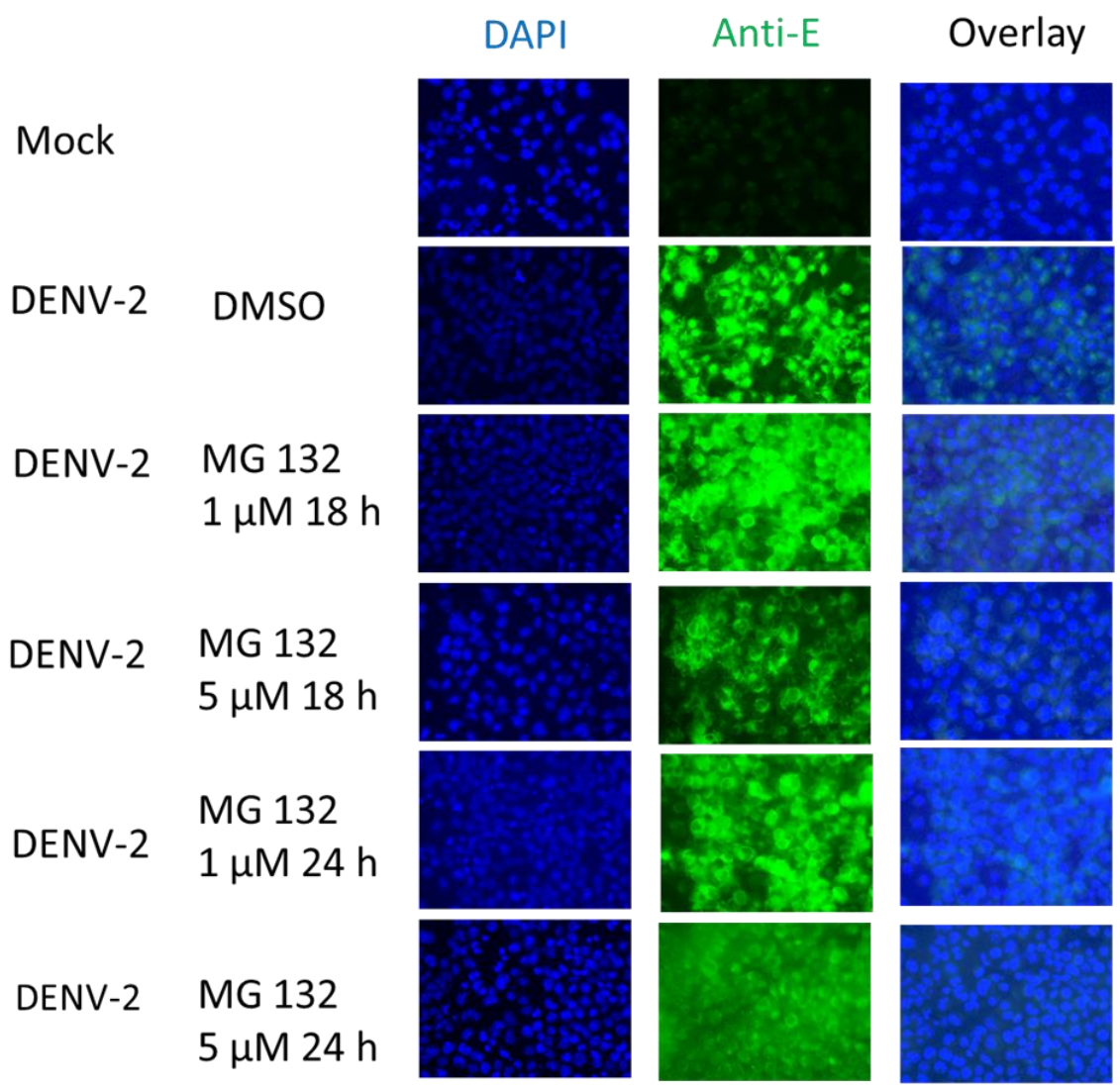

Figure 7.10 Analysis of the effects of MG132 on DENV-2 infection of Huh-7 cells by IFA.

Huh-7 cells were infected with DENV-2 at a MOI of 5 or mock infected. MG132 (1 and 5 µM in DMSO) or DMSO alone as indicated was added at 6 and 12 hpi. After 18 h or 24 h of MG132 or DMSO treatment, the cells were fixed and immunostained with an antibody against the DENV-2 E protein (Anti-E, green), nuclear DNA was visualised with DAPI (blue). Images were taken using a Leica widefield microscope with 40X magnification.

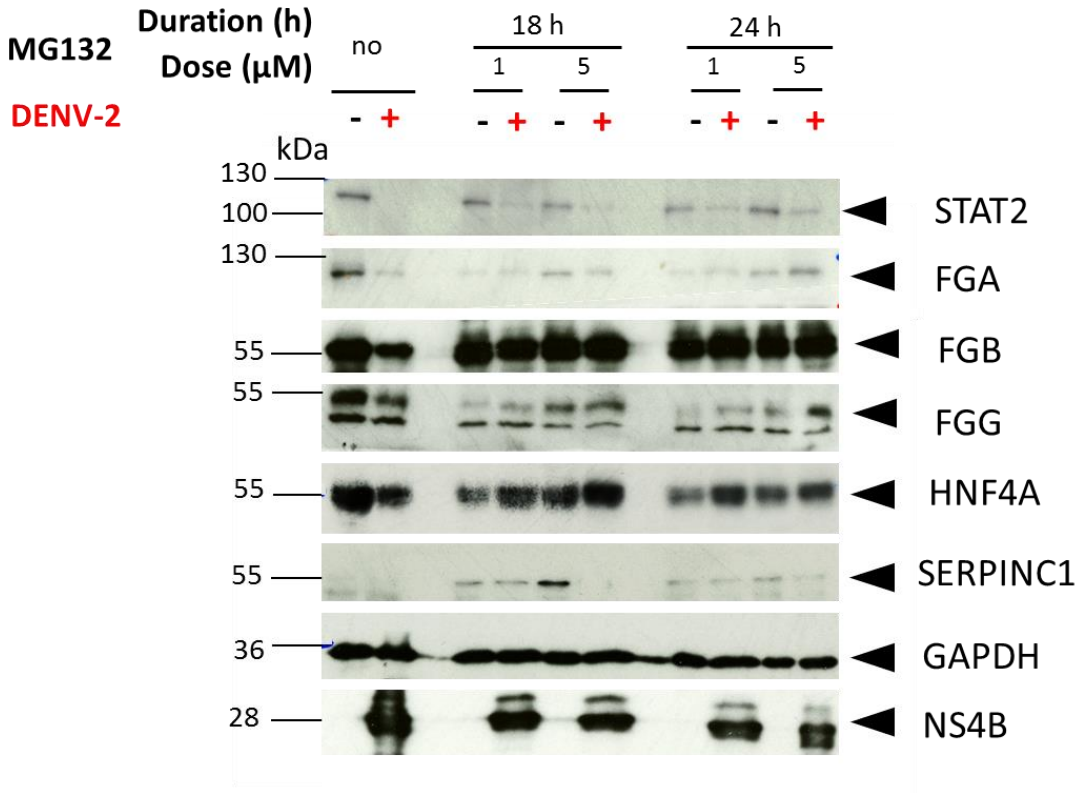

Figure 7.11 Analysis of the effects of MG132 on FBG, HNF4A and SERPINC1 amounts in DENV-2 infected Huh-7 cells by Western blotting.

Huh-7 cells were infected with DENV-2 at a MOI of 5 or mock infected. MG132 (1 or 5 µM in DMSO) or DMSO alone as indicated was added. After 18 and 24 h of MG132 or 24 h of DMSO treatment, the cells were harvested as total cell lysates. Twenty µg of cell lysate were loaded in each lane and the proteins separated by SDS-PAGE prior to Western blotting. Antibodies against STAT2, FGA, FGB, FGG, HNF4A, SERPINC1, NS4B and GAPDH were used to detect the amount of relevant proteins. GAPDH and NS4B were used as a loading control and marker of infection, respectively. The positions of relevant molecular mass markers are shown in kDa.

7.6 Imaging analysis of FGB and FGG

The intracellular level and/or distribution of the FBGs proteins in DENV-2 infected Huh-7 cells was examined by IFA. FGB and FGG were successfully immunostained while attempts to immunostain FGA were unsuccessful (data not shown for FGA) (Figure 7.12). There was no obvious change in the staining of FGB, but a decrease in the staining of FGG in response to DENV-2 infection. The distribution of FGG was also altered in DENV-2 infected Huh-7 cells. Further analysis by confocal microscopy was then performed to examine the change in the distribution of FGB and FGG in DENV-2 infected cells at both low and high MOI (MOI of 1 and 5) (Figures 7.13 and 7.14). In mock infected cells, FGB and FGG had a diffuse cytoplasmic distribution. Whereas in DENV-2 infected cells, FGG showed a more speckled cytoplasmic distribution and was found to condense in some area as bright spots. The patterns of FGB and FGG in DENV-2 infected Huh-7 cells were not obviously different when cells were infected at a low and high MOI (Figure 7.13 for FGB and 7.14 for FGG). Interestingly, the distribution of FGG in infected cells was similar to that of the DENV E protein used as marker of infection.

A further experiment was done examining potential co-localisation between FGB / FGG and the E protein. Huh-7 cells were infected with DENV-2 at varying MOIs (MOI of 1-5). The degree of co-localisation was measured by the Pearson's correlation coefficient (R) using the ImageJ program. The Pearson's R value ranges from -1 (perfect negative correlation) to 1 (perfect positive correlation); however, only a score <0.5 or >0.5 can be considered as showing a degree of correlation (Adler and Parmryd, 2010). Preliminary analysis revealed a Pearson's R score for co-localisation of the FGB and E protein of 0.35, so a conclusive correlation could not be made (Figure 7.13). By contrast the Pearson's R score for co-localisation of the FGG and E protein showed a positive correlation at the two different MOIs used for infection (Figure 7.14). Thus, the co-localisation of the FGG and E proteins was more extensively examined in both DENV-2 infected Huh-7 and mock infected cells (10 fields each) which revealed a Pearson's R score of 0.62 ±0.10 (mean ±SD) for DENV-2 infected cells compared with 0.089 ±0.05 in mock cells (P-value = 2.40E-11) (Figure 7.14B).

In summary, FGB and FGG showed a different distribution pattern in DENV-2 infected cells compared to mock infected Huh-7 cells. Co-localisation between the FGG and E proteins was demonstrated.

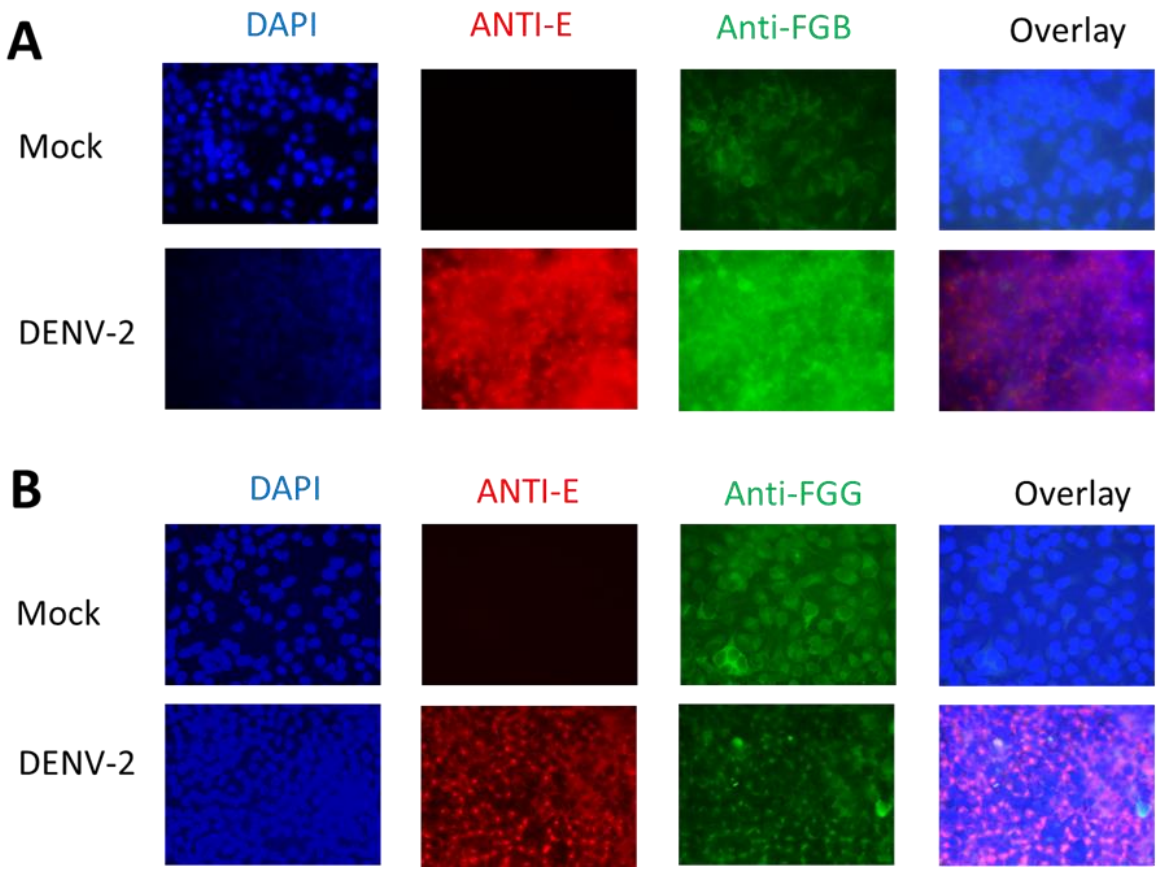

Figure 7.12 Analysis of FGB and FGG in DENV-2 infected Huh-7 cells by IFA.

The amount and pattern of distribution of FGB **(A)** and FGG **(B)** in DENV-2 infected cells compared with mock infected cells were analysed by IFA. Huh-7 cells were infected with DENV-2 at a MOI of 5 or mock infected. At 30 hpi, the cells were fixed and immunostained with an antibody against the DENV-2 E protein (Anti-E, red) and either FGB or FGG (Green), nuclear DNA was visualised with DAPI (blue). Images were taken using a Leica widefield microscope with 40X magnification.

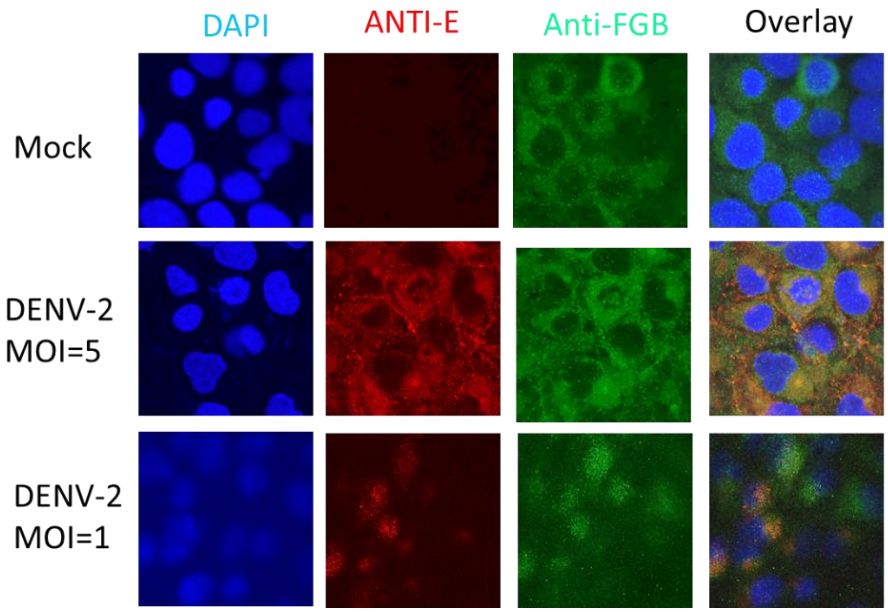

Figure 7.13 Confocal microscopic analysis of FGB in DENV-2 infected Huh-7 cells.

The pattern of distribution of FGB in DENV-2 infected cells compared with mock infected cells was analysed by confocal microscopy. Huh-7 cells were infected with DENV-2 (at a MOI of 1 and 5) or mock infected. At 30 hpi, the cells were fixed and immunostained with an antibody against the DENV-2 E protein (Anti-E, red), and FGB (Green), nuclear DNA was visualised with DAPI (blue). Images were taken using Leica SP5-AOBS confocal laser scanning microscope.

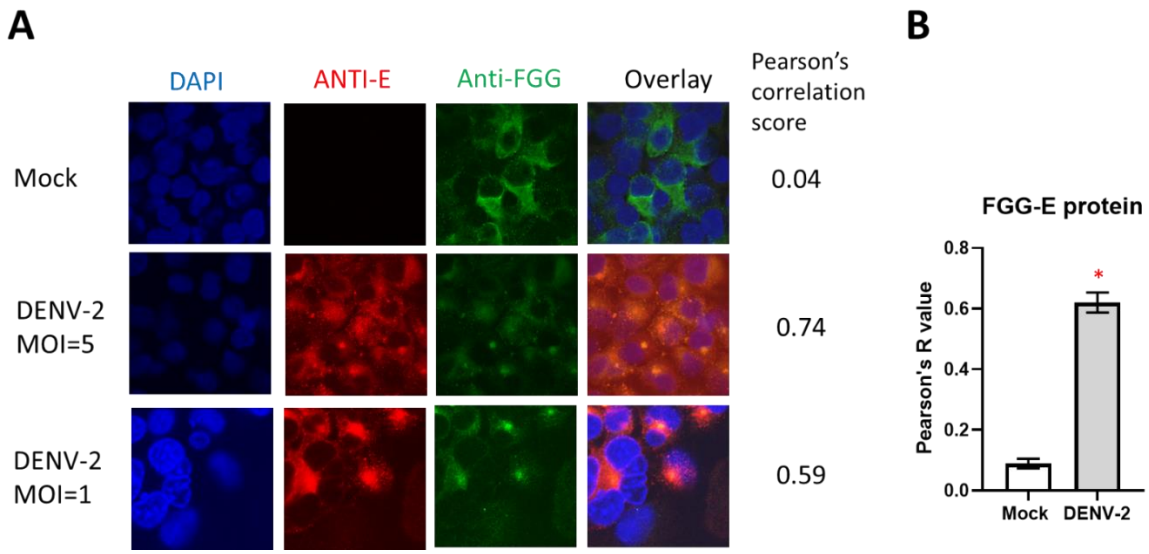

Figure 7.14 Confocal analysis of FGG in DENV-2 infected Huh-7 cells.

(A) The pattern of distribution and co-localization of FGG with the E protein in DENV-2 infected cells compared with mock infected cells was analysed by confocal microscopy. Huh-7 cells were infected with DENV-2 (at a MOI 1-5) or mock infected. At 30 hpi, the cells were fixed and immunostained with an antibody against the DENV-2 E protein (Anti-E, red), and FGG (Green), nuclear DNA was visualised with DAPI (blue). Images were taken using Leica SP5-AOBS confocal laser scanning microscope. **(B)** Co-localisation was determined using the Pearson's correlation coefficient using the ImageJ program. Statistical analysis was performed to compare co-localisation of FGG and E protein in DENV-2 infected and mock cells, using 10 images per group. Data is shown in terms of the mean ±SEM. * = P-value < 0.05

7.7 FGG-virus protein-protein interaction (PPI) analysis

Previous interactomic studies have identified an interaction between FGA and the DENV NS2A and NS5 proteins as well as an interaction between FGB and NS3 (Khadka *et al.,* 2011). FGG has not been detected to interact with DENV proteins. In this study, an examination of potential PPIs between FGG and DENV E proteins was undertaken as there was no change in the FGG mRNA transcript level in DENV-2 infected Huh-7 cells and FGG and the DENV E protein were identified to co-localise. Co-IP analysis using an anti-FGG antibody was performed to identify potential interactions between FGG and DENV proteins as well interactions between FGG and other FBG chains. Lysates prepared from DENV-2 (at MOI of 5) and mock infected Huh-7 cells were incubated with either anti-FGG (a mouse monoclonal) or control mouse serum (described in section 2. and Table 2.5). After Co-IP, the protein eluates were analysed by SDS-PAGE and Western blotting using antibodies against FGA, FGB and DENV E protein.

The detection of FGG bands in FGG-IPs from both mock and DENV-2 infected cells (but not using control serum) indicated the IP was successful (Figure 7.15). Although interactions between FGG and both FGA and FGB were expected, the results revealed a detectable interaction only between FGG and FGB. Stronger FGB bands were observed in the FGG-IP using the mock cell lysate compared with the lysate from DENV-2 infected cells. Interestingly, there were a consistent detection of the E protein in the FGG-IP compared to the serum control, indicating an interaction between FGG and the DENV E protein. The results for other viral proteins (prM, NS4B and NS5) were inconclusive due to inconsistent results between experiments (data not shown).

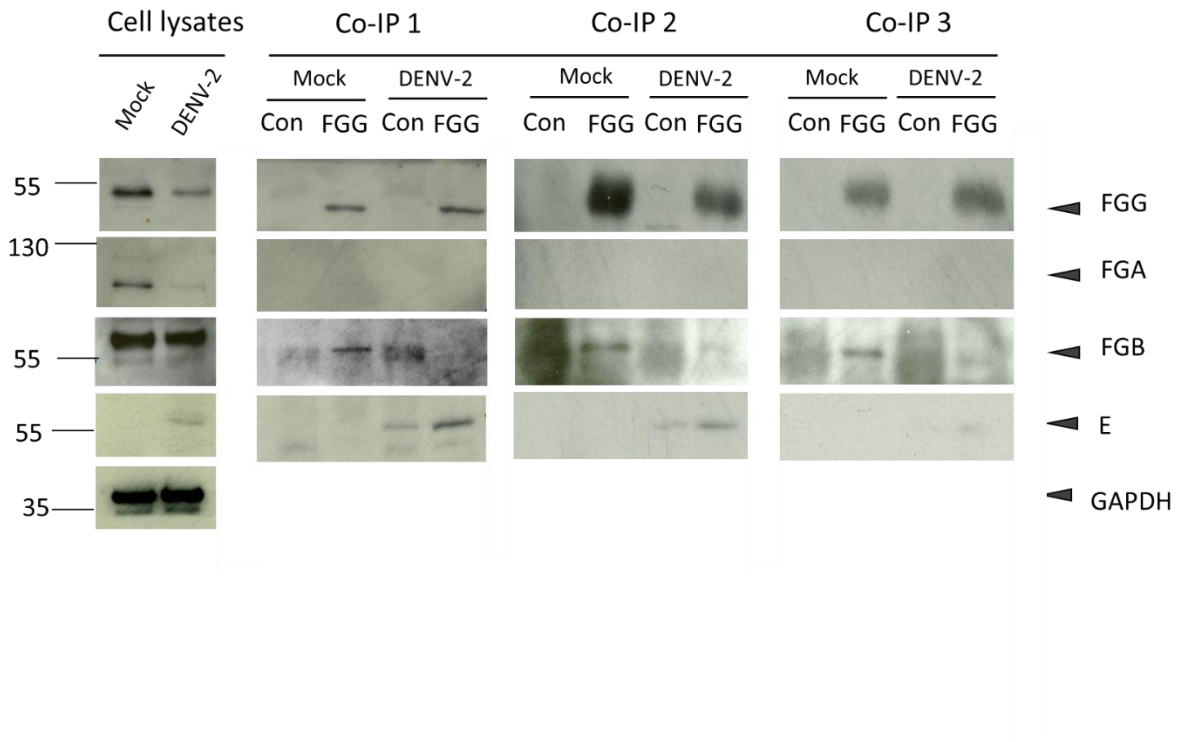

Figure 7.15 Protein-protein interactions with FGG identified by Co-IP.

Co-IP analysis was performed using cell lysates from DENV-2 (at MOI of 5) and mock infected Huh-7 cells. Equal amounts of cell lysates and anti-FGG antibody was used for Co-IP. A matched mouse serum was used as a negative control (Con). Western blotting analysis of the immunoprecipitates was performed using antibodies against FGG, FGA, FGB, DENV E and GAPDH. The experiment was done in triplicate (Co-IP 1-3). The positions of relevant molecular mass markers are shown in kDa.

7.8 Discussion

In this chapter, the results of experiments investigating the dysregulation of FBG and APPs during DENV infection of infected liver cell lines are described. Multiple techniques were applied to identify the mechanism/s underlying the decrease in liver APPs in DENV infected cells.

Optimisation of IL-6 stimulation condition

To study the cytokine response of APPs in an experimental setting, IL-6 which is the key regulator of APPs was selected. The secretion and effects of IL-6 in Huh-7 and HepG2 cells are different from those of type I IFNs. The hepatoma derived cell lines, both Huh-7 and HepG2 have a low basal level of IFN signaling proteins and needs higher doses of IFNα to stimulate the antiviral response compared with non-hepatoma derived cancer cell lines (Melen *et al.*, 2000). In contrast, previous studies revealed that both the Huh-7 and HepG2 cell lines exhibited robust IL-6 responses and as such, have been widely used to study the effect of IL-6 on APPs *in vitro* (Ray *et al.*, 2000; Ait-Goughoulte *et al*., 2009; Brock *et al*., 2011; Lukowski *et al*., 2015). In i*n vivo* conditions, IL-6 is secreted from endothelial cells, monocytes and macrophages and transported to the liver *via* blood circulation. Furthermore, Kupffer cells in the liver also secrete local IL-6 to neighbouring hepatocytes (Schmidt-Arras and Rose-John, 2016). A previous study reported that Huh-7 and HepG2 cells neither express IL-6 mRNA nor secret IL-6 (Matsuguchi *et al.,* 1990). In support of this finding, neither intracellular IL-6 nor a IL-6 RT-PCR product were detected using Huh-7 cell lysate in this study (proteomic results from Chapter 5 and RT-PCR results in this chapter). Thus, IL-6 was added to liver cells to mimic *in vivo* conditions.

The effect of IL-6 on the level of APPs in (uninfected) hepatocytes in this study was similar to the effects reported in previous studies. There was an increase in the effect/s of IL-6 with increased dose and duration of IL-6 treatment. The effect reached a peak at 50 ng/ml (final concentration) and 24 h of treatment after which there was a decreased effect with a high dose of Il-6 (100 ng/ml) and a longer duration of treatment (30 h). A previous study in which HepG2 cells were treated with different doses of IL-6 (ranging from 5-100 ng/ml) followed by measurement of the mRNA transcript levels of FGG and HP (after 24

h of treatment) reported a peak effect at a dose of 20-50 ng/ml and a decrease in mRNA levels at the dose of 100 ng/ml (Brock *et al*., 2011). The effect of treatment time on IL-6 stimulation of APPs was studied in primary human hepatocytes (PHH) and revealed parallel increases of positive APPs (FBG, CRP and SERPINA1) with the duration of treatment until a steady state was reaching after 25-30 h (Heinrich *et al*., 1990).

Dissimilar to type I IFN (Diamond *et al.,* 2000), the addition of IL-6 both pre- and post-infection did not lead to a significant decrease in the efficiency of DENV infection (determined by IFA) or viral production from liver cells. In this study, IL-6 was added to DENV infected liver cells after infection to mimic the *in vivo* pathophysiology of DENV infection on APPs.

Alteration in proteins and mRNA levels of FBG and APPs in Huh-7 and HepG2 cells in response to DENV infection with and without IL-6.

At the protein level, the results revealed similar changes in the amounts of the proteins of interest (all FBG, HNF4A and SERPINC1) in Huh-7 and HepG2 cells in response to DENV infection. Thus, the decreases in liver APPs during DENV infection was not specific to a particular liver cell line. However, it is should be kept in mind that both cell lines may share similar characteristics as they are hepatoma-derived in nature. HNF4A is the key hepatic gene regulator, the decrease in HNF4A during infection may contribute to the decrease in proteins regulated by HNF4A, including the FBG proteins and SERPINA1.

Overall the analysis of FBG and APP mRNA transcript levels in Huh-7 and HepG2 cells in response to DENV infection showed the same trends. The significant decreases in the mRNA transcript levels of *FGA*, *FGB*, *HP* and *HNF4A* in DENV-2 infected Huh-7 cells as well as those of *FGA* and *FGG* in HepG2 cells correlated with decreases in the amounts of the corresponding proteins. However, the mRNA transcript levels of *FGG*, *SERPINA1*, and *SERPINC1* in DENV infected Huh-7 cells and *SERPINC1* and *HNF4A* in DENV infected HepG2 cells did not correlate with the decreases in protein amounts. In a previous study that analysed changes in the transcriptome in response to DENV-2 infection of Huh-7 cells (using a whole genome microarray), no changes were detected in the mRNA transcript levels of all the genes examined in this investigation (Goh *et al.,* 2016). The

differences in the results may be from the different experimental conditions and techniques used in the studies. Goh's study were performed by using MOI of 10 and studying mRNA level at 24 hpi using microarray technique, while this study used MOI of 5 and studied mRNA level at 30 hpi with qRT-PCR. However, collectively, the changes in mRNA transcript levels detected in this and previous studies do not fully explain all of the decreases in the FBG proteins and APPs found in liver cells in response to DENV infection in this study. Several studies have previously documented the disagreement between gene expression and protein levels in human cell lines; for example, a study analysing the transcriptome and proteome of a medulloblastoma cell line (by microarray and LC-MS/MS, respectively) demonstrated that mRNA abundance could explain only 67% of protein abundance variation, with a positive correlation score (R^2) of 0.32 (Vogel *et al*., 2010). Moreover, changes in mRNA transcripts in response to DENV infection is a dynamic process. For example, a study of gene expression signatures associated with lipid metabolism in DENV-2 infected HepG2 cells by qRT-PCR revealed increases in specific mRNA transcripts until 24 hpi before decreases at 48 and 72 hpi (Tongluan *et al*., 2017). The mRNA transcript levels in this study were measured at the same time as protein levels (30 hpi). Thus, the results from single time point measurement might not explain the relationship between mRNA and protein levels of all the selected APPs.

As expected, IL-6 treatment resulted in an increase in the FBG and HP protein and mRNA transcript levels in both liver cell lines. Increases in the mRNA transcript levels of *FGA, FGB, FGG* (Lukowski *et al*., 2015) and *HP* (Brock *et al.*, 2011) in HepG2 cells after 24 h treatment with IL-6 have been reported. The decrease in the mRNA transcript and protein level of SERPINC1, which is a negative APP was expected. An increase in the protein level of SERPINA1 after IL-6 treatment for 24 h in Huh-7 cells in this study was similar to the results found using HepG2 cells and human liver tissue (Heinrich *et al*., 1990). However, there was a significant decrease in *SERPINA1* mRNA levels in Huh-7 cells in response to IL-6. As mentioned earlier, changes in mRNA transcripts level might not correlate with a similar change in protein amount. Another possibility is the mRNA level might be modulated by miRNAs.

Infection with DENV was found to blunt the effect of IL-6 stimulation on the protein levels of all positive APPs in both Huh-7 and HepG2 cells. Small increases in the levels of some APPs (eg. HP in Huh-7 and FBG in HepG2 cells) in cells treated with IL-6 and DENV infected were observed; however, overall the protein levels still decreased when compared with untreated mock infected cells for both cell lines. The analysis of the corresponding mRNA transcripts revealed a more marked response to IL-6 treatment. In contrast to the protein levels, the mRNA transcript levels of almost all of the positive APPs (except *FGA* and *FGB* in Huh-7 cells) in DENV infected cells treated with IL-6 increased to level higher than in mock infected cells not treated with IL-6. These results suggested that the decreases observed in the amounts of APPs in liver cells in response to DENV infection is mainly due to a mechanism distinct from any changes observed in APP gene transcription.

It was concluded that even under conditions of high IL-6 stimulation (mimicking the pathophysiology of a severe DENV infection), there were still decreases in APP protein amounts that in turn, led to decreased secretion of liver APPs. The increases in mRNA transcript levels but decreases in protein amounts for FBG and APPs during DENV infection and IL-6 stimulation suggested post-transcriptional changes. However, apart from an increase of IL-6, increases in the amounts of other cytokines including IL-8 and IL-1β (another key regulator of APPs) have been reported in DEN patients (Bozza *et al*., 2008; Priyadarshini *et al.*, 2010). This may explain the different results observed between this study and studies investigating *in vivo* pathophysiology.

Post transcriptional regulation of FBG and APPs

The APPs are known to be post-transcriptionally regulated by transcript stability, miRNA dependent transcriptional control and protein degradation (Bode *et al*., 2012). Several studies have reported post-transcriptional modulation of APPs; for example, degradation of the SAA mRNA transcript mediated by the 3´-untranslated regions was reported in IL-1β and IL-6 stimulated HepG2 cells (Longley *et al*., 1999).

The role of miRNAs in the regulation FBG and APPs has been widely documented. For example, a study in which Huh-7 cells were transfected with a library of human miRNAs enabled the identification of 23 and 4 miRNAs that significantly decreased and

increased FBG production, respectively (Fort *et al.*, 2010). Furthermore, over expression of miR-18a could induce both mRNA and protein levels of HP and FBG in IL-8 stimulated HepG2 cells (Brock *et al*., 2011). Dysregulation of miRNA in DENV infection has been widely studied in both cell-based experiments (Escalera-Cueto *et al*., 2014; Kanokudom *et al*., 2017) and using patient blood samples (Diosa-Toro *et al*., 2017). An upregulation of miR-let7c (measured by microarray and qRT-PCR) in DENV-2 infected Huh-7 and U937 DC-SIGN cells has been reported since 12 hpi (Escalera-Cueto *et al*., 2014). An overexpression of miR-let7c after miR-let7c transfection resulted in a significant decrease in FBG secretion from Huh-7 cells (Fort *et al.,* 2010). Collectively, these studies suggest an increase in miR-let7c may contribute to a decrease in FBG levels in DENV infected Huh-7 cells. Thus, further experiments investigating the role of miRNAs in the modulation of FBG and APPs in the context of DENV infection should be performed.

The instability and degradation of APPs was previously mentioned. After assembly of FBG in the ER, the unassembled/misfolded FBG chains are degraded by the ERAD using a proteasomal dependent system (Redman and Xia, 2001). A previous study using an ERAD assay proposed that the mutant FGG chain, named fibrinogen Aguadilla, was targeted by ERAD and subsequently degraded by the proteasome (Kruse *et al.,* 2006). Furthermore, the excess fibrinogen Aguadilla that accumulated in ER was also sent to the vacuole *via* autophagy (Kruse *et al*., 2006).

According to the published literature, this is the first time that proteasomal degradation has been demonstrated to be a mechanism used to decrease key coagulation proteins and APPs in DENV infection. Furthermore, both positive (FBG) and negative (SERPINC1) APPs were degraded in DENV infection. It is well established that an interaction between DENV NS5 and STAT2 results in a decrease in STAT2 *via* proteasome-mediated degradation during DENV infection (Ashour *et al*., 2008; Mazzon *et al.,* 2009). Thus, based on the results produced in this investigation it is hypothesised that interaction/s between APPs and DENV proteins results in misfolded APPs that are then degraded in a proteasome dependent manner. Alternatively, DENV replication on ER membranes leads to ER stress and dysfunction which may cause a defect in assembly of APPs (that occurs in ER lumen). Together with the increased APP production due to

stimulation *via* cytokines released during DENV infection, the overexpressed unassembled APPs are then processed *via* proteasomal degradation (which is the part of ERAD). Furthermore, DENV infection itself also stimulates ER stress, which triggers UPR responses and ERAD functions which may lead to increased degradation of multiple proteins including APPs in hepatocytes.

The results from Chapter 5 revealed decreases in multiple coagulation proteins and APPs as well as proteins involved in complement systems and lipid metabolism. However, only FBG and key APPs were selected for investigation in this chapter. Thus, further experiments to investigate the effect of proteasomal degradation in the proteomes of DENV-2 infected Huh-7 cells with high throughput LC-MS/MS should be done.

FGG and DENV E protein PPI

Co-localisation of FGG and the DENV-2 E protein was observed. Theoretically, co-localisation means two proteins are present in the same area or associated with the same structure in cells (Dunn *et al.,* 2010). The change in the distribution of FGG and co-localisation of FGG and the E protein in DENV infected Huh-7 cells may be a result of an interaction between FGG and the DENV E protein (or other proteins that bound with E protein e.g. prM) leading to a change in the distribution of FGG in DENV infected cells. Another possible explanation is that both the FGG and E proteins are present in the same organelle/structures such as in ER. The ER is where FBG assembly, degradation of unassembled/misfolded FBG and DENV replication occur. Further co-localisation studies examining the localization of FGG and ER or UPS markers may provide a better understanding of this process.

To provide more evidence for the interaction between FGG and the E protein, co-IP analysis was done which confirmed an interaction between FGG and the E protein. As the DENV prM protein interacts with the E protein in the immature virion, an antibody against the DENV prM was also used to analyse the immunoprecipitates by Western blotting. However, an interaction between prM and FGG was not detected (data now shown). The FBG-DENV protein interaction was previously identified in one study (Khadka *et al.,* 2011). Using yeast two-hybrid analysis, Khadka *et al*., reported an interaction between FGA and both NS2A and NS5, whilst interactions between FGB and

NS3 and FGA and FGB were also detected (Khadka *et al.*, 2011). Thus, this is the first time that an interaction between FGG and a DENV protein has been identified. The results of the FBG co-IP analysis were limited as the co-IP was performed only for FGG and analysed with limited antibodies against DENV proteins. Future studies using a combined co-IP / LC-MS/MS approach may provide more information about proteins that interact with FBG.

It is established that DENV NS5 targets proteins for degradation *via* the proteasome in DENV infected cells (Ashour *et al*., 2008) and the DENV E protein interacts with key ER chaperones, including HSPA5 (Limjindaporn *et al*., 2009). Collectively, the interaction between FGG and DENV E protein identified here and the interaction between FGA and NS5 previously suggests multiple DENV proteins may contribute to proteasomal degradation of FBG.

One of the limitations of this study is that the experiments performed only with DENV-2 may not be generalised to other serotypes. Although the results from previous proteomic analyses of DENV-2 and DENV-4 infected Huh-7 cells (done in the laboratory) revealed similar trends (Chiu, 2014; Yousuf, 2016), the serotype-specific differences in the properties of DENV proteins have been previously reported. For example, the nuclear localisation of DENV-2 and DENV-4 NS5 differs in infected cells (Hannemann *et al*., 2013) as well as the interaction between ERC1 and NS5, which was determined to be serotype 2 specific (Chiu, 2014).

In conclusion, the investigations reported in this chapter suggest the mechanisms underlying the alterations in APPs are multifactorial. Evidence was provided of dysregulation at both the mRNA transcript and proteins stability levels but the major determinant appears to be proteasomal degradation of the FBG proteins and APPs. An interaction between FGG and the DENV-2 E protein was identified by co-localisation and co-IP. Furthermore, using experimental conditions mimicking *in vivo* infection, IL-6 stimulation could not overcome the degradation of FBG and APPs proteins. Future high throughput studies and protein interaction studies are required to further understand the role of proteasomal degradation on the whole proteome in DENV infected liver cells, and

whether this effect is entirely mediated by viral host protein interactions or due to a dysregulation of specific cellular processes.

CHAPTER 8. GENERAL DISCUSSION AND FUTURE PERSPECTIVES

As an emerging disease, DEN has become a major global public health issue within decades of the first isolation of DENV in 1943. The disease not only effects people in endemic areas but also international travellers. The high number of cases and the complicated course of disease have stimulated intensive research into identifying the underlying causes of DEN pathogenesis, which would facilitate the development of treatments for clinical intervention, that are limited. Unfortunately, despite much effort and many studies, good biomarkers to either diagnose DEN in the late stage of disease or to predict disease severity are lacking and there are no specific antiviral treatments or a fully safe and protective vaccine. The lack of an animal model to study pathogenesis is a major impediment in DEN research. As such, pathogenesis studies have used clinical samples or relevant cell-based models. Most clinical studies have focussed on the analysis of blood from DEN patients to quantify mRNA, proteins or cytokines. Studies using cell-based systems should be used with caution when trying to understand pathogenesis, which should ideally be done in clinical studies. Multiple cell lines have been used in DENV studies, to date, there is no consensus concerning the most relevant cell models for studying DEN pathogenesis. In addition, studies systematically comparing the results of cell-based studies with those using clinical specimens are limited. In this study, high throughput proteomic analyses of the proteomes and secretomes of DENV infected HEK293T and Huh-7 cells were simultaneously done and the results reported in Chapters 4 and 5 respectively. Importantly, an integrated analysis of the proteome and secretome of DENV infected cells was performed for the first time. Furthermore, a comparative proteomic analysis of cells stably maintaining a DENV replicon (which is a useful model for studying DENV intracellular replication) and DENV infected cells was described in Chapter 4. The results from cell-based models were then compared with the results of a proteomic analysis of serum from patients with differing grades of DEN and described in Chapter 6. This comparison identified decreases in FBG and liver APPs as common to DEN patient serum and DENV infected liver cell lines. The potential mechanisms underlying the decreases in

FBG and liver APPs were further investigated as described in Chapter 7. Importantly, the work described in this thesis demonstrates the use of cell based models for the study of clinically relevant proteins and highlights cellular processes perturbed during DENV replication which have direct relevance to DEN pathogenesis.

8.1 Secretome analysis: challenges and potential applications

Overall, analysis of the proteomes and secretomes of REP cells (in Chapter 4) and DENV infected Huh-7 cells (in Chapter 5) showed that the changes that occurred in protein levels in the cellular proteome were reflected in the secretome, suggesting that dysregulation of protein levels intracellularly, led to the alterations observed in the secretome. The relationship between the cellular proteome and secretome of DENV infected HEK293T cells could not be explored due to the low number of proteins that significantly changed in amount. Furthermore, comparison of the proteomic analyses obtained using the Huh-7 cell model (in Chapter 5) with that using serum from DEN patients (in Chapter 6) demonstrated the relationships between the cellular proteome, secretome and serum proteome. This highlighted the potential of secretome studies for increasing our understanding of DEN pathogenesis.

Interestingly, a large number of proteins were detected in the secretomes but not detected in the proteomes, 883 and 342 proteins in the HEK293T (Figure 4.3) and Huh-7 cell (Figure 5.3) secretomes respectively. These proteins might not accumulate or function intracellularly but be secreted to act as signal proteins or components of the extracellular matrix. This hypothesis is supported by the results of the STRING analysis of the 883 proteins detected only in secretome of HEK293T cells, which revealed an enrichment of proteins associated with the GOBP term “cell adhesion”, GOCC term “collagen-containing extracellular matrix” and GOMF term “signaling receptor binding”. The group of DDX proteins that significantly changed only in the secretomes of DENV infected cells and/or REP cells (but not in the proteomes) were highlighted in Chapter 4 as proteins potentially involved in the host antiviral immune response.

However, there are many challenges in secretome analysis that need to be solved. Firstly, methods to minimise the amount of BSA in cell culture supernatants need to be improved. Growing cells in SFM affects their energy metabolism and may affect proteomic analysis of proteins involved in energy metabolism. Secondly, ideally the concentration method needs to be effective and fast (as described in Chapter 3) so that proteins are not unequally concentrated from the secretome or subject to proteolytic activity. Thirdly, the method used to validate the proteomic results requires consideration. Many previous secretome studies were not able to validate the results of LC-MS/MS analyses; for example, a previous study examining the secretome of DENV infected HepG2 cells (Higa *et al*., 2008). Western blotting was not always sensitive enough to detect proteins which were present in low amounts in the secretome samples, even though there was a large fold increase in the amount of a protein between conditions. Only proteins that are known to be secreted in high amounts such as FBG and APPs were successfully validated in this study.

8.2 Applications of *in vitro* cell models for the study of DENV infection

Unfortunately, despite a number of advantages of HEK293T cells for general molecular virology studies on DENV, as mentioned in Chapter 4, they appear not to be an optimal cell line for studies related to DEN pathogenesis. However, this study demonstrated that there was a good overall correlation between the proteomic results obtained using DENV infected HEK293T cells and the same cells expressing a DENV replicon. Few studies have compared changes in the transcriptome or proteome in cells containing a DENV replicon to those infected with DENV, although replicon systems are widely employed for antiviral screening. This finding supports the use of a DENV replicon system for studying general host cell responses to DENV replication, and the interaction of viral and cellular proteins. Recently, Huh-7 cells stably maintaining a DENV replicon were developed in the laboratory by Dr. Maia Kavanagh Williamson. As the results from this study revealed that Huh-7 cells were a useful model for some aspects of DEN pathogenesis, the replicon containing Huh-7 cells will be useful to dissect these processes further.

Although PHHs are the ideal model for studying human liver pathophysiology, their use is limited by low reproducibility (batch-to-batch variability), a high cost with a

low passage lifespan and limited availability (Zeilinger *et al*., 2016; Shi *et al.*, 2018). Thus, transformed hepatic cell lines have been extensively used in biological studies to overcome the limitations of PPH. Huh-7 and HepG2 cell lines are derived from well differentiated hepatocellular carcinoma liver tissue. Both cell lines are highly permissive to DENV infection and widely used as *in vitro* models for DENV studies. At the protein level, a proteomic study using high throughput LC-MS/MS and targeted proteomics to compare liver microsomes isolated from pooled liver samples (membrane fragments prepared from homogenized liver) using three hepatoma-derived cell lines (HepG2, Hep2B and Huh-7) revealed a correlation among the three cellular proteomes of 0.65, by principal component analysis (PCA)) (Shi *et al*., 2018). However, a marked difference between the protein profiles of pooled liver microsomes and the hepatoma cell lines was observed (Shi *et al*., 2018). Pathway analysis revealed significant differences between human liver cells and Huh-7 / HepG2 cells in biological processes related to metabolism including; drug metabolism-cytochrome P450, steroid hormone biosynthesis, spliceosome and ribosomes (Shi *et al.*, 2018), however, these processes were not dysregulated in response to DENV infection in Huh-7 cells in the experiments presented in this thesis. Unfortunately, there was no available data which could be used to compare the coagulation proteins and APPs in liver cell lines and human liver tissue.

Therefore, for the first time, the hepatoma derived cell line, Huh-7, has been demonstrated to be a relevant cell-based model to study changes in the serum proteome in response to DENV infection, particularly in regards to APPs and proteins involved in "complement and coagulation" and "lipid metabolism" pathways. To better model *in vivo* pathophysiology, future investigations using PHH or a 3-dimensional culture system which includes non-parenchymal cells (eg. Kupffer cells as the source of cytokines) will be of much use in studying the dysregulation of APPs in DEN (Zeilinger *et al.*, 2016).

8.3 Potential clinical applications of the study

8.3.1 Biomarkers to diagnose DEN and predict severity

The major problems in clinical practice are the lack of reliable test to diagnose DEN in late phase of disease and no available test to predict severity. An ideal biomarker should

be specific to DEN infection in all stages of disease (febrile, critical, recovery), not influenced by other host conditions (age, sex, race and comorbidity) and able to predict the severity of DEN. Unfortunately, this and previous studies have not identified a protein or set of proteins that satisfies all of these criteria. Moreover, although some candidate biomarkers have been proposed (ie. CRP, SERPINA1, SERPINC1 and HP) there are inconsistencies between different studies, as mentioned in the discussion of Chapter 6 and introduction of Chapter 7. NS1 has been widely used as marker for the diagnosis of DEN. Although NS1 based tests have great sensitivity and specificity in the acute phase of infection, they have a number of limitations (reviewed in Chapter 1) such that these tests are not ideal for diagnosis, especially in severe cases or cases that present in the late phase of disease.

Not all of the proteins that significantly differentiated between DEN patients and healthy controls (described in Chapter 6) potentially can be used as biomarkers for DEN diagnosis. Candidate protein biomarkers should alter (increase or decrease) in the same direction in all disease conditions. They should also be detectable in clinical specimens without ALB/IgG depletion, using routine clinical methods such as an ELISA assay. The relative alteration in protein amounts detected by shot-gun proteomics requires absolute quantification before use in clinical practice. Importantly, any candidate biomarkers need to be validated in much larger patient cohorts using quantitative methods that can determine the specificity and sensitivity values suitable for application in clinical practice. To decrease the time from discovery proteomics to biomarker validation, the selection of candidate protein biomarkers for which tests are already available with known information (ie approved clinical tests, normal healthy values, conditions that effect the level) is optimal, rather than validation of novel proteins for which no tests and little clinical information exists. Thus, coagulation proteins and APPs that are present in high amounts in blood, can be assayed using available tests, and have been studied in clinical conditions other than DEN (for which little information exists) were selected for further analysis in this study, although they are still not ideal biomarkers for predicting whether an individual will progress to severe DEN. Coagulation proteins and APPs (FBG, F2, SERPINC1, SERPINA1 and HP) are not only decreased in DEN but also in severe forms of many

infectious diseases, including bacterial sepsis. Furthermore, underlying liver diseases will affect the interpretation of liver APP amounts.

Although low levels of CRP were reported to distinguish viral disease (mainly DEN) from bacterial infection (Wangrangsimakul *et al.*, 2018), the study included only 24 cases of viral infection and did not mention DEN severity. In another study the CRP level in severe DEN was still high enough to overlap with the range observed in bacterial infections (Chen *et al*., 2015). Thus, CRP needs to be used in combination with other biomarkers for the diagnosis of DEN and the cut-off to predict severe diseases (in each age group) needs to be determined.

8.3.2 Potential therapeutic application of the results from this study

This study revealed a decrease in the serum level of liver APPs which the *in vitro* analyses suggested is a result of decreased production and secretion of these proteins from the liver. Moreover, proteasomal degradation was proposed as a key mechanism for the decrease in APPs. Since alterations in liver APPs occur to combat infection/inflammation, reversing the decrease in APPs, either by blocking proteasomal degradation or replacement therapy may restore the host immune response to DENV infection.

Apart from preventing the dysregulation of FBG and APPs in response to DENV infection shown in this study, the antiviral effect of proteasome inhibitors has been previously documented. Treatment of DENV infected BHK-21 cells with MG132 and curcumin (a traditional Asian herb with a proteasome inhibitory effect) resulted in reduced viral titres (Padilla *et al.,* 2014). Pre-incubating HepG2 cells with a low dose (as low as 0.4 μM) of MG132 and N-acetyl-leucinyl-leucinyl-norleucinal (ALLN) (another proteasome inhibitor) resulted in a decrease in viral titre from DENV infected HepG2 cells without cytotoxic effect (Fink *et al.,* 2007). Pre-treatment of THP-1 cells with β-lactone, a proteasome inhibitor, before infection with DENV-2, also resulted in a decrease in viral titre and accumulation of the DENV E protein, suggesting that DENV egress was blocked (Coy *et al.,* 2015).

Bortezomib is an FDA approved proteasome inhibitor used for cancer treatment. A study which investigated the effects of pre-treating THP-1 cells with Bortezomib before DENV infection reported a decrease in viral production for all serotypes of DENV with a

EC50 (a dose that can inhibit 50% of viral replication) of less than 20 nM while the cytotoxic dose was 1μM (Coy *et al.*, 2015). Bortezomib was also found to inhibit DENV-2 infection using a mouse model with decreased DENV replication in the spleen and a decrease in the severity of disease as determined by the levels of Hct, Plt, leakage and pro-inflammatory cytokines (Coy *et al*., 2015). Curcumin, a traditional herb with many medicinal properties including antiviral and anti-cancer effects, has been used safely in humans as a dietary complement (Hewlings and Kalman, 2017).

Another potential therapeutic approach is replacement therapy. The intravenous administration of concentrated proteins such as SERPINA1 and SERPINC1 is used as a replacement therapy for other conditions in clinical practice. Purified SERPINA1 prepared from pooled plasma has been used for decades as a therapeutic option for α1-antitrypsin deficiency, a genetic disease (Teschler, 2015). In this study it was proposed that decreased SERPINC1 was a result of decreased secretion from the liver, however increased filtration by the kidney has also been proposed to result in decreased SERPINC1 levels (Wills *et al*., 2004). A randomized control trial showed the potential benefit of high dose intravenous SERPINC1 (in a subgroup that did not receive concomitant heparin) in patients with severe sepsis (Warren *et al.,* 2001). Replacement therapy with purified coagulation proteins might have role in SD similar to the administration of fresh frozen plasma and concentrated Plt, that that is given to those with SD and uncontrolled bleeding. However, this strategy would need further investigation in a clinical trial.

Overall the *in vitro* results presented in this study may not be robust enough to demonstrate a clear therapeutic role for proteasome inhibitors in the treatment of DEN. However, given their potential for restoring liver/serum APP levels, in combination with their antiviral effects, the potential therapeutic use of proteasome inhibitors warrants further investigation.

APPENDIX A

Culture media

- **2X MEM**

  Prepared from 10X MEM (Invitrogen) containing 25 mM HEPES, 0.1 mM NEAA, 2 mM L-glutamine and 2% FCS, 100 μg/ml streptomycin and 100 U/ml penicillin

Protein analysis

- **1.5 M Tris-HCl pH 8.8**

  36.30 g Tris base in 100ml of dH_2O

  Adjust pH with HCl and make up to 200 ml with autoclaved dH_2O

- **0.5 M Tris-HCl pH 6.8**

  6 g Tris base in 60 ml of dH_2O

  Adjust pH with HCl and make up to 100 ml with autoclaved dH_2O

- **10% (w/v) SDS solution**

  20 g of SDS in 200 ml of autoclaved dH_2O

- **10% (w/v) ammonium persulphate for electrophoresis, ≥ 98% (APS)**

  0.05 g ammonium persulphate in 0.5 ml of autoclaved dH_2O

- **10X Electrode Buffer pH8.3 (not adjust pH)**

  30.3 g Tris base, 144 g Glycine, 10 g SDS in 1000 ml of dH_2O

- **6X sample buffer**

  7 ml 0.5 M Tris-HCl pH6.8, 3 ml Glycerol, 1.2 g SDS,

  1.2 mg Bromophenol blue

  Make up to 10 ml with autoclaved dH_2O

- **2X sample buffer**

  2 ml of 6X sample buffer added to 4 ml of autoclaved dH_2O

- **Coomassie Brilliant Blue R-250 staining solution**

  0.575 g Coomassie Brilliant Blue R-250, 200 ml methanol, 50 ml acetic acid, 250 ml dH_2O

- **SDS-PAGE Destain solution**

  Add 50 ml of glacial acetic acid to 350 ml of dH_2O

  Add 100 ml of methanol and mix

  Store at RT in sealable container

- **1X Western Blot transfer buffer**

  100 ml methanol, 12.5 g Tris base, 5.63 g glycine

  Make up to 500 ml with dH_2O
- **1X PBS**

  8 g NaCl, 0.2 g KCl, 1.44 g Na2HPO4, 0.24 g KH2PO4 in 1000 ml of dH2O

  Autoclave for 20 min at 121°C
- **PBST**

  1000 1X PBS, 1 ml Tween 20
- **10X TBS**

  12.115 g Trizma HCl (C4H11NO3), 40.03 g NaCl in 400 ml of dH_2O

  Adjust pH to 7.5 with HCl and make up to 500 ml with dH_2O

  Autoclave for 20 min at 121°C
- **TBST**

  50 ml 10X TBS, 450 ml dH_2O, 0.5 ml Tween 20
- **Western blot blocking solution**

  5 g skim milk powder added to 100 ml of PBST
- **Abcam mild stripping buffer**

  15 g glycine

  1 g SDS

  10 mL Tween 20

  Dissolve in 800 mL dH2O

  Adjust pH to 2.2

  Bring volume up to 1 L with dH_2O
- **Immunofocus assay blocking solution**

  10% (v/v) FBS in PBS
- **RIPA buffer**

  25 mM Tris-HCl pH 7.6

  150 mM NaCl

  1% (v/v) Tween-20

  1% (w/v) sodium deoxycholate

  0.1% (w/v) SDS

- **Protease inhibitor** (cOmplete, Mini, EDTA-free Protease Inhibitor Cocktail – Roche)

  1 tablet added directly to 10 ml of RIPA buffer
- **Co-IP lysis buffer (same as RIPA buffer)**
- **Co-IP wash buffer**

  25 mM Tris/Cl pH7.5

  150 mM NaCl

  0.05% - Tween-20

Resolving gel:

	10%
H_2O	1.9 ml
30% acrylamide mix	1.7 ml
1.5M Tris pH 8.8	1.3 ml
10% SDS	0.05 ml
10% APS	0.05 ml
TEMED	0.003 ml
TOTAL	5 ml

Stacking gel:

	5%
H_2O	2.2 ml
30% acrylamide mix	0.67 ml
0.5M Tris pH 6.8	1 ml
10% SDS	0.04 ml
10% APS	0.04 ml
TEMED	0.004 ml
TOTAL	4 ml

Electrophoresis of RNA and DNA

- **6X DNA loading dye**

  10 mM Tris-HCl pH 7.6, 0.03% bromophenol blue, 0.03% xylene cyanol FF, 60% glycerol and 60 mM EDTA

- **10X TBE Buffer**

  108 g Tris base, 55 g Boric acid, 40 ml 0.5M EDTA (pH 8.0)

  Adjust volume to 1 L with dH_2O

  Autoclave for 20 min at 121°C
- **1X TBE running buffer**

  50 ml 10X TBE buffer

  Adjust volume to 500 ml with dH_2O
- **4% (w/v) agarose**

  4 g agarose in 100 ml of 1X TBE
- **10 mg/ml ethidium bromide**

APPENDIX B

Link for Supplementary Tables:

https://uob-my.sharepoint.com/:f:/r/personal/vl15875_bristol_ac_uk/Documents/VL%20Supplementary%20Tables?csf=1&e=KjMGQM

REFERENCES

Adler, J., & Parmryd, I. (2010). Quantifying colocalization by correlation: the Pearson correlation coefficient is superior to the Mander's overlap coefficient. Cytometry A, 77(8), 733-742. doi:10.1002/cyto.a.20896

Afroz, S., Giddaluru, J., Abbas, M. M., & Khan, N. (2016). Transcriptome meta-analysis reveals a dysregulation in extra cellular matrix and cell junction associated gene signatures during Dengue virus infection. Sci Rep, 6, 33752. doi:10.1038/srep33752

Agrupis, K. A., Ylade, M., Aldaba, J., Lopez, A. L., & Deen, J. (2019). Trends in dengue research in the Philippines: A systematic review. PLoS Negl Trop Dis, 13(4), e0007280. doi:10.1371/journal.pntd.0007280

Ait-Goughoulte, M., Banerjee, A., Meyer, K., Mazumdar, B., Saito, K., Ray, R. B., & Ray, R. (2010). Hepatitis C virus core protein interacts with fibrinogen-beta and attenuates cytokine stimulated acute-phase response. Hepatology, 51(5), 1505-1513. doi:10.1002/hep.23502

Akey, D. L., Brown, W. C., Jose, J., Kuhn, R. J., & Smith, J. L. (2015). Structure-guided insights on the role of NS1 in flavivirus infection. Bioessays, 37(5), 489-494. doi:10.1002/bies.201400182

Albuquerque, L. M., Trugilho, M. R., Chapeaurouge, A., Jurgilas, P. B., Bozza, P. T., Bozza, F. A., . . . Neves-Ferreira, A. G. (2009). Two-dimensional difference gel electrophoresis (DiGE) analysis of plasmas from dengue fever patients. J Proteome Res, 8(12), 5431-5441. doi:10.1021/pr900236f

Alcaraz-Estrada, S. L., Manzano, M. I., Del Angel, R. M., Levis, R., & Padmanabhan, R. (2010). Construction of a dengue virus type 4 reporter replicon and analysis of temperature-sensitive mutations in non-structural proteins 3 and 5. J Gen Virol, 91(Pt 11), 2713-2718. doi:10.1099/vir.0.024083-0

Amemiya, T., Gromiha, M. M., Horimoto, K., & Fukui, K. (2019). Drug repositioning for dengue haemorrhagic fever by integrating multiple omics analyses. Sci Rep, 9(1), 523. doi:10.1038/s41598-018-36636-1

Argraves, W. S., Tanaka, A., Smith, E. P., Twal, W. O., Argraves, K. M., Fan, D., & Haudenschild, C. C. (2009). Fibulin-1 and fibrinogen in human atherosclerotic lesions. Histochem Cell Biol, 132(5), 559-565. doi:10.1007/s00418-009-0628-7

Arnaudeau, S., Frieden, M., Nakamura, K., Castelbou, C., Michalak, M., & Demaurex, N. (2002). Calreticulin differentially modulates calcium uptake

and release in the endoplasmic reticulum and mitochondria. J Biol Chem, 277(48), 46696-46705. doi:10.1074/jbc.M202395200

Arnold, P., Otte, A., & Becker-Pauly, C. (2017). Meprin metalloproteases: Molecular regulation and function in inflammation and fibrosis. Biochim Biophys Acta Mol Cell Res, 1864(11 Pt B), 2096-2104. doi:10.1016/j.bbamcr.2017.05.011

Ashour, J., Laurent-Rolle, M., Shi, P. Y., & Garcia-Sastre, A. (2009). NS5 of dengue virus mediates STAT2 binding and degradation. J Virol, 83(11), 5408-5418. doi:10.1128/jvi.02188-08

Avirutnan, P., Punyadee, N., Noisakran, S., Komoltri, C., Thiemmeca, S., Auethavornanan, K., . . . Malasit, P. (2006). Vascular leakage in severe dengue virus infections: a potential role for the nonstructural viral protein NS1 and complement. J Infect Dis, 193(8), 1078-1088. doi:10.1086/500949

Babeu, J. P., & Boudreau, F. (2014). Hepatocyte nuclear factor 4-alpha involvement in liver and intestinal inflammatory networks. World J Gastroenterol, 20(1), 22-30. doi:10.3748/wjg.v20.i1.22

Barbier, V., Lang, D., Valois, S., Rothman, A. L., & Medin, C. L. (2017). Dengue virus induces mitochondrial elongation through impairment of Drp1-triggered mitochondrial fission. Virology, 500, 149-160. doi:10.1016/j.virol.2016.10.022

Bartenschlager, R., & Miller, S. (2008). Molecular aspects of Dengue virus replication. Future Microbiol, 3(2), 155-165. doi:10.2217/17460913.3.2.155

Beatty, P. R., Puerta-Guardo, H., Killingbeck, S. S., Glasner, D. R., Hopkins, K., & Harris, E. (2015). Dengue virus NS1 triggers endothelial permeability and vascular leak that is prevented by NS1 vaccination. Sci Transl Med, 7(304), 304ra141. doi:10.1126/scitranslmed.aaa3787

Beltran Paschoal, J. F., Patiño, S. S., Bernardino, T., Rezende, A., Lemos, M., Pereira, C. A., & Calil Jorge, S. A. (2014). Adaptation to serum-free culture of HEK 293T and Huh7.0 cells. BMC Proceedings, 8(Suppl 4), P259-P259. doi:10.1186/1753-6561-8-S4-P259

Benjamini, Y., & Hochberg, Y. (1995). Controlling the False Discovery Rate: A Practical and Powerful Approach to Multiple Testing. Journal of the Royal Statistical Society. Series B (Methodological), 57(1), 289-300.

Bhatt, S., Gething, P. W., Brady, O. J., Messina, J. P., Farlow, A. W., Moyes, C. L., . . . Hay, S. I. (2013). The global distribution and burden of dengue. Nature, 496(7446), 504-507. doi:10.1038/nature12060

Biacchesi, S., Skiadopoulos, M. H., Yang, L., Murphy, B. R., Collins, P. L., & Buchholz, U. J. (2005). Rapid human metapneumovirus microneutralization

assay based on green fluorescent protein expression. J Virol Methods, 128(1-2), 192-197. doi:10.1016/j.jviromet.2005.05.005

Blazquez, A. B., Escribano-Romero, E., Merino-Ramos, T., Saiz, J. C., & Martin-Acebes, M. A. (2014). Stress responses in flavivirus-infected cells: activation of unfolded protein response and autophagy. Front Microbiol, 5, 266. doi:10.3389/fmicb.2014.00266

Bode, J. G., Albrecht, U., Haussinger, D., Heinrich, P. C., & Schaper, F. (2012). Hepatic acute phase proteins--regulation by IL-6- and IL-1-type cytokines involving STAT3 and its crosstalk with NF-kappaB-dependent signaling. Eur J Cell Biol, 91(6-7), 496-505. doi:10.1016/j.ejcb.2011.09.008

Bokisch, V. A., Top, F. H., Jr., Russell, P. K., Dixon, F. J., & Muller-Eberhard, H. J. (1973). The potential pathogenic role of complement in dengue hemorrhagic shock syndrome. N Engl J Med, 289(19), 996-1000. doi:10.1056/nejm197311082891902

Bozza, F. A., Cruz, O. G., Zagne, S. M., Azeredo, E. L., Nogueira, R. M., Assis, E. F., . . . Kubelka, C. F. (2008). Multiplex cytokine profile from dengue patients: MIP-1beta and IFN-gamma as predictive factors for severity. BMC Infect Dis, 8, 86. doi:10.1186/1471-2334-8-86

Brasier, A. R., Garcia, J., Wiktorowicz, J. E., Spratt, H. M., Comach, G., Ju, H., . . . Kochel, T. J. (2012). Discovery proteomics and nonparametric modeling pipeline in the development of a candidate biomarker panel for dengue hemorrhagic fever. Clin Transl Sci, 5(1), 8-20. doi:10.1111/j.1752-8062.2011.00377.x

Brock, M., Trenkmann, M., Gay, R. E., Gay, S., Speich, R., & Huber, L. C. (2011). MicroRNA-18a enhances the interleukin-6-mediated production of the acute-phase proteins fibrinogen and haptoglobin in human hepatocytes. J Biol Chem, 286(46), 40142-40150. doi:10.1074/jbc.M111.251793

Byk, L. A., & Gamarnik, A. V. (2016). Properties and Functions of the Dengue Virus Capsid Protein. Annu Rev Virol, 3(1), 263-281. doi:10.1146/annurev-virology-110615-042334

Byk, L. A., Iglesias, N. G., De Maio, F. A., Gebhard, L. G., Rossi, M., & Gamarnik, A. V. (2016). Dengue Virus Genome Uncoating Requires Ubiquitination. MBio, 7(3). doi:10.1128/mBio.00804-16

Cao, J., Shen, C., Zhang, J., Yao, J., Shen, H., Liu, Y., . . . Yang, P. (2011). Comparison of alternative extraction methods for secretome profiling in human hepatocellular carcinoma cells. Sci China Life Sci, 54(1), 34-38. doi:10.1007/s11427-010-4122-1

Capeding, M. R., Tran, N. H., Hadinegoro, S. R., Ismail, H. I., Chotpitayasunondh, T., Chua, M. N., . . . Bouckenooghe, A. (2014). Clinical efficacy and safety of a novel tetravalent dengue vaccine in healthy children in Asia: a phase 3, randomised, observer-masked, placebo-controlled trial. Lancet, 384(9951), 1358-1365. doi:10.1016/s0140-6736(14)61060-6

Caruso, M. B., Trugilho, M. R., Higa, L. M., Teixeira-Ferreira, A. S., Perales, J., Da Poian, A. T., & Zingali, R. B. (2017). Proteomic analysis of the secretome of HepG2 cells indicates differential proteolytic processing after infection with dengue virus. J Proteomics, 151, 106-113. doi:10.1016/j.jprot.2016.07.011

Chan, C. Y., & Ooi, E. E. (2015). Dengue: an update on treatment options. Future Microbiol, 10(12), 2017-2031. doi:10.2217/fmb.15.105

Chen, C. C., Lee, I. K., Liu, J. W., Huang, S. Y., & Wang, L. (2015). Utility of C-Reactive Protein Levels for Early Prediction of Dengue Severity in Adults. Biomed Res Int, 2015, 936062. doi:10.1155/2015/936062

Chen, K. (2004). Haemostatic disorder in Dengue hemorrhagic fever. Acta Med Indones, 36(2), 55-56.

Chen, L. C., Lei, H. Y., Liu, C. C., Shiesh, S. C., Chen, S. H., Liu, H. S., . . . Yeh, T. M. (2006). Correlation of serum levels of macrophage migration inhibitory factor with disease severity and clinical outcome in dengue patients. Am J Trop Med Hyg, 74(1), 142-147.

Chiu, H. C., Hannemann, H., Heesom, K. J., Matthews, D. A., & Davidson, A. D. (2014). High-throughput quantitative proteomic analysis of dengue virus type 2 infected A549 cells. PLoS One, 9(3), e93305. doi:10.1371/journal.pone.0093305

Choy, M. M., Zhang, S. L., Costa, V. V., Tan, H. C., Horrevorts, S., & Ooi, E. E. (2015). Proteasome Inhibition Suppresses Dengue Virus Egress in Antibody Dependent Infection. PLoS Negl Trop Dis, 9(11), e0004058. doi:10.1371/journal.pntd.0004058

Colpitts, T. M., Barthel, S., Wang, P., & Fikrig, E. (2011). Dengue virus capsid protein binds core histones and inhibits nucleosome formation in human liver cells. PLoS One, 6(9), e24365. doi:10.1371/journal.pone.0024365

Colpitts, T. M., Cox, J., Nguyen, A., Feitosa, F., Krishnan, M. N., & Fikrig, E. (2011). Use of a tandem affinity purification assay to detect interactions between West Nile and dengue viral proteins and proteins of the mosquito vector. Virology, 417(1), 179-187. doi:10.1016/j.virol.2011.06.002

Conde, J. N., da Silva, E. M., Allonso, D., Coelho, D. R., Andrade, I. D. S., de Medeiros, L. N., . . . Mohana-Borges, R. (2016). Inhibition of the Membrane Attack Complex by Dengue Virus NS1 through Interaction with Vitronectin

and Terminal Complement Proteins. J Virol, 90(21), 9570-9581. doi:10.1128/jvi.00912-16

Conde, J. N., Silva, E. M., Barbosa, A. S., & Mohana-Borges, R. (2017). The Complement System in Flavivirus Infections. Front Microbiol, 8, 213. doi:10.3389/fmicb.2017.00213

Cruz-Oliveira, C., Freire, J. M., Conceicao, T. M., Higa, L. M., Castanho, M. A., & Da Poian, A. T. (2015). Receptors and routes of dengue virus entry into the host cells. FEMS Microbiol Rev, 39(2), 155-170. doi:10.1093/femsre/fuu004

Daep, C. A., Munoz-Jordan, J. L., & Eugenin, E. A. (2014). Flaviviruses, an expanding threat in public health: focus on dengue, West Nile, and Japanese encephalitis virus. J Neurovirol, 20(6), 539-560. doi:10.1007/s13365-014-0285-z

Davalos, D., & Akassoglou, K. (2012). Fibrinogen as a key regulator of inflammation in disease. Semin Immunopathol, 34(1), 43-62. doi:10.1007/s00281-011-0290-8

de la Cruz-Hernandez, S. I., Flores-Aguilar, H., Gonzalez-Mateos, S., Lopez-Martinez, I., Alpuche-Aranda, C., Ludert, J. E., & del Angel, R. M. (2013). Determination of viremia and concentration of circulating nonstructural protein 1 in patients infected with dengue virus in Mexico. Am J Trop Med Hyg, 88(3), 446-454. doi:10.4269/ajtmh.12-0023

De La Guardia, C., & Lleonart, R. (2014). Progress in the identification of dengue virus entry/fusion inhibitors. Biomed Res Int, 2014, 825039. doi:10.1155/2014/825039

Desjardins, M. (2003). ER-mediated phagocytosis: a new membrane for new functions. Nat Rev Immunol, 3(4), 280-291. doi:10.1038/nri1053

Diamond, M. S., Roberts, T. G., Edgil, D., Lu, B., Ernst, J., & Harris, E. (2000). Modulation of Dengue virus infection in human cells by alpha, beta, and gamma interferons. J Virol, 74(11), 4957-4966. doi:10.1128/jvi.74.11.4957-4966.2000

Diosa-Toro, M., Echavarria-Consuegra, L., Flipse, J., Fernandez, G. J., Kluiver, J., van den Berg, A., . . . Smit, J. M. (2017). MicroRNA profiling of human primary macrophages exposed to dengue virus identifies miRNA-3614-5p as antiviral and regulator of ADAR1 expression. PLoS Negl Trop Dis, 11(10), e0005981. doi:10.1371/journal.pntd.0005981

Doerr, A. (2013). Mass spectrometry-based targeted proteomics. Nat Methods, 10(1), 23.

Dominiczak, M. H., & Caslake, M. J. (2011). Apolipoproteins: metabolic role and clinical biochemistry applications. Ann Clin Biochem, 48(Pt 6), 498-515. doi:10.1258/acb.2011.011111

El-Bacha, T., Midlej, V., Pereira da Silva, A. P., Silva da Costa, L., Benchimol, M., Galina, A., & Da Poian, A. T. (2007). Mitochondrial and bioenergetic dysfunction in human hepatic cells infected with dengue 2 virus. Biochim Biophys Acta, 1772(10), 1158-1166. doi:10.1016/j.bbadis.2007.08.003

Escalera-Cueto, M., Medina-Martinez, I., del Angel, R. M., Berumen-Campos, J., Gutierrez-Escolano, A. L., & Yocupicio-Monroy, M. (2015). Let-7c overexpression inhibits dengue virus replication in human hepatoma Huh-7 cells. Virus Res, 196, 105-112. doi:10.1016/j.virusres.2014.11.010

Fan, J., Liu, Y., & Yuan, Z. (2014). Critical role of Dengue Virus NS1 protein in viral replication. Virol Sin, 29(3), 162-169. doi:10.1007/s12250-014-3459-1

Faustino, A. F., Carvalho, F. A., Martins, I. C., Castanho, M. A., Mohana-Borges, R., Almeida, F. C., . . . Santos, N. C. (2014). Dengue virus capsid protein interacts specifically with very low-density lipoproteins. Nanomedicine, 10(1), 247-255. doi:10.1016/j.nano.2013.06.004

Feingold, K. R., & Grunfeld, C. (2000). Introduction to Lipids and Lipoproteins. In K. R. Feingold, B. Anawalt, A. Boyce, G. Chrousos, K. Dungan, A. Grossman, J. M. Hershman, G. Kaltsas, C. Koch, P. Kopp, M. Korbonits, R. McLachlan, J. E. Morley, M. New, L. Perreault, J. Purnell, R. Rebar, F. Singer, D. L. Trence, A. Vinik, & D. P. Wilson (Eds.), Endotext. South Dartmouth (MA): MDText.com, Inc.

Fink, J., Gu, F., Ling, L., Tolfvenstam, T., Olfat, F., Chin, K. C., . . . Hibberd, M. L. (2007). Host gene expression profiling of dengue virus infection in cell lines and patients. PLoS Negl Trop Dis, 1(2), e86. doi:10.1371/journal.pntd.0000086

Fischl, W., & Bartenschlager, R. (2011). Exploitation of cellular pathways by Dengue virus. Curr Opin Microbiol, 14(4), 470-475. doi:10.1016/j.mib.2011.07.012

Fish, R. J., & Neerman-Arbez, M. (2012). Fibrinogen gene regulation. Thromb Haemost, 108(3), 419-426. doi:10.1160/th12-04-0273

Fort, A., Borel, C., Migliavacca, E., Antonarakis, S. E., Fish, R. J., & Neerman-Arbez, M. (2010). Regulation of fibrinogen production by microRNAs. Blood, 116(14), 2608-2615. doi:10.1182/blood-2010-02-268011

Fragnoud, R., Flamand, M., Reynier, F., Buchy, P., Duong, V., Pachot, A., . . . Bedin, F. (2015). Differential proteomic analysis of virus-enriched fractions

obtained from plasma pools of patients with dengue fever or severe dengue. BMC Infect Dis, 15, 518. doi:10.1186/s12879-015-1271-7

Fragnoud, R., Yugueros-Marcos, J., Pachot, A., & Bedin, F. (2012). Isotope Coded Protein Labeling analysis of plasma specimens from acute severe dengue fever patients. Proteome Sci, 10(1), 60. doi:10.1186/1477-5956-10-60

Franceschini, A., Szklarczyk, D., Frankild, S., Kuhn, M., Simonovic, M., Roth, A., . . . Jensen, L. J. (2013). STRING v9.1: protein-protein interaction networks, with increased coverage and integration. Nucleic Acids Res, 41(Database issue), D808-815. doi:10.1093/nar/gks1094

Freeman, O. J., Unwin, R. D., Dowsey, A. W., Begley, P., Ali, S., Hollywood, K. A., . . . Gardiner, N. J. (2016). Metabolic Dysfunction Is Restricted to the Sciatic Nerve in Experimental Diabetic Neuropathy. Diabetes, 65(1), 228-238. doi:10.2337/db15-0835

Gabay, C., & Kushner, I. (1999). Acute-phase proteins and other systemic responses to inflammation. N Engl J Med, 340(6), 448-454. doi:10.1056/nejm199902113400607

Garin, J., Diez, R., Kieffer, S., Dermine, J. F., Duclos, S., Gagnon, E., . . . Desjardins, M. (2001). The phagosome proteome: insight into phagosome functions. J Cell Biol, 152(1), 165-180. doi:10.1083/jcb.152.1.165

Geddes, J. M., Croll, D., Caza, M., Stoynov, N., Foster, L. J., & Kronstad, J. W. (2015). Secretome profiling of Cryptococcus neoformans reveals regulation of a subset of virulence-associated proteins and potential biomarkers by protein kinase A. BMC Microbiol, 15, 206. doi:10.1186/s12866-015-0532-3

Geyer, P. E., Holdt, L. M., Teupser, D., & Mann, M. (2017). Revisiting biomarker discovery by plasma proteomics. Mol Syst Biol, 13(9), 942. doi:10.15252/msb.20156297

Godyna, S., Diaz-Ricart, M., & Argraves, W. S. (1996). Fibulin-1 mediates platelet adhesion via a bridge of fibrinogen. Blood, 88(7), 2569-2577.

Gonzalez, F. J. (2008). Regulation of hepatocyte nuclear factor 4 alpha-mediated transcription. Drug Metab Pharmacokinet, 23(1), 2-7.

Gualano, R. C., Pryor, M. J., Cauchi, M. R., Wright, P. J., & Davidson, A. D. (1998). Identification of a major determinant of mouse neurovirulence of dengue virus type 2 using stably cloned genomic-length cDNA. J Gen Virol, 79 (Pt 3), 437-446. doi:10.1099/0022-1317-79-3-437

Gubler, D. J., Suharyono, W., Tan, R., Abidin, M., & Sie, A. (1981). Viraemia in patients with naturally acquired dengue infection. Bull World Health Organ, 59(4), 623-630.

Guzman, M. G., & Harris, E. (2015). Dengue. Lancet, 385(9966), 453-465. doi:10.1016/s0140-6736(14)60572-9

Hafirassou, M. L., Meertens, L., Umana-Diaz, C., Labeau, A., Dejarnac, O., Bonnet-Madin, L., . . . Amara, A. (2017). A Global Interactome Map of the Dengue Virus NS1 Identifies Virus Restriction and Dependency Host Factors. Cell Rep, 21(13), 3900-3913. doi:10.1016/j.celrep.2017.11.094

Halstead, S. B. (1979). In vivo enhancement of dengue virus infection in rhesus monkeys by passively transferred antibody. J Infect Dis, 140(4), 527-533. doi:10.1093/infdis/140.4.527

Halstead, S. B., Porterfield, J. S., & O'Rourke, E. J. (1980). Enhancement of dengue virus infection in monocytes by flavivirus antisera. Am J Trop Med Hyg, 29(4), 638-642. doi:10.4269/ajtmh.1980.29.638

Hannemann, H., Sung, P. Y., Chiu, H. C., Yousuf, A., Bird, J., Lim, S. P., & Davidson, A. D. (2013). Serotype-specific differences in dengue virus non-structural protein 5 nuclear localization. J Biol Chem, 288(31), 22621-22635. doi:10.1074/jbc.M113.481382

Harlan, R., & Zhang, H. (2014). Targeted proteomics: a bridge between discovery and validation. Expert Rev Proteomics, 11(6), 657-661. doi:10.1586/14789450.2014.976558

Heaton, N. S., Perera, R., Berger, K. L., Khadka, S., Lacount, D. J., Kuhn, R. J., & Randall, G. (2010). Dengue virus nonstructural protein 3 redistributes fatty acid synthase to sites of viral replication and increases cellular fatty acid synthesis. Proc Natl Acad Sci U S A, 107(40), 17345-17350. doi:10.1073/pnas.1010811107

Heaton, N. S., & Randall, G. (2010). Dengue virus-induced autophagy regulates lipid metabolism. Cell Host Microbe, 8(5), 422-432. doi:10.1016/j.chom.2010.10.006

Heinrich, P. C., Castell, J. V., & Andus, T. (1990). Interleukin-6 and the acute phase response. Biochem J, 265(3), 621-636. doi:10.1042/bj2650621

Heinz, F. X., & Stiasny, K. (2012). Flaviviruses and their antigenic structure. J Clin Virol, 55(4), 289-295. doi:10.1016/j.jcv.2012.08.024

Hewlings, S. J., & Kalman, D. S. (2017). Curcumin: A Review of Its' Effects on Human Health. Foods, 6(10). doi:10.3390/foods6100092

Higa, L. M., Caruso, M. B., Canellas, F., Soares, M. R., Oliveira-Carvalho, A. L., Chapeaurouge, D. A., . . . Da Poian, A. T. (2008). Secretome of HepG2 cells infected with dengue virus: implications for pathogenesis. Biochim Biophys Acta, 1784(11), 1607-1616. doi:10.1016/j.bbapap.2008.06.015

Higa, L. M., Curi, B. M., Aguiar, R. S., Cardoso, C. C., De Lorenzi, A. G., Sena, S. L., . . . Da Poian, A. T. (2014). Modulation of alpha-enolase post-translational modifications by dengue virus: increased secretion of the basic isoforms in infected hepatic cells. PLoS One, 9(8), e88314. doi:10.1371/journal.pone.0088314

Ho, T. S., Wang, S. M., Lin, Y. S., & Liu, C. C. (2013). Clinical and laboratory predictive markers for acute dengue infection. J Biomed Sci, 20, 75. doi:10.1186/1423-0127-20-75

Huang da, W., Sherman, B. T., & Lempicki, R. A. (2009a). Bioinformatics enrichment tools: paths toward the comprehensive functional analysis of large gene lists. Nucleic Acids Res, 37(1), 1-13. doi:10.1093/nar/gkn923

Huang da, W., Sherman, B. T., & Lempicki, R. A. (2009b). Systematic and integrative analysis of large gene lists using DAVID bioinformatics resources. Nat Protoc, 4(1), 44-57. doi:10.1038/nprot.2008.211

Huerta, V., Ramos, Y., Yero, A., Pupo, D., Martin, D., Toledo, P., . . . Chinea, G. (2016). Novel interactions of domain III from the envelope glycoprotein of dengue 2 virus with human plasma proteins. J Proteomics, 131, 205-213. doi:10.1016/j.jprot.2015.11.003

Hung, C. W., & Tholey, A. (2012). Tandem mass tag protein labeling for top-down identification and quantification. Anal Chem, 84(1), 161-170. doi:10.1021/ac202243r

Huynh, K. K., Eskelinen, E. L., Scott, C. C., Malevanets, A., Saftig, P., & Grinstein, S. (2007). LAMP proteins are required for fusion of lysosomes with phagosomes. Embo j, 26(2), 313-324. doi:10.1038/sj.emboj.7601511

Idrees, S., & Ashfaq, U. A. (2014). Discovery and design of cyclic peptides as dengue virus inhibitors through structure-based molecular docking. Asian Pac J Trop Med, 7(7), 513-516. doi:10.1016/s1995-7645(14)60085-7

Igarashi, A. (1978). Isolation of a Singh's Aedes albopictus cell clone sensitive to Dengue and Chikungunya viruses. J Gen Virol, 40(3), 531-544. doi:10.1099/0022-1317-40-3-531

Inoue, Y., Peters, L. L., Yim, S. H., Inoue, J., & Gonzalez, F. J. (2006). Role of hepatocyte nuclear factor 4alpha in control of blood coagulation factor gene expression. J Mol Med (Berl), 84(4), 334-344. doi:10.1007/s00109-005-0013-5

Jacobs, R. H., Orr, J. L., Gowins, J. R., Forbes, E. E., & Langenecker, S. A. (2015). Biomarkers of intergenerational risk for depression: a review of mechanisms in longitudinal high-risk (LHR) studies. J Affect Disord, 175, 494-506. doi:10.1016/j.jad.2015.01.038

Jadhav, M., Nayak, M., Kumar, S., Venkatesh, A., Patel, S. K., Kumar, V., . . . Srivastava, S. (2017). Clinical Proteomics and Cytokine Profiling for Dengue Fever Disease Severity Biomarkers. Omics, 21(11), 665-677. doi:10.1089/omi.2017.0135

Jain, S., Gautam, V., & Naseem, S. (2011). Acute-phase proteins: As diagnostic tool. J Pharm Bioallied Sci, 3(1), 118-127. doi:10.4103/0975-7406.76489

Jayathilaka, D., Gomes, L., Jeewandara, C., Jayarathna, G. S. B., Herath, D., Perera, P. A., . . . Malavige, G. N. (2018). Role of NS1 antibodies in the pathogenesis of acute secondary dengue infection. Nat Commun, 9(1), 5242. doi:10.1038/s41467-018-07667-z

John, D. V., Lin, Y. S., & Perng, G. C. (2015). Biomarkers of severe dengue disease - a review. J Biomed Sci, 22, 83. doi:10.1186/s12929-015-0191-6

Kalayanarooj, S. (2011). Dengue classification: current WHO vs. the newly suggested classification for better clinical application? J Med Assoc Thai, 94 Suppl 3, S74-84.

Kalsheker, N., Morley, S., & Morgan, K. (2002). Gene regulation of the serine proteinase inhibitors alpha1-antitrypsin and alpha1-antichymotrypsin. Biochem Soc Trans, 30(2), 93-98. doi:10.1042/

Kanlaya, R., Pattanakitsakul, S. N., Sinchaikul, S., Chen, S. T., & Thongboonkerd, V. (2009). Alterations in actin cytoskeletal assembly and junctional protein complexes in human endothelial cells induced by dengue virus infection and mimicry of leukocyte transendothelial migration. J Proteome Res, 8(5), 2551-2562. doi:10.1021/pr900060g

Kanlaya, R., Pattanakitsakul, S. N., Sinchaikul, S., Chen, S. T., & Thongboonkerd, V. (2010). The ubiquitin-proteasome pathway is important for dengue virus infection in primary human endothelial cells. J Proteome Res, 9(10), 4960-4971. doi:10.1021/pr100219y

Kanokudom, S., Vilaivan, T., Wikan, N., Thepparit, C., Smith, D. R., & Assavalapsakul, W. (2017). miR-21 promotes dengue virus serotype 2 replication in HepG2 cells. Antiviral Res, 142, 169-177. doi:10.1016/j.antiviral.2017.03.020

Khadka, S., Vangeloff, A. D., Zhang, C., Siddavatam, P., Heaton, N. S., Wang, L., . . . LaCount, D. J. (2011). A physical interaction network of dengue virus and human proteins. Mol Cell Proteomics, 10(12), M111.012187. doi:10.1074/mcp.M111.012187

Kruse, K. B., Dear, A., Kaltenbrun, E. R., Crum, B. E., George, P. M., Brennan, S. O., & McCracken, A. A. (2006). Mutant fibrinogen cleared from the endoplasmic reticulum via endoplasmic reticulum-associated protein

degradation and autophagy: an explanation for liver disease. Am J Pathol, 168(4), 1299-1308; quiz 1404-1295. doi:10.2353/ajpath.2006.051097

Kuhn, P. H., Voss, M., Haug-Kroper, M., Schroder, B., Schepers, U., Brase, S., . . . Fluhrer, R. (2015). Secretome analysis identifies novel signal Peptide peptidase-like 3 (Sppl3) substrates and reveals a role of Sppl3 in multiple Golgi glycosylation pathways. Mol Cell Proteomics, 14(6), 1584-1598. doi:10.1074/mcp.M115.048298

Kumar, R., Singh, N., Abdin, M. Z., Patel, A. H., & Medigeshi, G. R. (2017). Dengue Virus Capsid Interacts with DDX3X-A Potential Mechanism for Suppression of Antiviral Functions in Dengue Infection. Front Cell Infect Microbiol, 7, 542. doi:10.3389/fcimb.2017.00542

Kumar, Y., Liang, C., Bo, Z., Rajapakse, J. C., Ooi, E. E., & Tannenbaum, S. R. (2012). Serum proteome and cytokine analysis in a longitudinal cohort of adults with primary dengue infection reveals predictive markers of DHF. PLoS Negl Trop Dis, 6(11), e1887. doi:10.1371/journal.pntd.0001887

Kuno, G., Chang, G. J., Tsuchiya, K. R., Karabatsos, N., & Cropp, C. B. (1998). Phylogeny of the genus Flavivirus. J Virol, 72(1), 73-83.

Kurosu, T., Chaichana, P., Yamate, M., Anantapreecha, S., & Ikuta, K. (2007). Secreted complement regulatory protein clusterin interacts with dengue virus nonstructural protein 1. Biochem Biophys Res Commun, 362(4), 1051-1056. doi:10.1016/j.bbrc.2007.08.137

Kuscuoglu, D., Janciauskiene, S., Hamesch, K., Haybaeck, J., Trautwein, C., & Strnad, P. (2018). Liver - master and servant of serum proteome. J Hepatol, 69(2), 512-524. doi:10.1016/j.jhep.2018.04.018

Kutsuna, S., Hayakawa, K., Kato, Y., Fujiya, Y., Mawatari, M., Takeshita, N., . . . Ohmagari, N. (2014). The usefulness of serum C-reactive protein and total bilirubin levels for distinguishing between dengue fever and malaria in returned travelers. Am J Trop Med Hyg, 90(3), 444-448. doi:10.4269/ajtmh.13-0536

Laemmli, U. K. (1970). Cleavage of structural proteins during the assembly of the head of bacteriophage T4. Nature, 227(5259), 680-685. doi:10.1038/227680a0

Lam, S. K. (2013). Challenges in reducing dengue burden; diagnostics, control measures and vaccines. Expert Rev Vaccines, 12(9), 995-1010. doi:10.1586/14760584.2013.824712

Le Turnier, P., Bonifay, T., Mosnier, E., Schaub, R., Jolivet, A., Demar, M., . . . Epelboin, L. (2019). Usefulness of C-Reactive Protein in Differentiating

Acute Leptospirosis and Dengue Fever in French Guiana. Open Forum Infectious Diseases, 6(9), ofz323. doi:10.1093/ofid/ofz323

Lee, Y. R., Kuo, S. H., Lin, C. Y., Fu, P. J., Lin, Y. S., Yeh, T. M., & Liu, H. S. (2018). Dengue virus-induced ER stress is required for autophagy activation, viral replication, and pathogenesis both in vitro and in vivo. Sci Rep, 8(1), 489. doi:10.1038/s41598-017-18909-3

Li, Y., Kakinami, C., Li, Q., Yang, B., & Li, H. (2013). Human apolipoprotein A-I is associated with dengue virus and enhances virus infection through SR-BI. PLoS One, 8(7), e70390. doi:10.1371/journal.pone.0070390

Libraty, D. H., Young, P. R., Pickering, D., Endy, T. P., Kalayanarooj, S., Green, S., . . . Rothman, A. L. (2002). High circulating levels of the dengue virus nonstructural protein NS1 early in dengue illness correlate with the development of dengue hemorrhagic fever. J Infect Dis, 186(8), 1165-1168. doi:10.1086/343813

Lietzen, N., Ohman, T., Rintahaka, J., Julkunen, I., Aittokallio, T., Matikainen, S., & Nyman, T. A. (2011). Quantitative subcellular proteome and secretome profiling of influenza A virus-infected human primary macrophages. PLoS Pathog, 7(5), e1001340. doi:10.1371/journal.ppat.1001340

Lima, W. G., Souza, N. A., Fernandes, S. O. A., Cardoso, V. N., & Godoi, I. P. (2019). Serum lipid profile as a predictor of dengue severity: A systematic review and meta-analysis. Rev Med Virol, 29(5), e2056. doi:10.1002/rmv.2056

Limjindaporn, T., Panaampon, J., Malakar, S., Noisakran, S., & Yenchitsomanus, P. T. (2017). Tyrosine kinase/phosphatase inhibitors decrease dengue virus production in HepG2 cells. Biochem Biophys Res Commun, 483(1), 58-63. doi:10.1016/j.bbrc.2017.01.006

Limjindaporn, T., Wongwiwat, W., Noisakran, S., Srisawat, C., Netsawang, J., Puttikhunt, C., . . . Yenchitsomanus, P. T. (2009). Interaction of dengue virus envelope protein with endoplasmic reticulum-resident chaperones facilitates dengue virus production. Biochem Biophys Res Commun, 379(2), 196-200. doi:10.1016/j.bbrc.2008.12.070

Lin, C.F., Lei, H.Y., Liu, C.C., Liu, H.S., Yeh, T.M., Chen, S.H., & Lin, Y.S. (2004). Autoimmunity in Dengue Virus Infection. Dengue Bull, 28, 51-57.

Lin, C. F., Wan, S. W., Cheng, H. J., Lei, H. Y., & Lin, Y. S. (2006). Autoimmune pathogenesis in dengue virus infection. Viral Immunol, 19(2), 127-132. doi:10.1089/vim.2006.19.127

Lin, C. W., Cheng, C. W., Yang, T. C., Li, S. W., Cheng, M. H., Wan, L., . . . Kao, M. C. (2008). Interferon antagonist function of Japanese encephalitis virus

NS4A and its interaction with DEAD-box RNA helicase DDX42. Virus Res, 137(1), 49-55. doi:10.1016/j.virusres.2008.05.015

Lin, S. W., Chuang, Y. C., Lin, Y. S., Lei, H. Y., Liu, H. S., & Yeh, T. M. (2012). Dengue virus nonstructural protein NS1 binds to prothrombin/thrombin and inhibits prothrombin activation. J Infect, 64(3), 325-334. doi:10.1016/j.jinf.2011.11.023

Lin, Y. S., Yeh, T. M., Lin, C. F., Wan, S. W., Chuang, Y. C., Hsu, T. K., . . . Lei, H. Y. (2011). Molecular mimicry between virus and host and its implications for dengue disease pathogenesis. Exp Biol Med (Maywood), 236(5), 515-523. doi:10.1258/ebm.2011.010339

Livak, K. J., & Schmittgen, T. D. (2001). Analysis of relative gene expression data using real-time quantitative PCR and the 2(-Delta Delta C(T)) Method. Methods, 25(4), 402-408. doi:10.1006/meth.2001.1262

Longley, D. B., Steel, D. M., & Whitehead, A. S. (1999). Posttranscriptional regulation of acute phase serum amyloid A2 expression by the 5'- and 3'-untranslated regions of its mRNA. J Immunol, 163(8), 4537-4545.

Low, J. G., Ooi, E. E., & Vasudevan, S. G. (2017). Current Status of Dengue Therapeutics Research and Development. J Infect Dis, 215(suppl_2), S96-s102. doi:10.1093/infdis/jiw423

Low, J. G., Sung, C., Wijaya, L., Wei, Y., Rathore, A. P. S., Watanabe, S., . . . Vasudevan, S. G. (2014). Efficacy and safety of celgosivir in patients with dengue fever (CELADEN): a phase 1b, randomised, double-blind, placebo-controlled, proof-of-concept trial. Lancet Infect Dis, 14(8), 706-715. doi:10.1016/s1473-3099(14)70730-3

Luvira, V., Silachamroon, U., Piyaphanee, W., Lawpoolsri, S., Chierakul, W., Leaungwutiwong, P., . . . Wattanagoon, Y. (2019). Etiologies of Acute Undifferentiated Febrile Illness in Bangkok, Thailand. Am J Trop Med Hyg, 100(3), 622-629. doi:10.4269/ajtmh.18-0407

Mairuhu, A. T., Mac Gillavry, M. R., Setiati, T. E., Soemantri, A., ten Cate, H., Brandjes, D. P., & van Gorp, E. C. (2003). Is clinical outcome of dengue-virus infections influenced by coagulation and fibrinolysis? A critical review of the evidence. Lancet Infect Dis, 3(1), 33-41.

Malavige, G. N., & Ogg, G. S. (2013). T cell responses in dengue viral infections. J Clin Virol, 58(4), 605-611. doi:10.1016/j.jcv.2013.10.023

Manchala, N. R., Dungdung, R., & Pilankatta, R. (2017). Proteomic analysis reveals the enhancement of human serum apolipoprotein A-1(APO A-1) in individuals infected with multiple dengue virus serotypes. Trop Med Int Health, 22(10), 1334-1342. doi:10.1111/tmi.12931

Marin-Palma, D., Sirois, C. M., Urcuqui-Inchima, S., & Hernandez, J. C. (2019). Inflammatory status and severity of disease in dengue patients are associated with lipoprotein alterations. PLoS One, 14(3), e0214245. doi:10.1371/journal.pone.0214245

Martina, B. E., Koraka, P., & Osterhaus, A. D. (2009). Dengue virus pathogenesis: an integrated view. Clin Microbiol Rev, 22(4), 564-581. doi:10.1128/cmr.00035-09

Martínez-Betancur, V., & Martínez-Gutierrez, M. (2016). Proteomic profile of human monocytic cells infected with dengue virus. Asian Pacific Journal of Tropical Biomedicine, 6(11), 914-923. doi:https://doi.org/10.1016/j.apjtb.2016.01.004

Masse, N., Davidson, A., Ferron, F., Alvarez, K., Jacobs, M., Romette, J. L., . . . Guillemot, J. C. (2010). Dengue virus replicons: production of an interserotypic chimera and cell lines from different species, and establishment of a cell-based fluorescent assay to screen inhibitors, validated by the evaluation of ribavirin's activity. Antiviral Res, 86(3), 296-305. doi:10.1016/j.antiviral.2010.03.010

Matsuguchi, T., Okamura, S., Kawasaki, C., & Niho, Y. (1990). Production of interleukin 6 from human liver cell lines: production of interleukin 6 is not concurrent with the production of alpha-fetoprotein. Cancer Res, 50(23), 7457-7459.

Mazzon, M., Jones, M., Davidson, A., Chain, B., & Jacobs, M. (2009). Dengue virus NS5 inhibits interferon-alpha signaling by blocking signal transducer and activator of transcription 2 phosphorylation. J Infect Dis, 200(8), 1261-1270. doi:10.1086/605847

Medin, C. L., Fitzgerald, K. A., & Rothman, A. L. (2005). Dengue virus nonstructural protein NS5 induces interleukin-8 transcription and secretion. J Virol, 79(17), 11053-11061. doi:10.1128/jvi.79.17.11053-11061.2005

Meng, F., Badierah, R. A., Almehdar, H. A., Redwan, E. M., Kurgan, L., & Uversky, V. N. (2015). Unstructural biology of the Dengue virus proteins. Febs j, 282(17), 3368-3394. doi:10.1111/febs.13349

Miao, M., Yu, F., Wang, D., Tong, Y., Yang, L., Xu, J., . . . Zhao, X. (2019). Proteomics Profiling of Host Cell Response via Protein Expression and Phosphorylation upon Dengue Virus Infection. Virol Sin. doi:10.1007/s12250-019-00131-2

Mishra, K. P., Shweta, Diwaker, D., & Ganju, L. (2012). Dengue virus infection induces upregulation of hn RNP-H and PDIA3 for its multiplication in the host cell. Virus Res, 163(2), 573-579. doi:10.1016/j.virusres.2011.12.010

Modhiran, N., Watterson, D., Muller, D. A., Panetta, A. K., Sester, D. P., Liu, L., . . . Young, P. R. (2015). Dengue virus NS1 protein activates cells via Toll-like receptor 4 and disrupts endothelial cell monolayer integrity. Sci Transl Med, 7(304), 304ra142. doi:10.1126/scitranslmed.aaa3863

Mongkolsapaya, J., Dejnirattisai, W., Xu, X.N., Vasanawathana, S., Tangthawornchaikul, N., Chairunsri, A., . . .Screaton, G. (2003) Original antigenic sin and apoptosis in the pathogenesis of dengue hemorrhagic fever. Nat Med,9(7), 921-7. doi: 10.1038/nm887

Morley, J. J., & Kushner, I. (1982). Serum C-reactive protein levels in disease. Ann N Y Acad Sci, 389, 406-418. doi:10.1111/j.1749-6632.1982.tb22153.x

Muller, D. A., Depelsenaire, A. C., & Young, P. R. (2017). Clinical and Laboratory Diagnosis of Dengue Virus Infection. J Infect Dis, 215(suppl_2), S89-s95. doi:10.1093/infdis/jiw649

Muller, D. A., & Young, P. R. (2013). The flavivirus NS1 protein: molecular and structural biology, immunology, role in pathogenesis and application as a diagnostic biomarker. Antiviral Res, 98(2), 192-208. doi:10.1016/j.antiviral.2013.03.008

Ng, C. Y., Gu, F., Phong, W. Y., Chen, Y. L., Lim, S. P., Davidson, A., & Vasudevan, S. G. (2007). Construction and characterization of a stable subgenomic dengue virus type 2 replicon system for antiviral compound and siRNA testing. Antiviral Res, 76(3), 222-231. doi:10.1016/j.antiviral.2007.06.007

Ngono, A. E., & Shresta, S. (2018). Immune Response to Dengue and Zika. Annu Rev Immunol, 36, 279-308. doi:10.1146/annurev-immunol-042617-053142

Nguyen, H., Trung, H., Trieu, Okamoto, K., Thi, T., Ninh, H., . . . Hirayama, K. (2013). Proteomic Profile of Circulating Immune Complexes in Dengue Infected Patients. J Trop Dis, 1, 109. doi:10.4172/jtd.1000109

Nguyen, N. M., Tran, C. N., Phung, L. K., Duong, K. T., Huynh Hle, A., Farrar, J., . . . Simmons, C. P. (2013). A randomized, double-blind placebo controlled trial of balapiravir, a polymerase inhibitor, in adult dengue patients. J Infect Dis, 207(9), 1442-1450. doi:10.1093/infdis/jis470

Nhi, D. M., Huy, N. T., Ohyama, K., Kimura, D., Lan, N. T., Uchida, L., . . . Hirayama, K. (2016). A Proteomic Approach Identifies Candidate Early Biomarkers to Predict Severe Dengue in Children. PLoS Negl Trop Dis, 10(2), e0004435. doi:10.1371/journal.pntd.0004435

Nightingale, K., Lin, K. M., Ravenhill, B. J., Davies, C., Nobre, L., Fielding, C. A., . . . Weekes, M. P. (2018). High-Definition Analysis of Host Protein Stability during Human Cytomegalovirus Infection Reveals Antiviral Factors and

Viral Evasion Mechanisms. Cell Host Microbe, 24(3), 447-460.e411. doi:10.1016/j.chom.2018.07.011

Nofrini, V., Di Giacomo, D., & Mecucci, C. (2016). Nucleoporin genes in human diseases. Eur J Hum Genet, 24(10), 1388-1395. doi:10.1038/ejhg.2016.25

Olagnier, D., Peri, S., Steel, C., van Montfoort, N., Chiang, C., Beljanski, V., . . . Hiscott, J. (2014). Cellular oxidative stress response controls the antiviral and apoptotic programs in dengue virus-infected dendritic cells. PLoS Pathog, 10(12), e1004566. doi:10.1371/journal.ppat.1004566

Olsavsky, K. M., Page, J. L., Johnson, M. C., Zarbl, H., Strom, S. C., & Omiecinski, C. J. (2007). Gene expression profiling and differentiation assessment in primary human hepatocyte cultures, established hepatoma cell lines, and human liver tissues. Toxicol Appl Pharmacol, 222(1), 42-56. doi:10.1016/j.taap.2007.03.032

Ong, E. Z., Zhang, S. L., Tan, H. C., Gan, E. S., Chan, K. R., & Ooi, E. E. (2017). Dengue virus compartmentalization during antibody-enhanced infection. Sci Rep, 7, 40923. doi:10.1038/srep40923

Orozco-García, E., & Gallego-Gómez, J.C. (2016). Autophagy and Lipid Metabolism – A Cellular Platform where Molecular and Metabolic Pathways Converge to Explain Dengue Viral Infection, Cell Biology - New Insights, Stevo Najman, IntechOpen, DOI: 10.5772/61305. Available from: https://www.intechopen.com/books/cell-biology-new-insights/autophagy-and-lipid-metabolism-a-cellular-platform-where-molecular-and-metabolic-pathways-converge-t (Accessed on 27 Aug, 2019)

Osuna-Ramos, J. F., Reyes-Ruiz, J. M., Bautista-Carbajal, P., Cervantes-Salazar, M., Farfan-Morales, C. N., De Jesus-Gonzalez, L. A., . . . Del Angel, R. M. (2018). Ezetimibe inhibits dengue virus infection in Huh-7 cells by blocking the cholesterol transporter Niemann-Pick C1-like 1 receptor. Antiviral Res, 160, 151-164. doi:10.1016/j.antiviral.2018.10.024

Osuna-Ramos, J. F., Reyes-Ruiz, J. M., & Del Angel, R. M. (2018). The Role of Host Cholesterol During Flavivirus Infection. Front Cell Infect Microbiol, 8, 388. doi:10.3389/fcimb.2018.00388

Padilla, S. L., Rodriguez, A., Gonzales, M. M., Gallego, G. J., & Castano, O. J. (2014). Inhibitory effects of curcumin on dengue virus type 2-infected cells in vitro. Arch Virol, 159(3), 573-579. doi:10.1007/s00705-013-1849-6

Pando-Robles, V., Oses-Prieto, J. A., Rodriguez-Gandarilla, M., Meneses-Romero, E., Burlingame, A. L., & Batista, C. V. (2014). Quantitative proteomic analysis of Huh-7 cells infected with Dengue virus by label-free LC-MS. J Proteomics, 111, 16-29. doi:10.1016/j.jprot.2014.06.029

Pathan, M., Keerthikumar, S., Ang, C. S., Gangoda, L., Quek, C. Y., Williamson, N. A., . . . Mathivanan, S. (2015). FunRich: An open access standalone functional enrichment and interaction network analysis tool. Proteomics, 15(15), 2597-2601. doi:10.1002/pmic.201400515

Pattanakitsakul, S. N., Poungsawai, J., Kanlaya, R., Sinchaikul, S., Chen, S. T., & Thongboonkerd, V. (2010). Association of Alix with late endosomal lysobisphosphatidic acid is important for dengue virus infection in human endothelial cells. J Proteome Res, 9(9), 4640-4648. doi:10.1021/pr100357f

Pattanakitsakul, S. N., Rungrojcharoenkit, K., Kanlaya, R., Sinchaikul, S., Noisakran, S., Chen, S. T., . . . Thongboonkerd, V. (2007). Proteomic analysis of host responses in HepG2 cells during dengue virus infection. J Proteome Res, 6(12), 4592-4600. doi:10.1021/pr070366b

Peerschke, E. I., Andemariam, B., Yin, W., & Bussel, J. B. (2010). Complement activation on platelets correlates with a decrease in circulating immature platelets in patients with immune thrombocytopenic purpura. Br J Haematol, 148(4), 638-645. doi:10.1111/j.1365-2141.2009.07995.x

Perera, R., & Kuhn, R. J. (2008). Structural proteomics of dengue virus. Curr Opin Microbiol, 11(4), 369-377. doi:10.1016/j.mib.2008.06.004

Petiot, E., Cuperlovic-Culf, M., Shen, C. F., & Kamen, A. (2015). Influence of HEK293 metabolism on the production of viral vectors and vaccine. Vaccine, 33(44), 5974-5981. doi:10.1016/j.vaccine.2015.05.097

Povoa, T. F., Alves, A. M., Oliveira, C. A., Nuovo, G. J., Chagas, V. L., & Paes, M. V. (2014). The pathology of severe dengue in multiple organs of human fatal cases: histopathology, ultrastructure and virus replication. PLoS One, 9(4), e83386. doi:10.1371/journal.pone.0083386

Prabhavathi, R., Madhusudan, S. R., Suman, M.G., Govindaraj, M., & Puttaswamy, M. (2017). Study of clinical and laboratory predictive markers of dengue fever and severe dengue in children. J PediatrRes. 4(06),397-404. doi:10.17511/ijpr.2017.06.08.

Priyadarshini, D., Gadia, R. R., Tripathy, A., Gurukumar, K. R., Bhagat, A., Patwardhan, S., . . . Cecilia, D. (2010). Clinical findings and pro-inflammatory cytokines in dengue patients in Western India: a facility-based study. PLoS One, 5(1), e8709. doi:10.1371/journal.pone.0008709

Prompetchara, E., Ketloy, C., Thomas, S. J., & Ruxrungtham, K. (2019). Dengue vaccine: Global development update. Asian Pac J Allergy Immunol. doi:10.12932/ap-100518-0309

Pryor, M. J., Carr, J. M., Hocking, H., Davidson, A. D., Li, P., & Wright, P. J. (2001). Replication of dengue virus type 2 in human monocyte-derived macrophages:

comparisons of isolates and recombinant viruses with substitutions at amino acid 390 in the envelope glycoprotein. Am J Trop Med Hyg, 65(5), 427-434. doi:10.4269/ajtmh.2001.65.427

Puschnik, A. S., Marceau, C. D., Ooi, Y. S., Majzoub, K., Rinis, N., Contessa, J. N., & Carette, J. E. (2017). A Small-Molecule Oligosaccharyltransferase Inhibitor with Pan-flaviviral Activity. Cell Rep, 21(11), 3032-3039. doi:10.1016/j.celrep.2017.11.054

Ranganathan, S., & Garg, G. (2009). Secretome: clues into pathogen infection and clinical applications. Genome Med, 1(11), 113. doi:10.1186/gm113

Rauniyar, N., & Yates, J. R., 3rd. (2014). Isobaric labeling-based relative quantification in shotgun proteomics. J Proteome Res, 13(12), 5293-5309. doi:10.1021/pr500880b

Ray, A. (2000). A SAF binding site in the promoter region of human gamma-fibrinogen gene functions as an IL-6 response element. J Immunol, 165(6), 3411-3417. doi:10.4049/jimmunol.165.6.3411

Ray, S., Patel, S. K., Kumar, V., Damahe, J., & Srivastava, S. (2014). Differential expression of serum/plasma proteins in various infectious diseases: specific or nonspecific signatures. Proteomics Clin Appl, 8(1-2), 53-72. doi:10.1002/prca.201300074

Ray, S., Srivastava, R., Tripathi, K., Vaibhav, V., Patankar, S., & Srivastava, S. (2012). Serum proteome changes in dengue virus-infected patients from a dengue-endemic area of India: towards new molecular targets? Omics, 16(10), 527-536. doi:10.1089/omi.2012.0037

Redman, C. M., & Xia, H. (2001). Fibrinogen biosynthesis. Assembly, intracellular degradation, and association with lipid synthesis and secretion. Ann N Y Acad Sci, 936, 480-495.

Rhea, J. M., Diwan, C. A., & Molinaro, R. J. (2010). Mass spectrometry-coupled techniques for viral-related disease biomarker identification. Biomark Med, 4(6), 859-870. doi:10.2217/bmm.10.110

Rivino, L. (2016). T cell immunity to dengue virus and implications for vaccine design. Expert Rev Vaccines, 15(4), 443-453. doi:10.1586/14760584.2016.1116948

Rivino, L. (2018). Understanding the Human T Cell Response to Dengue Virus. Adv Exp Med Biol, 1062, 241-250. doi:10.1007/978-981-10-8727-1_17

Rivino, L., Kumaran, E. A., Thein, T. L., Too, C. T., Gan, V. C., Hanson, B. J., . . . MacAry, P. A. (2015). Virus-specific T lymphocytes home to the skin during

natural dengue infection. Sci Transl Med, 7(278), 278ra235. doi:10.1126/scitranslmed.aaa0526

Rodenhuis-Zybert, I. A., Wilschut, J., & Smit, J. M. (2010). Dengue virus life cycle: viral and host factors modulating infectivity. Cell Mol Life Sci, 67(16), 2773-2786. doi:10.1007/s00018-010-0357-z

Romanello, M., Piatkowska, E., Antoniali, G., Cesaratto, L., Vascotto, C., Iozzo, R. V., . . . Brancia, F. L. (2014). Osteoblastic cell secretome: a novel role for progranulin during risedronate treatment. Bone, 58, 81-91. doi:10.1016/j.bone.2013.10.003

Rothman, A. L. (2011). Immunity to dengue virus: a tale of original antigenic sin and tropical cytokine storms. Nat Rev Immunol, 11(8), 532-543. doi:10.1038/nri3014

Salazar, M. I., del Angel, R. M., Lanz-Mendoza, H., Ludert, J. E., & Pando-Robles, V. (2014). The role of cell proteins in dengue virus infection. J Proteomics, 111, 6-15. doi:10.1016/j.jprot.2014.06.002

Schiodt, F. V., Ostapowicz, G., Murray, N., Satyanarana, R., Zaman, A., Munoz, S., & Lee, W. M. (2006). Alpha-fetoprotein and prognosis in acute liver failure. Liver Transpl, 12(12), 1776-1781. doi:10.1002/lt.20886

Schmidt-Arras, D., & Rose-John, S. (2016). IL-6 pathway in the liver: From physiopathology to therapy. J Hepatol, 64(6), 1403-1415. doi:10.1016/j.jhep.2016.02.004

Shepard, D. S., Suaya, J. A., Halstead, S. B., Nathan, M. B., Gubler, D. J., Mahoney, R. T., . . . Meltzer, M. I. (2004). Cost-effectiveness of a pediatric dengue vaccine. Vaccine, 22(9-10), 1275-1280. doi:10.1016/j.vaccine.2003.09.019

Shi, J., Wang, X., Lyu, L., Jiang, H., & Zhu, H. J. (2018). Comparison of protein expression between human livers and the hepatic cell lines HepG2, Hep3B, and Huh7 using SWATH and MRM-HR proteomics: Focusing on drug-metabolizing enzymes. Drug Metab Pharmacokinet, 33(2), 133-140. doi:10.1016/j.dmpk.2018.03.003

Shigaeva, M. I., Talanov, E., Venediktova, N. I., Murzaeva, S. V., & Mironova, G. D. (2014). [A role for calreticulin in functioning of mitochondrial ATP-dependent potassium channel]. Biofizika, 59(5), 887-894.

Silva, E. M., Conde, J. N., Allonso, D., Ventura, G. T., Coelho, D. R., Carneiro, P. H., . . . Mohana-Borges, R. (2019). Dengue virus nonstructural 3 protein interacts directly with human glyceraldehyde-3-phosphate dehydrogenase (GAPDH) and reduces its glycolytic activity. Sci Rep, 9(1), 2651. doi:10.1038/s41598-019-39157-7

Songprakhon, P., Limjindaporn, T., Perng, G. C., Puttikhunt, C., Thaingtamtanha, T., Dechtawewat, T., . . . Noisakran, S. (2018). Human glucose-regulated protein 78 modulates intracellular production and secretion of nonstructural protein 1 of dengue virus. J Gen Virol, 99(10), 1391-1406. doi:10.1099/jgv.0.001134

Srichaikul, T., Nimmanitaya, S., Artchararit, N., Siriasawakul, T., & Sungpeuk, P. (1977). Fibrinogen metabolism and disseminated intravascular coagulation in dengue hemorrhagic fever. Am J Trop Med Hyg, 26(3), 525-532. doi:10.4269/ajtmh.1977.26.525

Sridhar, S., Luedtke, A., Langevin, E., Zhu, M., Bonaparte, M., Machabert, T., . . . DiazGranados, C. A. (2018). Effect of Dengue Serostatus on Dengue Vaccine Safety and Efficacy. N Engl J Med, 379(4), 327-340. doi:10.1056/NEJMoa1800820

Srikiatkhachorn, A., & Green, S. (2010). Markers of dengue disease severity. Curr Top Microbiol Immunol, 338, 67-82. doi:10.1007/978-3-642-02215-9_6

Srikiatkhachorn, A., Rothman, A. L., Gibbons, R. V., Sittisombut, N., Malasit, P., Ennis, F. A., . . . Kalayanarooj, S. (2011). Dengue--how best to classify it. Clin Infect Dis, 53(6), 563-567. doi:10.1093/cid/cir451

Sripada, S., Srivastava, N., & Dayaraj, C. (2009). Dengue virus modulates mitochondrial dynamics during its replication. The FASEB Journal, 23(1_supplement), LB22-LB22. doi:10.1096/fasebj.23.1_supplement.LB22

St John, A. L., Abraham, S. N., & Gubler, D. J. (2013). Barriers to preclinical investigations of anti-dengue immunity and dengue pathogenesis. Nat Rev Microbiol, 11(6), 420-426. doi:10.1038/nrmicro3030

Stanaway, J. D., Shepard, D. S., Undurraga, E. A., Halasa, Y. A., Coffeng, L. E., Brady, O. J., . . . Murray, C. J. L. (2016). The global burden of dengue: an analysis from the Global Burden of Disease Study 2013. Lancet Infect Dis, 16(6), 712-723. doi:10.1016/s1473-3099(16)00026-8

Stastna, M., & Van Eyk, J. E. (2012). Investigating the secretome: lessons about the cells that comprise the heart. Circ Cardiovasc Genet, 5(1), o8-o18. doi:10.1161/circgenetics.111.960187

Stepanenko, A. A., & Dmitrenko, V. V. (2015). HEK293 in cell biology and cancer research: phenotype, karyotype, tumorigenicity, and stress-induced genome-phenotype evolution. Gene, 569(2), 182-190. doi:10.1016/j.gene.2015.05.065

Taguchi, K., Nishi, K., Chuang, V.T.G., Maruyama, T., & Otagiri, M. (2013). Molecular Aspects of Human Alpha-1 Acid Glycoprotein — Structure and Function, Acute Phase Proteins, Sabina Janciauskiene, IntechOpen, doi:

10.5772/56101. Available from: https://www.intechopen.com/books/acute-phase-proteins/molecular-aspects-of-human-alpha-1-acid-glycoprotein-structure-and-function (Accessed on 22 Aug, 2019)

Talens, S., Malfliet, J. J., van Hal, P. T., Leebeek, F. W., & Rijken, D. C. (2013). Identification and characterization of alpha1 -antitrypsin in fibrin clots. J Thromb Haemost, 11(7), 1319-1328. doi:10.1111/jth.12288

Teschler, H. (2015). Long-term experience in the treatment of alpha1-antitrypsin deficiency: 25 years of augmentation therapy. Eur Respir Rev, 24(135), 46-51. doi:10.1183/09059180.10010714

Thayan, R., Huat, T. L., See, L. L., Khairullah, N. S., Yusof, R., & Devi, S. (2009). Differential expression of aldolase, alpha tubulin and thioredoxin peroxidase in peripheral blood mononuclear cells from dengue fever and dengue hemorrhagic fever patients. Southeast Asian J Trop Med Public Health, 40(1), 56-65.

Thayan, R., Huat, T. L., See, L. L., Tan, C. P., Khairullah, N. S., Yusof, R., & Devi, S. (2009). The use of two-dimension electrophoresis to identify serum biomarkers from patients with dengue haemorrhagic fever. Trans R Soc Trop Med Hyg, 103(4), 413-419. doi:10.1016/j.trstmh.2008.12.018

Thio, C. L., Yusof, R., Ashrafzadeh, A., Bahari, S., Abdul-Rahman, P. S., & Karsani, S. A. (2015). Differential Analysis of the Secretome of WRL68 Cells Infected with the Chikungunya Virus. PLoS One, 10(6), e0129033. doi:10.1371/journal.pone.0129033

Thomas, P., & Smart, T. G. (2005). HEK293 cell line: a vehicle for the expression of recombinant proteins. J Pharmacol Toxicol Methods, 51(3), 187-200. doi:10.1016/j.vascn.2004.08.014

Thompson, A., Schafer, J., Kuhn, K., Kienle, S., Schwarz, J., Schmidt, G., . . . Hamon, C. (2003). Tandem mass tags: a novel quantification strategy for comparative analysis of complex protein mixtures by MS/MS. Anal Chem, 75(8), 1895-1904. doi:10.1021/ac0262560

Throop, J. L., Kerl, M. E., & Cohn, L. (2004). Albumin in health and disease: Causes and treatment of hypoalbuminemia. Compendium on Continuing Education for the Practicing Veterinarian, 26, 940-948.

Tongluan, N., Ramphan, S., Wintachai, P., Jaresitthikunchai, J., Khongwichit, S., Wikan, N., . . . Smith, D. R. (2017). Involvement of fatty acid synthase in dengue virus infection. Virol J, 14(1), 28. doi:10.1186/s12985-017-0685-9

Tseng, C. K., Lin, C. K., Wu, Y. H., Chen, Y. H., Chen, W. C., Young, K. C., & Lee, J. C. (2016). Human heme oxygenase 1 is a potential host cell factor against dengue virus replication. Sci Rep, 6, 32176. doi:10.1038/srep32176

Tyanova, S., Temu, T., Sinitcyn, P., Carlson, A., Hein, M. Y., Geiger, T., . . . Cox, J. (2016). The Perseus computational platform for comprehensive analysis of (prote)omics data. Nat Methods, 13(9), 731-740. doi:10.1038/nmeth.3901

Van Gorp, E. C., Setiati, T. E., Mairuhu, A. T., Suharti, C., Cate Ht, H., Dolmans, W. M., . . . Brandjes, D. P. (2002). Impaired fibrinolysis in the pathogenesis of dengue hemorrhagic fever. J Med Virol, 67(4), 549-554. doi:10.1002/jmv.10137

Vaughn, D. W., Green, S., Kalayanarooj, S., Innis, B. L., Nimmannitya, S., Suntayakorn, S., . . . Nisalak, A. (2000). Dengue viremia titer, antibody response pattern, and virus serotype correlate with disease severity. J Infect Dis, 181(1), 2-9. doi:10.1086/315215

Vetter, M. L., Rodgers, M. A., Patricelli, M. P., & Yang, P. L. (2012). Chemoproteomic profiling identifies changes in DNA-PK as markers of early dengue virus infection. ACS Chem Biol, 7(12), 2019-2026. doi:10.1021/cb300420z

Villar, L., Dayan, G. H., Arredondo-Garcia, J. L., Rivera, D. M., Cunha, R., Deseda, C., . . . Noriega, F. (2015). Efficacy of a tetravalent dengue vaccine in children in Latin America. N Engl J Med, 372(2), 113-123. doi:10.1056/NEJMoa1411037

Vogel, C., Abreu Rde, S., Ko, D., Le, S. Y., Shapiro, B. A., Burns, S. C., . . . Penalva, L. O. (2010). Sequence signatures and mRNA concentration can explain two-thirds of protein abundance variation in a human cell line. Mol Syst Biol, 6, 400. doi:10.1038/msb.2010.59

Vuilleumier, N., Dayer, J. M., von Eckardstein, A., & Roux-Lombard, P. (2013). Pro- or anti-inflammatory role of apolipoprotein A-1 in high-density lipoproteins? Swiss Med Wkly, 143, w13781. doi:10.4414/smw.2013.13781

Wain, H. M., Bruford, E. A., Lovering, R. C., Lush, M. J., Wright, M. W., & Povey, S. (2002). Guidelines for human gene nomenclature. Genomics, 79(4), 464-470. doi:10.1006/geno.2002.6748

Walldius, G., Jungner, I., Holme, I., Aastveit, A. H., Kolar, W., & Steiner, E. (2001). High apolipoprotein B, low apolipoprotein A-I, and improvement in the prediction of fatal myocardial infarction (AMORIS study): a prospective study. Lancet, 358(9298), 2026-2033. doi:10.1016/s0140-6736(01)07098-2

Wang, Y., Hao, J., Liu, X., Wang, H., Zeng, X., Yang, J., . . . Zhang, T. (2016). The mechanism of apoliprotein A1 down-regulated by Hepatitis B virus. Lipids Health Dis, 15, 64. doi:10.1186/s12944-016-0232-5

Wangrangsimakul, T., Althaus, T., Mukaka, M., Kantipong, P., Wuthiekanun, V., Chierakul, W., . . . Paris, D. H. (2018). Causes of acute undifferentiated fever

and the utility of biomarkers in Chiangrai, northern Thailand. PLoS Negl Trop Dis, 12(5), e0006477. doi:10.1371/journal.pntd.0006477

Ward, R., & Davidson, A. D. (2008). Reverse genetics and the study of Dengue virus. Future Virology, 3, 279-290.

Warren, B. L., Eid, A., Singer, P., Pillay, S. S., Carl, P., Novak, I., . . . Opal, S. M. (2001). Caring for the critically ill patient. High-dose antithrombin III in severe sepsis: a randomized controlled trial. Jama, 286(15), 1869-1878. doi:10.1001/jama.286.15.1869

Wati, S., Soo, M. L., Zilm, P., Li, P., Paton, A. W., Burrell, C. J., . . . Carr, J. M. (2009). Dengue virus infection induces upregulation of GRP78, which acts to chaperone viral antigen production. J Virol, 83(24), 12871-12880. doi:10.1128/jvi.01419-09

Weiskopf, D., & Sette, A. (2014). T-cell immunity to infection with dengue virus in humans. Front Immunol, 5, 93. doi:10.3389/fimmu.2014.00093

Welsch, S., Miller, S., Romero-Brey, I., Merz, A., Bleck, C. K., Walther, P., . . . Bartenschlager, R. (2009). Composition and three-dimensional architecture of the dengue virus replication and assembly sites. Cell Host Microbe, 5(4), 365-375. doi:10.1016/j.chom.2009.03.007

Whitehead, S. S. (2016). Development of TV003/TV005, a single dose, highly immunogenic live attenuated dengue vaccine; what makes this vaccine different from the Sanofi-Pasteur CYD vaccine? Expert Rev Vaccines, 15(4), 509-517. doi:10.1586/14760584.2016.1115727

Wills, B. A., Oragui, E. E., Dung, N. M., Loan, H. T., Chau, N. V., Farrar, J. J., & Levin, M. (2004). Size and charge characteristics of the protein leak in dengue shock syndrome. J Infect Dis, 190(4), 810-818. doi:10.1086/422754

Wills, B. A., Oragui, E. E., Stephens, A. C., Daramola, O. A., Dung, N. M., Loan, H. T., . . . Levin, M. (2002). Coagulation abnormalities in dengue hemorrhagic Fever: serial investigations in 167 Vietnamese children with Dengue shock syndrome. Clin Infect Dis, 35(3), 277-285. doi:10.1086/341410

World Health Organization (WHO) Regional Office for South-East Asia (2011). Comprehensive Guidelines for Prevention and Control of Dengue and Dengue Haemorrhagic Fever. Revised and expanded edition. India: WHO 2011. Retrieved from http://www.searo.who.int/entity/vector_borne_tropical_diseases/documents/SEAROTPS60/en/ (Accessed on June 10, 2019)

World Health Organization (WHO). (2009). Dengue: Guideline for Diagnosis, Treatment, Prevention and Control. Retrieved from

http://whqlibdoc.who.int/publications/2009/9789241547871_eng.pdf. (Accessed on January 10, 2016)

World Health Organization (WHO). (2019). Dengue and severe dengue. Retrieved from https://www.who.int/news-room/fact-sheets/detail/dengue-and-severe-dengue (Accessed on 12 July, 2019)

World Health Organization (WHO). (1997). Dengue hemorrhagic fever: diagnosis, treatment, prevention and control. 2nd ed. Geneva: WHO.

World Health Organization (WHO). (2012) TDR. Handbook for Clinical Management of Dengue. Geneva: WHO.

Wong, S. S., Haqshenas, G., Gowans, E. J., & Mackenzie, J. (2012). The dengue virus M protein localises to the endoplasmic reticulum and forms oligomers. FEBS Lett, 586(7), 1032-1037. doi:10.1016/j.febslet.2012.02.047

Woodson, S. E., Freiberg, A. N., & Holbrook, M. R. (2013). Coagulation factors, fibrinogen and plasminogen activator inhibitor-1, are differentially regulated by yellow fever virus infection of hepatocytes. Virus Res, 175(2), 155-159. doi:10.1016/j.virusres.2013.04.013

Woodson, S. E., & Holbrook, M. R. (2011). Infection of hepatocytes with 17-D vaccine-strain yellow fever virus induces a strong pro-inflammatory host response. J Gen Virol, 92(Pt 10), 2262-2271. doi:10.1099/vir.0.031617-0

Xie, X., Zou, J., Wang, Q. Y., & Shi, P. Y. (2015). Targeting dengue virus NS4B protein for drug discovery. Antiviral Res, 118, 39-45. doi:10.1016/j.antiviral.2015.03.007

Yacoub, S., Fox, A., Kinh, N.V., Screaton, G., & Wertheim, H. (2014). Biomarkers for dengue: prospects and challenges. In James W, Jeremy F. Clinical Insights: Dengue: Transmission, Diagnosis & Surveillance: Future Medicine Ltd. doi: 10.2217/ebo.13.499

Yang, S., McGookey, M., Wang, Y., Cataland, S. R., & Wu, H. M. (2015). Effect of blood sampling, processing, and storage on the measurement of complement activation biomarkers. Am J Clin Pathol, 143(4), 558-565. doi:10.1309/ajcpxpd7zqxntial

Yousuf, A. (2016). High-throughput quantitative proteomic analysis of host proteins interacting with dengue virus replication complex. University of Bristol.

Zeilinger, K., Freyer, N., Damm, G., Seehofer, D., & Knospel, F. (2016). Cell sources for in vitro human liver cell culture models. Exp Biol Med (Maywood), 241(15), 1684-1698. doi:10.1177/1535370216657448